University of Southampton

Faculty of Environmental and Life Sciences

School of Ocean and Earth Science

Development of a novel rapid screening technique for radionuclides using test-stick technology

by

Alexandre Duarte Correia Cabrita Margarido Tribolet

ORCID ID 0000-0001-7082-8100

Thesis for the degree of Doctor of Philosophy

February 2023

University of Southampton

Abstract

Faculty of Environmental and Life Sciences

School of Ocean and Earth Science

Thesis for the Degree of Doctor of Philosophy

Development of a novel rapid screening technique for radionuclides using test-stick technology

by

Alexandre Duarte Correia Cabrita Margarido Tribolet

The nuclear decommissioning authority (NDA) has been tasked with the decommissioning and clean-up of the UK's nuclear legacy. The NDA has identified methods to streamline the characterisation process by investing into the development of rapid screening techniques. Characterisation of non-gamma emitting radionuclides is currently relied upon off-site specialist radiochemical laboratories. Dependence on these off-site specialist laboratories for screening samples for non-gamma emitting radionuclides can increase the costs and timescales associated with reaching the desired end-states.

Test-stick technology looks to address this issue and provide a suitable candidate for on-site rapid screening of difficult-to-measure (DTM) radionuclides, such as ^{90}Sr. Strontium-90 has been selected as an exemplar for this technique to demonstrate the application of test-stick technology to screen for a DTM radionuclide and major contaminant in nuclear facilities.

A test-stick manufacture technique is presented along with the performance of two industrial extractive resins; TK100 and Clevasol. Both extractive resins were selected due to their operability in neutral conditions making them suited to sample groundwater and requiring no acids for experimental work. Operability conditions for both extractive resin test-sticks were determined including sampling time (40 to 60 minutes), sample volume (~4 mL) and the role of chemical interferences (Na, K, Ca and Mg). These studies provided insight into the test-stick performance for both extractive resins and how the performance between these extractive resin test-sticks compared. Optimisations for test-stick technology including test-stick manufacture and sampling time were identified and highlighted for future test-stick developments. Numerical simulations provided further insight into test-stick performance including over different extractive resin mass loadings on the test-stick as well as variable sample volumes. The performance of test-stick technology over a wide range of stable Sr concentrations was simulated and compared against real-world values for Sellafield.

Table of Contents

Table of Tables

Table of Tables

Table of Figures

Table of Figures

Table of Figures

Research Thesis: Declaration of Authorship

Print name: ALEXANDRE DUARTE CORREIA CABRITA MARGARIDO TRIBOLET

Title of thesis: Development of a novel rapid screening technique for radionuclides using test-stick technology

I declare that this thesis and the work presented in it are my own and has been generated by me as the result of my own original research.

I confirm that:

1. This work was done wholly or mainly while in candidature for a research degree at this University;
2. Where any part of this thesis has previously been submitted for a degree or any other qualification at this University or any other institution, this has been clearly stated;
3. Where I have consulted the published work of others, this is always clearly attributed;
4. Where I have quoted from the work of others, the source is always given. With the exception of such quotations, this thesis is entirely my own work;
5. I have acknowledged all main sources of help;
6. Where the thesis is based on work done by myself jointly with others, I have made clear exactly what was done by others and what I have contributed myself;
7. None of this work has been published before submission

Signature: Date: 17th February 2023

Acknowledgements

I would first like to thank my supervisors Phil Warwick and Ian Croudace for taking a chance on me with this project and tolerating me as their student. I would like to give an extra special thanks to Phil who has been not only a great supervisor and mentor but also a good friend. I could have never made it through without your support and passion for this project. Thank you for helping me to both conquer radiochemistry (funny, right?) and for providing so much support and time for me – I could never have got to this point without your insight, help, challenging-my-already-limited-knowledge and canteen cappuccinos – they were delicious. I want to thank my industrial supervisor Steve Walters at the National Nuclear Laboratory (NNL) for his help, knowledge, and enthusiasm throughout the project. I would also like to thank the Nuclear Decommissioning Authority and GAU Radioanalytical for funding this project. I would also like to thank the GAU Radioanalytical group, specifically Mark, Dave, Pawel, Maddie, Fran R., Rich and Fran B – you guys gave me such a warm welcome and provided an amazing basis for me to grow as a scientist. I am grateful for everything I've learned from you guys and I am sorry about the cap when I started – everything was new and the cap was all I had. Thank you Fran B. for being such an instrumental part in my numerical model chapter – couldn't have done it without you and I appreciate your patience.

When I moved to Southampton in 2017, I could never have imagined the amazing time and extraordinary people I would meet here and the profound impact they would have in my life and me as a person. Africa Gomez, Sarah Cryer, Emma Watts, David Riley, Emma Horn, Lina Zapata, Oana Dragomir, Koko Kunde, Millie Humphries and Jacob Harper – thank you for being amazing people who made my time in Southampton special. I want to give a special thanks to Elena Cerdan and Maarten Heijnen for being incredible people and inspiring me to be better. Thank you Maart for the consistent and always high-quality (especially the wine and company) boys nights – fly high kaiba boy. I want to thank Ben Chichester for being an awesome friend and incredible flatmate – that lockdown was long, but we made it work with our workouts (let people think what they will) and Beyblade theme tune dances. I couldn't have asked for a better flatmate and close friend – thank you. I want to thank my covfefe gang Sarah Ass-inta Howarth and Rachel BDS Shuttleworth – you guys are some of the funniest and most supportive friends I could have asked for. Thanks Rach for being a top-tier gym buddy – no one has ever made battle ropes look as funny as you do. Sarah, never stop playing rain chicken – you'll win it one day. I want to give a huge bro-shout-out to the bro triumvirate Duncan Stevens and Matthew Nichols – you lads exude bro-ness and I'm just here for the ride (take that what you will). I would also like to thank Alex Hately and Jess Stead for being brilliant officemates and friends – I miss you both. I'm sure I've forgotten other people but honestly, my Southampton journey over the last 5 years has been blessed by amazing people who have made

this experience reach heights I never dreamed it could have. Thank you, for everything. I miss you all so much.

Outside of the Southampton bubble, I also want to thank people who were as equally supportive throughout this journey. I would like to thank Sven Siedenberg for being a fantastic human being and genuinely one of my closest friends – it's been tough these last few years but you've reached new heights and I couldn't be happier for you. I want to thank one of my oldest friends, Ricardo Sanchez-Garcia, for being not only the buffest guy on here (sorry lads) but also for being one of my closest friends and supporters of everything I do. Thank you, brother. I would also like to give a special thank you to Leanne Tang for supporting me throughout this last year and being everything I could have asked for – and more. You're an incredible person and your support means everything to me - thank you batata. I would also like to thank Milo for being the true (purplegem) prince that he is and for lifting my spirit and my mood as easily and effortlessly as he does.

I want to give an incredibly special thanks to my parents, Humberto and Silvia Tribolet, who not only came up with my long name but also provided an incredible platform for me to reach where I am today. They gave everything to offer me and my sister a chance to become something and I will always be grateful for everything they've done. They have always been there when I really needed them and I couldn't have asked for any more from them. Obrigado – somos os melhores. I also want to thank my sister, Isis Tribolet, for putting up with me all these years – I know it hasn't been easy so I appreciate it! I want to also give a huge special thank you to the two most beautiful souls in my life: George and Juno. You guys bring me so much joy and happiness – the true heirs to the throne and I love you both more than words can describe.

Finally, I want to give a special and heart-filled thank you to the most special person on here, Apollo. You were the most beautiful and special soul in my life and there isn't a day that my heart doesn't search for you and wish you were still here. You were incredible and touched the soul of everyone you met and your patience was unending. You were my best friend, and my brother. And I miss you so much. This one is for you.

Thank you

Resins and reasons.

xx

Definitions and Abbreviations

Characterisation	Methods used to identify, quantify and isolate specific chemical nuclides and provide information regarding their chemical form.
Decommissioning	The process of dismantling and remediation of a site to the point where no further measures are in place regarding environmental and personnel safety.
Detection	Establishing the presence of a specific chemical or radionuclide from the background matrix and other nuclides that may also be present.
Monitoring	Repeated analysis for specific chemicals and/or radionuclides at a specific site that may have harmful effects for the environment and/or personnel.
Screening	The process of segregating specific chemicals based on their chemistry including decay mode, decay energy and/or chemical reactivity.

AGR	Advanced Gas-cooled Reactor(s)
DFR	Dounreay Fast Reactor(s)
DTM	Difficult To Measure radionuclide(s)
EAD	Early Alarm Detector(s)
EPR	Environmental Permitting Regulations
ETM	Easy To Measure
EXAFS	Extended X-ray Absorption Fine Structure
GO	Graphene Oxide
GO-COOH	Carboxylated Graphene Oxide

HDEHP	Di-(2-ethylhexyl)phosphoric acid
HLW	High Level Waste
IAEA	International Atomic Energy Agency
ICP-MS	Inductively Coupled Plasma Mass Spectrometry
ILW	Intermediate Level Waste
LLW	Low Level Waste
LLWR	Low Level Waste Repository
LSA	Liquid Scintillation Assay
LSC	Liquid Scintillation Counting
MES	Multiple Extractant System
MSS	Magnox Swarf Storage Silo
NDA	Nuclear Decommissioning Authority
NNL	National Nuclear Laboratory
PBO	Parent Body Organisations
PFR	Prototype Fast Reactor
PM	Photomultiplier
RTM	Real Time Measurement
SEM SDD EDS	Scanning Electron Microscopy Silicon Drift Detector Energy Dispersive X-ray Spectrometry
SES	Single Extractant System
SLC	Site License Company
SPEC	Spectroscopy Detector
TAWARA	TAp WAter RAdioactivity Real Time Monitor
THORP	Thermal Oxide Reprocessing Plant
UKAEA	United Kingdom Atomic Energy Agency

Chapter 1 Introduction

1.1 Nuclear legacy in the UK

With the conclusion of the Second World War and the United States passing the McMahon Act (Atomic Energy Act 1946 - which removed ties with the UK regarding the sharing of nuclear research) the UK began its own independent nuclear initiative [1,2]. This initiative was marked by the passing of the Atomic Energy Act 1946 by the UK followed by the Atomic Energy Authority Act 1954 that resulted in the creation of the UKAEA (United Kingdom Atomic Energy Authority) [3,4]. These legislations and especially the inception of the UKAEA set the precedence for the nuclear programme in the UK. This programme saw the initial development of nuclear research in the form of nuclear fuel production for military use before shortly shifting the focus to civil nuclear power generation in the form of Calder Hall in 1956 that saw the world's first purposely-built commercial civil nuclear power station coming online [5]. The following decades saw various reactor designs implemented for either research and/or civil power that resulted in the expansion of the number of nuclear sites across the UK. The existence of these driving forces including the development and construction of a range of technologies for nuclear power generation created a complex nuclear profile across the UK. This nuclear industry profile ranged from advanced gas-cooled reactors in Sellafield, Cumbria, to helium-cooled and steam-generating heavy water reactors in Winfrith and even DFR (Dounreay Fast Reactor) and PFR (Prototype Fast Reactor) fast-breeder reactors in Dounreay, Scotland. The fleet of nuclear reactors designed for larger scale energy generation for civil use were Magnox and AGR (Advanced Gas-cooled Reactors) nuclear power stations located in Dungeness B, Hunterston B, Hinkley Point B, Hartlepool, Heysham for AGR and Chapelcross, Hunterston A, Oldbury, Trawsfynydd, Wylfa, Berkely, Bradwell, Dungeness A, Hinkley Point A and Sizewell C for Magnox.

The UK nuclear programme had also expanded its focus onto the development of nuclear fuel manufacture (originally primarily for military applications but later for civilian power generation) and reprocessing plants for the recovery and processing of plutonium, which saw its inception in the UK after the Windscale piles and associated reprocessing plants were built in 1950. The Windscale piles were graphite moderated reactors designed to produce plutonium for military applications. This interest in nuclear fuel manufacture and reprocessing plants saw the construction of various nuclear fuel production and reprocessing plants with the last facilities consisting of the MAGNOX fuel reprocessing plant and THORP (Thermal Oxide Reprocessing Plant) at Sellafield, Cumbria, amongst others. Towards the end of the 20th century majority of these facilities faced closure and shut down due to various factors including end-of-life, lack of financial sustainability

and shift in focus of energy generation sources – the drive for more renewable energy sources as well as outsourcing energy from abroad. The nuclear programme led by the UKAEA has allowed for the development of a diverse range of nuclear facilities with the majority differing in operation/design and site geography. The result of this saw a large nuclear legacy built across the UK with most of these facilities either shut down or preparing to shut down in the next few years and with this the need to undertake a large-scale nuclear decommissioning project.

1.2 Nuclear Decommissioning in the UK

1.2.1 Nuclear Decommissioning Authority

A large nuclear decommissioning project is required to deal with the complex nuclear legacy that the UK has accumulated over the decades. Following a white paper *Managing the Nuclear Legacy—a Strategy for Action* (Cm 5552) and Energy Act 2004 the UK Government created the NDA (Nuclear Decommissioning Authority) to oversee this programme of civil nuclear decommissioning work [6]. The NDA is a non-departmental public body concerned with carrying out work, in this case nuclear decommissioning, on behalf of the Government. The NDA is sponsored by the Department for Business, Energy and Industrial Strategy and is accountable via Parliament for its progression throughout this decommissioning project [7]. The NDA is tasked and responsible for the management of all nuclear sites undergoing decommissioning and is responsible for the strategy undertaken to decommission these sites. Due to the complex decommissioning challenge presented by the UK's civil nuclear legacy as well as the magnitude of this legacy, the NDA undertakes this decommissioning project via management contracts with companies – known as Site License Companies (SLCs). SLCs are the legal entity which manage day-to-day site operation as well as the on-site decommissioning project and doing so in a safe and environmentally responsible manner. To ensure this, the SLCs are owned by the Parent Body Organisations (PBO), who are selected by the NDA through a contract competition process. These PBOs provide governance of the SLCs by arranging secondments and consultancy to provide expertise as well as financial and strategic management to the SLCs to optimise the decommissioning process. As the 'User' of the nuclear site, the SLCs are responsible for all on-site activities and for operating safely and legally within their nuclear site licenses and radioactive waste disposal authorisations. The SLCs must comply with these legislations whilst also meeting the NDA's goals and decommissioning project goals and in return the NDA allocates funding to SLCs to carry out their commitments [8].

The NDA is concerned with not only managing these sites and the decommissioning strategy but is also responsible for research and development in this sector. This includes optimising older technologies as well as developing new technologies all with the joint goal of providing the technical

means to deliver the decommissioning programme safely and in a time and cost-effective manner. This objective to incentivise research and development comes with the hopes of streamlining a project whose time projections looks to transcend generations coupled with a huge financial weight. It is this drive for research and development in this sector that gave origin to the NDA PhD bursary scheme that funds projects – such as this one – that aim to streamline and enhance the efficiency of this decommissioning process.

Figure 1.1: Workflow of operation regarding the NDA estates, demonstrating the role of regulators and government at the source of the workflow all the way to Site License Companies (SLCs) carrying out day-to-day operations at each nuclear decommissioning site [7].

1.2.2 Nuclear decommissioning challenge and the role of characterisation

To understand and explore the process by which decommissioning can be streamlined and aided through research and development, there is a need to first comprehend the magnitude of the nuclear decommissioning challenge being faced by the NDA. Currently 17 nuclear facilities ranging from Magnox civil nuclear power facilities such as Hinkley Point A in Somerset to the Low Level Waste Repository (LLWR) to nuclear fuel reprocessing plants in Sellafield, Cumbria are undertaking decommissioning activities. These sites even include the Magnox Swarf Storage Silo (MSSS) which has been assessed as the highest risk nuclear facility in the NDA's estate due to its aging structure, large stores of solid waste and ground contamination from leaking silos. The nuclear decommissioning project oversees different nuclear sites at different stages of the nuclear decommissioning process throughout the NDA's 17 current nuclear site portfolio (Figure 1.2) [9–11].

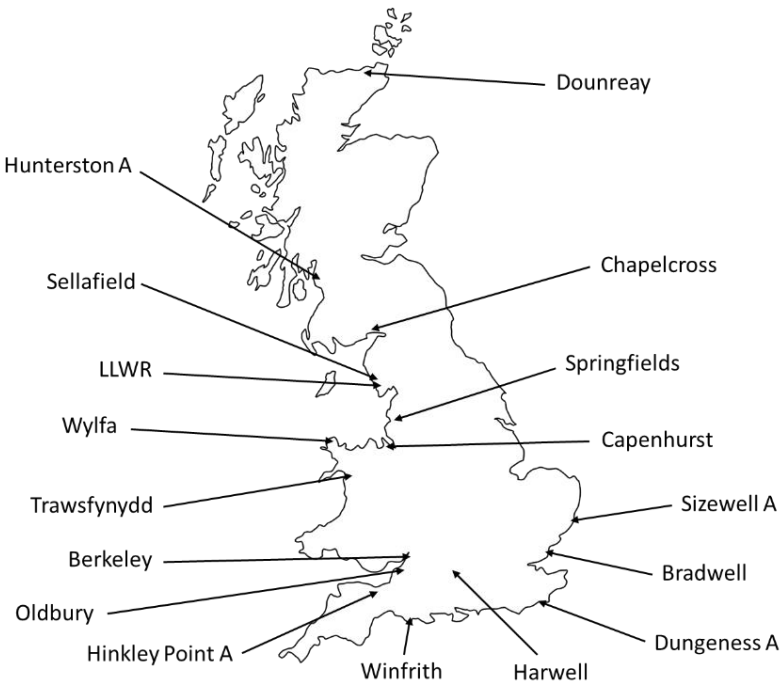

Figure 1.2: A nuclear site map of the UK outlining all the nuclear sites currently being decommissioned by the NDA and therefore the full magnitude of the large-scale nuclear decommissioning project.

However, despite the differences between each nuclear site including different types of nuclear facilities and the environment surrounding these nuclear sites one constant factor is the importance of characterisation. Waste segregation requires first carrying out characterisation to discover what tier specific types of waste fall into, from highly active cooling loop metal tubing to low level active (or out-of-scope activity) waste such as concrete from outer housing. The importance of knowing which categories of nuclear waste these wastes fall into is paramount as there are substantial costs attributed to each increasing nuclear waste category tier. This is due to the increasing number of precautions and safety measures taken to store waste in a manner appropriate to the level of contamination associated with that nuclear waste. For example, high level waste (HLW) is defined as being heat generating due to the substantial amount of radiation emitted from the waste and is normally comprised of spent nuclear fuel. This means that HLW requires storage in cooling ponds to allow the decay of short-lived radionuclides. HLW is then processed and resulting materials are blended with molten glass (in a process known as vitrification) before being stored in specially designed steel drums and stored again until the heat generation step passes. Intermediate-level waste (ILW) compromises 6% of radioactive waste obtained from nuclear sites by volume with major components of this waste being graphite from reactor core and sludges from radioactive waste effluent treatment. ILW requires no cooling-off period and waste is placed into a cement-based mixture before being stored into large, specialised steel drums and/or concrete boxes. These

large, specialised containers allow for the ILW to be safely transported and stored. ILW cannot be stored in near-surface repositories due to still requiring higher level of containment and isolation than can be provided by these repositories. Low-level waste (LLW) can be stored in near-surface repositories and is normally contained of scrap metal, paper and plastic, which makes up 94% of all radioactive waste by volume. Most LLW is disposed off in the Low-Level Waste repository in Cumbria where waste is mixed with cement and stored in large metal containers, which are stored in cement-lined vaults. Very Low-Level Waste (VLLW) can be disposed of in landfill sites with regular household waste as long as the landfill site holds the relevant permits to hold active waste. Regulations for VLLW waste state that low volume waste must contain a <400 kBq per 0.1 m^3 according, and/or <40 kBq for a single item with extra limits for ^{14}C and ^{3}H waste. High volume VLLW waste must not exceed 4 MBq per tonne with additional limits for wastes containing ^{3}H. Both of these tiers (HLW and VLLW) display the contrasting approaches to disposing of waste dependent on how (radio)active the waste is and the costs attributed with this (Figure 1.3) [12–14].

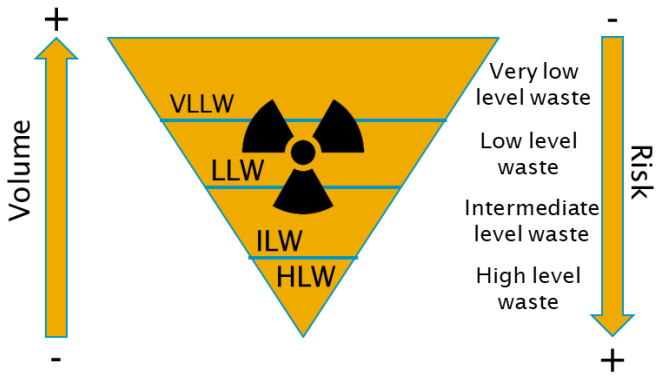

Figure 1.3: A diagram describing the nuclear waste hierarchy, which helps to organise and coordinate the disposal of nuclear waste dependent on how active the waste is and what its physical form is.

Planning and preparation are key in the process of decommissioning and characterisation plays a key role in this step. Characterisation determines simultaneously whether waste is active, and if so, what type of radiation is present: alpha, beta or gamma. This process is then normally followed by determining the amount of activity present along with the physical properties of this waste (solid or aqueous, for example) that then determines the waste category suitable for safe and effective waste disposal. Waste segregation follows the waste category system outlined above (Figure 1.3) with specific distinctions made between each waste segregation tier via the Environmental Permitting Regulations (EPR 2016) [15]. The NDA and other bodies including the Office for Nuclear Regulation has identified and highlighted the importance of waste characterisation in the nuclear decommissioning process.

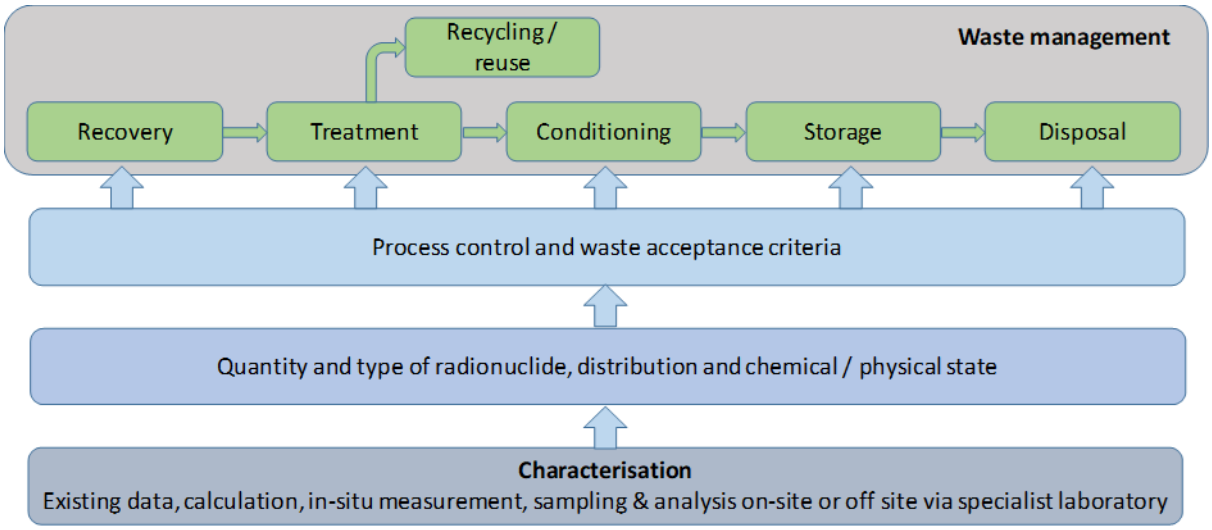

Figure 1.4: A flowchart demonstrating the role of characterisation in waste sentencing and management.

Emptage *et al.* concluded in their review that efficient radioactive waste management is dependent on a robust and efficient characterisation programme where contributions from in-*situ*, on-site and off-site characterisation can facilitate in reducing project risks and costs. This also means that the characterisation process must be not only robust but also constantly validated by regulators and quality control and assurance to maintain efficiency of the characterisation process whilst minimising costs and timescales. Characterisation in nuclear sites can be differentiated into off-site, on-site and in-*situ* analysis. Off-site characterisation is currently the predominant method of characterisation where samples are sent to specialist off-site laboratories and complex analytical methods are carried out. These analytical methods include carrying out radiochemical separations to isolate the radionuclide of interest before radiochemical analysis is carried out by techniques such as liquid scintillation (LSC), inductively coupled mass spectrometry (ICP-MS) and alpha spectroscopy. This method of characterisation is time consuming as the full analysis of the sample can take 20 to 30 days to be carried out – depending on the type of sample and the radionuclide of interest. On-site characterisation involves carrying out the analysis on-site using mobile adaptations of radiochemical techniques. On-site characterisation is less common, but interest is beginning to grow behind this type of characterisation. An example of an on-site technique is gamma spectroscopy where samples can be analysed directly for gamma-emitting radionuclides and scaling factors applied to determine the activity of non-gamma-emitting radionuclides from this. However, this type of on-site analysis is carried out for easy-to-measure radionuclides (ETM) only whilst current on-site analysis development targets difficult-to-measure (DTM) radionuclides. DTMs currently are unable to be directly measured without radiochemical separation and therefore why characterisation of DTMs is currently carried out off-site. In-*situ* techniques are also an emerging method of characterisation where sampling is carried out directly on the origin of the sample and

examples of these type of characterisation technique include gas proportional counters and plastic scintillators. It has been noted by the NDA, the Office for Nuclear Regulation and other bodies how advancements in waste characterisation, including the development of rapid screening techniques, could reduce projected time and costs. Despite deployment of rapid screening techniques in nuclear sites such as Harwell, these deployed rapid screening techniques currently involve screening for easy-to-measure (ETM) radionuclides. Difficult-to-measure (DTM) radionuclides are currently unable to be directly screened for on-site as they require radiochemical separation and therefore analysis is carried out off-site and away from the point of waste generation. These off-site analyses for DTM radionuclides are time consuming and cost intensive and therefore significant savings can be achieved by transferring this process to on-site. These savings include in shipping costs, turn around times for results and relieving the pressure on specialist radiochemical labs. Relieving the pressure on these specialist radiochemical labs allow for more time to analyse samples that have a complex mixture of radionuclides that requires specialist radiochemical separation and analysis to resolve. Advancement in rapid screening techniques would serve to promote timely characterisation and in turn complement off-site characterisation in specialist radioanalytical laboratories. The following statement has been made by the NDA and NNL in technical memorandums and reports:

"promoting timely characterisation and segregation of waste, which delivers effective waste management"[10,14]

This statement serves as a good example of the highlighted need for development of rapid screening techniques as well as a blueprint for in-development rapid characterisation techniques to follow including the focus of this project – test-stick technology. Furthermore, the UK nuclear decommissioning industry has also identified the current reliance on site-based expertise for waste characterisation including the utilisation of more specialist characterisation techniques. Therefore, the development of a technique that would be capable of providing in-*situ* rapid characterisation whilst requiring no expert/specialist to operate this technique is a further benefit to test-stick technology. The primary function and goal of rapid screening techniques, including test-stick technology, would be screening radioactive wastes and determining whether off-site analysis via a specialist off-site laboratory would be required. The importance of determining whether nuclear decommissioning waste is above or below specific thresholds (i.e. out-of-scope limits and VLLW as determined by the EPR 2016) lies in streamlining the characterisation of the waste materials (including groundwater, for example) and quickly determining whether[15]:

a) The presence of a specific radionuclide, or group of radionuclides, (in this case beta-emitting radionuclides with no detectable gamma-radiation) are detected

b) Whether the activity of this radionuclide(s) is above a specific legislative threshold (such as out-of-scope limits or VLLW, for example) that may then require further (off-site) radiochemical analysis.

Test-stick technology is a rapid screening technique that looks to implement currently established extractants that are specialised at extracting the radionuclide of interest (^{90}Sr in this case) and mount that extractant onto a small (1x1 cm^2) area. The test-stick are then submerged in the sample of interest (such as groundwater in this case) for a designated period of time before being removed from solution, washed to remove excess unwanted sample before being analysed via a scintillation counter. This relies on the concept of tabletop scintillation counters which already exist.

Characterisation of waste and determination of these factors within the space of 24 hours is what the NDA is currently aiming to achieve by 2025 and test-stick technology aims to complement this outlook. The NDA has also called for improvement in initial characterisation including the aim of having 70% of initial characterisation carried out in-*situ* to streamline the characterisation process and consequently the rest of the initial decommissioning process. Test-stick technology looks to primarily serve the role of both first-response and initial characterisation of waste in-*situ* to aid in the process of waste segregation and optimise the use of off-site specialist radiochemical analysis for samples that are both active above a specific legislative threshold (such as VLLW) and/or require complex radiochemical separation and analysis.[10,16]

1.3 Radionuclide characterisation

1.3.1 Radionuclide categorisation

Radionuclides can be organised into one of three groups dependent on the methods of detection of that said radionuclide. These three categories are known as easy-to-measure (ETM), difficult-to-measure (DTM) and impossible-to-measure (ITM) radionuclides. These categories reflect the ease or difficulty associated with detecting specific radionuclides attributing to their radiochemical properties such as type of radioactive decay, decay energy and half-life(s). ETM radionuclides are normally gamma emitters that can be easily detected using gamma spectrometers even without sample preparation or radionuclide separation techniques. DTM radionuclides present challenges in measuring the activity of these radionuclides primarily because these radionuclides are often alpha- and beta-emitters but can also be x-ray emitting radionuclides that require extensive sample preparation and radionuclide separation prior to measurement. This is often due to the surrounding mass (from the matrix) absorbing the majority of the radiation, which makes measurement of these radionuclides extremely challenging. Furthermore, some radionuclides may share similar decay

energies where spectral deconvolution is necessary and therefore may require further expertise. This difficulty often warrants the need to export samples to off-site specialist radioanalytical laboratories to carry out radiochemical separation and sample prep prior to measurement by either radiochemical or spectrometric techniques [13,17].

Table 1.1: A comparison between different categories of radionuclides reflecting the ease or difficulty to radioanalytically measure these radionuclides[17].

Radionuclide characterisation	Radionuclide detection method	Radionuclide examples
Easy-to-measure	Gamma spectroscopy	^{60}Co, ^{137}Cs
Difficult-to-measure	Alpha spectroscopy and scintillation counting	^{90}Sr, ^{99}Tc, ^{226}Ra

DTM radionuclides are dependent on the application of scaling factors which use known relationships between ETM and DTM radionuclides and analysing these ETM radionuclides directly to calculate the activity of the specific DTM radionuclide present in the sample. The basis of scaling factors is important in nuclear decommissioning and provides an indirect method of analysing for DTM radionuclides. However, this also highlights the issue that direct DTM analysis can currently only be carried out in off-site specialist laboratories, which are costly and time consuming. Therefore, this provides further emphasis for the need to develop new technologies which are capable of measuring DTM radionuclides at the point of waste generation. Test-stick technology is a viable candidate for this as it utilises industrially established extractants (such as TK100) bound on the test-stick in a 1x1 cm^2 solid phase to directly extract, in-*situ* and/or on-site, the radionuclide of interest. The test-stick is then placed into a scintillation counter and the activity of the radionuclide of interest measured. Test-stick technology looks to perform extraction of the target radionuclide in 60 minutes and complement this with 60-minute count times – therefore obtaining results in 2 hours. This would allow test-sticks to perform rapid screening of radionuclides in-*situ*/on-site and provide site operators with information regarding whether samples meet VLLW limits, are out-of-scope and/or whether any further off-site analysis is required.

1.3.2 Scaling factors

Scaling factors, also known as ‘vectors’ and ‘fingerprint ratios’, are an important technique for determining on-site activity of DTM radionuclides without directly measuring these radionuclides. This is using known distribution relationships in the environment between specific DTM and ETM radionuclides. By knowing this relationship, the ETM radionuclides can be directly measured using techniques such as gamma spectroscopy and from this measured activity (and applying the known

ratio between the ETM and DTM radionuclides) the activity of the DTM radionuclide can be calculated. Scaling factors present a method of dealing with (indirectly) measuring the activity of DTMs on-site rapidly however it must be noted that despite scaling factor ratios being obtained experimentally and through radiochemical analysis of various nuclear facilities, these ratios may sometimes change or alter. This change or alteration can be due to environmental factors such as changing plant equipment for maintenance, type of resin used in ion exchange barriers or different materials present in the wastewater stream between different nuclear facilities. This change in ratios for scaling factors must be monitored and requires the need to develop a technique that may serve to aid in monitoring scaling factor ratio stabilities. Test-stick technology would hypothetically be able to serve this purpose as a means of quickly determining whether the activity of a DTM radionuclide is present in activities that correlates positively with that calculated via scaling factors [17].

1.3.3 Rapid radionuclide characterisation methods

Traditional radiochemical analysis of DTM radionuclides, especially alpha- and beta-emitting radionuclides, involves using destructive techniques primarily due to the need to isolate the radionuclide in question. Alpha- and beta-emitting radionuclide measurements are complicated by the adsorption of emitted radiation by surrounding matter due to the poor penetrability of these types of radiation. Therefore, a series of radiochemical separation methods, commonly using column chromatography, have become standard in the characterisation of these radionuclides. The complexity of the process requires the analysis to be undertaken in off-site specialist laboratories. Radiometric methods include alpha spectrometry and liquid scintillation counting which depending on the number of radionuclides present in the samples can present spectral overlap, which can cause difficulty to measure accurately specific major radionuclide contaminants in nuclear decommissioning scenarios. An alternative method for measuring longer-lived radionuclides is mass spectrometry however, this type of technique also presents issues of its own including polyatomic and isobaric interferents (such as ^{90}Zr for ^{90}Sr measurement) which rely on complex chemical separation(s) to overcome [18].

In addition to the decommissioning industry, characterisation is also critical for a number of other applications including regulatory, emergency response and site safety management. The development and transformation of existing characterisation techniques into a more mobile and rapid form would be viewed extremely favourably in these industries. These different industries and applications present a series of directions for the development of rapid characterisation techniques to aim at. Development of rapid characterisation methods would also look to assist off-site specialist radiochemical laboratory work in which these laboratories handle samples from

different nuclear facilities at different stages of the nuclear facility life cycle. This may include nuclear facilities that are operating or that are undergoing decommissioning. Rapid characterisation developments would complement this work and provide a screening method to allow samples that are more physically and/or radiochemically complex to be analysed in off-site specialist laboratories. Turnaround time for nuclear waste characterisation is also an important fact to consider as turn-around time can affect project costs as well as projected timescales for work to be carried out. However, emergency response also requires techniques and methods that achieve a quick turnaround time. A method that could be capable of providing in-*situ* characterisation of a major radionuclide contaminant such as ^{90}Sr in the span of 24 hours, for example, would be instrumental in informing the relevant authorities. Relevant information regarding the spread of radionuclide contaminants including spatial distribution across a specific area and dosage estimates to the public and local wildlife would be highly beneficial to allow whether costly evacuation measures are required to be taken. This type of scenario has been highlighted previously and is a strong example of the importance of the development of rapid screening and characterisation techniques [19].

A standard method of measuring ^{90}Sr is to allow the sample to reach secular equilibrium (after approximately two weeks) and then measuring ^{90}Y, giving positive confirmation of the presence of ^{90}Sr in the sample. The high decay energy of 2.28 MeV allows direct measurement of Cherenkov radiation using liquid scintillation counters without the addition of an organic scintillator. Therefore, there has been work that has examined the application of TEVA extractants, amongst other extractants, on the radiochemical separation of ^{90}Y to confirm the presence and activity of ^{90}Sr due to their 1:1 relationship at secular equilibrium. This also highlights a further area of development for rapid characterisation of radionuclides – extractant resins. Novel extractant resins which can carry out specific radionuclide uptake (in this case ^{90}Sr) with higher efficiencies than currently established industrial extractants whilst maintaining a degree of selectivity would promote the development of rapid characterisation techniques even further. Higher uptake efficiencies would include faster kinetics, higher partitioning coefficients – measure of partitioning of the radionuclide between the solid phase and the sample – and loading capacities. Examples include TK100 which has incorporated the crown ether from Sr-resin and added an organic cationic exchanger to improve the performance of the extractant resin under neutral pH conditions. This promotes the application of crown ethers onto ^{90}Sr uptake and screening whilst removing the need for use of concentrated acids and harmful reagents. A rapid screening that could be operated using minimal amount of toxic reagents and take a few hours whilst additionally requiring no specialist knowledge would be extremely attractive – this project looks to provide a suitable candidate [20–22].

1.3.4 Radiometric detection

1.3.4.1 Gamma spectroscopy

Gamma spectrometry is a commonly used non-destructive technique to characterise decommissioning samples. Gamma spectroscopy can also be carried out on samples without requiring radiochemical separation and therefore has seen deployment on some nuclear decommissioning sites such as Harwell. Gamma spectrometry can also be used to facilitate monitoring of the movement of radionuclides and in this project was used to give initial information regarding radiostrontium uptake by different extractants. However, its application is limited and radionuclides such as ^{90}Sr produce no gamma radiation and therefore require other techniques, such as LSC [23].

1.3.4.2 Gas detector systems

Gas detector systems operates using the concept that during emission of ionising radiation surrounding matter including gases can absorb this energy and either be ejected into a higher state or ionised if the radiation energy is high enough. If the gas is ionised and a sufficiently strong electric field is applied, then the charged species separate into the positive (cathode) and negative (anode) electrodes at which point an electrical signal will be given indicating the presence of these ions. This basic principle forms the basis for gas detector systems. Three types of gas-filled detectors exist including Geiger-Muller counters, gas proportional counters and ion chambers – where the main difference lies in the strength of the electric field. These detectors can analyse both alpha- and beta-emitting radionuclides and contain α-β discrimination similar to LSC [24].

1.3.4.3 Solid plate scintillators

Solid plate scintillators incorporate the same principles as LSC instruments however the scintillator is in a solid form. This solid plate scintillator absorbs the ionizing radiation from alpha- and beta-emitting radionuclides and produces light emissions. These light emissions are then detected by PM tubes and the data is collected and processed. These light emissions can be quantified by the number of flashes (counts) and the energy (in keV) associated to them. Solid plate scintillators have been produced from materials including inorganic crystals (such as NaI) as well as plastic scintillators (such as polystyrene). Solid plate scintillators are used to characterise radionuclides that produce almost no gamma radiation, including ^{90}Sr and ^{99}Tc [25].

1.3.4.4 Liquid scintillation counting

Liquid scintillation counting (LSC) is a radiometric technique often used to characterise both alpha- and beta-emitting radionuclides in samples and is used to characterise samples from nuclear decommissioning sites. Liquid scintillation counting provides information regarding the activity of the radionuclide present but measuring its activity indirectly. The technique does also require adding a scintillation cocktail to the sample prior to counting. The scintillation cocktail allows radioactive decay energy to be converted into light emissions (photons). These light emissions are then detected by photomultipliers (light detectors) and a spectrum is obtained on a graph plot of number of light flashes versus energy (keV) [26]. LSC is a common characterisation technique for radionuclides such as ^{90}Sr and ^{99}Tc that also produce little to no gamma radiation.

1.3.4.5 Alpha spectrometry

Alpha spectrometry is a technique which directly counts alpha emissions from the sample using a surface-barrier semi-conductor detector. This semiconductor detects alpha emissions by recording the alpha particles colliding against the detector. This collision then results in a pulse of energy deposited on the detectors, where the detector then converts the pulse amplitude to an energy. Alpha spectrometers can only detect alpha-emitting radionuclides but with greater sensitivity than LSC, for example. This radiometric technique also requires the sample to be under vacuum during analysis. Alpha spectrometry is a common technique for analysing radionuclides such as ^{235}U and ^{241}Am [27].

1.4 Thesis overview

This thesis presents and evaluates a new rapid screening technique that incorporates commercially available extractive resins into a novel test-stick format that permits rapid on-site characterisation of difficult-to-measure radionuclides without the need for specialist analysts or facilities.

1.4.1 Aims and objectives

This project aims to develop and characterise test-stick technology for applications in characterising nuclear waste as well as other areas that would benefit from an easy-to-use, rapid screening technique. Strontium-90 has been selected as an exemplar to demonstrate this technique in this work. A difficult-to-measure radionuclide that is prevalent in nuclear sites due to its high fission yield (~5.7% for ^{235}U fission yield) and relatively long half-life (28.8 years) makes this a suitable radionuclide to demonstrate test-stick technology. Groundwater was selected as the matrix for test-stick development due to the presence and mobility of ^{90}Sr in groundwater at nuclear

decommissioning sites as well as forming a strong foundation for other future applications. Nuclear decommissioning sites such as Winfrith (Dorset, UK) would highly benefit from a groundwater rapid screening technique where information regarding ^{90}Sr spread could be achieved quickly and allow for decommissioning activities to take place swiftly. These future applications can include environmental monitoring of bodies of water such as lakes and rivers as well as contributing to future developments of test-stick application in higher ionic strength matrices such as seawater.

A series of experiments and assessment have been carried out to determine the operating conditions of ^{90}Sr test-sticks as well as highlight areas where future work and developments can optimise test-stick performance even further. Two extractive resins were selected, TK100 and Clevasol, which are known to operate under neutral conditions and therefore appropriate for screening ^{90}Sr in conditions including groundwater. These extractive resins represent contrasting uptake mechanisms – size exclusion (TK100) and cationic exchange (Clevasol) – and therefore present a further study comparing the performance of both ^{90}Sr extractive resin test-sticks. Comparison of these two test-sticks provides information regarding how easily extractive resins with different uptake mechanisms can be incorporated into the test-stick format and what factors influence their performance.

1.4.2 Thesis outline

Chapter 2 is a review of radiostrontium analysis and its radiochemical separation methods. This includes different types of rapid screening methods as well as a look into different extractant materials developed with the primary focus on radiostrontium uptake. The performance of different extractive resins as well as the different methods of rapid uptake of strontium are discussed. The chemistry of the two extractants used in this study are also described.

Chapter 3 provides information regarding the methodology used as well as a framework of the overall experimental work carried out.

Chapter 4 presents work regarding the test-stick manufacture and the properties underpinning this process. SEM analysis provides information regarding the distribution of the extractive resin particles on the test-stick surface. Mass loadings of the extractive resins on the test-sticks are examined and compared between both TK100 and Clevasol. This provides an important parameter to calculate partition coefficients (k') evaluating how well strontium is extracted by the test-sticks. The physical dimensions of the test-sticks are investigated including the impact of surface area and extractive resin particle sizes on test-stick performance. Reproducibility and durability experiments provide information regarding the statistical variance between test-stick results and the impact of shelf-life on test-stick performance, respectively.

Chapter 5 describes the development and optimisation of test-stick deployment protocols. This includes monitoring the performance of test-sticks over different contact times and determining the optimum sampling times that provides appreciable test-stick performance whilst minimising the turnaround in results. Test-stick response was evaluated over a range of ^{90}Sr activities to demonstrate the capability of test-sticks to distinguish whether ^{90}Sr activity was above or below specific permit limits (i.e. 1 Bq g^{-1} for ^{90}Sr – EPR2016). Diffusion control was also investigated to determine the impact of agitation on test-stick performance. Variable volumes examined whether sample volumes could be reduced from 4 mL and further mobilise test-stick technology. Strontium loading capacities provided insight into extractive resin test-sticks' loading capacities and whether mounting these extractive resins onto test-stick inert supports impacted this. Application of test-stick sampling with different chemical interferences presented insight into the performance of ^{90}Sr test-stick in real-world scenarios. Limit-of-detection and count times for test-stick technology are also discussed.

Chapter 6 describes a fundamental change in approaches to test-stick technology work, looking to utilise numerical simulations using LabVIEW (National Instruments) to provide further insight into test-stick performance. This numeric model was first optimised to test-stick technology by using input parameters derived from experimental work to improve model accuracy. The numerical model provided insight into conditions which would otherwise be difficult to replicate in the lab. These conditions included variable extractive resin loadings and variable sample volumes. Both tests provided insight into possible optimisations of test-stick performance, such as optimal extractive resin loadings. Further numerical models demonstrated the performance of the test-sticks over a wide range of stable Sr concentrations and how this performance may change, or not, due to factors such as changing mass ratios between the solid phase (the test-stick) and the aqueous phase (the sample).

Chapter 7 provides an overall conclusion to the work presented in this thesis and provides possible future work that can be carried out to optimise test-stick technology for field deployment.

Chapter 2 Review of approaches for rapid screening of ^{90}Sr

2.1 Rapid characterisation methods for radiostrontium

Sample preparation and isolation of radiometric species of interest for analysis is fundamental when concerned with alpha- and beta- emitting radionuclides. The nature of these types of radionuclides means that direct analysis is often impossible and radiometric separation and chemical work-up is required. The process of isolating these types of radionuclides has developed over time with increasing efficiency of separation, minimizing loss of species, and improving the time efficiency of this process. An example of this process is strontium separation for the analysis of strontium-90 (amongst other strontium radioisotopes). Historically, strontium purification was achieved by nitrate precipitation using fuming (~90-100%) nitric acid in repeated steps to selectively precipitate strontium nitrate and retain calcium and other ions in solution [28,29]. This method requires use of highly corrosive and hazardous fuming nitric acid and consequent methods looked to optimize this process concerning not only laboratory procedure and manual labor but also the safety risks posed to workers. Subsequent development of size exclusion chromatographic extractants by Horwitz and co. allowed for safer working environments whilst also improving the method for radiostrontium separation [30,31]. This process serves as an example for the pursuit of developing and optimizing radiometric separation techniques, especially for difficult-to-measure (DTM) radionuclides, such as strontium-90.

However, authors have looked to not only offer optimisations to the separation chemistry itself but also the technique as a whole. O'Hara *et al.* presented an interesting screening method combining chromatographic separation with scintillation analysis [32,33]. O'Hara *et al.* outlined the requirement for selective and sensitive sensors, which are required to have low enough detection limits for radiological applications. The solution was a column which would contain both the separation chemistry and the scintillation fluors in polymeric beads which were packed into the column, or in this case a minicolumn presumably to make the method more mobile and practical. The minicolumn was then placed, or somewhat sandwiched, between two photomultiplier tubes – this along with the scintillation fluors in the polymeric beads packed into the minicolumn would form the radiometric detection aspect of this method. Although non-extracted radionuclides (interferents) would produce some form of signal as they moved along the column and in close proximity to the scintillation fluors it was claimed that this would ultimately not affect the final analysis. The radionuclide of interest would build-up in the minicolumn as it continuously adsorbs onto the

polymeric beads eventually giving a steady signal which would become more pronounced than that of the passing interferent radionuclides. Traditionally, delivery of a large volume of sample through a chromatographic column can help increase the sensor's efficiency but as long as the large volume of the sample does not induce breakthrough of the column. O'Hara *et al.* looked to almost do the opposite with their minicolumn as they encouraged the process of breakthrough to reach a point at which the concentration of the analyte departing the column was equal to that of the sample entering the column. In doing so, an equilibrium would form between the sensing materials located within the column with that of the analyte concentration in the mobile phase. Under trace detection levels (which are desirable in this case), the amount of sample captured would be proportional to the analyte concentration. Although the technique seemed promising as a rapid-screening method, it was found to be a largely time consuming process. A derivation of these analysis which measured the controlled in-growth of ^{90}Y (daughter nuclide of ^{90}Sr) was found to take approximately 41.5 hours for the entire analysis, from sample collection to report of results.

An alternative technique to the minicolumn sensor was attempted by Uesugi *et al.* which looked to develop a rapid screening method for application in the Fukushima disaster zone. Uesugi *et al.* suggested a method to minimise the steps and complexity of the standard method used in Japan to analyse for ^{90}Sr, using solid phase extraction disks. As a reference point, the Japanese standard radioanalytical method for analysing ^{90}Sr in edible plant matter can take more than 2 weeks. Which in the circumstances of a nuclear accident (such as Fukushima 2011) or nuclear decommissioning (where the process is both time and financially demanding) this Japanese standard radioanalytical method is unsuitable due to time constraints. The method presented by Uesugi and his co-workers is found to be applicable for seawater samples of up to 1.0 L. Low volume samples require only one Sr Rad disk (the solid phase extraction disk) whilst samples reaching the sample load limit of 1.0 L require the combination of two Sr Rad disks. Sample preparation includes using magnesium phosphate removal followed by hydroxyapatite addition in the presence of citric acid to remove further interferences. Subsequent desorption of the ^{90}Sr from these Sr Rad disk was achieved using diammonium hydrogen citrate mixed with sodium hydroxide solution [34]. Interestingly, Uesugi *et al.* commented that the extraction of ^{90}Sr was highly influenced by changing pH and that increasing citric ion concentration reduced the extraction of ^{90}Sr. However, it must be understood that this method was applied on seawater samples and is therefore not comparative to applications in the nuclear decommissioning environment. Furthermore, the authors noted that Pb and Ba could be persistent interferents and therefore problematic with respect to this technique. Although Uesugi and his co-workers argued that removal of the interferent via citric acid complexation and co-precipitation with barium sulphate, respectively, could resolve this issue. Even so, the authors expressed some difficulty in determining exactly if these interferents, especially Pb, were actually

successfully removed and therefore calls into question the authenticity of these claims. Overall, Uesugi and co. claim that analysis could take approximately one day from sample receipt to analytical results and believe this method to be simple, safe and robust. However, it can be argued that the large volume of steps, reagents to remove interferents and waiting time could compare unfavourably against other published methods such as minicolumn sensors by O'Hara *et al.*

Another approach to analysing for radiostrontium in seawater was undertaken by Tayeb *et al.* Their method consisted of treating seawater samples (approximately 0.1 L) with pH adjustment to a pH of 10 using Na_2CO_3 followed by centrifugation. The supernatant was then discarded whilst the precipitate was dissolved and applied through a double stacked Sr-resin system followed by a DGA-N resin (all produced by TrisKem International™) for sequential separation. The columns are then split, with the double stacked Sr-resin cartridges producing a strontium fraction which is then analysed via Cherenkov radiation for ^{89}Sr and then liquid scintillation assay (LSA) for ^{90}Sr. The DGA-N resin is used to extract Y for LSA analysis. Double Sr-resin cartridges were utilised to minimise Sr loss whilst enhancing separation of Sr from Ba and Ca. Increasing the 8M HNO_3 resin rinsing solution to 30 mL allowed almost complete removal of Ba from the resin cartridges and therefore removal of this interferent. Chemical recoveries attained by this method were high: 85.4 ± 3.3% for Sr and 86.0 ± 9.7% for Y. Authors argue that small sample size (0.1L), simultaneous quantification of ^{89}Sr and ^{90}Sr, quick sample preparation (less than 4 hours for a batch of 10 samples) and the fact that the method detection limit meets the requirements of routine and emergency limits set by Canadian regulations demonstrates the value of this method [35]. Despite the authors claim, both of these methods utilise a whole series of reagents and equipment to achieve analysis with legislative-abiding accuracy. A technique that could minimise the use of multiple reagents and encourage simplicity in the procedure for application in nuclear scenarios where non-specialised personnel could use the technique would be beneficial. These ideals form part of the basis and validity as to why the development of test-stick technology as a viable candidate for rapid-screening of major contaminant radionuclides could be feasible.

Further radioanalytical studies were carried out on radiostrontium content in plant matter by Amano and his colleagues who identified, much like Tayeb and Vos van Avezathe, the need for evaluation and optimisation of standard radioanalytical technique [35–37]. These standard radioanalytical techniques have often been found to be either considerably time consuming or too complex for application in real-word nuclear scenarios such as an accident or decommissioning. Vos van Avezathe and co. claim the Netherlands standard method for analysing edible plant matter to require approximately 56 hours whilst Tayeb *et al.* were able to develop a method that requires only 4 hours to produce results that meet Canadian legislation requirements. Amano and his colleagues have also made similar statements, stating that the Japanese standard analytical method

takes up to two weeks to provide results (Amano et al., 2016). Amano and co. stated further that in the context of fast screening methods this method is unsatisfactory especially in respect to time sensitive applications such as nuclear forensics and nuclear accident responses. Amano *et al.* proposed a method which consisted of dry ashing edible plant matter before extraction with concentrated HNO_3 or 6M HCl, co-precipitation with $Fe(OH)_3$ followed by double oxalic acid precipitation. After this sample preparation was complete, the sample is loaded into an extraction column to obtain the ^{90}Y fraction. The extraction column consisted of a N,N,N',N',-tetra-n-octyldiglycolamide resin known commercially as DGA and provided by the same manufacturer as Sr-resin and TK100 (TrisKem International, 2015a). Measurement of ^{90}Y was carried out using a triple-double coincidence ratio LSC instrument with decay correction being set from the time of ^{90}Y co-precipitation with $Fe(OH)_3$ to the middle of radioactivity measurements. Average counting efficiency of ^{90}Y by LSC was worked out to be 57% and the calculated MDA (minimal detectable activity) for the method was 14 mBg kg^{-1}. The authors argued that the MDA was sufficient for analyses of past atmospheric nuclear detonation effects on edible plant matter as well as for applications for the state of edible plant matter post-2011 after the Fukushima disaster. It was also argued that if U and/or Th was believed to be also present in the edible plant matter that the method could be modified to include the use of TRU resins (also produced by TrisKem International™). The TRU resin is specialised at extracting U as well as Th and their daughter radionuclides, which does not include ^{90}Y (TrisKem International, 2015b). Application of this TRU resin would occur post co-precipitation of ^{90}Y with $Fe(OH)_3$ and just before separation via the DGA resin. This, as argued by the authors, would ensure removal of the U and Th content believed to be in the edible plant matter but still maintain the ^{90}Y for extraction and analysis. Possible presence of ^{91}Y, which is an interferent to the analysis of ^{90}Y, would require a waiting period of approximately 2 years before this method could be applied. Therefore, this method is not applicable under circumstances that include nuclear accidents and is more suitable for environmental monitoring. Total analysis time was 3 days, which makes its classification as a fast screening method debatable but a major improvement over the Japanese standard radioanalytical method nonetheless. However, the work here is valuable as a demonstration of how modifications can be made to a technique to minimise other interferences present in the sample that cannot be removed by the originally developed method. In this case, Amano *et al.* used a TRU resin cartridge prior to the DGA resin cartridge to remove U and Th (as well as their daughter nuclides) from the sample before isolating the Y fraction. Test-stick technology would look to minimise the need for this by using resins which can uptake and isolate the radionuclide of interest, in this case of this project being ^{90}Sr, whilst limiting the retention of non-desirable radionuclides or accounting for these.

Methods for monitoring waste water systems for radionuclide contamination have also been looked into including the WILMA and TAWARA (TAp WAter RAdioactivity Real Time Monitor) systems. WILMA is a system designed by LabLogic Systems, Inc. which utilises a fluid handling system coupled with a scintillation counter for real time measurement of gross alpha and beta emitters. The system uses a proprietary scintillation cocktail and PM tubes to detect the gross alpha/beta emitters. The TAWARA system was developed for detection of radionuclide contamination in wastewater treatment using its EAD (Early Alarm Detector), RTM (Real Time Monitor) and SPEC (Spectroscopy Detector). These three units are comprised of a gamma detector, a scintillation detector and a spectroscopy detector, respectively. Both of these systems demonstrated limits of detection for gross alpha/beta emitters of 370 Bq L^{-1} and 1 Bq L^{-1}, respectively [38,39]. However, both monitoring systems operate on detection of gross alpha/beta emitters and therefore provide limited radionuclide-specific information of the samples. A simple radionuclide-specific screening technique capable of deployment by non-specialists with readily deployable instrumentation is therefore required. [40].

2.2 Extraction technologies

The fundamental aspect of this project that underpins the characterisation performance is the method of uptake – the extractant. The extractant plays a critical role in the uptake of the desired radionuclide and therefore is the primary focus of this project. Previous studies have looked to utilise various extractants from commercially available resins such as SuperLig 620 and TK100 (TrisKem International) to novel extractant resins such as calcium oxalate monohydrate and graphene-based materials. Approaches have even varied in the format of extractants, sometimes referred to as the resin or the extractant chromatographic component of a method, from commercially available extraction disks to scintillation coated polymeric beads [32,34].

Arguably the most well-known and documented chromatographic extractant resin for strontium is Sr-resin [41]. Details of the extractant were first published by Horwitz in 1992 and is based on size exclusion chromatography which separates the species of interest based on ionic radii or sometimes even the molecular size of that species from others. Structurally, it is a 4,4’(5’)-di-t-butylcyclohexano-18-crown-6 with the size exclusion component consisting of the crown ether ring [30,31].

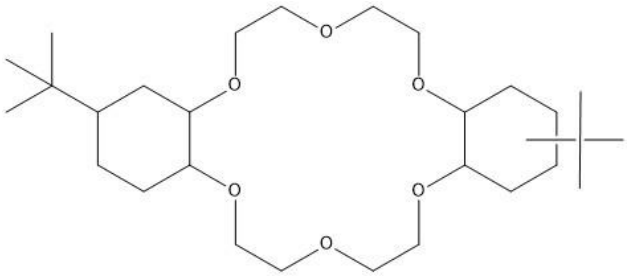

Figure 2.1: Chemical structure of the Sr-resin, with the size exclusion process occurring in the crown ether ring. Cavity size of the crown ether is reported to be between 2.6 and 3.2Å [31].

Sr-resin has seen various applications from radiostrontium isolation in milk to seawater samples as a viable post-disaster method for isolating ^{89}Sr and ^{90}Sr for environmental monitoring [35,42]. The major drawback of Sr-resin, as reported by previous authors, is the extremely acidic range at which it functions optimally, which is equivalent to that of ca. 8 M HNO_3 [40,43]. This may not be problematic for techniques which incorporate sample preparation and acid work-up prior to analysis however these techniques are often lab-based and not suitable for on-site rapid screening. However, handling of this type of acidic media, especially 8 M HNO_3 for example, is unfavourable in nuclear decommissioning where access to on-site radiometric laboratories and specialised personnel is often limited. This is especially true if test-stick technology were to explore its utilisation in nuclear disaster and forensic scenarios where rapid-screening techniques have extremely feasible application. However, Sr-resin was one of the first resins attempted in a test-stick technology format by Warwick and Croudace along with TEVA for ^{99}Tc uptake [40]. This attempt at manufacturing and using test-sticks demonstrated the feasibility and application potential of test-stick technology and provided the initial groundwork for this project. Warwick and Croudace found that for the Sr-resin-based test-sticks there was a strong correlation between the quantity of ^{90}Sr adsorbed onto the test-stick and the initial activity concentration of ^{90}Sr in solution. These findings did indicate that the test-stick concept does work but required further method optimisation and accounting for factors such as competing ions and uptake kinetics.

In 2014, Surman and co-workers published a study into a novel Sr-resin adaptation that had undergone a modification to make up for the drawback of the original crown ether extractant – Sr-resin. Surman *et al.* tested a newly manufactured resin which contained the same extractant as Sr-resin but had been combined with an organic cation exchanger; di(2-ethyl-hexyl)phosphoric acid (HDEHP) [30,31]. This new modified Sr-resin is manufactured by TrisKem International who also manufacture the Sr-resin [44]. This study identified how the TK100 resin works by using HDEHP which exchanges a H^+ ion for the Sr^{2+} and with the strontium ion in the organic phase it can now bind more easily to the crown ether [43]. The only difference between the Sr- and TK100 resins lies in what the crown ether co-exists with; 1-octanol (Sr resin) or HDEHP (TK100). This modification proved

effective as Surman *et al.* showed that the addition of the HDEHP organic cationic exchanger allows the crown ether extractant to operate at a wider range of pH. Using the equation below for data analysis, the D_w (distributed weight coefficient) value was found to be above 10^4 mL g^{-1} for most pH values except 2 (~3300 mL g^{-1}) and 6 (~8800 mL g^{-1}).

$$D_w = \frac{\left[\frac{(A_0 - A_S)}{M_r}\right]}{\left(\frac{A_S}{V_S}\right)}$$

D_w = distribution weight coefficient (mL g^{-1})

A_0 = initial activity in solution (Bq L^{-1} or mg L^{-1})

A_S = final activity in solution (Bq L^{-1} or mg L^{-1})

V_S = volume of the solution (mL)

M_r = mass of the resin (g)

The study carried out analysis using multiple elemental standards such as Sr, Y, U, Pb, Bi, Cs, Co, Ba, Ca, K, Mg, ^{226}Ra and ^{241}Am to demonstrate the performance of TK100 against these species which are commonly found in nuclear decommissioning sites. Additionally, the multi-elemental analysis also looked to monitor the behaviour of the resin in the presence of other species and which elemental species could act as interferents. Ca and K were found to cause the most interference whilst Mg was negligible. Ba was also noted by the authors to not act as an interferent in batch uptake analysis via ICP-MS but radio element uptake analysis showed it was an interferent along with Pb, Am, Bi, U and Y. However, noticeably and importantly for nuclear decommissioning the authors noted a lack of affinity of the TK100 resin for Co or Cs which are both prevalent beta-emitting radionuclides alongside ^{90}Sr. Ionic strength of the media in the form of NaCl content was found to deter the efficiency of strontium uptake by TK100 with increasing NaCl content in the aqueous phase. The capacity of the TK100 resin was also analysed and found to be ~7.7 mg Sr g^{-1}, which was observed to be below its predecessor Sr-resin (27 mg Sr g^{-1}). Kinetic analysis showed TK100 could reach equilibrium in roughly 30 minutes, which was also inferior to its predecessor Sr-resin (around 3 minutes for a 5 M HNO_3 media), but the authors argued that these final two points did not deter greatly the suitability of TK100 for environmental sample analysis. Despite the relatively recent development of TK100, its application in ^{90}Sr uptake has seen limited work and offers an opportunity to look experimentally closer and evaluating TK100 as a potential test-stick active site candidate. Some work has been carried out on TK100 however not all of this work has been specific to ^{90}Sr with some focussing on ^{226}Ra. Russell *et al.* looked to incorporate TK100 to the development of an optimised method for analysing nuclear decommissioning wastes, more

specifically ^{90}Sr, and compare against its predecessor Sr-resin [22]. However, the work carried out by Russell *et al.* looked to use ICP-QQQ-MS as the detector method rather than radiometric such as liquid scintillation counting. Mixed standards of stable Sr and Zr were used to assess the separation capabilities of both Sr-resin and TK100. The Sr-resin exhibited good retention of Sr but poor retention of Zr, whilst TK100 showed good retention of Zr. Russell and his co-workers theorised that the organic cationic exchanger HDEHP was the cause of this as it was the major difference chemically between the Sr-resin and the TK100. Although this is an important factor for mass spectrometric methods due to ^{90}Sr and ^{90}Zr in nuclear decommissioning waste sharing almost identical mass-to-ion ratio (m/z), it is not of great importance to radiometric techniques. Russell noted that TK100 offered an alternative separation method to Sr-resin as it could be used to retain Zr. Therefore, both extractant resins could be potentially incorporated into an optimised lab method for analysing ^{90}Sr along with other sample preparation methods such as hydroxide and carbonate precipitation. Mohamud and her group, including Russell who authored the study just mentioned, used synthesised crown ethers identical to the extractant of both Sr-resin and TK100 [45]. This synthesised extractant was immobilised onto a SiO_2 disk and used to uptake ^{226}Ra. Although this work did not focus on ^{90}Sr it still establishes the potential for TK100 to be used in a multi-extractant system in future work.

Clevasol is another extractant that shows the potential to be adopted into test-stick technology to target ^{90}Sr analysis. Clevasol is an inorganic cationic exchange extractant and therefore has an uptake mechanism that differs greatly to that of TK100 – a size exclusion extractant. Clevasol is a novel inorganic polymer made up of regular boron icosahedron monomers which are then cross-linked to form the ionic polymer $[B_{12}H_{(12-x)}L_x]_n^{2n-}$. The ionic polymer is formed of borane clusters with certain hydrogens (referred to as X in the chemical formula) in the borane cluster replaced with functional groups that influences the number of active sites available for species uptake. These functional groups also introduce a degree of size exclusion but to a lesser extent than that of TK100. Clevasol forms an interesting alternative extractant versus TK100 for application in test-stick technology for ^{90}Sr screening. The product sheet provided by LemerPax has stated Clevasol to have a greater affinity for more positively charged ions ($M^{4+} > M^{3+} > M^{2+} > M^{+}$). This could prove useful for applications in strontium-specific test-sticks where Sr^{2+} could be extracted favourably over other major cations (such as Cs^{+}, for example) [46,47]. Furthermore, the lack of published literatures on Clevasol prior to the start of this project means that working with Clevasol presents an opportunity to present data on this new extractant including its performance in test-stick technology.

Other resins used in previous research for radiostrontium uptake included calcium oxalate monohydrate. Singer and his co-workers looked to utilise calcium oxalate monohydrate, which is also produced by two-thirds of all plant families, for sequestration of Sr^{2+} [48]. Batch-uptake

experiments were carried out over a series of weeks (ranging from one week to ten weeks) and were done within commonly established pH ranges from 4 to 10. Analysis of these batch-uptake experiments, however, were carried out via ICP-MS instead of the more representative radiometric techniques for this project. Interestingly, strontium uptake was found to be independent of pH as well as ionic strength. Further observations were made including the increasing concentration of Ca^{2+} in solution with increasing initial concentration of Sr^{2+}. This observation was suggested by the authors to indicate an almost 1:1 ratio between Ca^{2+} released into solution and Sr^{2+} uptake onto the solid phase (bound with oxalate ligands). Signer *et al.* noted that due to the small increase in oxalate removed from solution at the different pH intervals with increasing initial Sr^{2+} suggests that almost 90% removal of Sr^{2+} from solution was achieved. This value was given considering that oxalate removal increase was almost an order of magnitude smaller than the observed changes in Sr^{2+} and Ca^{2+} concentrations. Singer *et al.* believed that the mechanism for the exchange between the Ca^{2+} and Sr^{2+} from the aqueous to the solid phase was dissolution-reprecipitation and the final solid could be comprised of either a strontium oxalate mixed hydration form ($SrOx{\cdot}nH_2O$, where n = 0, 1 or 2) or a Sr-Ca-oxalate solid solution. EXAFS (Extended X-ray Absorption Fine Structure) analyses were executed and gave strong evidence for the presence of a strontium oxalate mixed hydration form rather than the Sr-Ca-oxalate form. However, the large timescale with which these experiments took place (weeks) is not a favourable feature of this resin when considered for application in rapid screening test-stick technology.

An alternative approach to ^{90}Sr detection is by leaving the sample to stand to allow ingrowth of ^{90}Y ($t_{1/2}$ = 64 hours, $E_{\beta max}$ = 2.28 MeV) and reach secular equilibrium. Yttrium-90 is then analysed via either LSC or Cerenkov counting and the activity of ^{90}Sr calculated from this. Work by Froidevaux *et al.* demonstrated this process whilst using a novel ion imprinted polymer which focussed on ^{90}Y uptake. Despite this ion imprinted polymer focussing on ^{90}Y instead of ^{90}Sr, like previous authors mentioned so far, it demonstrates a possible alternative route for developing ^{90}Sr test-sticks that focus on ^{90}Y uptake instead. Although this process requires an ingrowth period of approximately two weeks it is still a viable alternative method for measuring ^{90}Sr and its applications can include both environmental and site safety monitoring [49].

Interestingly, work has also been carried out on radionuclide separation using graphene oxide-based resins[50]. Several literatures looked to use graphene and both its carboxyl and oxide derivatives as an extractant for clean environmental wastewater treatment [21,51,52]. It must be noted that Mohamud and Sun focused on U(IV) uptake whilst Bubeníková focused on ^{90}Sr however both studies introduce the capabilities and properties of graphene as an extractant. Mohamud *et al.* looked to address the need to develop a rapid and effective treatment method(s) for dealing with aqueous nuclear waste produced in activities relating to the nuclear fuel cycle. Mohamud stated

that the sorption method they introduced demonstrates an alternative wastewater treatment method that exhibits favourable properties such as ease of operation, limited use of solvents and simplicity. It is this same type of advantageous properties which test-stick technology looks to implement to allow ease of field deployment by non-specialised personnel. Graphene oxide (GO) is looked at due to its various intrinsic properties including a wide range of chemical functionalities (including carboxylated GO which was also used by Bubeníková *et al.*) and a very high contact surface area. Surface complexation processes (such as the inner- and outer-sphere surface complexation mechanisms) are what dominate the adsorption of uranyl species onto the GO surface. Mohamud *et al.* looked to study the effect of pH, contact time and the influence or not of competing ions prior to analysis, which in this case consisted of ICP-MS. Synthesis followed a modified Hummer's method which generated the GO from graphite flakes – a method which was also used by Bubeníková *et al.* [53]. Mohamud and company found that the sorption efficiency of carboxylated-GO (GO-COOH) had a gradual increase for pH values up to pH 7 which the authors justified to be due to the negatively charged surface of GO($-COO^-$) (and GO) exhibiting favourable electrostatic interactions with uranyl species (UO_2^{2+}). At higher pH the formation of negatively charged U species (such as $[UO_2(CO_3)_3]^{4-}$) no longer formed favourable electrostatic interactions with the negatively charged GO-COOH surfaces. It was also found that graphite, GO and GO-COOH demonstrated strong sorption efficiencies of 94.3 ± 1.7%, 98.7 ± 1.3% and 88.9 ± 1.9% respectively. Kinetics results showed that high sorption efficiencies were obtained in as quickly as 5 minutes with equilibrium attainment observed at approximately 80 minutes. This study also revealed that both GO and graphite were impacted negatively by competing ions with respect to observed distribution coefficients, however, only GO-COOH was able to retain U consistently. Observed distribution coefficient values of GO-COOH with increasing exposure to competing ions decreased marginally from 4.11 ± 0.1 $x10^3$ mL g^{-1} to 3.72 ± 0.19 $x10^3$ mL g^{-1}. These findings strongly suggest that the presence of carboxylic acid functional groups impacts the selectivity of the sorbent material in a favourable manner. This work presented by Mohamud *et al.* demonstrated the potential in GO-based materials and although this work was carried out for U(IV) species specifically, it also demonstrates the potential this material has for multi-extractant systems which are of strong interest to this project. More importantly, this work promoting the application of GO-based materials as an extractant resin was also backed up with prior work by Bubeníková *et al.* who focussed on ^{90}Sr uptake.

Bubeníková also noted that nanomaterials have higher efficiencies and show faster reaction rates due to their increased surface areas and large number of active sites. Restriction on usage of nanomaterials for wide application has been determined to be due to the complex and costly procedures involved in preparing the nanomaterials. A simple procedure (Hummels' method) for

synthesis of GO and GO-based materials is seen in this study as advantageous for the usage of GO(-based materials) in wastewater treatment applications. GO-based materials also possess biodegradable and non-toxic properties which are viewed favourably for the implementation of GO-based materials in the nuclear industry. However, hydrophilicity of GO-based materials have led to difficulty in recovery of the materials post-wastewater treatment as the GO-based material is found to remain dispersed in the aqueous medium. This factor can be seen as problematic for application in groundwater but it must be noted that the adhesive and/or the method of test-stick manufacture can perhaps avoid this issue. Unlike Mohamud *et al.* who used GO-based materials in bulk, Bubeníková looked to carry out a study into the preparation of nanocomposite GO-based polymeric matrices and applications of these matrices in batch uptake experiments. This approach is highly interesting for this project that also looks to use extractant resin(s) bound onto an inert support rather than in bulk form. Factors that were looked at in these batch uptake experiments included ionic strength, contact time and pH stability. Batch uptake experiments included experimenting with different pH, ranging from ~2 to 10 using NaOH or $HClO_4$ to achieve this. Ionic strength was also studied and different ionic strength solutions were prepared using 0.01 or 0.1 mol L^{-1} $NaClO_4$. Strontium-85 radiotracer was used to analyse and monitor the batch uptake experiments via gamma spectroscopy, which was a useful source of information for this project that also looked to use radiometric detection in test-stick technology post-sampling. Kinetic studies conducted by the authors showed relatively fast sorption by all GO-based polymeric matrices, with equilibrium being reached within 30 minutes. Sorption was found to increase up to pH 6 to 7 before achieving ~97% uptake at higher pHs; which is indicative of the pH stability of the GO and GO-based materials. Changing pH towards lower values caused a pattern of decreasing uptake percentage observed in the order of 15%-weight GO, 25%-weight GO and 15%-weight GO-COOH to ~87%, ~85% and ~80%. Sorption isotherms revealed GO nanocomposites to comply with the Langmuir model, which suggests monolayer adsorption whilst GO-COOH nanocomposites were found to comply with the Freundlich model. Utilising the Langmuir model for both GO-based materials allowed the maximum sorption capacity, q_{max}, to be calculated. GO-COOH was found to hold the highest maximum sorption capacity, which demonstrates that addition of carboxylated functional groups on the original GO surface led to higher adsorption of Sr^{2+}. Work on isotherms shown by Bubeníková was also useful as a reference for isotherm work in this project to determine sorption mechanisms exhibited by the test-stick extractants. This work cements GO-based materials as a viable candidate for future work in strontium-selective test-stick technology. This is of extreme importance as it shows potential for test-sticks in the future to be manufactured with the extractant that is best suited to rapidly screen the radionuclide of interest in a specific setting and/or set of conditions. This is not only advantageous to the credibility of test-stick technology as a rapid-screening technique but also as a characterisation technique that can potentially be adaptable to

various environments. GO-based extractants were not selected for test-stick application due to the need to manufacture in-house the extractant itself whilst both Clevasol and TK100 were both readily available extractants in the lab. However, this should not detract from the potential of GO-based extractants from future applications in test-stick technology as attractive future test-stick extractant candidates.

2.3 Test-stick technologies

Test-stick technology is not a completely novel technique as it has famously seen application in the biomedical field initially for pregnancy test-sticks before being applied in rapid one-step immunochromatographic assays[54]. This project looks to replicate this type of technique but in a nuclear scenario to aid both time and costs the decommissioning process. Warwick and Croudace presented the first step in the implementation of test-stick technology as a viable option for rapid screening analysis in a conference in August 2017 [40]. Warwick and Croudace identified essentially a three-stage process of analysis: manufacture of a compact and optimised extraction system, uptake of contaminant radionuclide of interest and a scintillation-based detection system capable of measuring alpha, high-energy beta and low-energy beta emissions. Their work and others found that traditional methods were unsatisfactory with respect to time efficiency and cost-effective characterisation of nuclear waste [16]. The methodology of this study consisted of five test-sticks prepared with two types of extractant (Sr-resin and TEVA-resin, both provided by TrisKem International) with both extractants manufactured in 100-150 µm particle sizes. Test solutions were prepared by spiking the target solution with known activities of ^{90}Sr or ^{99}Tc. For ^{90}Sr the target solution was 8 M HNO_3 and for the ^{99}Tc the target solution was water at pH 7. This difference in pH conditions was based on the known window of operation of both extractants [31,55]. The test-stick(s) was placed in an unstirred solution for a consistent period of time, then removed and rinsed to remove any leftover adhering solution. Blank test-sticks were also prepared using pre-filter material for comparative analysis. Activities of ^{90}Sr and ^{99}Tc were measured using LSC analysis, with the mass of the resin present on the test-stick being calculated from the measured activity.

Results obtained by the authors found that roughly 4 mg of Sr- and TEVA- (100-150 µm) resins were present on an area of ~1 cm^2; masses included both the resin and the adhesive used to mount the extractant(s). An analogue of Sr-resin with 50-100 µm particle size was also investigated and calculated to have a mass of approximately 2 mg of resin, onto a ~1 cm^2 area. TEVA-resin analysis including the measured activity of ^{99}Tc via LSC analysis found the measured value to be 8.4 ± 0.6 kBq ^{99}Tc per gram of loose TEVA-resin which correlated well with theoretical loading of 8.5 kBq; indicating near quantitative uptake of the ^{99}Tc onto the resin. Calculated uptake coefficient was greater for Sr-SES (50-100 µm) than for Sr-SES (100-150 µm) and even greater for TEVA-SES (100-

150 µm) than either of the latter. Proportionality constants b_t (equation shown below) that were measured were found to be consistent with calculated effective distribution coefficients at equilibrium. The authors state that these findings indicate that the radionuclide partitioning is not thermodynamically controlled, especially because the systems were not mixed. Blank test-stick test showed uptake of the radionuclide on the Sr-SES dip-stick involved active interaction with the extractive resin and not passive physisorption to the test-stick. This factor is important as it demonstrates the extractant, including the type of extractant and particle size of the extractant are all important factors for consideration in the development of these test-sticks.

$$A_{(s,t)} = b_t \cdot [A_{aq}]_0$$

$A_{(s,t)}$ = activity of radionuclide on the dip-stick at time t

b_t = proportionality constant for time t

$[A_{aq}]_0$ = initial activity concentration of the radionuclide in the test solution

The work carried out by Warwick and Croudace essentially laid the foundations as well as the potential that test-sticks have as an effective radionuclide rapid-screening technique. The potential to streamline decommissioning processes especially the characterisation and consequently optimise the segregation of nuclear waste is a major focal point to this project.

A table summarising works carried out by previous authors in the separation and characterisation of radiostrontium as well as studies utilising extractants of interest is shown below. The table outlines target radionuclides, methods and extractant resins used, and summarises the literature used to develop the concepts and methods used in this study, as described in Chapter 3.

Authors	**Radionuclide/s of interest**	**Work-up**	**Method**	**Extractant resin**
Oleg B. Egorov *et al.*, 2006	^{99}Tc, ^{90}Sr, Cr	No consumable reagents. Experimentation consisted of spiking the well water with known amounts of ^{99}Tc, ^{90}Sr and Cr in individual well water sample.	Minicolumn sensor, consisting of a separating column with scintillation beads containing both the separation chemistry and the scintillation fluors in polymeric beads, sandwiched in between two photomultipliers.	AG 4-X4 100-200 (^{99}Tc, Cr), SuperLig 620 (^{90}Sr)
Matthew J. O'Hara *et al.*, 2008	^{99}Tc	Use of fast-flow hydroxylapatite to remove trace organic matter interferents. Remainder of the measurement process consisted of spiking	Minicolumn sensor comprising of a column packed with polymeric beads containing the scintillation fluors and the chromatographic resin. Column is placed between	AG 4-X4 100-200

		groundwater with known and controlled amounts of ^{99}Tc.	two photomultiplier tubes. Further calculations and corrections for scintillation errors applied compared to previous.	
Matthew J. O'Hara *et al.*, 2009	^{90}Y	Acid work-up (3M HNO_3) to remove residual ^{90}Sr followed by usage of solutions such as sodium bicarbonate to induce a higher pH solution to encourage uptake of ^{90}Y by the resin.	Flow cell sensor which utilises a flow cell compiled between two photomultiplier tubes to measure the Cherenkov radiation emitted by ^{90}Y. Also used an automated fluidic layout consisting of pumps and columns with a Cherenkov radiation sensor located at the end of the analytical system.	Superlig 620

Masaki Uesugi *et al.*, 2017	^{90}Sr	Magnesium phosphate followed by hydroxylapatite in the presence of citric acid for the removal of trace organic matter and interferents.	Utilises one to two solid phase extraction disks (termed "Sr Rad disks") to extract the ^{90}Sr, followed by desorption of the ^{90}Sr using diammonium hydrogen citrate and sodium hydroxide solution. Subsequent analysis carried out via liquid scintillation analysis. "Sr Rad disk" is based on the HDEHP extraction method.	Sr-rad disks (solid phase extraction disks)
Mária Bubeníková *et al.* 2018	^{90}Sr	Preparation of GO-based nanocomposite polymeric material. No work-up specific to the sample indicated by the authors.	Application of GO (graphene oxide) based materials, such as GO-COOH (carboxylated graphene oxide) coated onto two different polymeric inert	Graphene oxide-polymeric matrix. Polystyrene and PA66 matrix, covered with graphene (GO – oxidised graphene, and GO-COOH –

			supports, such as polystyrene and PA66. Adsorption of Sr(II) ions onto the surface of said nanocomposites. Wastewater treatment.	carboxylated graphene oxide).
H. Mohamud *et al.* 2018	U(IV) e.g. UO_2^{2+}, $[UO_2(CO_3)_3]^{4-}$	Preparation of GO and GO-COOH using modified Hummers' method including work-up to form GO-COOH and purifying. No indication of possible sample preparation required prior to sorbet material application.	Simple application of graphite, GO and GO-COOH in experimental conditions that looked to study the effects of pH, competing ions and kinetics of sorbent materials with look towards applications in wastewater treatment.	Graphene-oxide and GO-COOH sorbent material. Graphite also investigated and used for comparative purposes. No inert support required.
David M. Singer *et al.* 2008	Sr(II)	Preparation of calcium oxalate monohydrate using a technique which was	Cationic exchange system in which the already-present Ca^{2+} in the oxalate system	Calcium oxalate monohydrate

		previously established by another study.[1]	displaces Sr^{2+} in the solution, releasing Ca^{2+} into the aqueous media in the process. A strontium oxalate with water of crystallisation product is formed ($SrOx \cdot nH_2O$) in this process.	
J.J. Surman *et al.* 2014	$^{89, 90}Sr$	Minimal work-up as study is carried out with laboratory prepared samples. Consists of spiking milli-Q water based samples and some acidified samples. Spike samples with a range of both stable and active isotopes of elements present in nuclear environments.	Modify existing strontium-selective extractant resin (Sr-resin) with organic cationic exchanger instead of 1-octanol as is present in the Sr-resin. New resin is then tested for uptake under different pH, ionic strength media and presence of different both stable and	TK100 resin

			active species to identify possible interferents.	
E. Kabai *et al.* 2011	$^{89, 90}$Sr	Isolation of fat and proteins via protein precipitation followed by oxalate complexation to co-precipitation strontium along with the remaining alkaline earth metals. Final step involves using extractant chromatography to isolate the strontium fraction.	Use 2,2,2-trichloroacetic acid to separate the fat and protein from the milk to produce the clean filtrate containing the strontium. Oxalic acid is added to the clean filtrate and pH adjusted to 5-6 to precipitate out the alkaline earth metals including strontium. Sr-resin is then used to isolate the strontium fraction via multiple washes of 3M HNO_3 and deionised water.	Sr-resin

H. Amano *et al.* 2016	^{90}Sr, ^{90}Y	Dry ashing edible plant matter before extraction with concentrated HNO_3 or 6M HCl. Iron hydroxide co-precipitation of yttrium is carried out before double oxalic acid precipitation.	After sample preparation is complete, the oxalic acid precipitation of yttrium amongst other elements is then placed through a DGA resin which separates out the elements to obtain the ^{90}Y fraction. This fraction is then analysed by triple-double coincidence ratio LSC instrument for Cherenkov counting. TRU resin can also be implemented before the DGA resin to remove suspected U and Th isotopes from the sample.	DGA resin

M. Tayeb *et al.* 2016	^{89}Sr, ^{90}Sr, ^{90}Y	Firstly, adjust pH of sweater sample (0.1L) to 5-6 and add Na_2CO_3 followed by centrifugation. Precipitate is collected and sequential extractant chromatography is applied.	Post-sample preparation, the sample is passed through a double-stacked Sr-resin cartridges and one DGA-N cartridge before the cartridges are split into two groups. One contains the double-stacked Sr-resin cartridges and elutes both ^{89}Sr and ^{90}Sr for LSA analysis. Whilst the second groups consists of the DGA-N cartridge and is used to elute ^{90}Y for Cherenkhov counting.	Sr-, DGA-N resins
A. Vos van Avezathe *et al.* 2015	^{90}Sr, ^{90}Y	Sample (which is fresh produce such as spinach and beetroot) is simply grinded	Method 1: consists of grinding the sample, microwave digesting the	No resin.

		before being put through one of three methodologies.	sample and then analysing via Cherenkov counting. Method 2: consists of grinding the sample, microwave digesting, evaporating the sample and then analysis via LSC. Method 3: Sample is grinded before being mixed with the scintillation cocktail in a gel media before direct analysis via LSC.	
Warwick *et al.* 2017	^{90}Sr, ^{99}Tc	Samples were milli-Q water and spiked with ^{99}Tc. Samples were also prepared in 8M HNO_3 and spiked with ^{90}S.	Test-sticks prepared using cellulose acetate, adhesive and TEVA (for ^{99}Tc) or Sr-resin (for ^{90}Sr) were submerged into the sample for up to 60	Sr-, TEVA resins

			minutes. Test-sticks were then removed from the sample, washed and placed into a scintillation vial along with scintillation cocktail. The test-sticks were then counted via LSC.	

Chapter 3 Methodology

3.1 Reagents and materials

Stable strontium solution was prepared using $SrCl_2 \cdot 6H_2O$ (May & Baker, London, UK) dissolved in 3 M HNO_3 before being dried down and then made up to 1000 ppm stock solutions for experiments. Aqueous samples containing ionic interferences were prepared from analytical grade $MgSO_4 \cdot 7H_2O$ (BDH Chemicals Ltd., Poole, England), $KHCO_3$ (BDH Chemicals Ltd., Poole, England), $CaCl_2 \cdot 2H_2O$ (Acros Organics, New Jersey, USA) and $NaHCO_3$ (Fischer Scientific, Loughborough, UK). Radiotracer used was ^{90}Sr (AEA Technology QSA, Germany) and all other reagents including acids were sourced from Fischer Scientific, Loughborough, UK unless specifically stated otherwise. SprayMount™ (3M, UK) adhesive was used in test-stick manufacture.

3.2 Resins and reasons

Extraction materials used in this project included both TK100 from TrisKem International and Clevasol from LemerPax. TK100 was selected due to being a size exclusion extractant and an industry standard in extracting ^{90}Sr as well as having the capability to operate at neutral pH compared to its predecessors (such as Sr-resin from TrisKem International). Clevasol represents an extractant that operates differently to that of TK100 by opting for a cationic exchange mechanism instead of size exclusion. This difference in uptake mechanism between extractants can be used to demonstrate test-stick technology's capability to operate using different types of extractant. Clevasol is an extractant originally designed for water treatment and therefore also presents an extractant with a much higher ^{90}Sr capacity (243 mg g^{-1}) compared to TK100 (8 mg g^{-1}).

3.3 Procedures

3.3.1 Batch uptake experiments

Five solutions of variable concentration of stable strontium were prepared from a 1000 ppm stable strontium stock solution into 4 mL aliquots per experimental run. Each solution was spiked with ^{90}Sr and the test-sticks were then immersed into the samples for approximately 60 minutes. Agitation is carried out during this 60-minute sampling period depending on the objectives of the specific experiment. The test-stick(s) were then removed from the samples, washed, cut into 22 mL scintillation vials and 20 mL of scintillation cocktail was added. The samples were then placed into LSC instrumentation and counted for 60 minutes. This experimental procedure was carried out for

both TK100 and Clevasol test-sticks. In some experiments, where stated, a 1 mL aliquot of the aqueous phase post-sampling time was taken, added into a 22 mL scintillation vial and 19 mL of scintillation cocktail was added. These samples were also counted for 60 minutes.

3.3.2 Test-stick manufacture

Cellulose acetate sheets were cut into ~1 cm wide and approximately 4 cm length strips and each cellulose acetate strip tip was coated with a spray adhesive. The adhesive coated-acetate sheets were manually coated uniformly with TK100 and left to stand for 24 hours. This allowed the adhesive to set and prevent degradation of the extractant resin during sample submersion. The area of the test-stick that was coated with spray adhesive prior to resin coating was ~1 cm^2. This procedure was also replicated for the manufacture of the Clevasol test-sticks (figure 3.1).

3.3.3 Extractive resin mass loadings

Extractant resin was tagged with a radiotracer to establish the mass of extractant loaded on the test-sticks for both TK100 and Clevasol. Extractant (100 mg) was mixed with approximately 0.130 kBq of ^{90}Sr and equilibrated for 60 minutes before being vacuum filtrated. The extractant was then collected and dried for 24 hours. After this, the extractant was weighed into four vials containing 5, 10, 15 and 20 mg of the ^{90}Sr-tagged extractant resin(s). The remaining extractant resin was then used to prepare test-sticks. The test-sticks active sites (~1x1 cm) were then cut from the test-sticks themselves, transferred into 22 mL scintillation vials and 20 mL of scintillation cocktail was added. The calibration standards were added directly into 22 mL scintillation vials and 20 mL of scintillation cocktail was added. Analyses were carried out via LSC instrumentation with count times of 30 minutes. This procedure was applied to both TK100 and Clevasol. Gravimetric analysis of test-sticks was also carried out by weighing the individual test-stick inert support prior to test-stick manufacture. Once the test-stick manufacture had completed, the test-sticks were weighed again, and the mass of the individual test-stick inert support and the final manufactured test-stick were then compared to obtain the mass of the extractive resin.

3.3.4 Uptake kinetics

Kinetic studies consisted of submerging test-sticks into a series of samples (seven to twelve), each spiked with approximately 5.0 to 10.0 Bq of ^{90}Sr in milli-Q water. The test-sticks were submerged into the samples for different time intervals; 5, 10, 15, 20, 40, 60 minutes and 24 hours with later experiments including additional samples at 1-, 2-, 30-, 50-minutes and 48- and 72-hour time intervals. The test-sticks were then removed, washed with milli-Q water, cut into 22 mL scintillation

vials and 20mL of scintillation cocktail was added. LSC instrumentation analyses were then carried out with count times of approximately 60 minutes. Aliquots of the aqueous phase for each sample was also taken of approximately 1 mL, added into a 22 mL scintillation vial along with 19 mL of scintillation cocktail, and counted for 60 minutes. This procedure was repeated for both TK100 and Clevasol.

3.3.5 Other experiments

For other experiments pertaining to changing variables such as sample volume, acid spiking and diffusion control the experimental procedure followed similarly to that of the protocol set out in section 3.3.1. as well as that graphically presented in the following figure (figure 3.1).

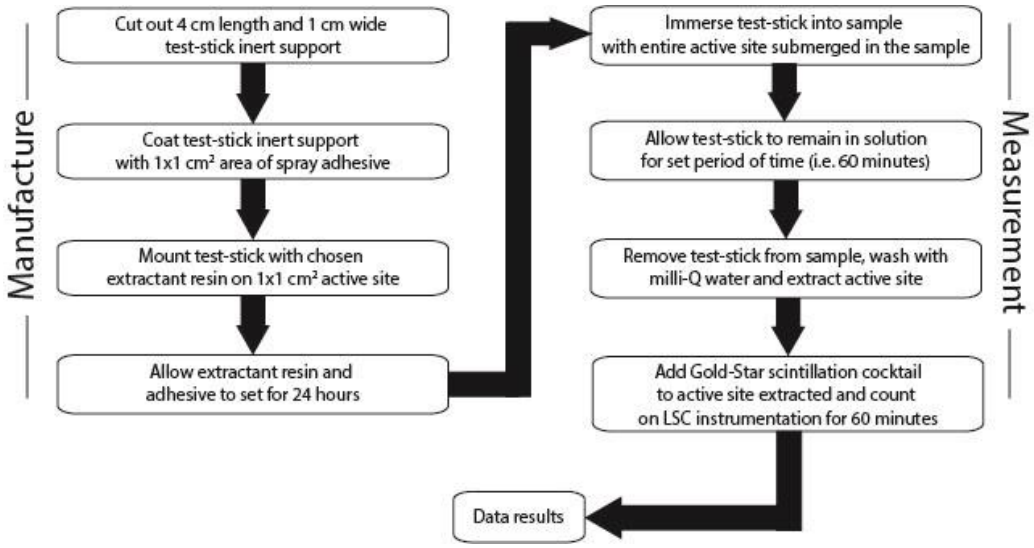

Figure 3.1: Flow chart demonstrating the typical methodology of test-stick technology from manufacture to data acquisition. Changes to some steps may have occurred such as changing the active site area from 1x1 cm^2 to a variable surface area to investigate the effect of this on the performance of the test-stick(s).

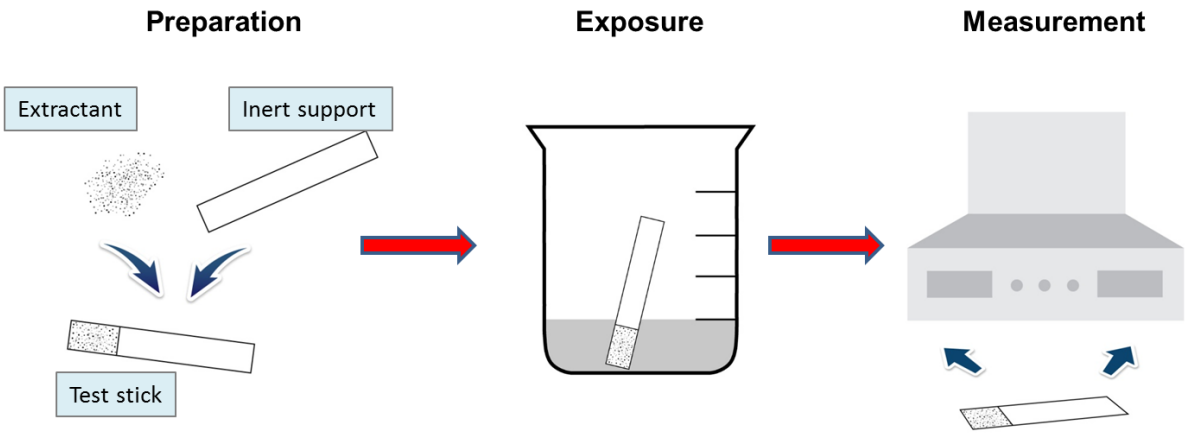

Figure 3.2: Diagram demonstrating the simplicity and systematic procedure to test-stick technology. Preparation step can be referred to as the "Manufacture" phase shown in figure 3.1. Both the 'Exposure' and 'Measurement' steps can also be referred to in the same previous figure (figure 3.1) as the "Measurement" phase of the procedure.

The table below summarises comparatively the different types of experiments carried out:

Table 3.1: A list and comparison of the different types of batch uptake experiments carried out including some of the differences in experimental variables between experiments.

Experiment name	Extractant/s	Sampling Time (mins)	Agitation	Aqueous phase	Approximate surface area
Strontium loading/capacity (bulk phase and test-stick)	TK100, Clevasol	60	No	Milli-Q water with 0.01, 0.1, 1, 10 and 100 ppm ^{88}Sr.	1x1 cm^2
			Yes	Milli-Q water with 0.01, 0.1, 1, 10, 100, 200, 500, 700 and 1000 ppm ^{88}Sr. The added solutions with 200, 500, 700 and 1000 ppm ^{88}Sr were carried out for Clevasol test-sticks only.	
Mass loading	TK100, Clevasol	-	-	-	1x1 cm^2

Uptake kinetics	TK100, Clevasol	5, 10, 15, 20, 40, 60 and 1440 (24 hours) mins.	Yes	Milli-Q water.	1x1 cm^2
		1, 2, 5, 10, 15, 20, 30, 40, 50, 60, 1440 (24 hours) and 4320 (72 hours) mins.	Yes		
Particle size effect	TK100 (50-100 and 100-150 µm), Clevasol	60	Yes	Milli-Q water.	1x1 cm^2
Chemical interferences	TK100, Clevasol	60	Yes	Milli-Q water, Ca, Na, K and Mg.	1x1 cm^2
Test-stick response	TK100, Clevasol	60	Yes	Milli-Q water spiked with 0.1, 1.0, 10, 100 Bq ^{90}Sr.	1x1 cm^2
				Milli-Q water spiked with 10, 30, 50, 70 and 100 Bq ^{90}Sr.	

Test-stick diffusion control	TK100, Clevasol	60	No	Milli-Q water spiked with variable ^{90}Sr (0.1, 1.0, 10, 100 Bq)	1x1 cm^2
			Yes	Milli-Q water spiked with 0.1, 1.0, 10, 100 Bq ^{90}Sr.	
Surface area	TK100, Clevasol	60	Yes	Milli-Q water with variable ^{90}Sr (0.1, 1.0, 10, 100 Bq).	0.8, 1.2, 1.4, 1.8 and ~2.0 cm^2.
Variable volume	TK100, Clevasol	60	Yes	Milli-Q water with variable ^{90}Sr (0.1, 1.0, 10, 100 Bq). Volume of aqueous phase controlled to approximately 1.0, 1.5, 2.0, 3.0 and 4.0 mL.	1x1 cm^2

Reproducibility	TK100, Clevasol	60	Yes	Milli-Q water with constant ^{90}Sr activity (approximately 100 Bq). Volume of aqueous phase also kept constant and 5 experimental repeats were set up per extractant test-stick.	1x1 cm^2
Durability	TK100, Clevasol	60	Yes	Milli-Q water with constant ^{90}Sr activity (approximately 10 Bq). Volume of aqueous phase also kept constant and test-sticks were allowed to sit for approximately 4 weeks	1x1 cm^2

				prior to experiment. Normal wait time is 48 hours.	

3.4 Instrumentation

3.4.1 Radiometric techniques

Liquid scintillation counting was carried out in this project to analyse the test-sticks post-sampling to determine whether uptake of the desired radiochemical species was successful and by how much. Liquid scintillation counting was carried out on a PerkinElmer 1220 Ultra Low Level Liquid Scintillation Spectrometer (PerkinElmer, Waltham, MA, USA) set to low coincidence bias, 14C (high energy beta) configuration and 60 minute count times unless stated otherwise. Gold Star (Meridian Biotechnologies Ltd, Epsom, UK) liquid scintillation cocktail was added to samples prior to LSC analysis. WinQ data acquisition software was used for LSC data processing

3.4.2 Other instruments

Scanning electron microscopy analysis of different resins were carried out using a Leo 1450VP SEM (Zeiss, Oberkochen, Germany) and an Oxford Instruments X-Act 10 mm2 area SDD EDS Detector. Software used to run this equipment was an Aztec Energy software system (Oxford Instruments, Oxfordshire, UK).

3.5 Simulations and computational modelling

Simulations were carried out on LabVIEW 2015 (National Instruments UK, Newbury) using ODE (ordinary differential equations) solver VI to solve sets of differential equations that monitored a change in one specific variable (such as initial concentration, volume and/or mass) against another variable such as time. The coding had been developed prior to this project by another project and the code was originally used to predict behaviour of the analyte in batch experiments and later developed for column conditions [56,57]. The simulations monitored and predicted the performance of different extractants under these two experimental conditions. Runge-Kutta 45 (variable) was the continuous solver used to evaluate the differential equations in the code that dealt with calculating changing in concentration with respect to time from the input forward and back rate constant (*k*) values.

The extractant used in these simulations was TK100 100-150µm. Input values for the code were updated to match the conditions of these experiments including loading mass, density and volume. The code calculated forward and backward *k* values for analyte movement between the lumped solid phase (the extractant on the test-stick during sampling) and the aqueous phase (the sample). However, the code also introduced a modification for unstirred experiments where the aqueous

phase was split into a surface layer phase and a bulk phase with a mass transfer constant added. Simulations for agitated experiments did not require this modification and therefore maintained the default lumped solid and aqueous phases. Calculated forward and backward '*k*' rate constants were derived from experimental data carried out in this project and provided the basis for the simulation to run. The simulation was looped until the experiment had achieved 'equilibrium' in which the concentration of ^{90}Sr in the solid phase (known as lumped solid concentration) between simulation iterations was less than a specificed value or until stopped by the user. Upon completion of the simulation, a .CSV file is produced which provides time (in seconds), concentration in lumped solid phase (Bq mL^{-1}) and in aqueous phase (Bq mL^{-1}) and these values used to calculate activity (either in Bq or/and in Bq g^{-1} if the density of the extractant is known) on the test-stick with respect to time. Distribution coefficients can then be calculated from these factors as well as from running multiple simulations in which input parameters are varied.

Chapter 4 Assessment of test-stick production and properties underpinning this process

4.1 Abstract

Nuclear site decommissioning is underpinned by robust radioanalytical waste characterisation and therefore the UK and European nuclear industries are investing in research into next generation characterisation technologies to meet the increasing demands for efficient waste characterisation. Test-stick technology aims to characterise significant non-gamma emitting radionuclides such as ^{90}Sr using an approach that is readily deployable by non-specialists. Strontium-90 has been identified as one of the major radionuclide contaminants in nuclear decommissioning due to its high fission yield and pure beta-emitting properties. This study investigates the application of test-stick technology for screening of ^{90}Sr in aqueous samples and evaluate factors involving test-stick manufacture that impacts test-stick performance including surface area, extractant particle sizes, reproducibility, and durability. The extractants investigated in this study include a commercial extractant TK100 (TrisKem International, France) and a novel extractant Clevasol (LemerPax, France) which were selected for their ability to extract ^{90}Sr at near neutral pH conditions. This makes them suitable for a wide number of applications including groundwater screening. The comparison of both extractants serves to provide insight into the flexibility of test-stick technology to adopt other extractants despite contrasting uptake mechanisms; TK100 (size exclusion) and Clevasol (cationic exchange). This rapid screening approach provides potentially significant advantages over time and financial constraints through on-site deployment for the initial identification and characterisation of ^{90}Sr.

4.2 Introduction

The UK is currently undergoing a large-scale decommissioning programme led by the NDA (Nuclear Decommissioning Authority) to manage the UK's civil nuclear legacy and remediate its nuclear sites. Current estimates place the cost to complete this project at over £100 billion and a duration of more than 100 years [7,58]. The complexity of this challenge lies in the diversity of the nuclear legacy spread across the UK, from the helium-cooled DRAGON reactor in Winfrith to the fast-breeder reactor in Dounreay. The most notable challenge for the NDA is Sellafield as it contains a plethora of different nuclear facilities including power stations and nuclear fuel reprocessing plants [7,59]. The decommissioning approach comprises a step-by-step process consisting of removal of the nuclear fuel followed by dismantling of buildings and other structures with low contamination. Upon

achieving this the focus of the decommissioning process shifts to the reactor itself and the surrounding (more) highly contaminated structures [60,61]. Throughout this procedure characterisation of nuclear decommissioning waste is essential to waste segregation and sentencing. The NDA has subsequently identified the need to develop technologies and methods that could meet these complex technical challenges and streamline the project in terms of cost and delivery time. Characterisation of materials is fundamental in underpinning the decommissioning and associated waste sentencing with an emphasis on in-*situ*/on-site characterisation methodologies. The NDA baseline has identified and promoted the development of rapid screening technologies to complement off-site laboratory sample analysis [9]. Previous studies had also highlighted the need for deployable mobile laboratory systems to aid in both nuclear forensic and decommissioning scenarios [19]. Development of gamma-emitting screening techniques have already been routinely implemented at sites such as Harwell and are used in conjunction with scaling factors. These scaling factors are based on sampling and measurement of specific and designated areas of the decommissioning site. Scaling factors, also known as "finger-prints", provide information about the presence of difficult-to-measure (DTM) radionuclides, for example ^{90}Sr, using calculated ratios between these DTM and easy-to-measure (ETM) radionuclides [13,17]. Despite this, deployment of on-site screening techniques for alpha- and beta-emitting radionuclides are not routinely undertaken, including techniques to monitor scaling factor stability.

On-site and automated screening of ^{90}Sr has been previously attempted using minicolumn sensors which combine separation chemistry with detection via scintillation[32,33]. This technique involves passing the aqueous sample through a minicolumn which detects the activity of ^{90}Sr via the column solid phase consisting of beads of a polymeric matrix with fluors imbedded which act as scintillators. Photomultiplier (PM) tubes placed either side of the column then detect this scintillation process and data collection is carried out by a computer system connected to the PM tubes. This is an interesting approach which achieves detection limits of 0.3 Bq L^{-1} for >0.2 L samples but requires substantial set-up which site operators would be unlikely to carry out. Other methods have included utilising on-site wastewater monitoring systems such as WILMA (LabLogic systems, Inc, UK) and TAWARA (TAp WAter RAdioactivity Real Time Monitor) as an option however both these systems operate on detecting gross alpha/ beta emitters and therefore provide limited radionuclide-specific information of the samples. Rapid screening techniques would require techniques which would be capable of providing radionuclide-specific information including whether the activity of this specific radionuclide, such as ^{90}Sr, is above or below specific legislative thresholds. The NDA has outlined objectives for rapid screening techniques to be developed with quick turnover of results and easy data manipulation. These objectives, which were also outlined by the NDA in a recent report, include carrying out majority of initial characterisation in-*situ* with turnover of results achieved

within 24 hours[10]. Therefore, rapid screening techniques must also contain a degree of mobility to facilitate these objectives as well provide results quickly.

Test-stick technology is a viable technique to meet these objectives set out by the NDA by providing a mobile rapid screening technique with targeted turnover in results within the space of a few hours. However, before the potential of test-stick technology in rapid screening can be explored the fundamental components of test-stick production must first be investigated. Using the current test-stick manufacturing technique, determination of factors such as mass loadings, active site surface area and particle distribution on the uptake performance will provide information regarding the efficiency of the current test-stick manufacturing process. Additionally, work on test-stick durability will provide further information regarding shelf-life of test-sticks as well as their performance variability over time. This investigation will also set out the guidelines for future test-stick manufacture developments to meet in order to maximise test-stick performance for rapid screening of specific radionuclides.

Performance of the test-sticks will be measured using a partitioning constant, k', to evaluate the performance of the test-stick

$$\left(\frac{A_s}{A_{aq}}\right) = k' \times \left(\frac{M_s}{M_{aq}}\right)$$

Where, A_s is the activity of the species on the solid phase (test-stick) in Bq, A_{aq} is the activity of the species on the aqueous phase in Bq, M_{aq} is the mass of the aqueous phase in g, M_s is the mass of the solid phase in g and k' is the partition coefficient. The k' constant describes the partitioning of the species in question, in this case ^{90}Sr, between the solid and aqueous phases for test-stick technology. This k' value relates to the partitioning at a given exposure time and does not assume equilibrium as this is not realistic for test-stick technology that looks to target rapid screening (<24-hours) applications. The selected extractants for this work are TK100 and Clevasol that represent contrasting approaches to ^{90}Sr uptake. TK100 is based on an industrially standard crown ether extractant that is specialised in selectively targeting ^{90}Sr but also uses an organic cationic exchanger di(2-ethyl-hexyl) phosphoric acid (HDEHP) to facilitate Sr extraction at more neutral pH conditions. The addition of this organic cationic exchanger HDEHP allows for crown ether extractants to be applied to groundwater samples without the addition of concentrated (8 mol dm^{-1}) HNO_3 as required by its predecessor, Sr-resin. Alternatively, Clevasol is a novel cationic exchange extractant based on a borane polymer that was originally developed for wastewater treatment and therefore contains a high capacity (243 mg g^{-1} for ^{90}Sr) compared to TK100 (8 mg g^{-1}). A comparison between the properties of the two extractive resins and their impact on test stick performance will be undertaken.

4.3 Methodology

4.3.1 Test-stick manufacture

The test-sticks were manufactured according to the method described in section 3.3.2. An industrial spray adhesive was used to bind the extractive resin onto the test-stick inert plastic support forming an approximately 1x1 cm^2 active area. The test-stick was allowed to set for a period of time (24 to 48 hours) in a dark container. During this period of time the test-sticks were placed into air-tight containers to prevent any contamination from the air or sunlight which may affect the extractant and that could potentially impact test-stick performance. This waiting period also allowed the adhesive to fully set and reduce the risk of the adhesive breaking down during sample submersion and therefore causing test-stick failure.

4.3.2 Test stick performance assessment

Scanning electron microscope (SEM) analysis determined the physical distribution of the extractive resin onto the test-stick. SEM data were analysed using image processing software ImageJ™ which applied enhanced contrast (saturation) of 2.0 to 8.0% to emphasise the contrast between light and dark in the SEM images to improve saturation cover percentage calculations. Saturation cover percentage calculations were then carried out using ImageJ™ before this data was then transferred to Excel and the final surface coverage percentages were calculated. See section 3.4.2. for further details

Mass loading experiments involved radiolabelling the extractants with ^{90}Sr before different extractant masses were weighed out and measured via LSC. The remaining radiolabelled extractant was used to manufacture test-sticks (see section 4.3.1.) which were then also measured via LSC. This analysis measured the activity of ^{90}Sr associated with different extractant masses and then correlated with the mass of the extractant mounted onto the test-stick. A different method was also approached for obtaining the mass of the extractive resin using gravimetric analysis. Gravimetric analysis involved weighing the individual test-stick inert support followed by weighing the final manufactured test-stick and comparing these two masses to obtain the mass of the extractive resin on the test-stick. Please see section 3.3.3. for more details of both methods.

The effect of surface area on test-stick performance was investigated by preparing a series of test-sticks with different surface areas – approximately ~0.8, 1.2, 1.4, 1.8 and 2.0 cm^2. This was prepared for both TK100 and Clevasol test-sticks. See section 3.3.5. for further details.

Particle size effect was evaluated for on test-stick performance where different extractant resins with different particle sizes were utilised. TK100 was selected due to availability of different particle sizes for this extractive resin whilst maintaining the same composition of the extractant (4,4'(5')-di-t-butylcyclohexano-18-crown-6) and the organic cationic exchanger HDEHP. TK100 test-stick with 50-100 µm and 100-150 µm particles were evaluated to determine the impact of the particle size on test-stick performance. Please refer to section 3.3.5. for the full procedure.

Reproducibility of the test-sticks was investigated by preparing five test-sticks and all five test-sticks screened identically prepared solutions to compare the k' values obtained between all five test-sticks. This procedure was carried out for both TK100 and Clevasol extractive resins and the full procedure can be found in section 3.3.

Durability experiments were similar to that of the reproducibility experiments where five test-sticks were prepared before screening the same sample to compare the k' values achieved between all five test-sticks after. However, before these test-sticks experiments were carried out the test-sticks were allowed to stand in an airtight container for approximately four weeks. This procedure was carried out for both TK100 and Clevasol extractive resins. Further information regarding the experiment procedure can be found in section 3.3.

Experiments were carried out via batch-uptake experiments with sampling times of 60 minutes, unless stated otherwise. After sampling was complete, test-sticks were then placed into separate 22 mL scintillation vials along with 10 to 20 mL of Gold Star scintillation cocktail and counted via LSC for approximately 60 minutes, unless otherwise stated. The full procedure is described in section 3.3.1.

4.3.3 Data analysis and processing

Data collection on LSC instrumentation was achieved via WinQ data acquisition software which provided data in CPM (counts per minute). These data were then extracted and analysed on Excel™ where ^{90}Sr activity was calculated whilst considering counting efficiencies and ^{90}Y ingrowth. Counting efficiencies were determined to be 95% for both ^{90}Sr and ^{90}Y from QC (quality control) data and ^{90}Y ingrowth determined from recording the time of separation (when the test-stick was removed from the sample) and the time of measurement (provided by registry files produced by WinQ software). Using count times which were two weeks apart from the time of separation allowed for secular equilibrium to be established and therefore there was no requirement to account for ^{90}Y uptake by the test-sticks. All graph plots were carried out on SigmaPlot™ graph plotting and statistical software.

4.4 Results and discussion

4.4.1 Test-stick manufacture

Test-sticks were manufactured onto the plastic inert support of the test-sticks by binding the extractive resin of choice, either TK100 or Clevasol, onto this support using a spray adhesive. The test-stick manufacturing process looks to implement an 'easy-to-use' and simple principle to the manufacture of the test-sticks. This provides the potential for the test-stick manufacturing to be easily modified to meet the demands of the customer. This includes controlling the extractive resin mass loadings to improve radionuclide uptake kinetics or lowering the manufacturing costs whilst still obtaining test-stick performance where results turn around is obtained within 24 hours. These principles will be discussed throughout the next few chapters. Current test-stick dimensions are 4x1 cm^2, where the extractive resin is bound onto the edge of the test-stick in a 1x1 cm^2 active site. A further advantage of constraining the active site to a 1x1 cm^2 surface area allows to further control the extractive resin mass loadings. These test-stick dimensions were chosen as the test-stick experiments are currently carried out inside 5 mL cryogenic tubes, which promote mobility of the technique, with ~4 mL sample volume. The sample volume was chosen to match the 5 mL container whilst allowing ~1 cm of room on the top for test-stick removal. The remainder of the test-stick (3x1 cm^2) provides a non-active component to handle safely the removal of the test-stick from the sample. This test-stick manufacturing process and design forms the baseline for future experimental work to optimise and therefore improve the performance of the test-sticks, including sample volume, surface area and particle size effect.

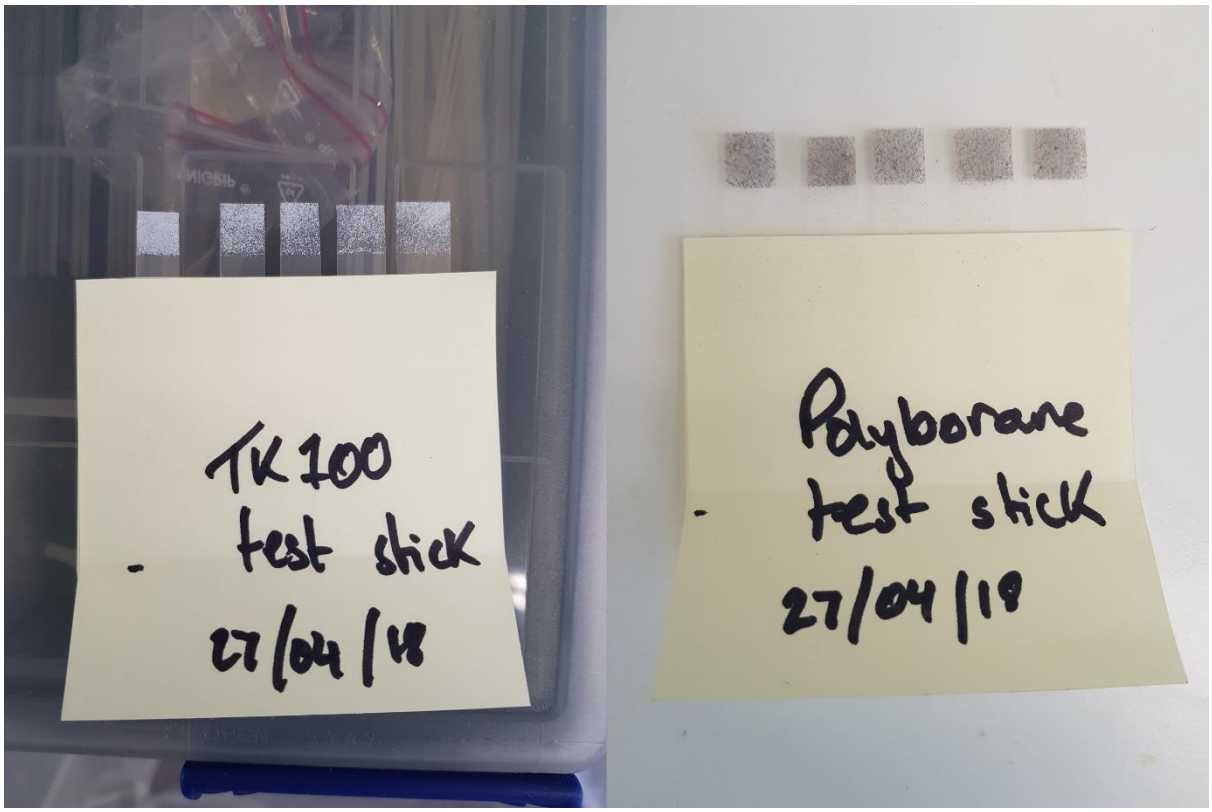

Figure 4.1: Manufactured test-sticks. The post-it notes were used to maintain the test-sticks in place whilst the adhesive set. Post-it notes were also used to control the active site area whilst spray adhesive and extractive resins were applied onto the test-stick inert support during manufacture.

4.4.2 SEM analysis of surface coverage

SEM analysis provides helpful insight into the spatial distribution of the solid phase onto the test-sticks' support and provides information regarding the physical appearance of the TK100 and Clevasol extractant particles. SEM analysis provides not only qualitative information regarding the test-stick solid phase but can also be used to calculate surface coverage percentage to better understand how spatially efficient the current test-stick manufacture procedure is.

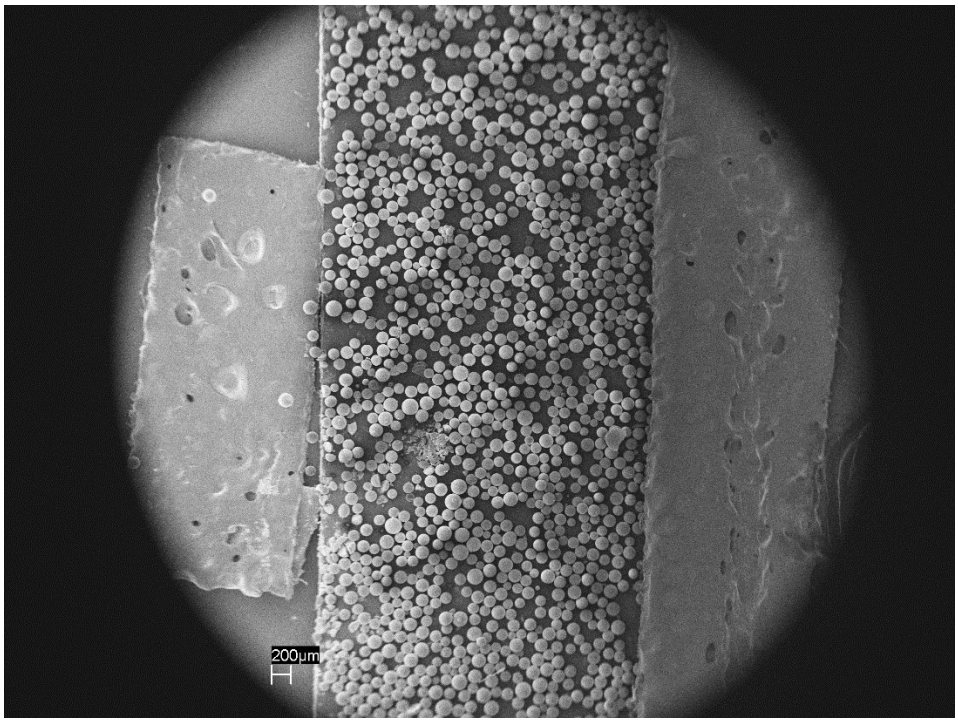

Figure 4.2: SEM image of the active site of the 100-150 µm TK100 test-stick demonstrating the extractant spread and binding. (Magnification: 45x)

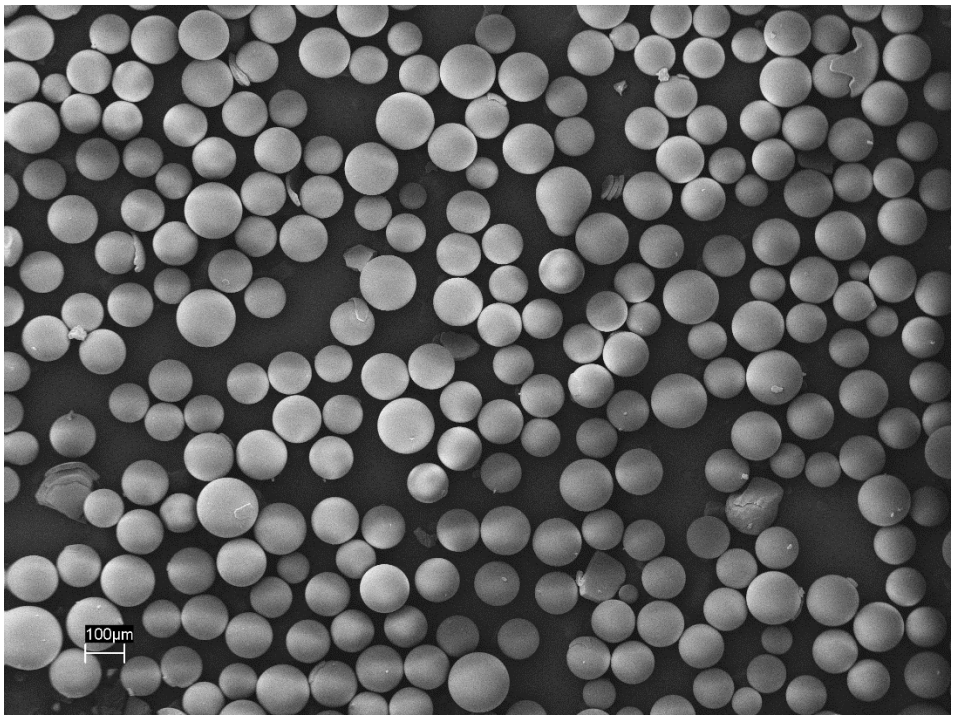

Figure 4.3: SEM image featuring a close-up of the 100-150 µm TK100 test-stick showing the shape of the TK100 particles and their distribution over a smaller space. (Magnification 250x)

SEM images confirm the findings from literatures regarding the spherical shape including the homogenous and smooth exteriors featuring the extractant coating on the polymeric beads. Some damages on the beads are evident in the SEM images including some form of 'shelling' taking place.

This could be due to the friction occurring between the beads during transport and also some batch-to-batch manufacture variations however this is not believed to noticeably impact the extractant's performance [43].

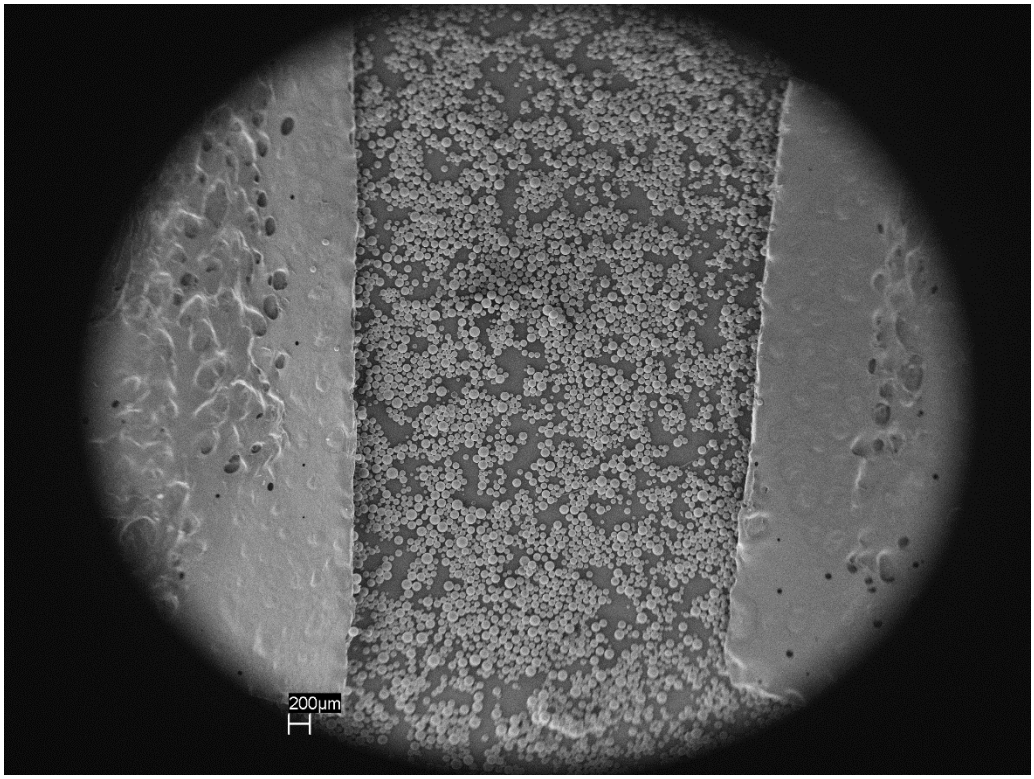

Figure 4.4: SEM image of the active site of the 50-100 µm TK100 test-stick demonstrating the extractant spread and binding. (Magnification: 45x)

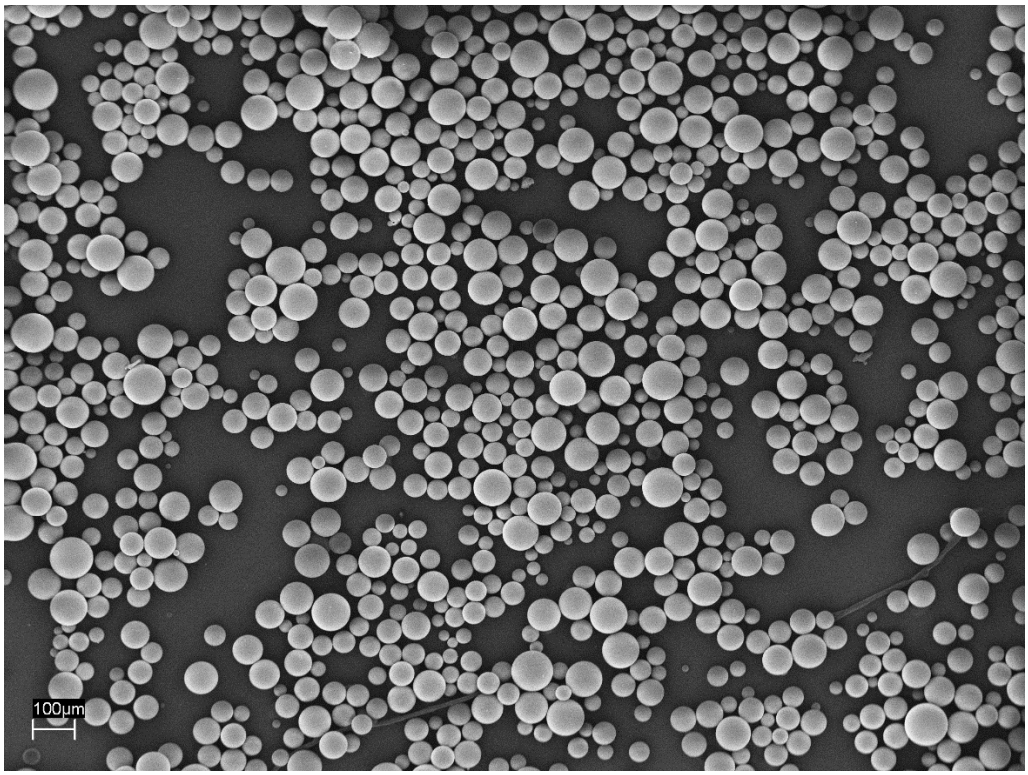

Figure 4.5: SEM image featuring a close-up of the 50-100 µm TK100 test-stick showing the shape of the TK100 particles and their distribution over a smaller space. (Magnification: 250x)

For comparative purposes, 50-100 µm TK100 test-sticks were also prepared to evaluate the impact of reducing particle sizes onto the test-stick manufacturing process.

Further SEM images were taken of 50-100 µm TK100 test-sticks demonstrating a comparison between both extractant's particle sizes as well as particle distribution across the active site of the test-sticks. Both test-stick particle sizes (50-100 µm- and 100-150 µm-TK100) show mostly consistent particle sizes across all the beads albeit with some outliers where noticeably smaller bead sizes are seen. This observation is mostly found for 50-100 µm TK100 however this is believed to be residual unfiltered particles from the extractant's manufacture. Calculated surface coverage percentages carried out using ImageJ™ software are shown below:

Table 4.1: Tabulated results showing the percentage coverage of the active site of both TK100 test-sticks containing different particle sizes, taken at different magnifications.

Sample	Magnification	%background	%coverage
TK100_100-150_1	45x	42.43	57.57
TK100_100-150_2	250x	42.93	57.07
TK100_100-150_3	750x	38.71	61.29
		Mean:	58.64
		Standard deviation:	1.88
		2σ:	3.77
TK100_50-100_1	45x	47.08	52.92
TK100_50-100_2	250x	47.51	52.49
TK100_50-100_3	750x	41.48	58.52
		Mean:	54.64
		Standard deviation:	2.75
		2σ:	5.49

Different magnifications of the test-stick solid phase provided repeats for surface coverage threshold analysis and results were found to be consistent throughout the different magnifications. Calculated relative standard deviations (%RSD) of 3.77% and 5.49% for 100-150 µm and 50-100 µm, respectively, demonstrates this consistency throughout the different magnifications. This suggests that packing coverage was relatively consistent throughout the solid phase.

Mean %coverage of 58.64 ± 3.77 for 100-150 µm and 54.64 ± 5.49 for 50-100 µm TK100 also shows that particle sizes have minimal impact on the performance of the current test-stick manufacturing process. However, it is believed that the development of more automated test-stick manufacturing processes would improve the surface coverage efficiency of the current test-stick manufacturing process. Improvement in surface coverage efficiency would potentially reflect in improved ^{90}Sr uptake performance due to increased number of active sites present across the solid phase.

Clevasol particles were found to be much rougher in comparison and lack the smooth homogenous particle surface seen in TK100 particles. These irregularly shaped and highly variably sized Clevasol particles can introduce uptake steric constraints and therefore interrupt species uptake by the extractant. This could potentially impact the performance of the solid phase and the irregularity of the particle sizes and topography could introduce inconsistencies of the solid phase's performance.

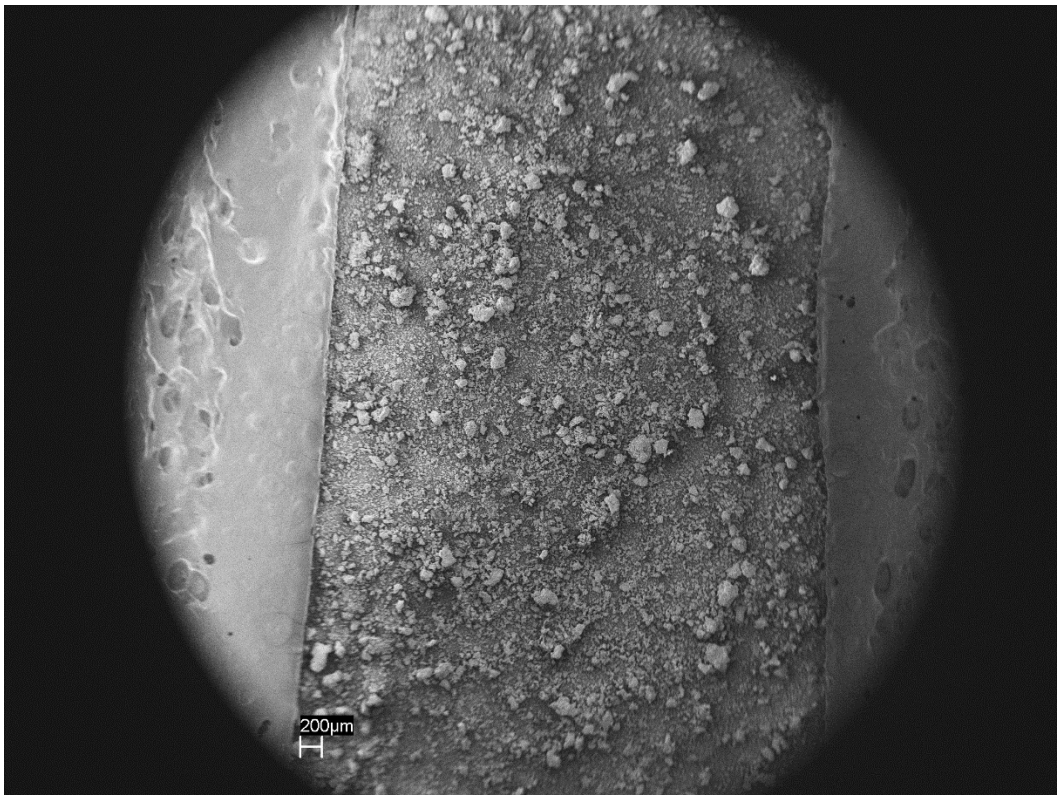

Figure 4.6: SEM image of the active site of the 200 ± 100 µm Clevasol test-stick demonstrating the extractant spread and binding. (Magnification: 45x)

Figure 4.7: SEM image featuring a close-up of the 200 ± 100 µm Clevasol test-stick showing the shape of the Clevasol particles and their distribution over a smaller space. (Magnification: 250x)

Coverage percentage calculations using ImageJ™ software provided useful insight into the spatial distribution of Clevasol, especially when taking into account the irregular shape and variable sizes of Clevasol particles as discussed above.

Table 4.2: Tabulated results showing the percentage coverage of the active site of Clevasol test-sticks, taken at different magnifications.

Sample	Magnification	%background	%coverage
Clevasol_1	45x	45.33	54.67
Clevasol_2	250x	46.26	53.77
Clevasol_3	750x	26.21	73.79
		Mean:	60.74
		Standard deviation:	9.23
		2σ:	18.47

Different magnifications of the solid phase provided much greater variability in solid phase coverage% for Clevasol test-sticks. A calculated %RSD of 18.47% is much higher than that seen for 100-150 µm (3.77%) and 50-100 µm (5.49%) TK100 test-sticks. This demonstrates the effect of the highly variable Clevasol particle sizes and particle surface topology where efficient 'packing' of the extractant particles is less likely to occur. However, surface saturation calculations showed that Clevasol (60.74 ± 18.47%) had slightly better coverage on the solid phase over both size variants of TK100 ($TK100_{50\text{-}100\ \mu m}$ = 54.64 ± 5.49%, $TK100_{100\text{-}150\ \mu m}$ = 58.64 ± 3.77%,). Increasing saturation coverage of the test-stick active site with increasing particle sizes may be due to the presence of 'layering' occurring in which larger sized particles may seem to cover the surface more but without either being sufficiently bound onto the test-stick or covering the active sites of other neighbouring particles. A manufacturing method that would be capable of introducing a tightly packed monolayer system would be highly beneficial and reduce factors, such as steric hindrance, that may impact test-stick performance. SEM analysis has provided useful insight into the extent of extractant 'packing' onto the test-stick inert support and highlighted the need for future test-stick manufacturing techniques to improve this. Manufacturing methods may adopt processes such as electroplating and 3-D printing which would grant more consistent methods of manufacturing test-sticks with tight packing of the solid phase.

4.4.3 Solid phase mass loadings

Evaluation of test-stick performance is carried out by calculating the partitioning constant, k', which reflects the partitioning of the species of interest between the solid and the aqueous phase. However, calculation of k' requires knowledge of not only the activity of ^{90}Sr in both the solid phase (A_s) and the aqueous phase (A_{aq}) but also the mass of both the solid phase (M_s) and the aqueous phase (M_{aq}).

$$\left(\frac{A_s}{A_{aq}}\right) = k' \times \left(\frac{M_{aq}}{M_s}\right)$$

Activities of both the solid and aqueous phases can be determined by radiometric analysis of the test-stick and the aqueous phase. Mass of the aqueous phase (sample) can be determined in the methodology and for the majority of the work carried out in this project this is 4 mL. However, the mass of the solid phase is unknown and therefore must be determined so k' calculations can be carried out to evaluate test-stick performance. To measure the mass of the solid phase both radiolabelling and gravimetric analysis were carried out of both extractant test-sticks. Radiolabelling provided short term mass loading information whilst gravimetric analysis provided insight into the batch manufacture reproducibility as well as the long-term manufacture reproducibility.

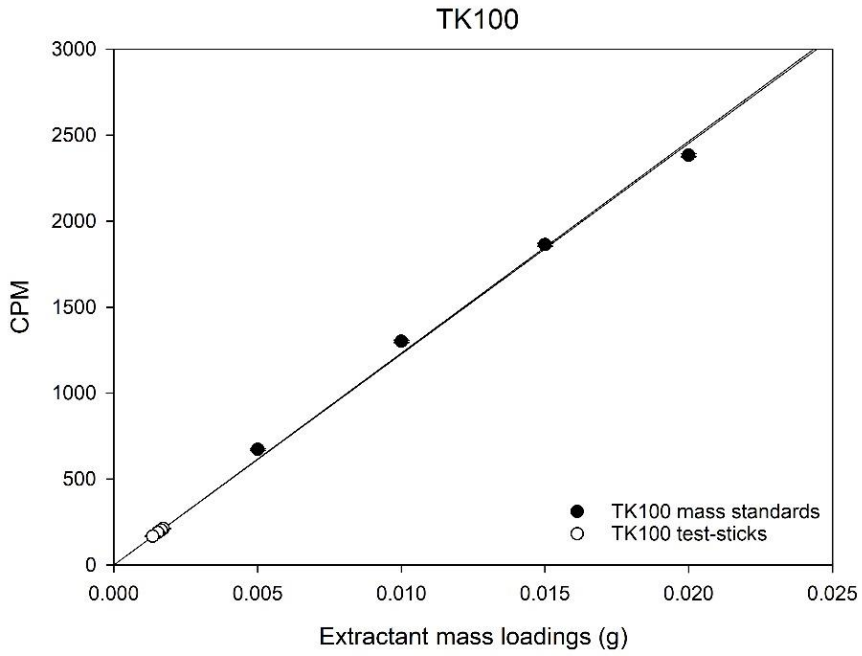

Figure 4.8: Extractant loading data for TK100 test-sticks using radiolabelling.

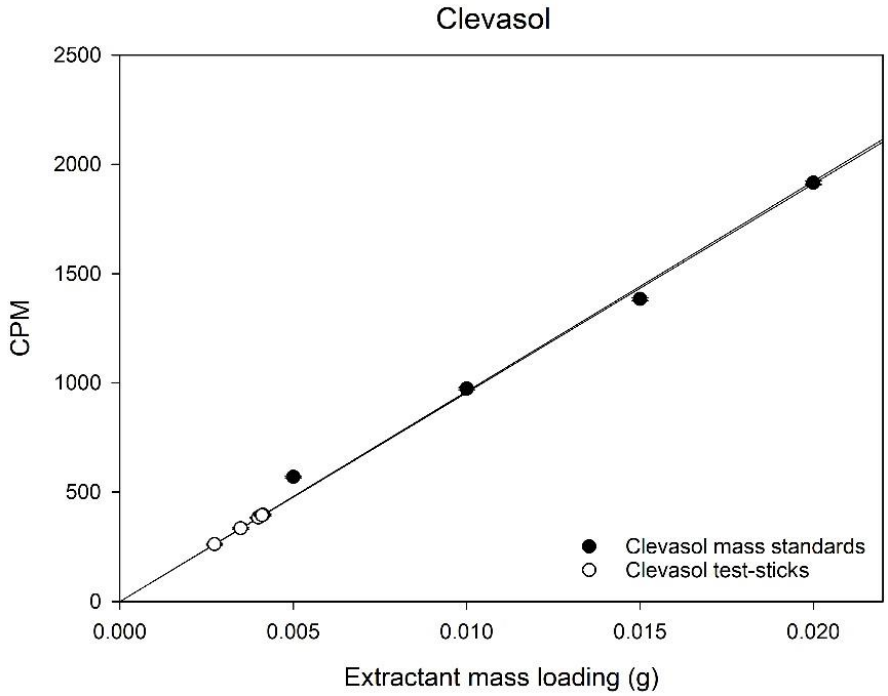

Figure 4.9: Extractant loading data for Clevasol test-sticks using radiolabelling.

Radiolabelling showed TK100 test-sticks to have an average mass loading of 1.6 mg ± 0.4 mg and presented an RSD of 25%. Clevasol had higher test-stick average mass loadings of 3.6 mg ± 1.2 mg and presented an increased RSD of 30%. These results show a relatively large variance in average mass loadings for both TK100 and Clevasol-test-sticks however this may be understandable due to the relatively small particle sizes of both extractants, especially TK100 (100-150 µm) when compared against Clevasol (200 ± 100 µm). The observed variance in extractant mass loadings for both extractants may also be due to the test-stick manufacture process in which spray adhesive is utilised as the binding mechanism for extractant(s) onto the test-stick inert support. Inadequate or inconsistent spray coverage on the inert support prior to mounting the extractants may also have contributed to the observed wide mass range. This is emphasised when considering that spherical beads such as those of TK100 require sufficient coverage of spray adhesive in order to bind sufficiently well to the inert support. These results also further cemented the need for future work to investigate other test-stick manufacturing methods. These test-stick manufacturing methods could potentially be electroplating or 3-D printing, for example. Test-stick manufacturing developments would need to provide better adhesive coverage on the inert support, and consequently binding strength, whilst impacting as little as possible to the performance of the test-sticks themselves [43,44,46].

Gravimetric analysis provided further insight into the variability in solid phase mass loadings and demonstrated the reproducibility of the current test-stick manufacturing method. Both intra-batch and inter-batch reproducibility over extended time periods was assessed.

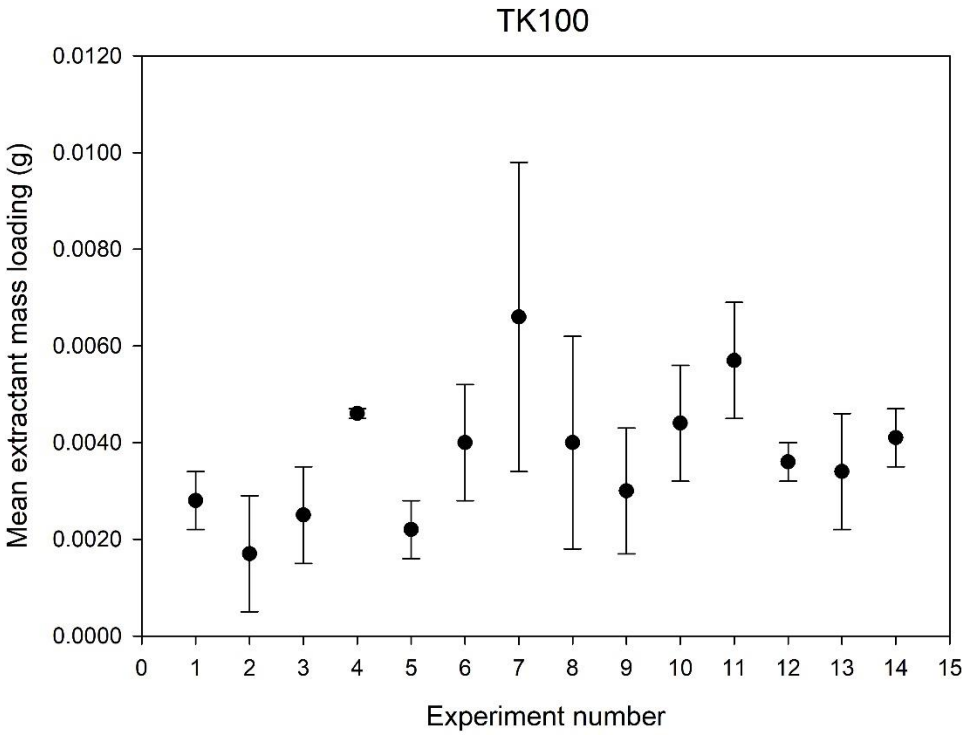

Figure 4.10: Gravimetric analysis of TK100 mass loadings on test-sticks over a span of 14 different experiments. Error bars reflect variance in gravimetric analysis across test-sticks for that experiment.

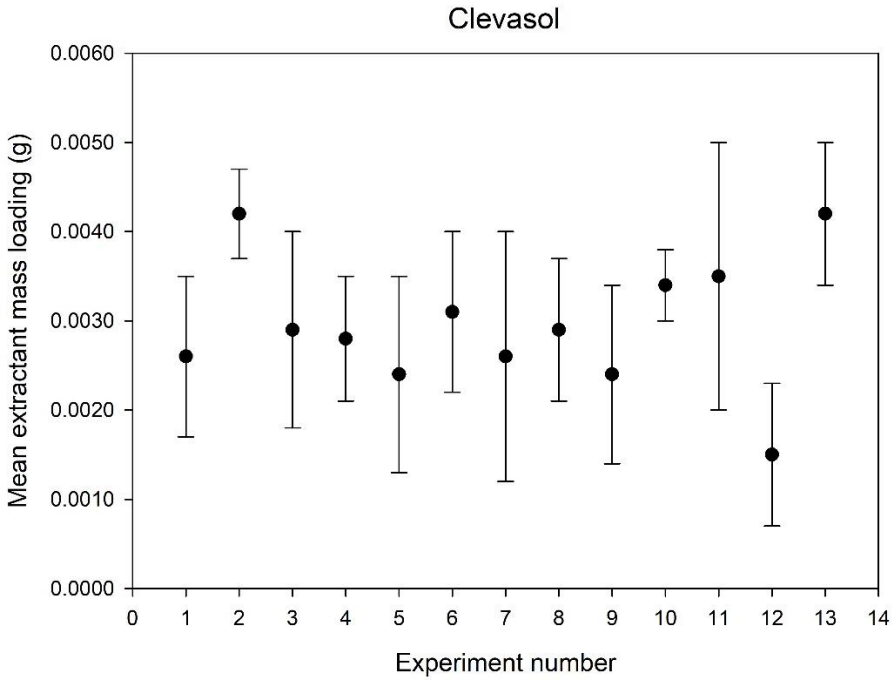

Figure 4.11 Gravimetric analysis of Clevasol mass loadings on test-sticks over a span of 13 different experiments. Error bars reflect variance in gravimetric analysis across test-sticks for that experiment.

Average solid phase mass loadings of 3.8 ± 1.1 mg (2σ, *n* = 14) for TK100 test-sticks and 3.0 ± 0.9 mg (2σ, *n* = 13) for Clevasol test-sticks were found across multiple experiments. These gravimetric results showed an increase in average mass loadings for TK100 (from 1.6 mg to 3.8 mg) whilst Clevasol results showed similar results (radiolabelling 3.6 mg vs gravimetric 3.0 mg) to radiolabelling mass loading experiments. Calculated %RSD for TK100 and Clevasol test-sticks were also both lower at 16.2% and 17.4%, respectively, compared to radiolabelling data. The observed change in mass loading can be associated to human error during test-stick manufacture. This human error can be attributed to inconsistent application of spray adhesive from one test-stick manufacture batch to another. This human error factor can also apply to the application of the extractant onto the test-stick after the spray adhesive has been applied. This change in mass loading is not observed for Clevasol test-sticks although this may be attributed to the larger particle size of Clevasol (200 ± 100 µm) by comparison to TK100 (100-150 µm). The lower particle sized TK100 may be more susceptible to solid phase mass variability than Clevasol and therefore future test-stick manufacture techniques will have to account for this. Future development in test-stick manufacturing will have to be able to manufacture test-sticks with consistent solid phase masses regardless of extractant's particle sizes.

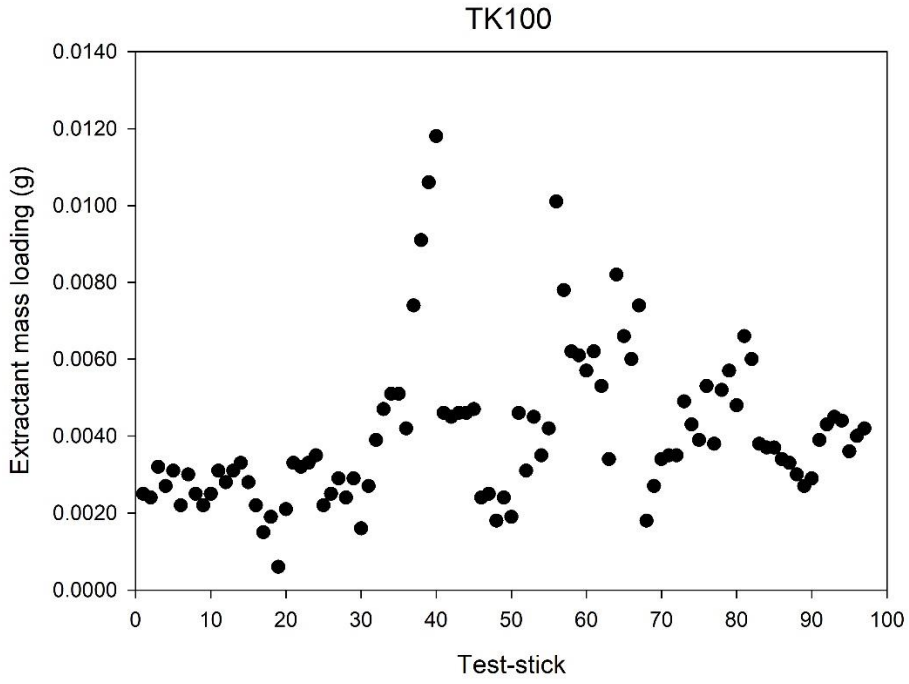

Figure 4.12: Individual gravimetrically weighed TK100 test-sticks over the span of 14 different experiments.

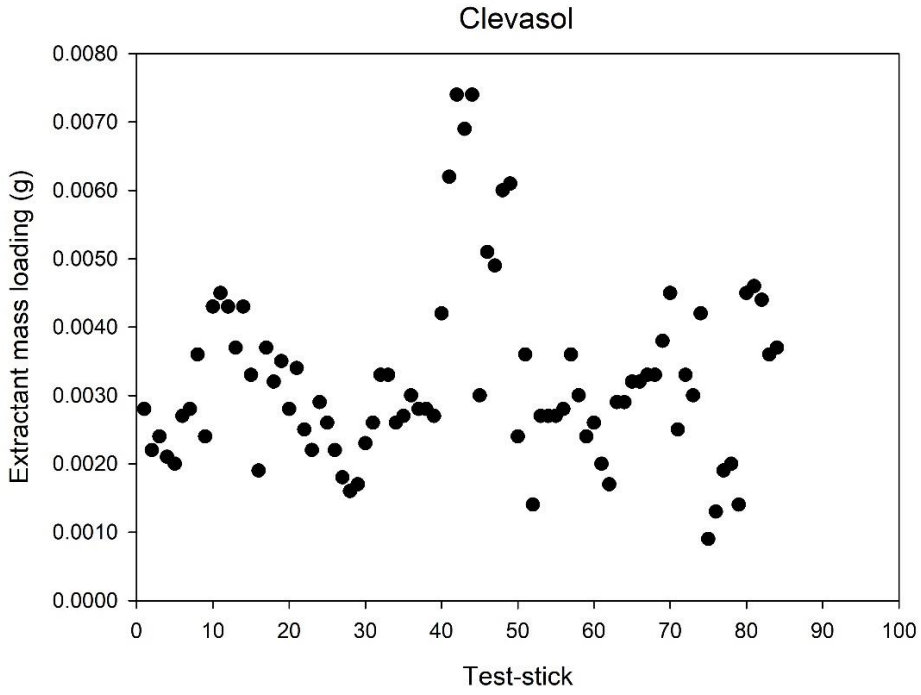

Figure 4.13: Individual gravimetrically weighed Clevasol test-sticks over the span of 13 different experiments.

Figures 4.12 and 4.13 expand on the data shown in figures 10 and 11 revealing all of the individually gravimetrically analysed test-sticks over the span of the 14 (TK100) and 13 (Clevasol) different experiments. These figures show the observed spread of the data with respect to the relevant extractants' mass loadings where TK100 is shown to have marginally more consistent mass loading measurements with some spread in the middle test-sticks measured. Clevasol, on the other hand, shows a far greater spread in mass loadings over the different test-sticks and therefore less consistent. This data demonstrates that the larger average particle sized Clevasol plays an influential role in the observed solid phase mass loadings of the Clevasol test-sticks as well as its greater spread in test-stick mass loadings when compared against the smaller particle sized TK100. TK100 average mass loadings over the individual samples is 4.1 ± 4.0 mg whilst Clevasol is 3.2 ± 2.6 mg showing that the large data spread encountered in the middle portion of samples in figure 4.12 increases the variability in TK100 test-sticks loadings. These results overall show that a future need for optimising the test-stick manufacture including minimising the human aspect of this process would be beneficial to reduce the variance of test-stick mass loadings for both extractant test-sticks. Minimising human error would reduce statistical variance and potentially provide less ^{90}Sr uptake variability across test-sticks. This would increase the confidence in results obtained as well as potentially improve LODs (limit of detection).

4.4.4 Surface area

Analysis of the surface area of the test-sticks' solid phase provides information regarding the physical parameters of the test-stick that can be modified and investigated. Analysis of the effect of increasing the surface area on the test-stick performance will help determine the optimum surface area for future test-stick design and manufacture. Throughout the experiments in this project the standard surface area of the test-stick solid phase is 1x1 cm^2 located at the edge of a 4x1 cm^2 test-stick inert support. For this experiment additional solid phase areas were tested, which included approximately 0.8, 1.2, 1.4, 1.8 and 2.0 cm^2 in a 4 mL sample volume. These surface areas were chosen to monitor the effect of surface area on test-stick performance as well as maintaining space on the upper section of the test-stick to allow removal from the sample once sampling was complete. The dimension of the test-stick inert support (4x1 cm^2) did not change. The choices in the solid phase area and inert support physical dimensions were selected to accompany the 5 mL vials that were adapted to carry out test-stick experiments and introduced further mobility to the technique. It must be noted that the solid phase surface area should not supersede the top of the sample line (sample meniscus) meaning that the entire solid phase must be submerged in the sample. This is to prevent any drying of the solid phase or inconsistent sampling carried out throughout the solid phase to maintain the data comparable.

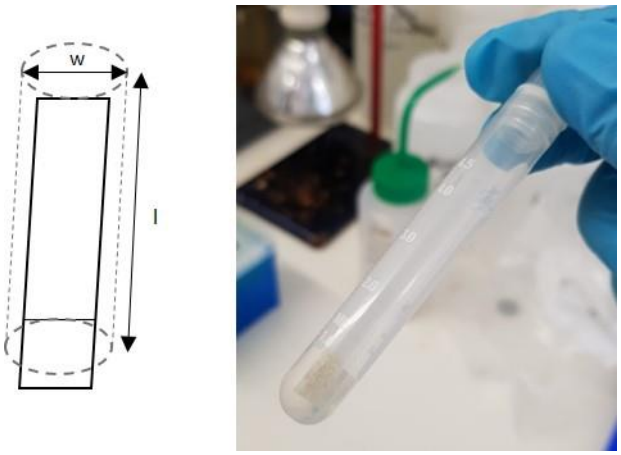

Figure 4.14: Dimensions of the test-stick in the vial with dotted outline of the 5 mL vial (left) and a photographic example of a Clevasol test-stick inside the 5 mL vial (right).

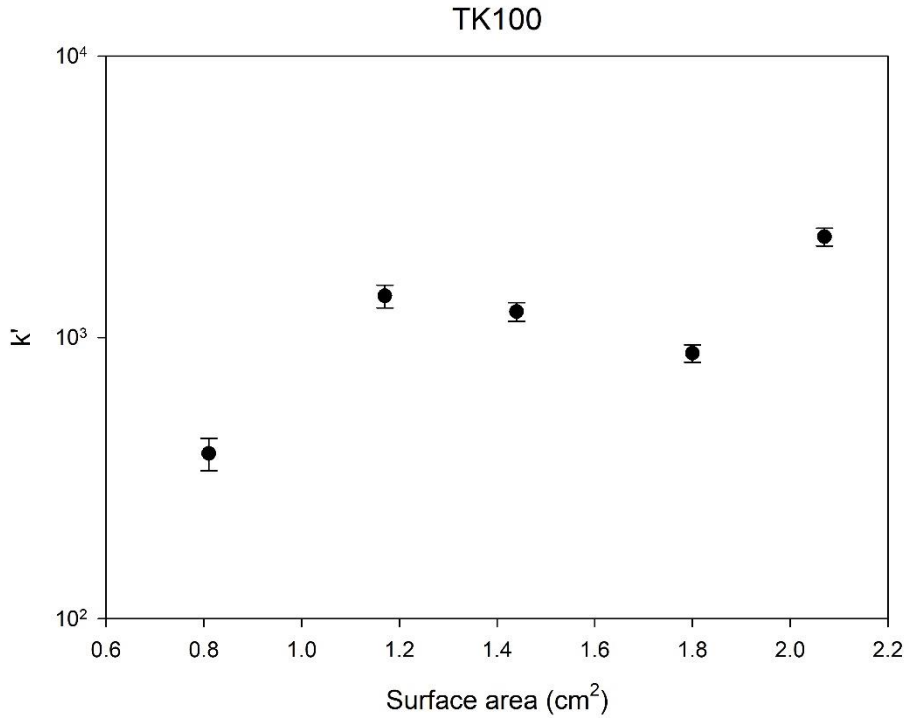

Figure 4.15: Partition coefficients obtained at different surface areas for the TK100 test-stick active site. Error bars represent uncertainty calculated from counting statistics.

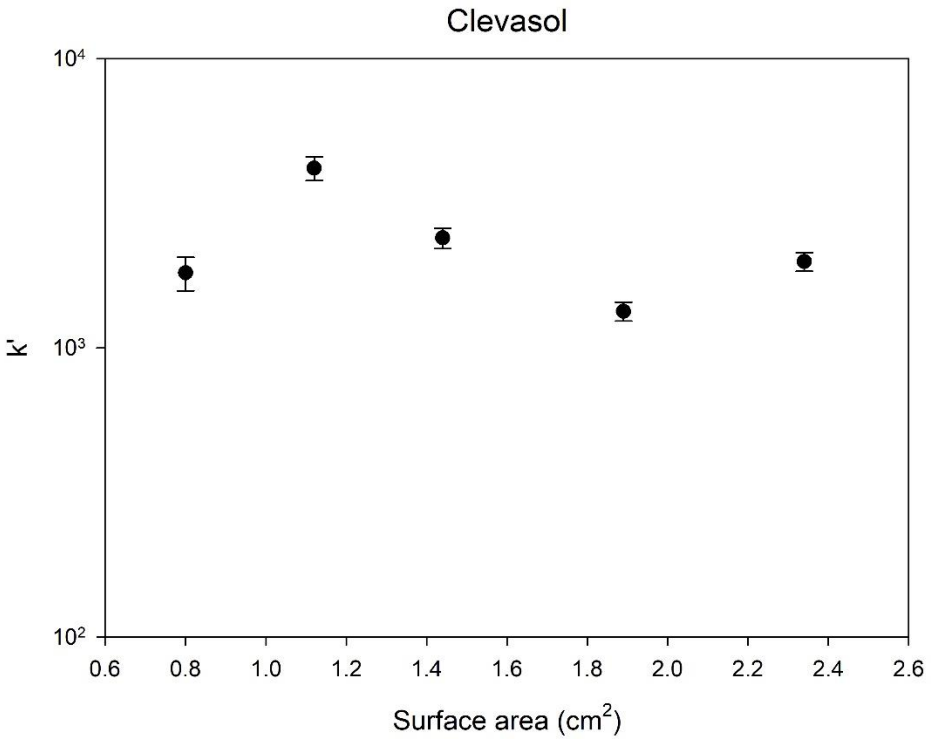

Figure 4.16: Partition coefficients obtained at different surface areas for the Clevasol test-stick active site. Error bars represent uncertainty calculated from counting statistics.

Partition coefficients obtained for TK100 test-sticks revealed a general increase in k' values with increasing surface area. Increasing the surface area from 0.81 cm^2 to 1.17 cm^2 saw a noticeable increase in k' values from 386 to 1405 before k' values for 1.17 cm^2 and 1.44 cm^2 stabilised at 1405

and 1236, respectively. Observed k' values then decreased at 1.80 cm^2 to 879. Active site surface area of 2.07 cm^2 saw the k' value peak at 2281, which further confirms that increasing the surface area of the test-stick active site does improve the strontium-partitioning performance of TK100 test-sticks. Clevasol test-sticks showed less correlation between k' values and surface area. Distribution coefficient values obtained for 0.80 (k' = 1818 ± 241), 1.12 (k' = 4182 ± 396), 1.44 (k' = 2402 ± 195), 1.89 (k' = 1339 ± 99) and 2.34 cm^2 (k' = 1990 ± 147) surface areas showed minor k' differences between all surface areas except 1.12 cm^2. Active site surface area of 1.12 cm^2 corresponds to the normal active site of the test-stick manufactured throughout most other experiments in this project and showed the highest k' value of 4182. These results are surprising considering the performance of TK100 test-sticks where increasing surface area showed an overall improvement in k' values. Clevasol test-sticks however do not show this trend and instead show minimal change in k' values between most surface areas except 1.12 cm^2 – the optimal surface area for Clevasol test-sticks. This observed minimal change in k' value may be due to the particle topography described in section 4.4.1. where the rough particle texture and Clevasol test-stick mounting may introduce a degree of steric hindrance which introduces a limiting step to mass transfer of ^{90}Sr onto the Clevasol test-stick solid phase. Improvement in test-stick manufacturing, including particle packing throughout the solid phase, could potentially overcome this issue for Clevasol test-sticks. This improvement in particle packing throughout the solid phase could potentially provide Clevasol test-sticks with a correlation similar to TK100 test-sticks, where an increase in solid phase surface area correlates in an increase in k' value.

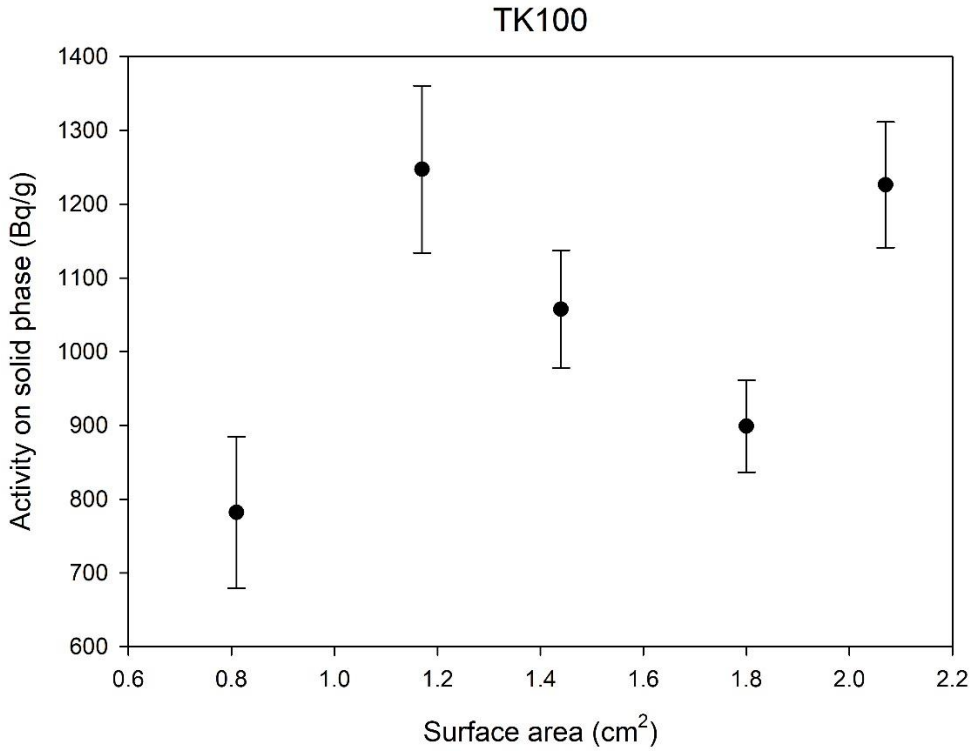

Figure 4.17: Measured uptake activity of ^{90}Sr over different surface areas for TK100 test-sticks. Error bars represent uncertainty calculated from counting statistics.

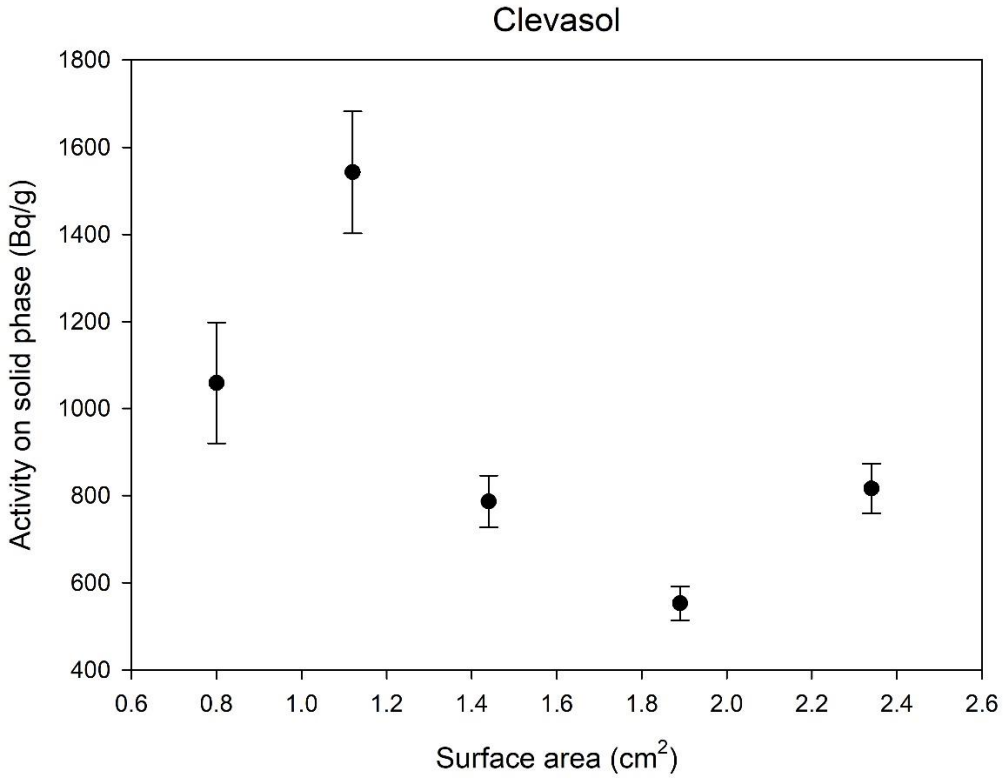

Figure 4.18: Measured uptake activity of ^{90}Sr over different surface areas for Clevasol test-sticks. Error bars represent uncertainty calculated from counting statistics.

TK100 test-sticks showed the largest uptake of ^{90}Sr at 1.17 cm^2 (1247 ± 113 Bq g^{-1}) followed by 2.07 cm^2 (1226 ± 85 Bq g^{-1}) with remaining surface areas showing ^{90}Sr uptake between 781 (± 103) and 1057 (± 80) Bq g^{-1}. The general trend here has shifted from that seen in k' work (see figure 4.15) where a general increase in TK100 test-stick performance with increasing surface area was observed. The general trend for ^{90}Sr loadings shifted to a more subtle increase in ^{90}Sr uptake on test-sticks, with solid phase surface areas of 1.17 and 2.07 cm^2 showing the highest ^{90}Sr loadings. The justification for this observation is most likely due to how well distributed the TK100 extractant on the surface of each test-stick is, as shown in the SEM work carried out in section 4.4.1. The results still show that approximately 1x1 cm^2 active site remains suitable for efficient uptake performance of ^{90}Sr by TK100 test-sticks. This data is also important for future systems where development of MES (multi extractant systems) will look to simultaneously screen multiple radionuclides of nuclear decommissioning importance – such as ^{99}Tc and ^{137}Cs, for example – at once and therefore if the solid phase surface area can be kept compact then theoretically more extractants can be mounted onto the test-sticks. This would mean test-sticks would be capable of characterising more radionuclides at once, further streamlining the characterisation process.

Strontium-90 uptake on Clevasol test-sticks showed a similar pattern to that seen when evaluating k' values (Figure 4.16) and shows once again superior performance at 1.12 cm^2 (1542 ± 140 Bq g^{-1}) on Clevasol test-sticks. The justification for why this is observed for both k' values and ^{90}Sr loadings may be due to the high loading capacity of Clevasol (243 mg g^{-1} for ^{90}Sr). Increasing the surface area of the solid phase, and therefore increasing the number of total active sites, could potentially have no effect on an extractant with a loading capacity thirty times greater than TK100 (8 mg g^{-1} Sr) for ^{90}Sr. Therefore, the solid phase surface area for Clevasol test-sticks should be maintained at 1 cm^2 as increasing the solid phase surface area brings no improvement to the performance of the Clevasol test-stick. This investigation, for both Clevasol and TK100 test-sticks, also serves to reinforce the need to investigate test-stick manufacturing methods that introduces a degree of automation. This would reduce human error in manufacture and carry out test-stick manufacture with consistent mass loadings, extractant particle distribution and surface area to optimise test-stick performance.

4.4.5 Particle size effect

Particle size effect deals directly with the physical parameters of the extractant including the extractant's surface area and active site availability for species uptake – in this case ^{90}Sr. An understanding of the impact of the particle size effect on test-stick performance would help to optimise future designs including extractant candidature for future test-sticks that focus on different species of interest.

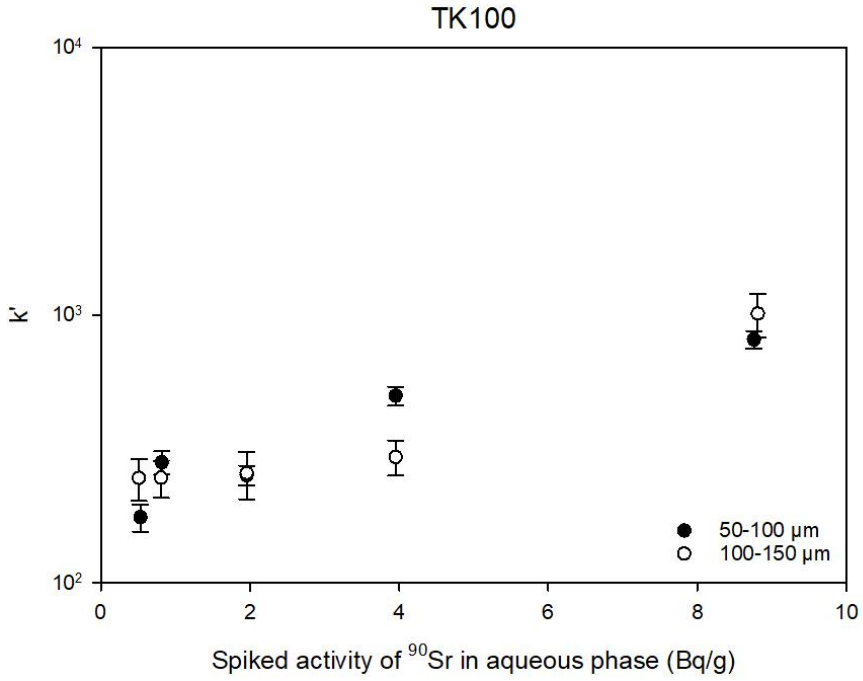

Figure 4.19: Comparison between 50-100 µm and 100-150 µm TK100 test-sticks and their performance presented as k' values. Error bars represent uncertainty calculated from counting statistics.

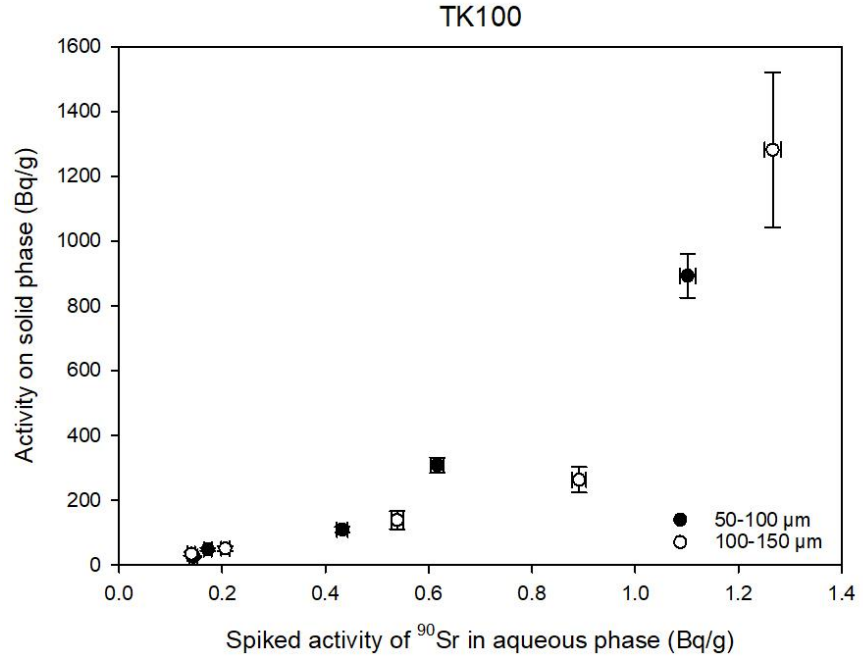

Figure 4.20: Comparison between 50-100 µm and 100-150 µm TK100 test-sticks and their performance with respect to measured activity of ^{90}Sr on the solid phase. Error bars represent uncertainty calculated from counting statistics.

Observed k' values for both 50-100 µm and 100-150 µm TK100 test-sticks showed a general increase with increasing ^{90}Sr in the aqueous phase. Despite 100-150 µm test-sticks exhibiting higher k' values ($k'_{100\text{-}150\mu m}$ = 1012 versus $k'_{50\text{-}100\ \mu m}$ = 811) both particle sizes exhibited largely similar k'

values at different activity spikes of 0.5, 0.8, 2.0, 4.0 and 8.8 Bq in 4mL aqueous samples. Activity loadings of ^{90}Sr on the solid phase in figure 4.20 showed a larger distinction between both particle sizes with 100-150 µm TK100 test-sticks demonstrating higher ^{90}Sr activity in the solid phase. This observation may be justified when considering an adhesive coating is applied during test-stick manufacture which may reduce the number of active sites available in TK100 test-sticks, especially for smaller extractant particles such as 50-100 µm TK100. Examined linearity between both particle sizes showed 50-100 µm TK100 test-sticks obtaining an $R^2 = 0.94$ versus an $R^2 = 0.76$ for 100-150 µm TK100 test-sticks. This observed linearity demonstrates that despite the lower activity of ^{90}Sr in the solid phase, 50-100 µm TK100 test-sticks showed stronger conformity to the proportional mechanism that test-sticks operate by and is therefore an important consideration. Works by Warwick *et al.* drew similar conclusions from the effect of particle size, using Sr-resin instead, at similar particle sizes (50-100 µm and 100-150 µm) – same manufacturer (TrisKem International), uptake mechanism (size exclusion) and extractant (crown ether) with Sr-resin containing 1-octanol whilst TK100 contains an organic cationic exchanger HDEHP as well. Warwick *et al.* found 50-100 µm Sr-SES (single extractant stick) to exhibit higher k_{eq} (effective distribution coefficient, mL g^{-1}) and twice as high *r* (rate constants, s^{-1}) values when compared against 100-150 µm test-sticks. These findings correlate well with those presented here where despite 50-100 µm TK100 test-sticks exhibiting lower activities of ^{90}Sr on the solid phase (than 100-150 µm TK100 test-sticks) these smaller particle size systems exhibited stronger linearity and therefore conformed more to a proportional mechanism. The importance of the proportional mechanism in test-stick technology is fundamental and therefore must be reminded. The stronger the proportional mechanism of the system is then the more accurately the ^{90}Sr in the sample can be determined by measuring the activity of ^{90}Sr on the test-stick and calculating from this using a proportionality constant.

$$A_{s,t} = b_t \times [A_{aq}] \therefore \frac{A_{s,t}}{b_t} = [A_{aq}]$$

Where, A_s is the activity on the test-stick at time *t* in Bq, b_t is the proportionality constant for time *t* in Bq mL Bq^{-1} and $[A_{aq}]$ is the activity on the aqueous phase/sample in Bq mL^{-1}.

These observations strongly suggests that different particle sizes can play an influential role on test-stick performance and therefore should be considered in future test-stick development and design. A preference for smaller particle sized extractants, if available, may be desirable when selecting test-stick candidate extractants for specific radionuclide uptake. This would potentially provide confidence regarding the performance of test-stick technology and its ability to exhibit a strong proportionality mechanism. The importance in the strength of the proportionality mechanism is so the radionuclide of interest in the sample can be more accurately calculated from the activity of said radionuclide on the test-stick. If future test-stick manufacturing techniques for ^{90}Sr, as well as

other radionuclides, can incorporate the idea of using smaller particle sized extractants then it could potentially improve the performance of the test-sticks without the need for more complex or expensive extractants.

4.4.6 Reproducibility

The performance of the test-sticks, regardless of the radiochemical species being screened or the sampling environment, must be able to exhibit reproducibility. If the test-sticks are not capable of determining, with confidence, if a specific sample has no activity (activity is out-of-scope) or has enough activity to require further (off-site) analysis then test-sticks would be unsuitable for field deployment. Screening techniques do not require the same reproducibility as lab techniques (such as mass spectrometric techniques) as they are field deployed and therefore require sufficient reproducibility to determine confidently whether a sample has activity below or above a specific threshold. For ^{90}Sr, the EPR 2016 activity limit for very low-level waste is 1 Bq g^{-1} meaning that test-stick technology must be able to distinguish this in a sample even with reproducibility of the test-sticks accounted for. For example, if the calculated activity of ^{90}Sr in a sample is 0.4 ± 0.2 Bq g^{-1} then it can be confidently stated that this sample does not exceed the 1 Bq g^{-1} limit stated by EPR 2016. Determination of the reproducibility of the test-sticks will consist of evaluating five test-sticks' performance under identical conditions and outline whether results obtain are concordant and reliable.

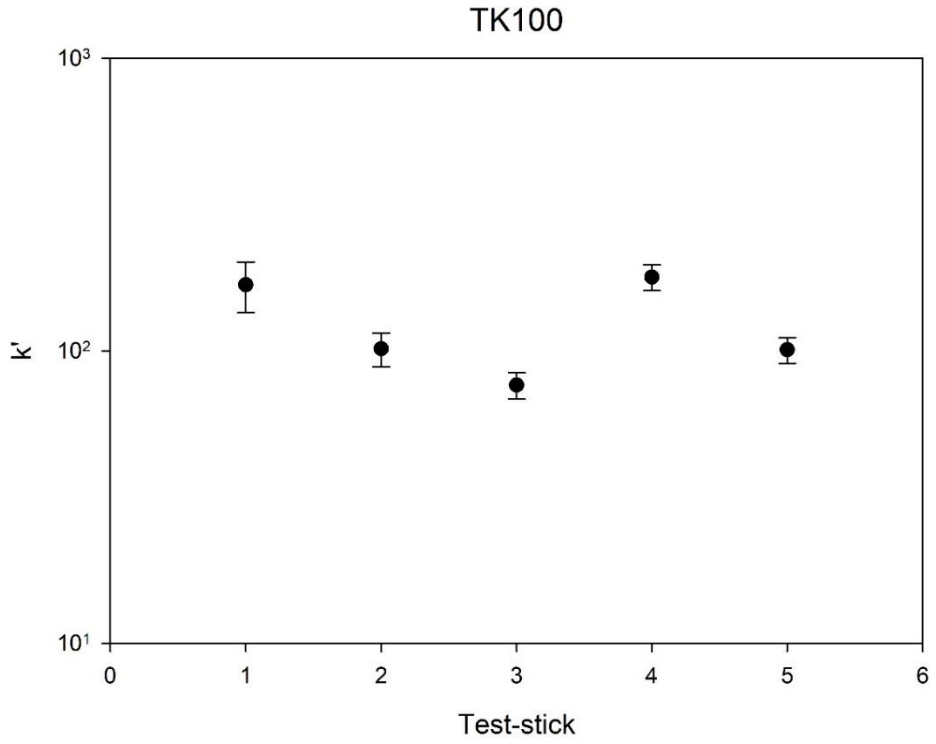

Figure 4.21: Distribution coefficients obtained for TK100 test-sticks over five repeats. Spiked activity of ^{90}Sr = approx 100 Bq. Error bars represent uncertainty calculated from counting statistics.

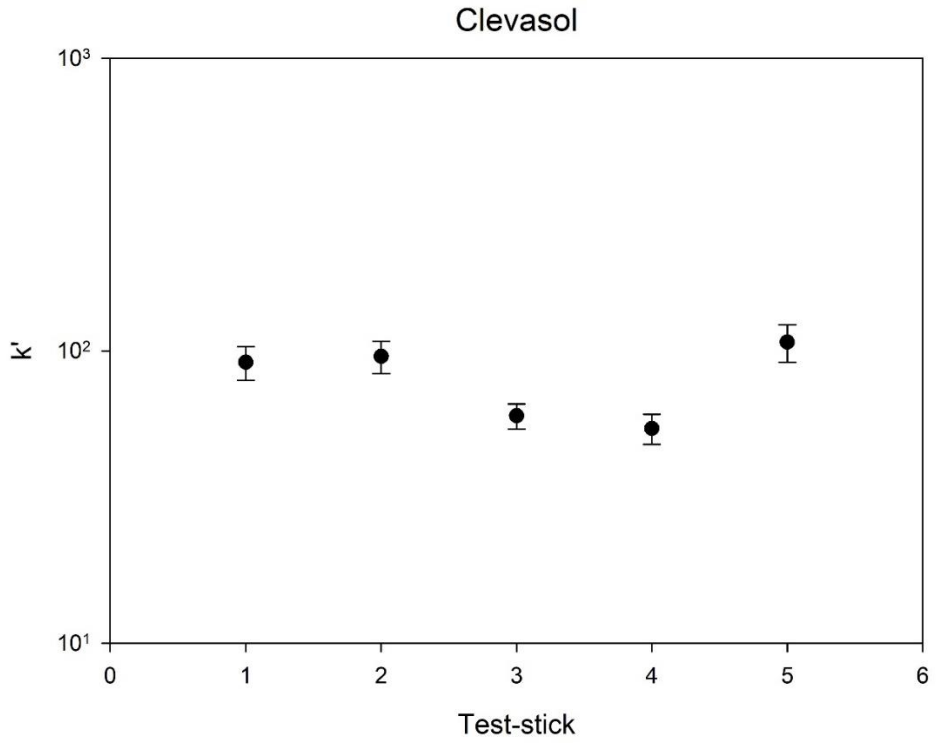

Figure 4.22: Distribution coefficients obtain for Clevasol test-sticks over five repeats. Spiked activity of ^{90}Sr = approx 100 Bq. Error bars represent uncertainty calculated from counting statistics.

Mean k' values across TK100 test-sticks were 125 ± 40 whilst Clevasol test-sticks had mean k' values of 82 ± 21 across all five test-sticks. This mean distribution coefficient for TK100 corresponded to a deviation of 32.0% RSD across the five test-sticks whilst Clevasol test-sticks showed a slightly lower variation of 25.9% RSD. TK100 test-stick were shown to perform at slightly higher k' values compared to Clevasol test-sticks. TK100 weighing uncertainty provided even less variance in these results with TK100 RSD of 13.2% whilst Clevasol showed weighing uncertainty RSD of 12.8%. This could indicate that solid phase mass loading uncertainty may be playing a minor role in the observed reproducibility of both extractant test-sticks. Even so, there is a strong indication that improvement in test-stick manufacture, which includes improving batch-to-batch variance, could have an impact on the reproducibility of both extractant test-sticks. This would be an easier way of improving test-stick k' variability without altering the extractant choice or the operating procedure. Despite both extractant test-sticks differing in uptake mechanisms both exhibited similar reproducibility of 32.0% (TK100) and 25.9% RSD (Clevasol). This indicates both TK100 and Clevasol test-stick performances are similarly reproducible.

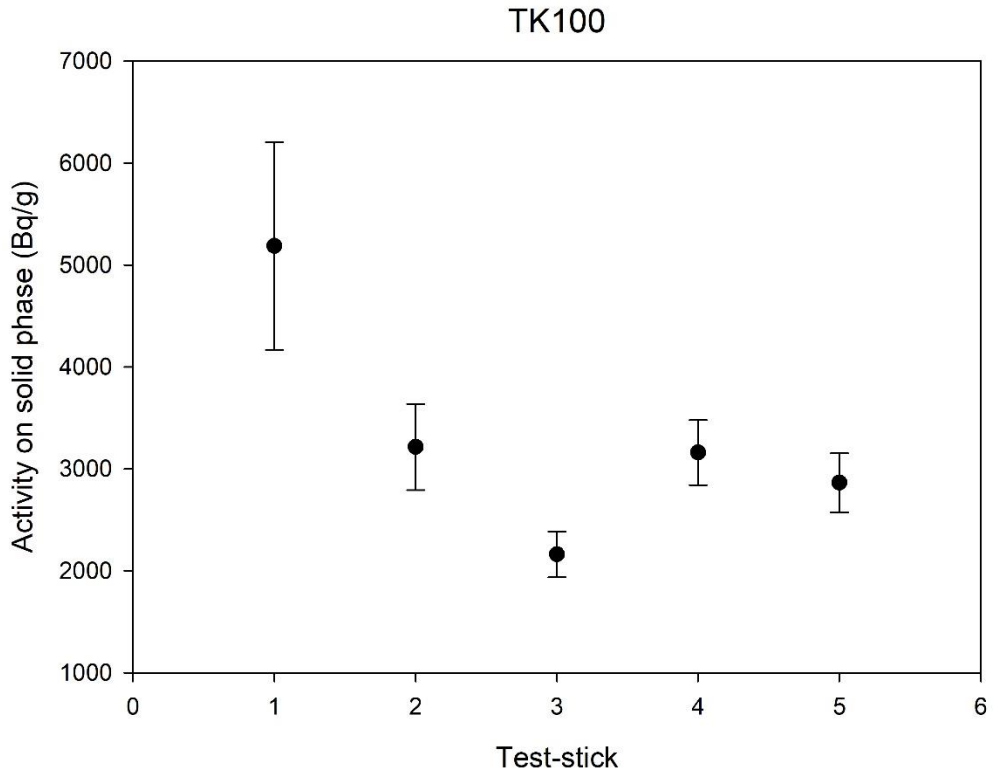

Figure 4.23: Test-stick activity obtained for TK100 test-sticks over five repeats. Spiked activity of ^{90}Sr = approx 100 Bq. Error bars represent uncertainty calculated from counting statistics.

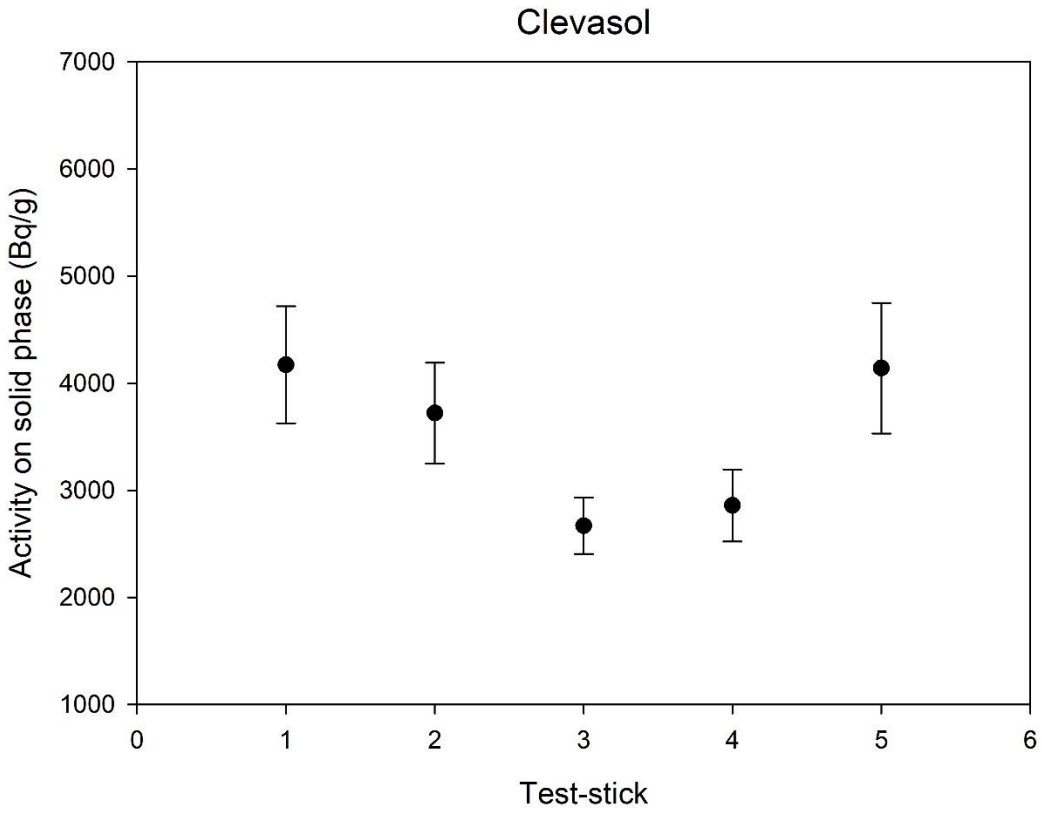

Figure 4.24: Test-stick activity obtained for Clevasol test-sticks over five repeats. Spiked activity of ^{90}Sr = approx 100 Bq. Error bars represent uncertainty calculated from counting statistics.

Mean measured activity of ^{90}Sr across TK100 test-sticks was 3317 ± 1007 Bq g^{-1} whilst Clevasol test-sticks showed ^{90}Sr activity uptake of 3511 ± 635 Bq g^{-1}. Both extractants exhibited similar ^{90}Sr activity uptake whilst doing so over almost identical average mass loadings – 30 mg for TK100 test-sticks and 29 mg for Clevasol test-sticks. These results showed that both candidates performed similarly well, and it can be observed in the above figures (Figures 4.23 and 4.24) that Clevasol exhibited qualitatively greater consistency across the results including maintaining variances across each test-stick comparable to that of the TK100 test-sticks. This last observation is especially important as due to Clevasol's rough and non-homogenous surface it has often been found to complicate the consistency of Clevasol test-sticks' performance. However, these results should serve to demonstrate the potential for Clevasol to be a viable test-stick candidate for ^{90}Sr screening should the Clevasol manufacturing process improve and allow for this topological influence on Clevasol's test-stick-to-test-stick variance to minimise. Furthermore, the calculated RSD%s suggest both test-sticks are suitable for field deployment and can be further optimised via future development in test-stick manufacture that can improve solid phase mass loading precision.

4.4.7 Durability

An important aspect of optimising test-stick manufacture is accounting for shelf life and the durability of test-sticks to withstand long periods of wait until they are required for field deployment. On-site deployment will often require the technique to be readily deployable. If the site does not have the necessary equipment or technology to manufacture the test-sticks, then the test-sticks will be required to be manufactured off-site and then delivered. Transportation of test-sticks coupled with the wait times on site before being required for site deployment means test-sticks must be capable of maintaining their performance after several weeks or potentially even months. If test-sticks could perform similarly after this amount of time, then it would lower the costs of the technique even further and even allow the test-sticks to be manufactured in bulk rather than on demand. This section looks to evaluate the effect of leaving test-sticks to stand for a period of approximately four weeks before screening samples with known spikes of ^{90}Sr.

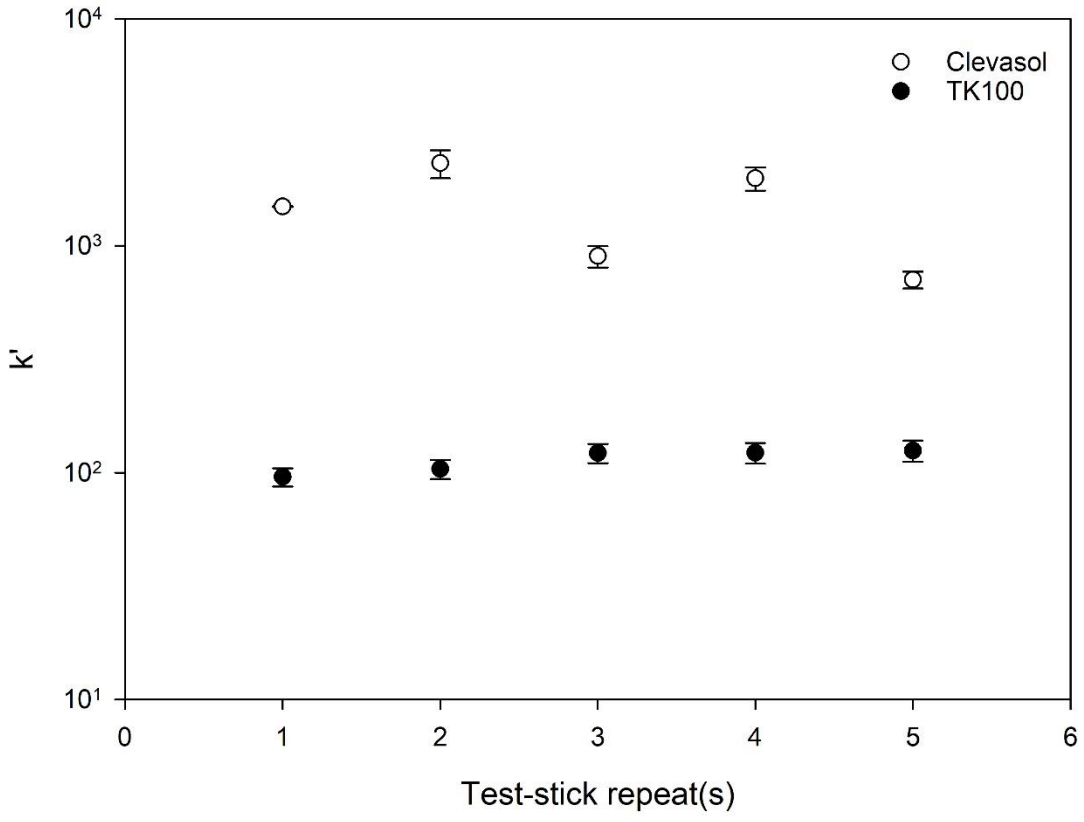

Figure 4.25: Distribution coefficients of TK100 and Clevasol test-sticks that were left to sit for a period of approximately four weeks prior to screening samples with spiked ^{90}Sr. Spiked activity of ^{90}Sr = approx. 103 Bq. Error bars represent uncertainty calculated from counting statistics.

Experiments showed TK100 test-sticks to exhibit an average k' value of 113 ± 12 whilst the average k' value for Clevasol test-sticks was 1479 ± 612. Clevasol test-sticks exhibited k' values that were an order of magnitude higher than those of TK100 test-sticks. This difference is most likely reflected in the differing capacities between TK100 (8 mg g^{-1}) and Clevasol (243 mg g^{-1}) for ^{90}Sr causing a noticeable difference in strontium partitioning between both extractant test-sticks. However, despite Clevasol test-stick exhibiting higher average k' values, TK100 test-sticks demonstrated results that were more consistent across all five repeats. Calculated %RSD of 10.3% for TK100 test-sticks and 41.4% for Clevasol test-sticks demonstrates TK100 test-sticks to be far more consistent between test-stick repeats than Clevasol test-sticks.

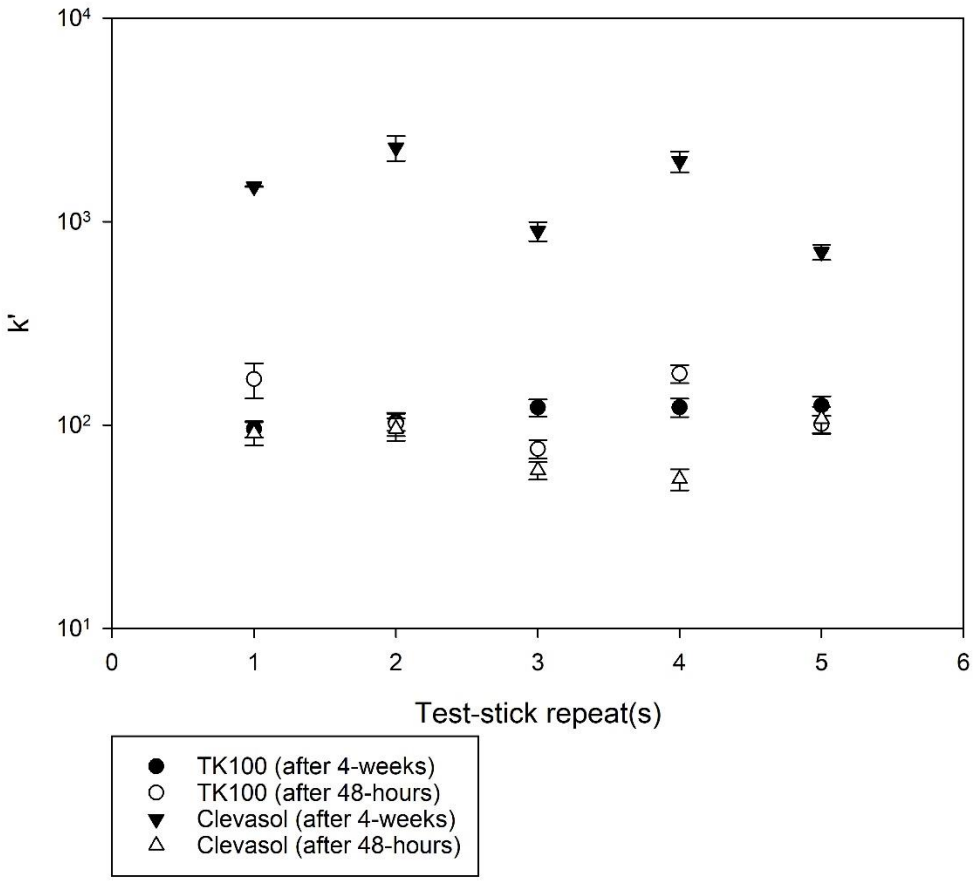

Figure 4.26: Distribution coefficient for both TK100 and Clevasol test-sticks for both timescales; test-stick that were left for 4-weeks and test-sticks that were left to stand for approximately 48 hours prior to sampling, as outlined in the original test-stick methodology (see section 3.3.1). Error bars represent uncertainty calculated from counting statistics.

Comparison of test-stick performance between both timescales (figure 4.26) demonstrates the differences in uptake potential with respect to shelf life for both extractant test-sticks. It can be observed that for TK100 the k' values sit closely within each other across five test-stick repeats for both timescales whilst Clevasol data shows the 'after 48-hours' data (from section 4.4.6) where test-sticks were left to stand, post-manufacture, for 48 hours sit closely with TK100 data for both timescales. However, Clevasol test-sticks that were left to sit for 4 weeks showed superior performance to the rest with k' values an order of magnitude above the rest. Reasons as to why this has occurred are unknown and further work is required to investigate this including whether 'conditioning' Clevasol prior to sampling is required to achieve maximum performance, as potentially observed here. This data also calls into question the long-term stability of Clevasol test-sticks and therefore an important consideration for test-stick manufacture is the long-term stability of extractants mounted onto the test-sticks.

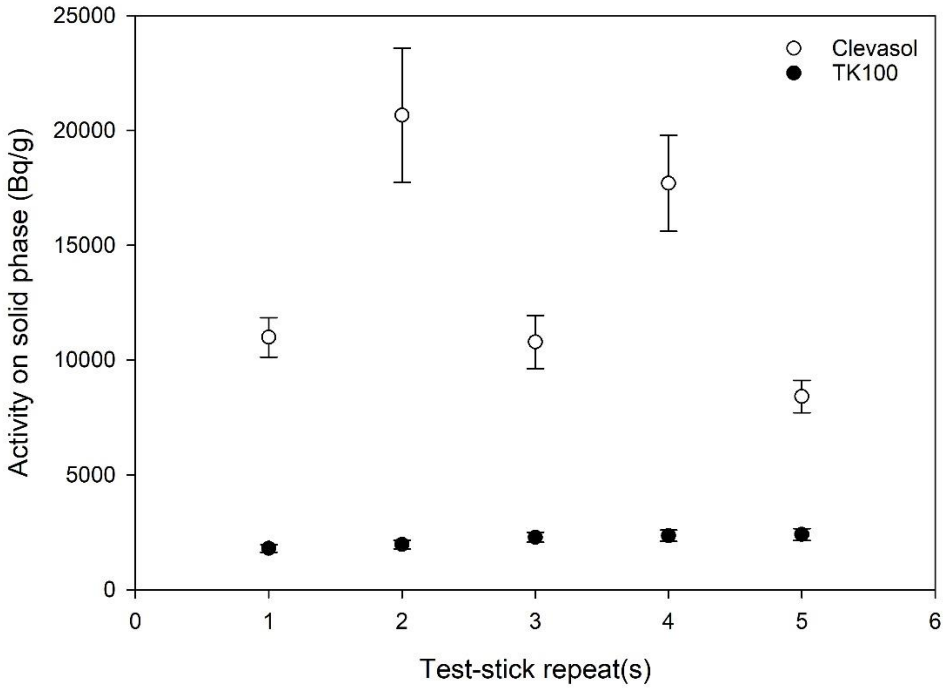

Figure 4.27: Measured activity of ^{90}Sr on test-sticks (for both TK100 and Clevasol) that were left to stand for approximately four weeks prior to analysis, over five repeats. Spiked activity of ^{90}Sr = approx. 103 Bq. Error bars represent uncertainty calculated from counting statistics.

Measured activity of ^{90}Sr on test-sticks revealed a similar pattern to that found in the results that looked at k' values across five repeats for both extractant test-sticks (Figure 4.25). Clevasol once again exhibited far greater performance, with a higher average activity of ^{90}Sr on the test-stick (13,708 ± 4654 Bq g^{-1}) when compared to TK100 (2157 ± 237 Bq g^{-1}). However, as previously

observed, TK100 exhibited much lower variance in per sample run (%RSD = 11.0%) when compared to Clevasol (%RSD = 33.9%) and therefore showed much more precision in the results obtained. These results show that leaving test-sticks standing for a period of approximately four weeks causes Clevasol test-sticks to retain their high uptake performance but with a large test-stick-to-test-stick variance in the results obtained. These results are not surprising due to the unrefined manufacturing process of the batch obtained in these studies and therefore it is believed that refinement in the manufacturing process including smoother surfaces and/or more restrained particle sizes would allow Clevasol test-sticks to overcome this large batch-to-batch variance across test-sticks. TK100 test-sticks on the other hand show inferior performance but instead couples this inferior performance with more consistency between test-stick repeats. This inferior performance by TK100 test-sticks compared against Clevasol is not surprising considering the gap in extractant capacity (TK100 = 8 mg g^{-1}, vs. Clevasol 243 mg g^{-1} for ^{90}Sr). However, the more refined and controlled manufacturing process culminating in restrained particle sizes (100-150 µm) and bead-like smooth extractant surface allows for more consistent results to be obtained between repeats even after allowing test-sticks to stand an extended period of time.

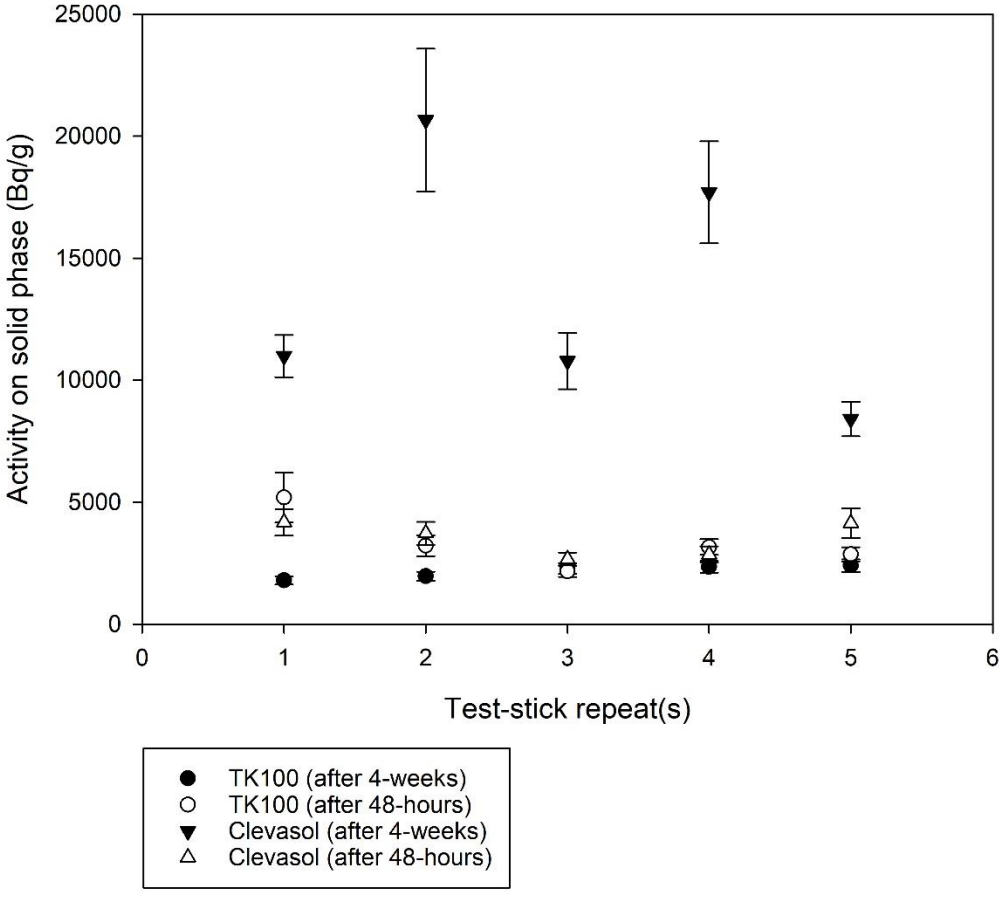

Figure 4.28: Measured activity of ^{90}Sr on test-sticks for both TK100 and Clevasol for both timescales; test-stick that were left for 4-weeks and test-sticks that were left to stand for

approximately 48 hours prior to sampling, as outlined in the original test-stick methodology (see section 3.3.1). Error bars represent uncertainty calculated from counting statistics.

Comparison of measured ^{90}Sr activities on both TK100 and Clevasol test-sticks between the two timescales (figure 4.28) reveal the same pattern as that seen for k' values (figure 4.26) where TK100 test-sticks repeats at both timescales perform similarly. The performance of both timescale TK100 test-sticks are also similar to 'after 48-hours' Clevasol (left to stand for ~48 hours), however, Clevasol test-sticks left to stand for 4 weeks show superior uptake of ^{90}Sr activity and again reasons as to why this is observed here are unknown. Future work looking at potential methods of 'conditioning' the Clevasol test-sticks as well as even different timescales may provide more information.

Overall, these results show that extractant stability over time is an important consideration in extractant candidature for application in test-stick technology. An extractant with poor stability over time can impact the shelf-life of the test-stick and therefore make it less suitable to be stored on-site ready for field deployment when required. These findings feed directly into future test-stick manufacturing techniques where extractant choice will be an important part of the manufacturing process.

4.5 Conclusion

A series of experiments have been carried out and presented here that look to assess the impact of the test-stick production process on test-stick performance. Additionally, work presented here has also provided a framework of factors for future developments in test-stick manufacturing to consider that have been found to be influential on test-stick performance. This includes the impact of particle distribution on the solid phase where more packing of extractant particles on the solid phase could potentially improve the precision of the test-stick performance. Furthermore, it was found that 'layering' occurred in the current test-stick manufacturing technique where instances of particles being mounted on top of each other were discovered. This can potentially impact the performance of the test-stick as the number of potential active sites has been decreased. A lack of control in mounting extractant particles evenly across the surface in a monolayer system means that variability in test-stick performance is present which was reflected in the %RSD values for TK100 (25%) and Clevasol (30%) in mass loading experiments via radiolabelling. Despite the observed variance in mass loadings being reflected in the reproducibility performance of both extractant test-sticks, this does not detract from the potential of test-stick technology as a rapid screening technique. The nature of on-site screening of samples does not require high precision as

seen in lab-based techniques such as ICP-MS (inductively-coupled mass spectrometer). On-site rapid screening techniques are required to simply distinguish whether a sample is potentially above a legislative threshold for the radionuclide of interest. In this project, the radionuclide of interest is ^{90}Sr and therefore test-stick technology must be capable of distinguishing whether samples contain ^{90}Sr activity above or below 1 Bq g^{-1}. If the test-sticks detect activity close to or above this threshold then further, off-site, analysis may be carried out to provide complex characterisation of the sample. If the sample does not contain ^{90}Sr activity close to 1 Bq g^{-1} then no further, off-site, analysis is required and the sample may be disposed of normally. Reproducibility experiments demonstrated that sample-to-sample variance was 32.0% for TK100 test-sticks and 25.9% for Clevasol test-sticks. These RSD% values are suitable for determining whether a sample has ^{90}Sr activity above or below the EPR 2016 guideline limits and therefore demonstrates the suitability of both extractant test-sticks as on-site rapid screening methods. Durability experiments provided information regarding the shelf-life of test-sticks and their suitability for remaining on standby until required. This analysis also provides initial information regarding the potential for test-stick technology to be applied in emergency response applications. TK100 test-sticks showed similar performance to normal conditions when test-sticks are manufactured 24 hours before sampling. Clevasol showed poor performance and demonstrated evidence of degradation in extractant performance over time. This formulated an important point of consideration for test-stick manufacture – extractant choice. Extractants must be selected based on a number of different factors including extractant stability as well as particle sizes. Experiments showed that smaller particle sized TK100 (50-100 µm versus the standard 100-150 µm TK100 used in this project) demonstrated better proportionality mechanism than its bigger particle sized TK100 sibling. Therefore, extractants that have smaller particle sizes may be selected over bigger particle sized extractants or extractants with a large particle size variance. However, if test-stick manufacture could be improved to allow tight monolayer packing of the extractant particles then particle sizes may not matter as much if particle size variability is low.

Chapter 5 Development and optimisation of test-stick deployment protocols

5.1 Abstract

The Nuclear Decommissioning Authority (NDA) has outlined in a recent document the need for initial characterisation to be carried out on-site and with result turnover within 24 hours. Test-stick technology looks to address this and provide a technique that can be deployed on-site and provide rapid screening of difficult-to-measure (DTM) radionuclides, such as ^{90}Sr, within the space of a few hours. Strontium-90 has been identified as one of the major contaminants in nuclear decommissioning sites due to being a pure beta-emitter as well as having high mobility and fission yield (~5.7 %). A rapid screening technique for this radionuclide would be beneficial for not only characterisation purposes and to aid waste sentencing but also for monitoring fingerprint stability. This study looks to monitor the current deployment methodology for test-stick technology and outline its operational conditions as well as its limits and propose methods to overcome this. An assessment of the sensitivity and precision of this technique, including for two extractant test-sticks, will also be evaluated to present the suitability of these extractants for test-stick rapid screening of ^{90}Sr. The two extractants used are TK100 (TrisKem International, France) and Clevasol (LemerPax, France) which represent two extractants which are capable of operating under neutral pH conditions and represent two different uptake mechanisms for ^{90}Sr: size exclusion (TK100) and cationic exchange (Clevasol). Test-stick technology looks to facilitate the NDA's goal of streamlining the characterisation process and propose a rapid screening approach that can be readily deployed on-site and provide significant savings in time and costs.

5.2 Introduction

The nuclear decommissioning programme in the UK currently being undertaken by the NDA is projected to cost >£100 billion and require more than 100 years to complete. A project of this magnitude has seen the NDA revise its decommissioning programme to identify areas and methods that could reduce the current forecasted costs of the project as well as shorten the current predicted timescale as much as possible. One of the strategies the NDA has identified as a viable method to lower project costs and time is to expedite waste characterisation. The NDA has outlined an objective to move majority of initial characterisation methods to in-*situ* and have results from these in-*situ* characterisation methods achieved within 24 hours. The target is to accomplish this for 70% of all initial characterisation by 2025, demonstrating the NDA's ambition to achieve this

goal. Test-stick technology looks to be a viable candidate to facilitate this target set out by the NDA by expediting waste characterisation and waste sentencing processes. Test-stick technology looks to mobilise industrially established extractant resin technologies, such as TK100, to provide a rapid screening technique for in-*situ* deployment and characterisation. This would mean providing a simple technique requiring almost no specialist knowledge to carry out timely on-site characterisation and therefore streamline on-site decommissioning processes. However, the development and success of test-stick technology hinges on the availability and performance of extractant technologies and therefore this will be the focus of this chapter.

The role of characterisation is to identify radionuclides and the extent of radionuclide contamination in samples obtained from nuclear decommissioning sites and facilitate waste segregation. Developing rapid screening techniques would expedite the role of characterisation as well as relieve the pressure faced by off-site specialist laboratories. Radiochemical labs face large sample intake and time-consuming processes such as delivery and receipt of samples. Analyses of samples through complex analytical methods (such as ICP-MS) often require 20 to 30 days for specialist labs to carry out the necessary analysis and compile the reports for the customer. Test-stick technology would look to alleviate this pressure on radiochemical labs by screening samples for activities above or below thresholds established by the appropriate legislation – i.e. EPR 2016. This would help determine whether the sample in question would require further, more complex, radiochemical analysis and therefore enable radiochemical labs to focus solely on these specific samples.

On-site radiometric analysis has predominantly been that of easy-to-measure (ETM) radionuclides which are screened via gamma detectors. Gamma emitting radionuclides generally require minimal sample preparation prior to analysis and therefore present minimal issues for in-*situ* and on-site characterisation to be carried out. However, for difficult to measure (DTM) radionuclides such as ^{90}Sr this is not the case and sample preparation is often required to prevent radiation absorption by surrounding matrix. Original analysis dating back to 1936 used fuming HNO_3 to isolate Sr from other species including Ca. This is due to Sr sharing similar chemistry to calcium (and therefore why ^{90}Sr is referred to as a 'bone seeker') and this is reflected in the difficulty faced in the past when isolating Sr for analysis before chromatographic extractants were developed. These chromatographic extractants presented a safer and easier method for Sr separation, compared to the fuming HNO_3 method, to be carried out in radiochemical labs. One of the most popular extractants for Sr separation was a crown ether – di-*t*-butyl dicyclohexyl-18-crown-6. Horwitz *et al.* presented work on this crown ether where they found this size-exclusion extractant to be capable of extracting Sr from solution at low pH (approximately ~8M HNO_3 equivalent). Since then, other extractants have been developed including novel cationic exchange extractants such as the boron-

based extractant Clevasol. Clevasol is an extractant formed of borane clusters with hydrogens in the borane clusters replaced by different functional groups that also offer an element of size exclusion to Clevasol's performance.

Monitoring test-stick performance under different conditions such as variable volume and chemical interferences provides insight into the current performance of both extractant test-sticks and will aid in optimising future operating procedures for test-stick technology. The work in this chapter will not only look to provide information regarding how the test-sticks perform but will also outline possible limitations of the technique and potential solutions to overcome this. The emphasis will essentially be on the extractants themselves; TK100 and Clevasol, and the analysis will surround these as the extractants are fundamental to the performance of the test-sticks. The effect of factors such as diffusion control and ionic interferences onto test-stick performance will provide further information regarding the operating conditions of the test-sticks and what their limitations may be. Assessment of test-stick loading capacity and sample volume would also provide further information regarding the test-sticks' current uptake efficiency and potentially how this could be improved. Overall, this chapter looks to evaluate current test-stick performance and provide a framework of optimisation for future test-stick methodology.

Performance of both extractant test-sticks will be evaluated through measurement of the partition coefficient, k'. The relationship between the k' value and the activities on the solid (A_s in Bq) and aqueous phase (A_{aq} in Bq) as well as the masses of both phases (M_s and M_{aq}, both in g) is given by:

$$\left(\frac{A_s}{A_{aq}}\right) = k' \times \left(\frac{M_s}{M_{aq}}\right)$$

This chapter aims to evaluate factors relating to testing condition and sample composition, such as exposure time, mixing / stirring, chemical interference, test-stick volume and stable Sr concentration that may impact k' and hence on the observed $\left(\frac{A_s}{A_{aq}}\right)$ ratio. Understanding how these factors impact on test stick performance are critical in developing robust test stick deployment procedures for routine monitoring applications.

5.3 Methodology

5.3.1 Test-stick manufacture

The test-sticks used in this project were manufactured from 4x1 cm^2 inert (cellulose acetate) supports which were coated with the extractive resin a 1x1 cm^2 active site at the edge of the test-stick support. An industrial spray adhesive was used to fix the extractive resin to the support. The

test-sticks were left to set for 24 to 48 hours in an airtight container which also allowed no sunlight in to minimise any complications to the test-stick manufacture. This 'setting' period also allowed the adhesive to set completely and bind the extractant onto the test-stick support – forming the solid phase of the test-stick. The full methodology for test-stick manufacture is shown in section 3.3.2.

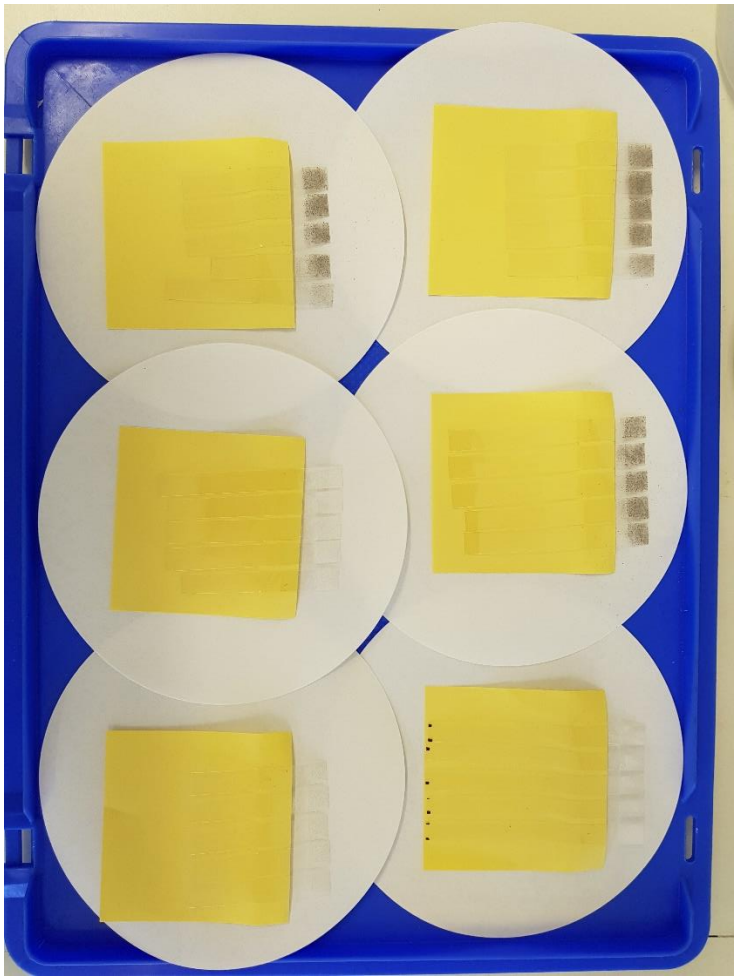

Figure 5.1: Image of manufactured test-sticks prior to allowing to set for 24 to 48 hours. White test-sticks represent TK100 test-sticks whilst dark test-sticks represent Clevasol test-sticks.

5.3.2 Experimental procedure

Uptake kinetics were investigated with test-sticks deployed at different contact time – 5, 10, 15, 20, 30, 40, 50, 60 and 1440 minutes. These contact times were selected to determine the optimum sampling time for test-stick deployment, where test-stick performance was appreciable within 24 hours to meet the goals of the NDA for rapid screening techniques. See section 3.3.4. for further details regarding the procedure.

Test-stick response was determined by deploying test-sticks, for both TK100 and Clevasol, in five samples with ^{90}Sr spikes of approximately 0.4, 0.8, 2.0, 4.0 and 8.8 Bq in a 4 mL sample volume.

These ^{90}Sr spikes are equivalent to 0.1, 0.2, 0.5, 1.0 and 2.2 Bq g^{-1} which correlates well with legislation threshold limits for ^{90}Sr (1.0 Bg g^{-1} in solids where test-sticks may application in rapid characterisation in acid leachates – further discussed in chapter 7) and therefore validates the application of test-stick technology to distinguish whether ^{90}Sr in nuclear site samples are above, or below, species waste sentencing thresholds. Test-sticks experiments in this work were carried out in a stirred system. Please refer to section 3.3 for further details.

Evaluation of the effect of agitation onto the test-stick system was conducted by deploying test-sticks into two sets of five samples each, where the activity of ^{90}Sr spike varied across these five samples (0.4, 0.8, 2.0, 4.0 and 8.8 Bq in 4 mL sample volumes). The performance of these test-sticks with increasing activity of ^{90}Sr was monitored whilst introducing agitation to one of the set of samples to monitor its effect and whether test-stick performance increased due to agitation. Further information regarding the procedure is found in section 3.3.

An assessment of the effect of variable volume on the performance of the test-sticks was carried out. The variable volumes examined were 1.0, 1.5, 2.0, 3.0 and 4.0 mL and both TK100 and Clevasol test-sticks were used in this experiment set. This experimental work provides information regarding the optimal sample volume to improve test-stick performance whilst still being compatible with the 5 mL sample vial design. For further information regarding the procedure used please refer to section 3.3.

Strontium loading capacity was evaluated by preparing solutions with stable Sr concentrations of 0.01, 0.1, 1.0, 10 and 100 ppm. Test-sticks were then sampled on these solutions and the results obtained. An extension of the stable Sr concentration range was carried out for Clevasol due to its higher loading capacity (according to LemerPax – the manufacturer) of 243 mg g^{-1} for ^{90}Sr compared to TK100 (8 mg g^{-1} Sr). The extended stable Sr concentration range incorporated the following concentrations: 100, 200, 500, 700 and 1000 ppm. For the full procedure please refer to section 3.3.

Chemical interferences were prepared individually at concentrations reflecting those found in Sellafield groundwater. The chemical interferences chosen were Na, K, Ca and Mg and they were chosen due to both their chemical similarity (group 1 and 2 metals – Sr is a group 2 metal) and prevalence in groundwater. Experiments into chemical interferences provides insight into the performance of both extractive resin test-sticks. This includes how well the test-sticks perform in the presence of ionic interferences that are likely to be present when test-sticks are deployable on the field. For further information please refer to section 3.3 and for ionic interference concentrations in Sellafield groundwater please refer to section 3.1.

The experimental procedure involved a standard batch-uptake procedure carried out for nearly all experiments in this chapter. Once manufacture of the test-sticks were complete, the test-sticks were submerged into 5 mL vials containing the sample for approximately 60 minutes unless stated otherwise (and for uptake kinetic experiments). After sampling was complete, the test-sticks were removed from the sample, washed with Milli-Q water to remove any residual non-adsorbed sample from the test-stick and the solid phase cut into a 22 mL scintillation vial. Gold star scintillation cocktail was added up to 20 mL and the sample was counted in LSC instrumentation for approximately 60 minutes, unless stated otherwise. The full detailed methodology for all experiments is discussed in section 3.3.3.

5.3.3 Data analysis and processing

WinQ software was used as the method for data acquisition in LSC instruments which provided data including CPM (counts per minute) and measurement times. These data were then extracted from registry files produced by the WinQ software during analysis of the samples via LSC. The activity of ^{90}Sr was calculated taking into account ^{90}Y ingrowth and counting efficiencies. Most experimental data shown involved secondary counts of the samples taken after secular equilibrium had been established to account for any ^{90}Y uptake by the extractants. However, in rare cases this was not possible and therefore a mathematical approach was used to deconvolve the ^{90}Sr and ^{90}Y activities.

To account for ^{90}Sr and possible ^{90}Y uptake by the extractants the following simultaneous equations were used to solve for this which included using two different count times.

Therefore, the following equations were used:

$$CPS_{t_1} = k_1 A_{Sr-90} + k_2 A_{Y-90}$$

$$CPS_{t_2} = k_3 A_{Sr-90} + k_4 A_{Y-90}$$

Where,

$$CPS_{t_x} = \text{counts per second at time x}$$

$$k_1 = (1 - e^{-\lambda t_1}) \cdot \varepsilon_{Sr-90} \cdot \varepsilon_{Y-90}$$

$$k_2 = e^{-\lambda t_1} \cdot \varepsilon_{Y-90}$$

Where, λ is decay constant in s^{-1}, t is time in seconds and ε is counting efficiency for specific species. The above equations can be derived into the following equation:

$$A_{Sr-90} = \left(\frac{c_1 - \frac{k_2 c_2}{k_4}}{k_1 - \frac{k_2 k_3}{k_4}} \right)$$

Additionally, an equation to calculate the activity of ^{90}Y was also derived and used:

$$A_{Y-90} = \left(\frac{c_1 - k_1 A_{Sr-90}}{k_2} \right)$$

The derivation for the above equations is shown in the appendix for reference. It must be noted that these calculations were not carried out for experimental data sets unless stated so.

5.4 Results and Discussion

5.4.1 Uptake kinetics

Uptake kinetics underpin the importance of rapid screening techniques as it fundamentally determines the time required for optimal uptake of the species of interest. Determining the uptake kinetics and by extension the factors influencing how quickly kinetic equilibrium is achieved can aid in increasing the uptake kinetics of a technique and work under a time frame that is practical for deployment. Optimum uptake kinetics balances the performance of the extractant(s) test-sticks alongside the requirements of on-site challenges. The NDA has outlined under the recent baseline document the need for rapid screening techniques to provide characterisation of the species of interest within 24 hours [7]. Therefore, experiments in this section provide information regarding the uptake kinetics of both extractant test-sticks over the same time intervals – 5, 10, 15, 20, 30, 40, 50, 60 and 1440 mins (24 hours).

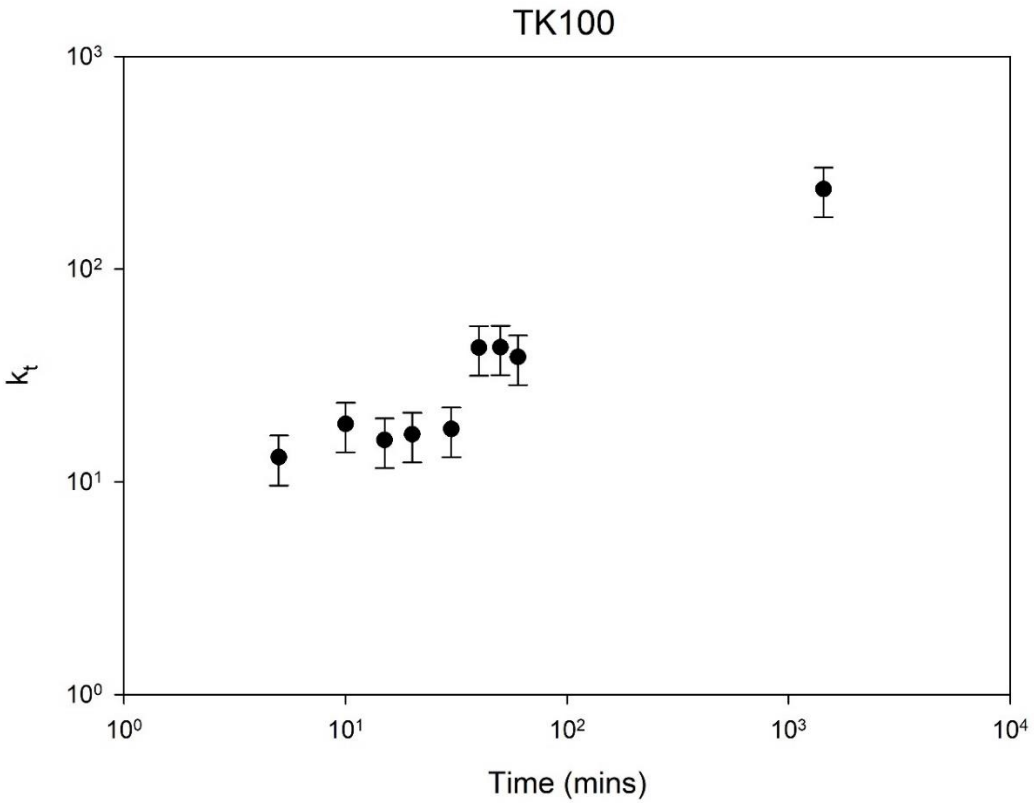

Figure 5.2: Effective distribution coefficient of ^{90}Sr uptake on TK100 test-sticks, from 5 mins to 24 hours. Activity of ^{90}Sr spike = approx. 5.0 Bq. Error bars represent mass loading uncertainties determined in mass loading experiments (see section 4.4.3).

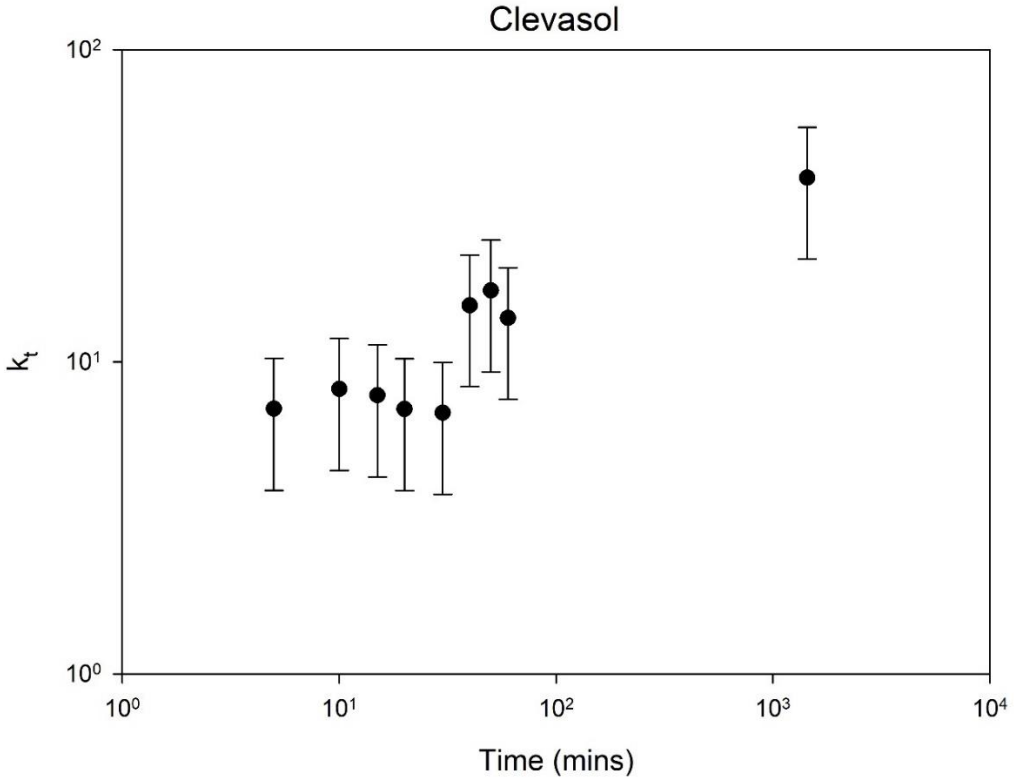

Figure 5.3: Effective distribution coefficient of ^{90}Sr uptake on Clevasol test-sticks, from 5 mins to 24 hours. Activity of ^{90}Sr spike = approx. 5.0 Bq. Error bars represent mass loading uncertainties determined in mass loading experiments (see section 4.4.3).

The effective distribution coefficient was calculated using the following formula:

$$k_t = \left(\frac{A_{stick}}{[A_{aq}]_t \times M_s}\right)$$

Where k_t is the effective distribution coefficient in g^{-1}, A_{stick} is the activity on the solid phase in Bq, $[A_{aq}]_t$ is the activity in the aqueous phase at time *t* in Bq and M_s is the mass of the solid phase in g.

Effective distribution coefficient values showed TK100 test-sticks to have a small plateau in uptake kinetics achieved between 40 to 60 mins where k_t values fluctuated between 39 and 43 before strontium partitioning increased afterwards to a k_t = 238 at 24 hours (1440 mins) (figure 5.2). Reasons as to why k_t values increase after 24 hours may be due to diffusion effects influencing k_t over timescales > 1 hour, improving uptake - this is further investigated and discussed in chapter 6. Despite this, the kinetic behaviour of TK100 test-sticks agrees well with those observed by Surman *et al.* where TK100 reached equilibrium at approximately 30 mins. It was also noted by Surman *et al.* that this was noticeably longer than Sr-resin, the predecessor to TK100, which reached kinetic equilibrium within 3 minutes but required using 5M HNO_3 whilst TK100 operates at neutral pH conditions. Analysis was carried out using mass loadings determined in prior experiments (see

section 4.4.2) where the mass loading for TK100 test-sticks was calculated to be 1.6 ± 0.4 mg. The noticeably lower effective distribution coefficients could be due to factors such as the manufacture of the test-sticks where spray adhesive could have affected active site availability along with extractant loading variability. This extractant loading variability has been considered in uncertainty calculations represented by the error bars in figures 5.2 and 5.3. Factors regarding the test-stick manufacture and methods to improve this process were discussed in chapter 4. The data shown here agrees well with Surman *et al.* and shows that mounting TK100 on test-sticks does not substantially delay the extractant reaching kinetic equilibrium allowing for the extractant to operate closer to its design. However, this should not detract from the value in these experiments which serve to demonstrate a kinetic uptake profile of ^{90}Sr on TK100 test-sticks over increasing time sampling intervals. Despite the observed lower effective distribution coefficients, the test-sticks still demonstrated appreciable uptake of ^{90}Sr around 40 to 60 minutes and introduction of more efficient and robust agitation methods and test-stick manufacture could potentially improve this.

Clevasol test-sticks' kinetics showed lower k_t values compared to TK100 test-sticks, with $k_t = 38$ at 24 hours, versus $k_t = 238$ at 24 hours for TK100 test-sticks. Mass loadings used for Clevasol test-sticks were 3.6 ± 0.4 mg which were determined in previous mass loading experiments (see section 4.4.2). Interestingly, despite the differing uptake mechanism adopted by TK100 (size exclusion) and Clevasol (cationic exchange), Clevasol test-sticks were also found to reach a small plateau in kinetic uptakes at time intervals of 40 to 60 mins (figure 5.3) suggesting a limiting step in ^{90}Sr uptake which may be caused by mass transfer factors where ^{90}Sr is required to diffuse through the solid phase. The increase in k_t values after 24 hours (1440 mins) may, again, be down to diffusion control factors like that discussed above for TK100 however this is further investigated in the next chapter (chapter 6). Additionally, the rough surface topology of Clevasol test-sticks may also mean that diffusion through the solid phase to enable chemical transfer between the sample and the solid phase is slower compared to TK100 which contains smooth bead-like particles (see section 4.4.1). However, this potentially still means that Clevasol test-stick sampling can be carried out in 40 minutes instead of 60 minutes. Furthermore, this data suggests that despite both extractants utilising different methods of extracting ^{90}Sr, both extractant test-sticks can be deployed for 40 to 60 minutes to achieve optimal uptake performance for rapid screening applications. This means that test-stick sampling can comply comfortably within the NDA target of carrying out initial characterisation in-*situ* and obtaining results within 24 hours, regardless of which extractant test-stick is deployed.

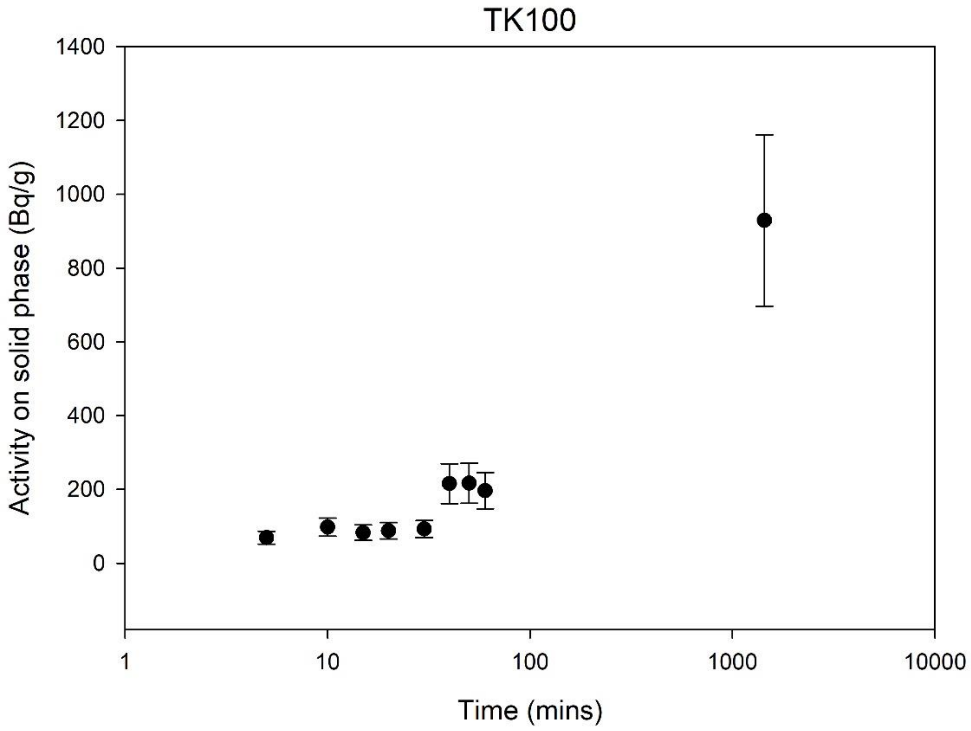

Figure 5.4: Measured activity of ^{90}Sr on TK100 test-sticks from 5 mins to 24 hours. Activity of ^{90}Sr spike = approx. 5.0 Bq. Error bars represent mass loading uncertainties determined in mass loading experiments (see section 4.4.3).

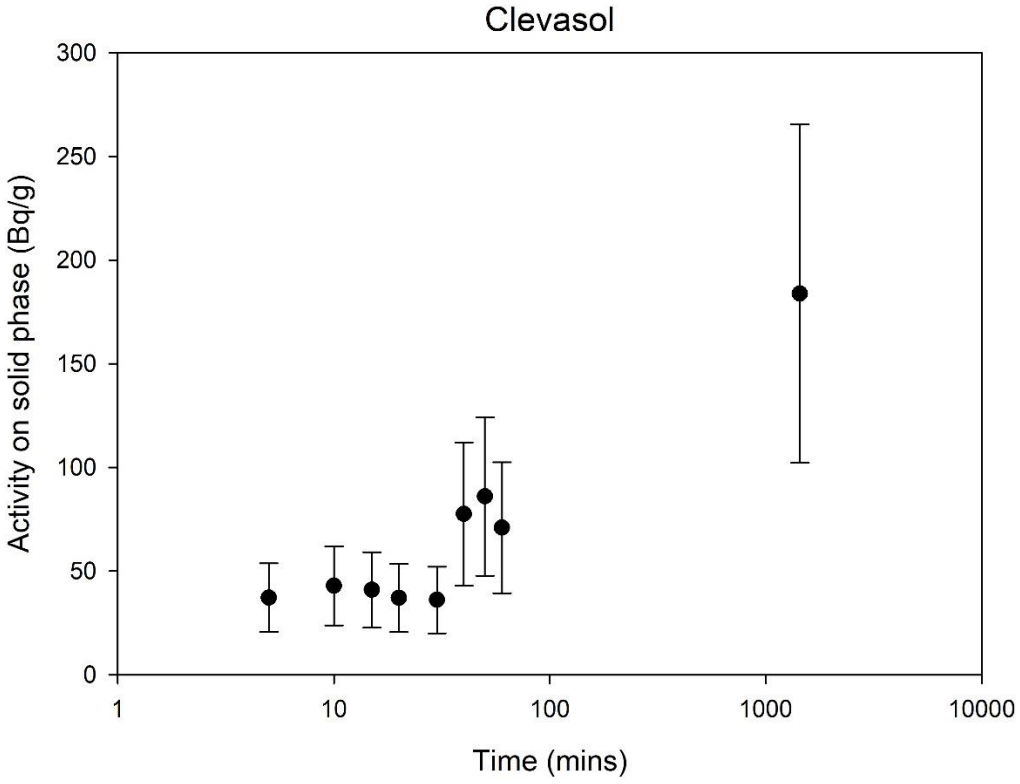

Figure 5.5: Measured activity of ^{90}Sr on Clevasol test-sticks from 5 mins to 24 hours. Activity of ^{90}Sr spike = approx. 5.0 Bq. Error bars represent mass loading uncertainties determined in mass loading experiments (see section 4.4.3).

TK100 test-sticks demonstrated high ^{90}Sr activity loadings of approximately 210 ± 53 Bq g^{-1} for time intervals of 40 to 60 mins further indicating that sampling time could be reduced to 40 minutes and performance would be observably similar (figure 5.4). Kinetic equilibrium was reached after 24 hours with ^{90}Sr activity loadings of 929 ± 232 Bq g^{-1}. Clevasol test-sticks showed comparatively lower ^{90}Sr activity loadings of 78 ± 34 Bq g^{-1} for time intervals of 40 to 60 minutes (figure 5.5). Clevasol test-sticks' kinetic performance also demonstrated the potential for test-stick sampling time to be reduced to as low as 40 minutes and provide similar performance to 60-minute sampling times. Kinetic equilibrium for Clevasol test-sticks was reached after 24 hours with ^{90}Sr activity loadings of 184 ± 82 Bq g^{-1}. Analysis of ^{90}Sr loadings for both test-sticks showed similar findings to that of effective distribution coefficients where TK100 test-stick kinetic performance was superior to Clevasol test-sticks. However, the observed plateau in test-stick performance at 40 to 60 minutes time intervals for both extractants is an important consideration for the development of test-stick technology's standard operating procedure. Lowering the sampling time even further without impacting the performance of the test-sticks will only serve to expedite on-site characterisation of important waste packages as well as the potential for monitoring fingerprint ratio stability. It is interesting to note that this 'plateau' at 40 to 60 minutes suggests that limitations in mass transfer may also be present for TK100 test-sticks, where diffusion of the ^{90}Sr species through the solid phase is slow as active sites become occupied. The large variance in the activities obtained in these experiments are attributed to mass loading errors and raises the importance of test-stick manufacture which was discussed in chapter 4. Overall, uptake kinetic studies of both TK100 and Clevasol test-sticks showed that sampling times could be potentially lowered even further to 40 minutes and still provide similar performance to 60-minute sampling times. This means that test-stick technology comfortably complies with the NDA's objective to provide on-site screening results for DTM radionuclides within 24 hours.

5.4.2 Test-stick response

An important aspect of test-stick technology concerns the range of operability of the test-sticks, especially their capability to characterise samples in-*situ* and provide radiochemical information for these samples. This requires investigating the test-stick activity response and evaluating the applicability of test-stick technology in determining whether sample activity is above, or below specific thresholds outlined by legislation (such as the EPR 2016 guidelines). The data presented below investigates the performance of both extractive resin test-sticks, stirred, over specific activity ranges and determines the lowest ^{90}Sr activity(s) that the test-sticks can begin to operate at. A further consideration for this work, especially for TK100, is ^{90}Y uptake. Work by Surman *et al.* showed TK100 extractant to extract ^{90}Y preferably over ^{90}Sr at low HCl (~0.01M) and HNO_3

(~0.01M) concentrations. Therefore, this will be an important consideration when evaluating the test-stick response to variable ^{90}Sr activities. For this work, simultaneous equations described in section 5.3.3. were solved to account for both ^{90}Sr and ^{90}Y activities on both extractant test-sticks.

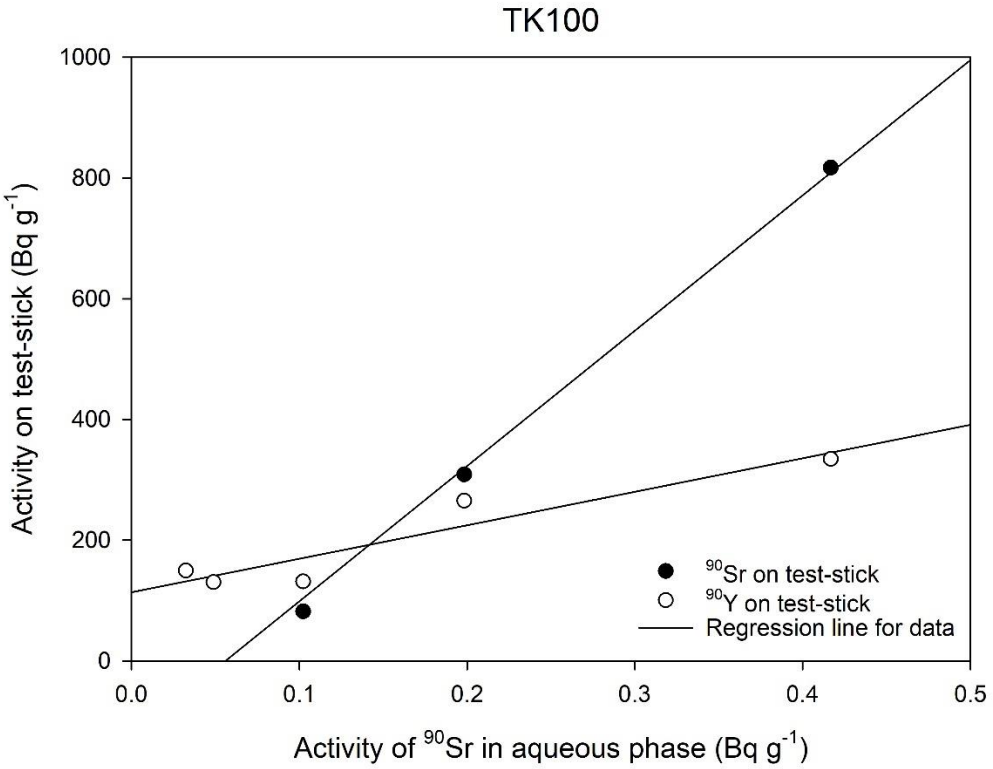

Figure 5.6: Measured activities of ^{90}Sr and ^{90}Y on stirred TK100 test-sticks and aqueous phase. Missing data points correspond to values below zero indicating no species present. Spiked ^{90}Sr activities: approximately 0.4, 0.8, 2.0, 4.0 and 8.8 Bq

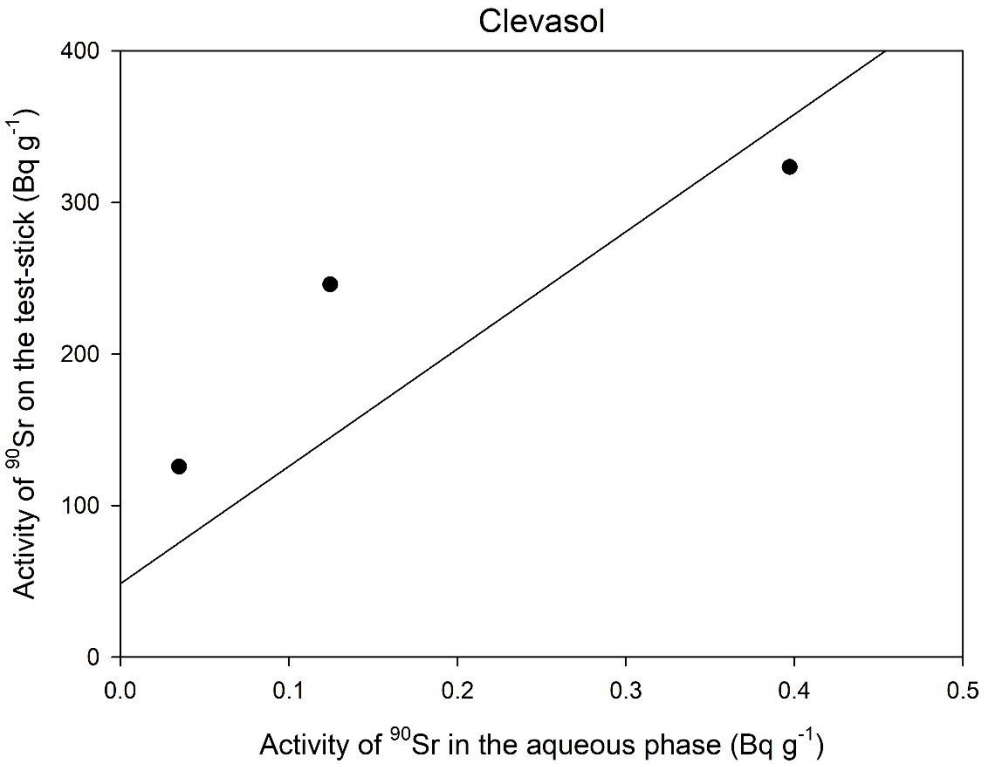

Figure 5.7: Measured activities of ^{90}Sr on stirred Clevasol test-sticks and aqueous phase. Missing data points correspond to values below zero indicating no ^{90}Sr present. Spiked ^{90}Sr activities: approximately 0.4, 0.8, 2.0, 4.0 and 8.8 Bq

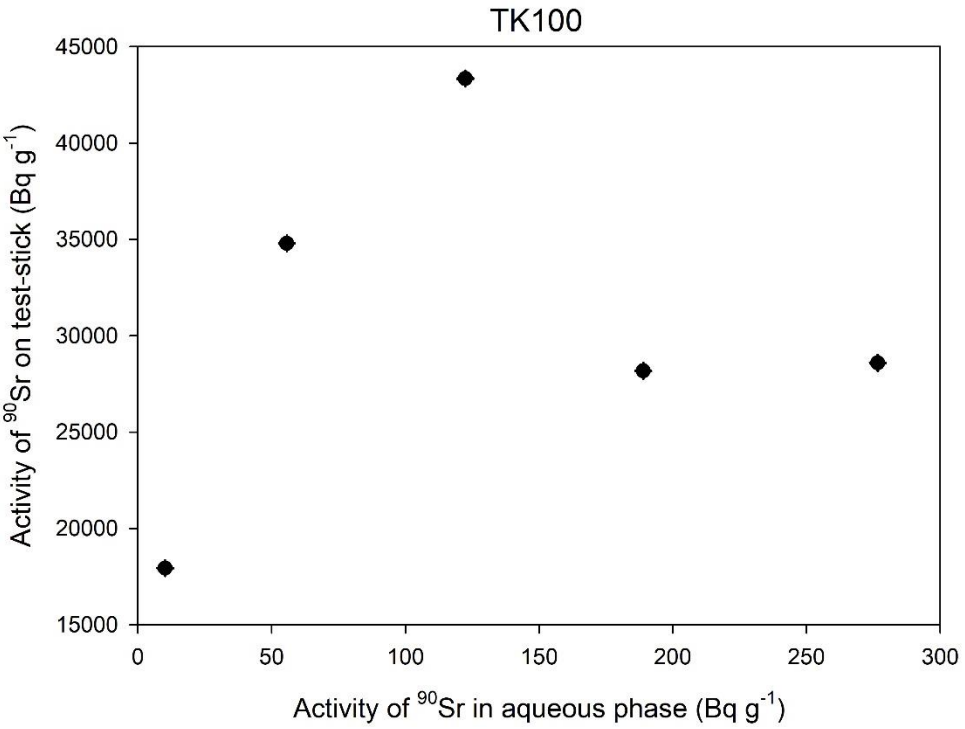

Figure 5.8: Measured activities of ^{90}Sr on stirred TK100 test-sticks and aqueous phase. Spiked ^{90}Sr activities: approximately 150, 450, 775, 1100 and 1550 Bq.

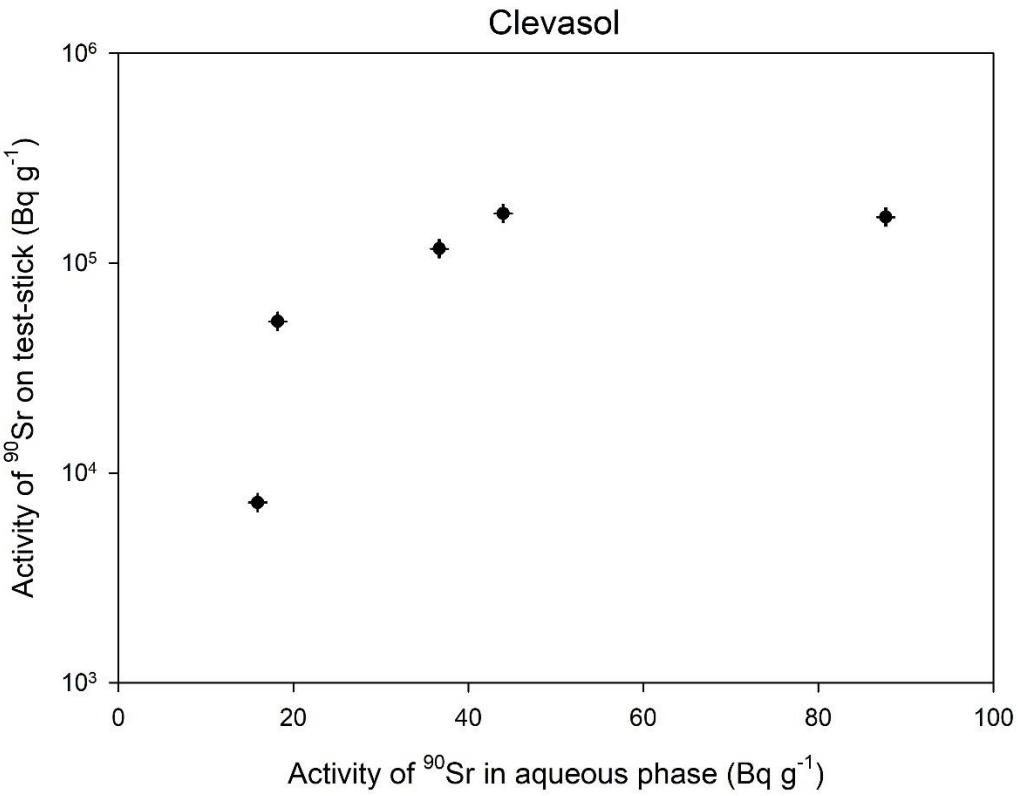

Figure 5.9: Measured activities of ^{90}Sr on stirred Clevasol test-sticks and aqueous phase. Spiked ^{90}Sr activities: approximately 150, 450, 775, 1100 and 1550 Bq.

Activity response of stirred TK100 test-sticks showed loadings of both ^{90}Sr and ^{90}Y on the test-sticks with regression analysis finding ^{90}Sr (R^2 = 0.998) uptake to be more proportional than that of ^{90}Y (R^2 = 0.889). Despite Surman *et al.* finding ^{90}Y to be preferably extracted over ^{90}Sr in low acid concentrations, this was only observed for low activity spikes of 0.4 and 0.8 Bq ^{90}Sr. If ^{90}Y uptake is of concern, then a simple method to circumvent this was suggested by Surman *et al.* which involved washing the extractant with 10 mL of 8M HNO_3. This solution could be easily adopted into test-stick methodology as part of the test-stick wash process where TK100 test-sticks could be washed with concentrated nitric acid, as opposed to Milli-Q water post-sampling. This test-stick wash method alteration would allow both TK100-bound ^{90}Y as well as any unbound radiochemical residue still present on the test-stick to be washed off and improve TK100 test-stick performance. Clevasol test-sticks showed no ^{90}Y uptake despite being a cationic exchange resin. This may be due to Clevasol preferably extracting $^{90}Sr^{2+}$ over $^{90}Y^{3+}$ where exchange of two oxonium ions (H_3O^+) may be more favourable to carry out than the exchange of three oxonium ions. Clevasol test-sticks demonstrated a poorer linear relationship (R^2 = 0.739) between activity of ^{90}Sr on the test-stick and activity of ^{90}Sr in the aqueous phase, however as with TK100 test-sticks, several data points were below zero showing that at low spike activities both extractant test-sticks struggled to extract ^{90}Sr. Both extractant test-sticks showed measurable uptake ^{90}Sr spikes of 2.0 Bq (which equates to 0.5 Bq g^{-1}

^{90}Sr) onwards which correlates well with the legislative threshold of 1.0 Bq g^{-1} of ^{90}Sr provided by the EPR 2016.

This test-stick data also demonstrates the proportional mechanism in action where an increase in the activity of ^{90}Sr in the aqueous phase is reflected in a proportional increase in the activity of ^{90}Sr adsorbed onto the test-stick. This relationship is demonstrated in the equation below:

$$A_{s,t} = b_t \times [A_{aq}] \therefore \frac{A_{s,t}}{b_t} = [A_{aq}]$$

Where $A_{s,t}$ is the activity of the radiochemical species on the test-stick at time *t* in Bq, b_t is the proportional constant for time *t* in Bq mL Bq^{-1} and $[A_{aq}]$ is the activity of the radiochemical species in the aqueous phase (sample) in Bq mL^{-1}.

The proportional mechanism forms the fundamental basis of test-stick technology which aims to characterise the activity of the radiochemical species of interest (^{90}Sr in this case) in samples via a proportional mechanism instead of a quantitative process. An increase in the activity of ^{90}Sr in the sample will reflect in a proportional increase in ^{90}Sr detected on the test-stick after sampling has taken place – proportional mechanism. The proportional constant, b_t, can be derived from experimental work and used to convert the activity of ^{90}Sr found on the test-stick to calculate the theoretical activity of ^{90}Sr in the original sample. This calculated activity of ^{90}Sr would be compared against legislative thresholds, including accounting for measurement error, and determine whether ^{90}Sr activity of the sample is below the threshold or if further off-site analysis is required. The table below shows calculated values from the data obtained in this section. Please note the units.

Table 5.1: Calculated proportionality constant, b_t, for both extractive resin test-sticks for test-stick response experiments. Please note that TK100 test-sticks under a higher activity range of ^{90}Sr did not demonstrate linearity in the results obtained.

Test-stick	^{90}Sr activity range (Bq)	b_t constant (Bq mL Bq^{-1})
TK100	0.4 to 8.8	1.709
Clevasol	0.4 to 8.8	0.825
TK100	150 to 1550	n/a
Clevasol	150 to 1550	7.717

Repeat activity response experiments were carried out with increased ^{90}Sr spike activities to investigate when test-stick ^{90}Sr uptake performance would begin to stabilise, and the proportional mechanism would no longer operate (Figure 5.8 and 5.9). The proportional mechanism could stop

working if the environment on the extractive resin changes – this includes saturation of the extractive resin. TK100 test sticks showed ^{90}Sr loadings increasing until reaching >1 kBq ^{90}Sr spikes where ^{90}Sr loadings on TK100 test-sticks began to decrease rapidly. Clevasol test-sticks on the other hand showed ^{90}Sr loadings to increase up to >1 kBq ^{90}Sr spikes before ^{90}Sr loadings stabilised. These observed variations in ^{90}Sr loadings across both extractant test-sticks over high ^{90}Sr spikes may be due to the disparity in extractant loading capacities between both extractants – TK100 (8 mg g^{-1}) and Clevasol (3.5 meq = 243 mg g^{-1} for ^{90}Sr). This work provides useful insight into the possibility of test-stick application in sampling materials that were either used or encountered higher activity level waste and the possibility of applying test-stick technology to other aspects of nuclear decommissioning characterisation work with higher activities.

5.4.3 Diffusion control

Application of test stick technology for DTM screening relies on a test stick activity that is proportional to the activity of the target nuclide in solution. In addition to thermodynamic controls, the response may be impacted by the rate of diffusion of the analyte from the bulk solution to the extractant on the test stick. Ensuring that the system is well-mixed and that there is no significant diffusion gradient around the test stick active area would improve the linearity in response. This would consequently improve the accuracy and reproducibility of ^{90}Sr activity measurement in the sample using the measured activity of ^{90}Sr on the test-stick. One method thought to improve test-stick performance in this way is by introducing agitation to the system. Agitation could be introduced by either manually stirring or using automated 'rollers' to agitate the test-stick during sampling and improve test-stick performance. This section looks to investigate and compare an unstirred system vs a stirred (via automated rollers) system for both extractant test-sticks and monitor the impact of introducing agitation to both extractant test-sticks' performance. Simultaneous equations described in section 5.3.3. were used to account for both ^{90}Sr and ^{90}Y activities on both extractant test-sticks for this section.

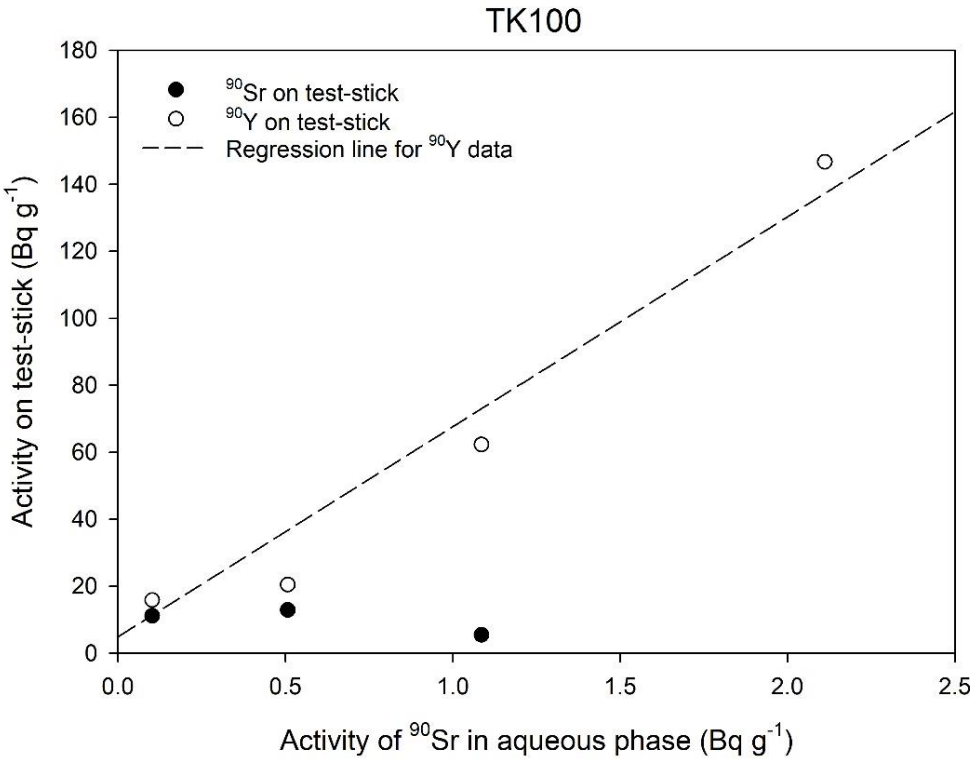

Figure 5.10: Measured activity of ^{90}Sr loadings on TK100 test-sticks in an unstirred system. Spiked ^{90}Sr activities = approximately 0.4, 0.8, 2.0, 4.0 and 8.8 Bq

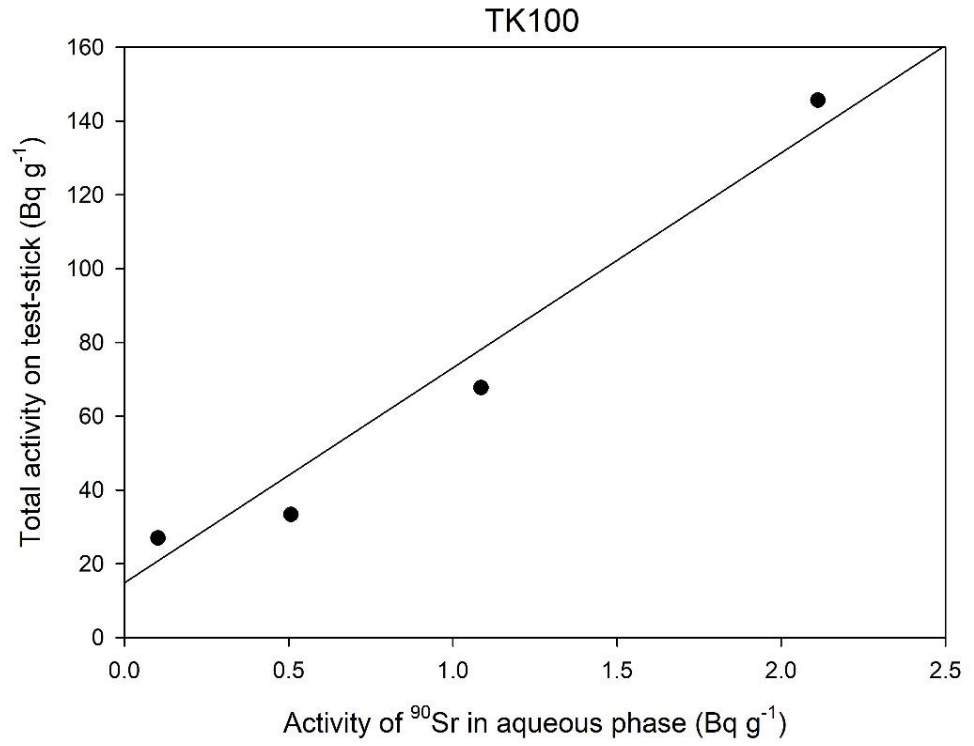

Figure 5.11: Measured activity of total loadings (^{90}Sr + ^{90}Y) on TK100 test-sticks in an unstirred system. Spiked ^{90}Sr activities = approximately 0.4, 0.8, 2.0, 4.0 and 8.8 Bq

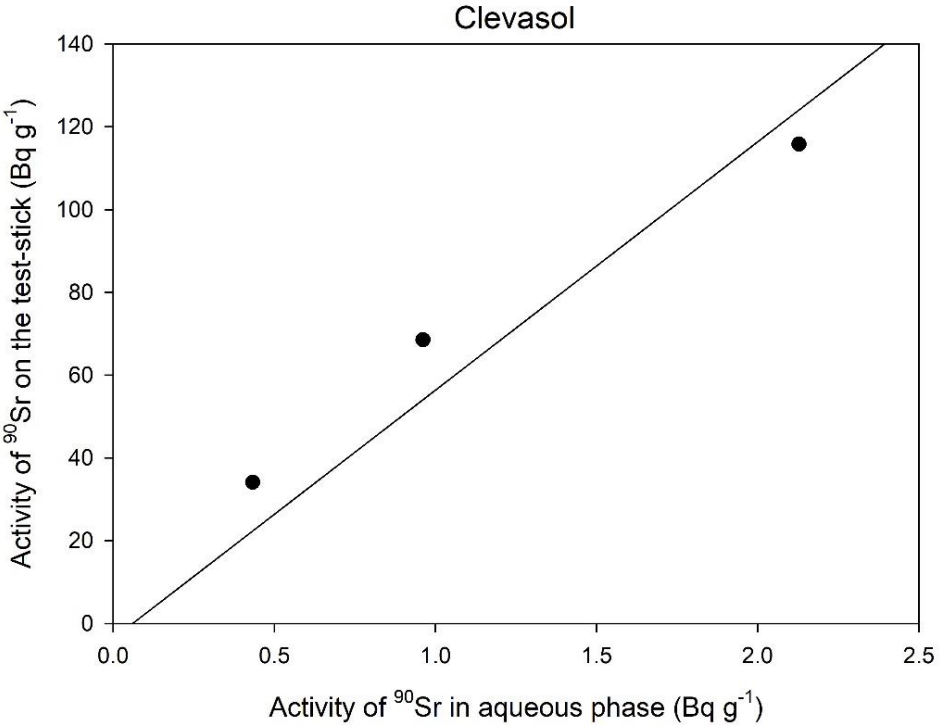

Figure 5.12: Measured activity of ^{90}Sr loadings on Clevasol test-sticks in an unstirred system. Spiked ^{90}Sr activities = approximately 0.4, 0.8, 2.0, 4.0 and 8.8 Bq

Initial experiments investigated both extractant test-sticks' performance in an unstirred system. TK100 test-sticks struggled to uptake ^{90}Sr over the activity range with ^{90}Y outcompeting the ^{90}Sr for uptake. Preferential uptake of ^{90}Y by the unstirred TK100 test-sticks agrees well with the work carried out by Surman *et al.* who showed that at low acid concentrations ^{90}Y uptake outcompetes ^{90}Sr uptake. No linear relationship was observed for ^{90}Sr uptake whilst ^{90}Y uptake demonstrated good linearity with an R^2 = 0.734. Analysis of total activity loadings on TK100 test-sticks in an unstirred system revealed a linear relationship (R^2 = 0.804) primarily due to ^{90}Y uptake. However, this data also demonstrated that TK100 test-sticks (in an unstirred system) could still be viable if ^{90}Y:^{90}Sr ratios were calculated and utilised in combination with the proportionality constant, b_t, to calculate an approximation of ^{90}Sr present in the sample.

For example:

Hypothetical ratio of ^{90}Y:^{90}Sr in TK100 test-sticks = 0.8

Proportionality constant, b_t = 0.125 Bq mL Bq^{-1}

Measured total activity in TK100 test-stick = 0.225 Bq

Using the proportional mechanism equation (for test-sticks) below,

$$A_{s,t} = b_t \times [A_{aq}] \therefore \frac{A_{s,t}}{b_t} = [A_{aq}]$$

$$0.225 \text{ Bq } \times 0.8 = 0.180 \text{ Bq of Sr-90 } \left(\frac{0.180 \text{ Bq}}{0.125 \text{ Bq g mL Bq}^{-1}}\right) = 1.440 \text{ Bq of Sr-90 in the sample}$$

The above example is a simplified demonstration of a possible method of utilising TK100 test-sticks in an unstirred system to screen for ^{90}Sr in aqueous samples. This theoretical ^{90}Y:^{90}Sr, much like the proportionality constant, would be dependent on factors such as sample matrix and type of extractant test-stick. This example forms a feasible path of future work for test-stick technology that would aim to account for uptake of ^{90}Y and subtract from total activity to give the true activity of ^{90}Sr on the test-sticks and by extension the sample itself. Clevasol test-sticks showed a good linear relationship between the activity of ^{90}Sr on the test-stick and the aqueous phase (R^2 = 0.946) and suggests that agitation is not required to achieve a proportional mechanism with these extractant test-sticks. This is a beneficial advantage of Clevasol test-sticks and a factor to take into consideration for Clevasol as a test-stick extractant candidate for ^{90}Sr screening.

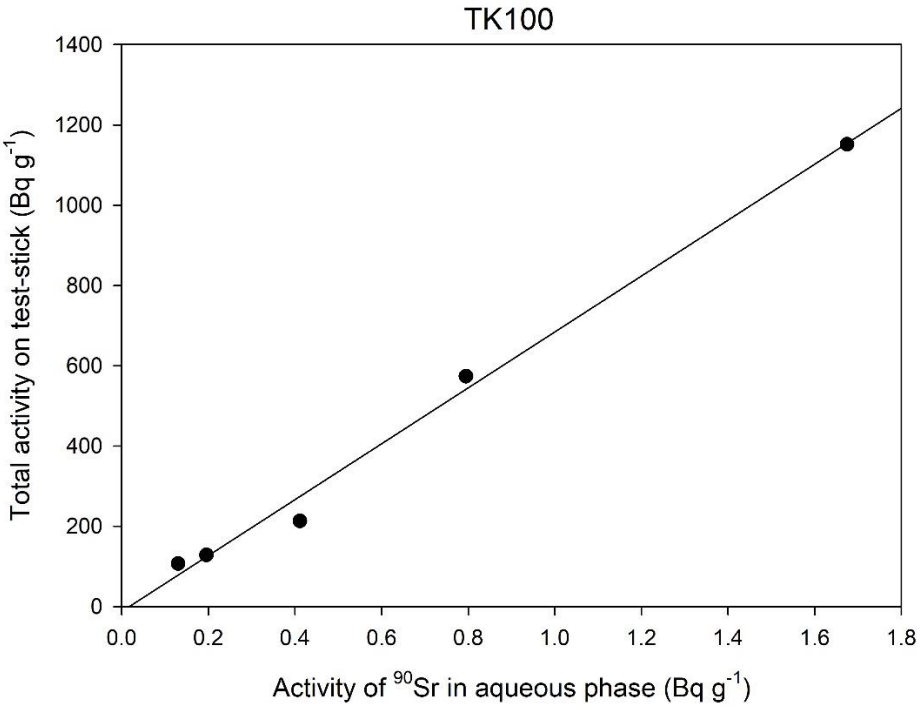

Figure 5.13: Measured activity of total loadings (^{90}Sr + ^{90}Y) on TK100 test-sticks in a stirred system. This figure combines the data points from figure 5.6. Spiked ^{90}Sr activities = approximately 0.4, 0.8, 2.0, 4.0 and 8.8 Bq

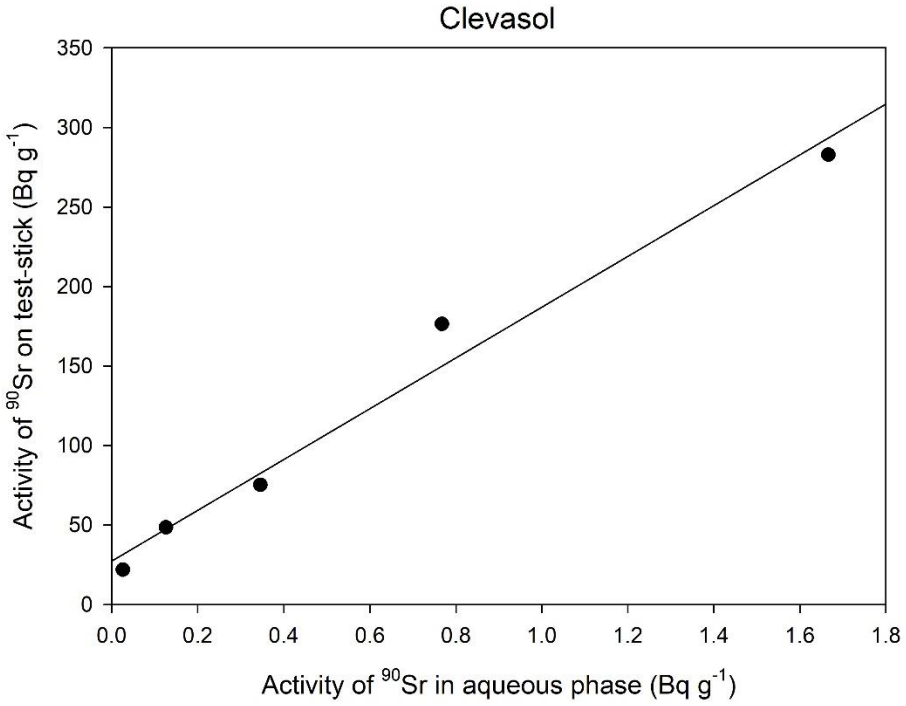

Figure 5.14: Measured activity of ^{90}Sr loadings on Clevasol test-sticks in a stirred system. Spiked ^{90}Sr activities = approximately 0.4, 0.8, 2.0, 4.0 and 8.8 Bq

Introduction of agitation to TK100 test-sticks improved ^{90}Sr uptake performance and introduced a linear uptake of ^{90}Sr with increasing activity of ^{90}Sr spikes. Furthermore, a stronger linear relationship for ^{90}Sr (R^2 = 0.998) versus ^{90}Y (R^2 = 0.889) was observed suggesting that introducing agitation resolved the previous observations where ^{90}Y outcompeted ^{90}Sr for uptake onto TK100 test-sticks in an unstirred system (please refer to figure 5.6 for this data). Linearity of total activity loadings on TK100 test-stick also improved, as a reflection of the improved ^{90}Sr uptake, from R^2 = 0.804 to 0.993. These findings strongly suggest that introducing a simple concept such as agitation that is easy to integrate into test-stick methodology can improve TK100 test-stick performance greatly.

Clevasol test-sticks retained their linear relationship (R^2 = 0.979) in a stirred system which agrees well with unstirred experiments (R^2 = 0.946) as Clevasol test-sticks had already shown strong linearity in unstirred systems between loadings of ^{90}Sr on the test-sticks and ^{90}Sr spikes. Therefore, results suggest that agitation may not be as important for Clevasol test-sticks as it is for TK100 test-sticks where no linearity of ^{90}Sr uptake is present if there is no agitation of the system during sampling. These findings suggest that Clevasol test-sticks may have applications in sampling large bodies of water, such as old fuel ponds, directly without the need to agitate the entire system. These findings are helpful as they assist in optimising test-stick methodology moving forward including incorporating agitation into the test-stick methodology as well as suggesting further possible in-*situ* applications of Clevasol test-stick sampling. Furthermore, a theoretical

mathematical approach to utilising TK100 test-sticks in unstirred systems is also presented and is a point of consideration moving forward for future work in the potential application of TK100 test-sticks in unstirred systems.

5.4.4 Variable volume

Test stick response may be impacted by the total sample volume that the test stick is exposed to. Optimisation of the aqueous test volume for test-stick performance may aid in designing future test-stick product kits ready for field deployment. The ratio between the test-stick active site (normally 1x1 cm) and the sample volume (~4 mL) has remained constant throughout majority of experiments in this project and therefore a series of different volumes have been investigated. These different volumes will help to determine which volume provides the highest uptake efficiency of ^{90}Sr for both extractant test-sticks. It must be noted that the central focus of this work is still for the development of a mobile rapid screening technique and therefore must be kept in consideration throughout this investigation. This means that test-stick optimal volumes must not exceed the maximum volume of the 5 mL vial as it is unlikely that test-sticks may be able to operate at higher volumes due to being able to only 'see' a local volume of solution. These experiments will help to determine what that local volume of solution is. Sample volumes investigated were 1.0, 1.5, 2.0, 3.0 and 4.0 mL.

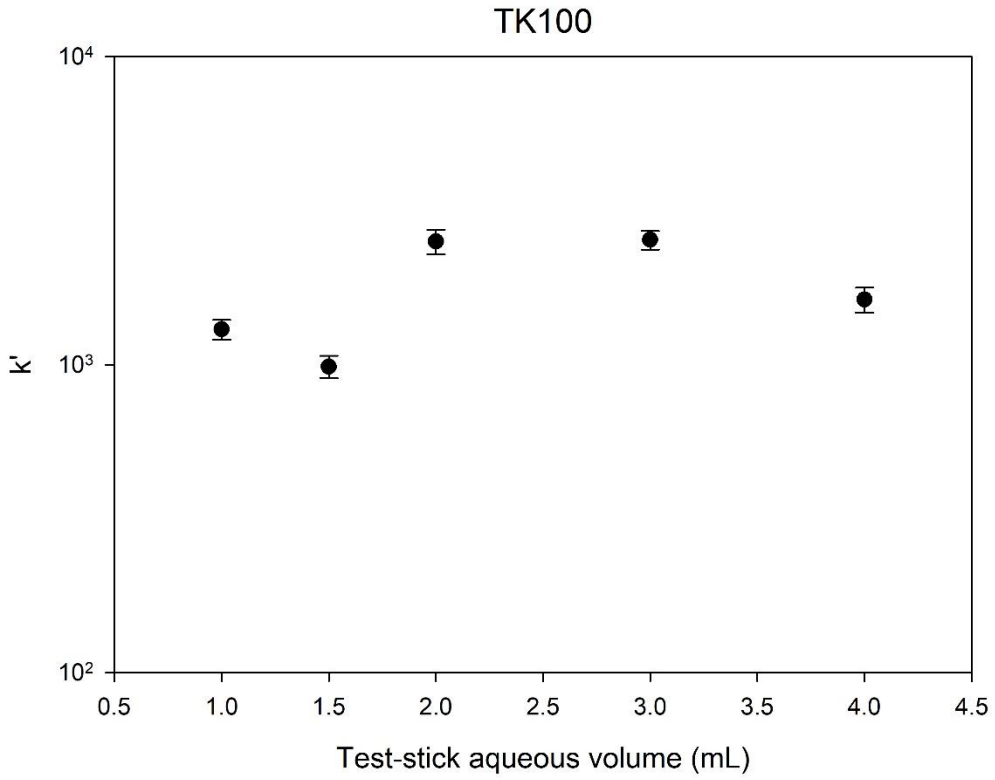

Figure 5.15: Measured partitioning coefficients obtained over a range of volumes for TK100 test-sticks. Spiked ^{90}Sr activity = approx. 10 Bq. Error bars represent uncertainty calculated from counting statistics.

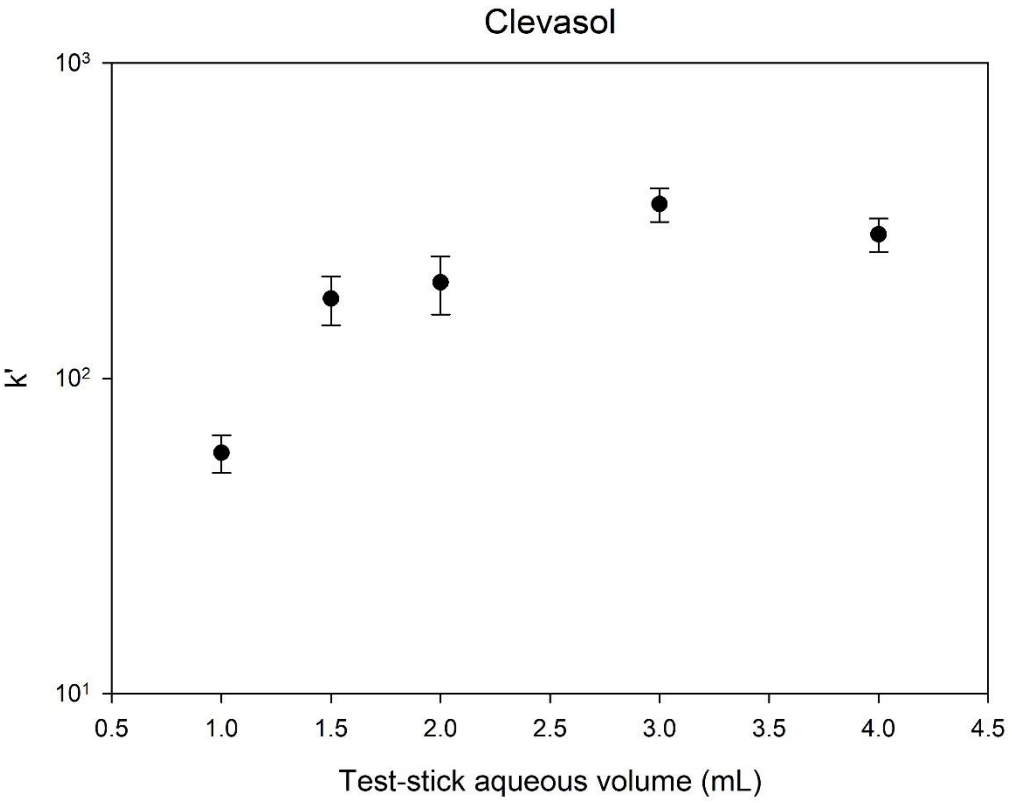

Figure 5.16: Measured partitioning coefficients obtained over a range of volumes for Clevasol test-sticks. Spiked ^{90}Sr activity = approx. 10 Bq. Error bars represent uncertainty calculated from counting statistics.

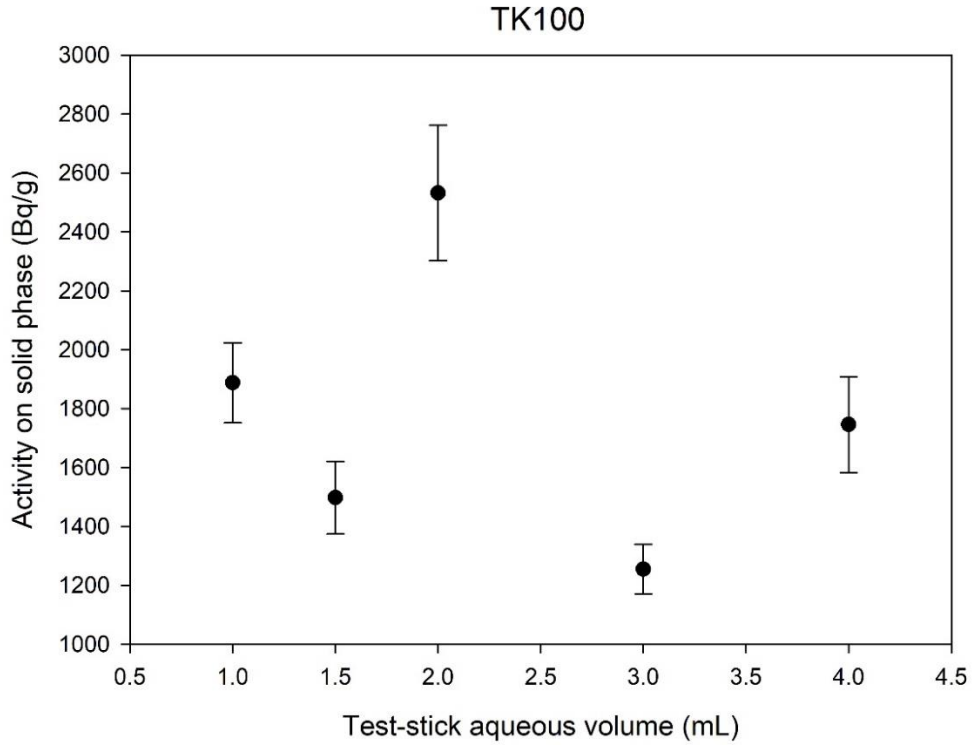

Figure 5.17: Strontium-90 activity measured on the solid phase (TK100 test-sticks) over a range of sample volumes. Error bars represent uncertainty calculated from counting statistics.

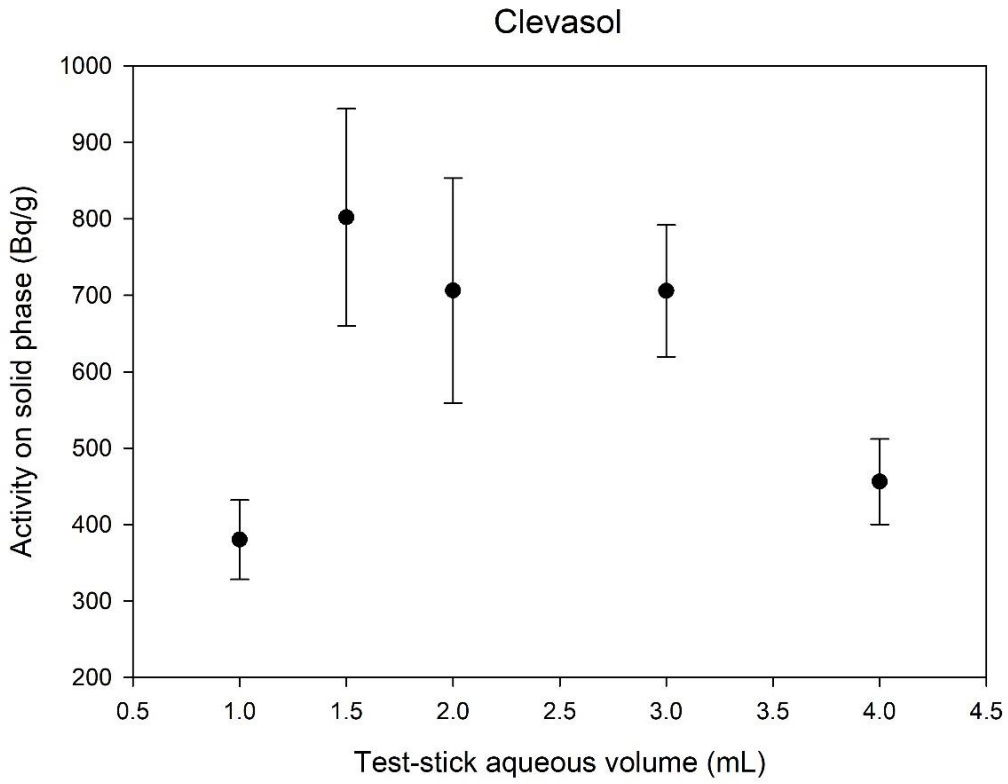

Figure 5.18: Strontium-90 activity measured on the solid phase (TK100 test-sticks) over a range of sample volumes. Error bars represent uncertainty calculated from counting statistics.

Measured partitioning coefficients for TK100 test-sticks provided insight as it showed TK100 test-sticks to largely exhibit increasing k' values with increasing sample volumes. Partitioning coefficient values varied slightly across the different volumes of sample which is comparable to the reproducibility of TK100 test-sticks. Reproducibility experiments (see section 4.4.6.) showed calculated relative standard deviation (RSD) values of 32% whilst variable volume experiments showed RSD values of 35%. This is similar to the reproducibility data where the samples used were identical, including sample volume (4 mL), and five test-stick repeats were used. This suggests that variable volume (from 1.0 to 4.0 mL) has minimal impact on test-stick performance, or at least at a less of an impact on test-stick performance than TK100 test-sticks' reproducibility. This further strengthens the idea that test-stick manufacture improvements would improve the test-stick performance in general. Clevasol test-sticks showed a greater range in k' values between the different sample volumes. Additionally, all k' values were far lower when compared against TK100 test-sticks. The reasons for this have been discussed in chapter 4 and highlight the irregular particle surface topology of Clevasol compared to the smooth bead-like surface of TK100 particles. These factors may impact extraction of ^{90}Sr by the Clevasol test-sticks and uptake kinetics (section 5.4.1.) demonstrated this even further where Clevasol test-stick performance was lower than TK100 at throughout the different contact times. Clevasol test-sticks once again demonstrated large variance in the data when accounting for weighing uncertainty and counting statistics (errors bars shown in

Figures 5.17 and 5.18) compared to TK100 test-sticks. Lowest k' value obtained was for 1.0 mL (k' = 58) and the highest was for 3.0 mL (k' = 357). These findings are similar to TK100 test-sticks where 1.0 mL sample volumes provided the lowest test-stick performance whilst 3.0 mL volumes provided the best uptake performance for both extractant test-sticks. This strongly suggests that test-stick sampling volumes could be decreased to 3.0 mL in future test-stick methodology.

Measured activity of ^{90}Sr on the solid phase for TK100 test-sticks provided further information regarding which volumes showed the highest ^{90}Sr uptake. TK100 test-sticks showed higher ^{90}Sr activity uptake at a volume of 2.0 mL (2532 Bq g^{-1}) and the standard 4.0 mL sample volume showed ^{90}Sr uptake of 1746 Bq g^{-1}. Despite sample volume of 3.0 mL exhibiting the highest k' value ($k'_{3.0\ mL}$ = 2545) its ^{90}Sr uptake was the lowest (1254 Bq g^{-1}). Although 4.0 mL sample volume did not present the highest strontium partitioning data or the highest ^{90}Sr uptake onto the test-stick it still exhibited similar performance to most of the other sample volumes. This suggests that 4.0 mL may be a good compromise sample volume to obtain both appreciable uptake performance and good ^{90}Sr loadings. Clevasol test-sticks presented a similar variation in ^{90}Sr uptake onto the test-sticks, with 1.0 mL exhibiting the lowest uptake activity (380 Bq g^{-1}) and 1.5, 2.0 and 3.0 mL exhibiting similar ^{90}Sr uptake (802, 706 and 706 Bq g^{-1}, respectively). This observed lower ^{90}Sr loadings at 1.0 mL volume further confirms that insufficient volume of sample was present to make sufficient contact with the solid phase during sampling, even whilst agitating the system on an automated roller system. Clevasol test-sticks also showed characteristically high error bars across most data points when measuring the activity of ^{90}Sr on the test-sticks. This is not surprising when considering points already brought up in chapter 4 where particle size variation (200 ± 100 µm) and non-homogenous (rough) particle surface topology means that uptake potential of Clevasol test-sticks can vary greatly. This work demonstrated that extractant particle size and surface topology play a bigger role in affecting the performance of the (Clevasol) test-sticks and may be a point of concern for the viability of Clevasol as a test-stick extractant candidate for ^{90}Sr uptake [46].

5.4.5 Strontium loading capacity

Strontium partition experiments are important to determine the point at which ^{88}Sr concentration begins to impact test-stick performance. Analysis of test-stick performance across a range of ^{88}Sr concentrations allows for test-stick saturation to be identified and therefore determine the limits of test-stick performance. Once the Sr concentration limit for both extractant test-sticks has been determined, it can be compared against real-world stable Sr concentrations in groundwater from a nuclear site – such as Sellafield. This will provide an evaluation of both extractant test-sticks' sensitivity to stable Sr concentrations and provide insight into their current suitability for on-site

deployment. Simultaneous equations described in section 5.3.3. were solved to account for both ^{90}Sr and ^{90}Y activities on both extractant test-sticks, in this work.

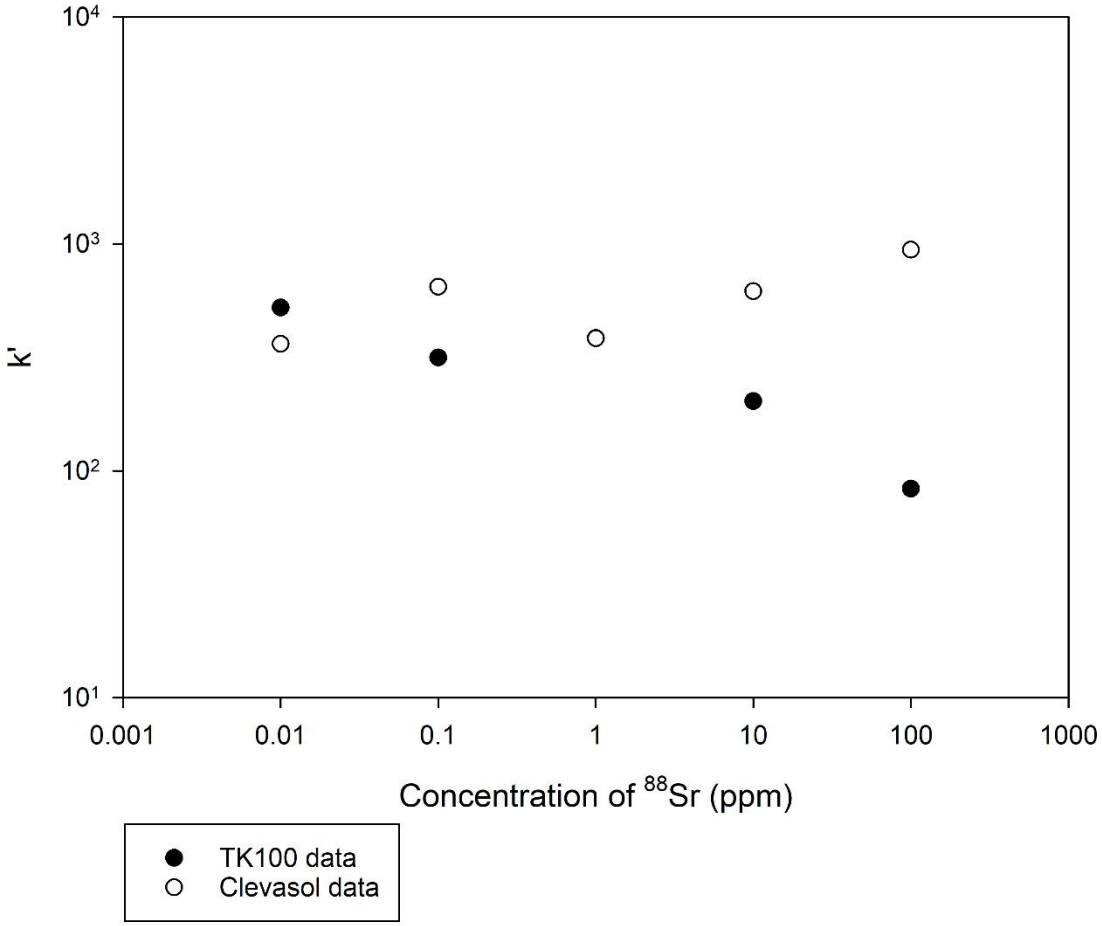

Figure 5.19: Partitioning coefficients for TK100 and Clevasol test-sticks over variable concentrations of stable Sr: 0.01, 0.1, 1.0, 10 and 100 ppm. Activity of ^{90}Sr spike was approximately 3.2 Bq. Note: data points for both Clevasol and TK100 at 1 ppm ^{88}Sr are superimposed as they were found to have almost identical k' values.

Initial studies tested the performance of both TK100 and Clevasol test-sticks over a specified range of ^{88}Sr solutions with concentrations of 0.01, 0.1, 1.0, 10 and 100 ppm. TK100 test-sticks were found to have k' values decrease from 524 to 83 with increasing initial ^{88}Sr concentration. This is expected as fewer active sites become available due to increased number of ^{88}Sr species in solution and therefore competition for active sites increases. Information regarding Sr loadings onto the test-sticks would help to demonstrate this and are shown below. Interestingly, Clevasol test-sticks partitioning coefficients increased from 363 to 942 with increasing initial ^{88}Sr concentration which contrasts with that observed for TK100 test-sticks. The original patent for Clevasol described borane clusters to potentially introduce a degree of size exclusion to the extractant. This, coupled with the

fact that the Clevasol used in these experiments showed irregularity in particle sizing and topography (see section 4.4.2.) strengthens the argument that inconsistent active site availability across different test-sticks may be present. These findings led to a further investigation into the performance of Clevasol test-sticks over a wider range of initial ^{88}Sr concentrations.

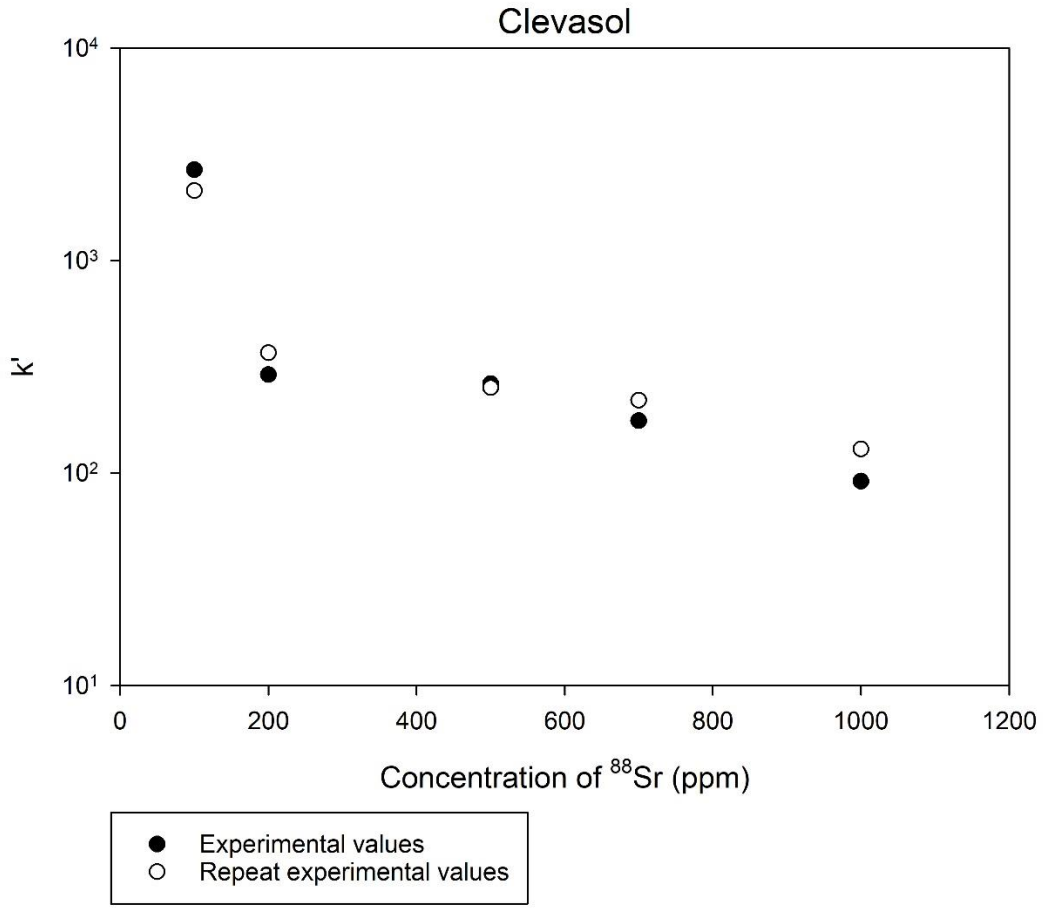

Figure 5.20: Distribution coefficients for Clevasol test-sticks over a wider range of stable Sr concentrations: 100, 200, 500, 700 and 1000 ppm. Activity of ^{90}Sr spike was = 8.5 Bq

Performance of Clevasol test-sticks over ^{88}Sr concentrations from 100 to 1000 ppm were found to decline appreciably from 200 ppm ^{88}Sr onwards. This indicates that at >200 ppm ^{88}Sr active site competition had become dominant and therefore the limiting step to uptake performance. These results demonstrate that Clevasol test-sticks operate at higher ^{88}Sr concentrations than TK100 test-sticks and can therefore potentially operate in higher ionic strength samples. This is expected for an extractant marketed for applications in wastewater treatment where high capacity extractants are required to maximise uptake and increase efficiency of wastewater treatment. However, extractants for wastewater treatment normally possess high capacities but poor selectivity and therefore it will be interesting to investigate whether this is the case in the next section.

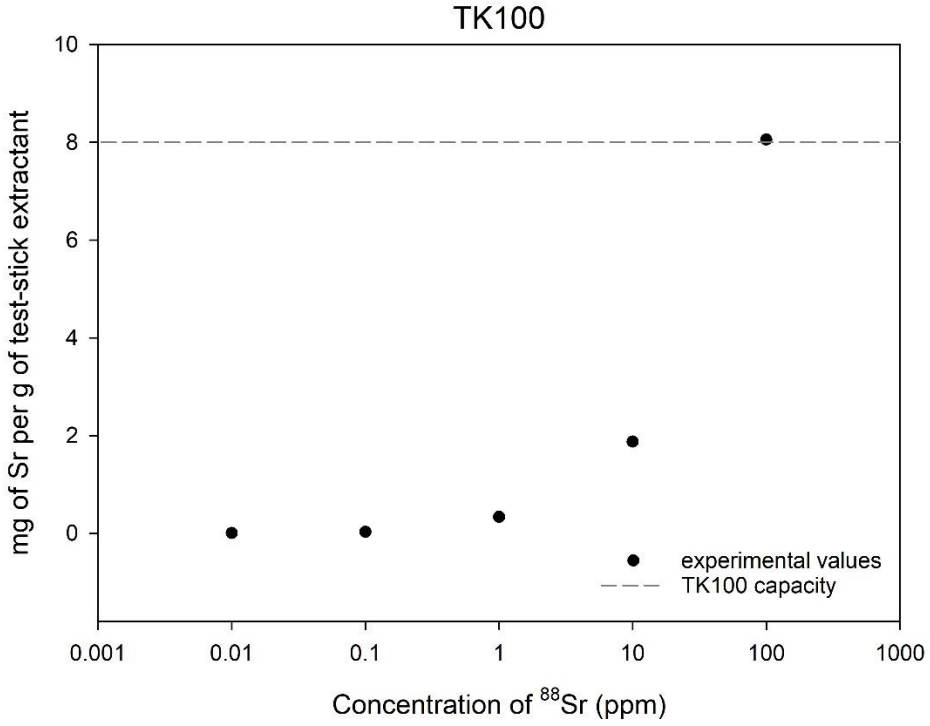

Figure 5.21: Calculated Sr loadings on TK100 test-sticks. Grey dashed line represents the TK100 product sheet value for Sr capacity on the TK100 extractant.

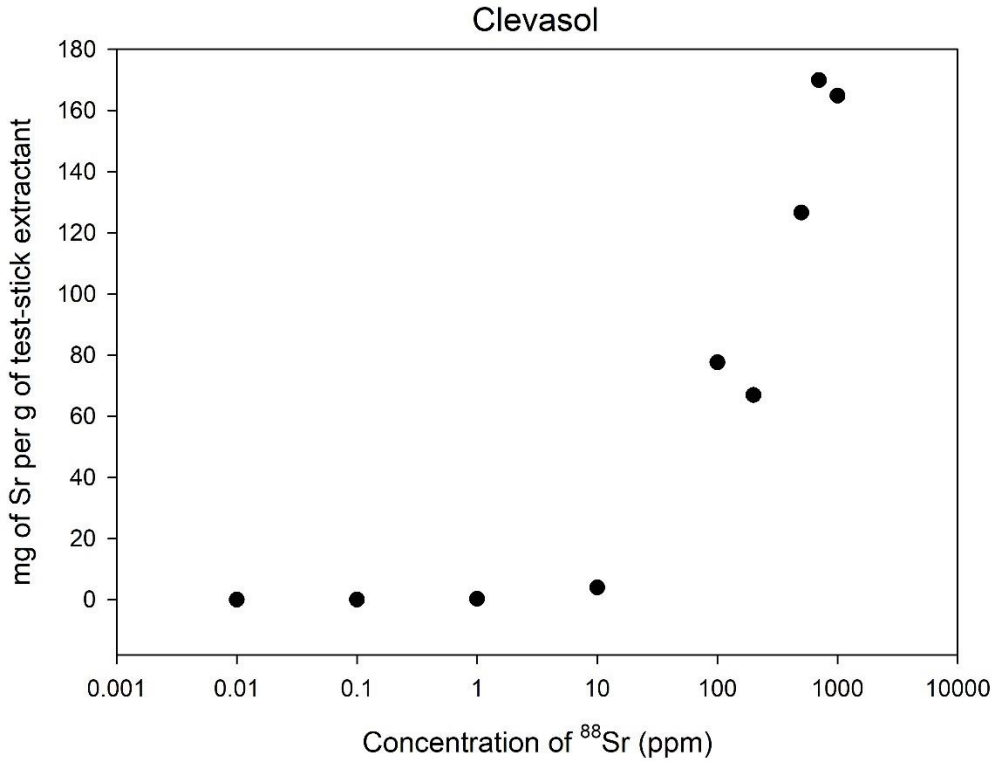

Figure 5.22: Calculated Sr loadings on Clevasol test-sticks. Lack of grey dashed line is due to literature value for capacity of Clevasol extractant to be much higher – 243 mg g^{-1} for ^{90}Sr (3.5 meq g^{-1}).

Strontium loadings on TK100 test-sticks showed Sr mass loadings approaching close to the literature value for TK100 capacity (8 mg g^{-1}). This data shows that at 100 ppm ^{88}Sr TK100 test-sticks begin to saturate and therefore are not suitable for applications in conditions where ^{88}Sr concentration approaches 100 ppm. Despite this limitation, literature values for groundwater composition in Sellafield found ^{88}Sr concentration to be approximately 1 ppm (0.82 µg L^{-1}) for the 95th percentile of samples making the TK100 test-sticks suitable for screening groundwater samples. It is also interesting to note that despite the TK100 extractant being bound to the test-stick and exhibiting a 2-D uptake geometry it has still been able to retain the same capacity as that stated in the manufacturer's product sheet. This suggests that current test-stick methodology, including manufacture, does not greatly impact the extractant's chemistry and therefore demonstrates the flexibility of test-stick technology in utilising extractants without noticeably impacting their capacity. Strontium loadings on Clevasol test-sticks were found to be greater at the same concentrations as TK100 test-sticks – 80 mg g^{-1} for Clevasol test-sticks versus 8 mg g^{-1} for TK100 test-sticks in 100 ppm of ^{88}Sr solutions. Partitioning coefficients for Clevasol test-stick showed performance decreasing from 200 ppm ^{88}Sr onwards however strontium loading calculations showed that even at 1000 ppm ^{88}Sr concentrations the stated maximum capacity (3.5 meq g^{-1}, which is equal to 243 mg g^{-1} for ^{90}Sr) for Clevasol was not reached. This may be due to the inconsistent particle sizes and topography of the Clevasol extractant as well as the extractant chemistry. More specifically, the borane clusters which literatures have stated present an element of size exclusion to the extractant may have impeded Sr uptake and therefore prevented extractant capacity from being reached. It is believed that refinement in both extractant manufacture (to restrict particle sizes and homogenise particle surface topology) as well as test-stick manufacture (to improve extractant particle distribution across the active site) may solve this. However, both extractant test-sticks were found to perform optimally at stable Sr concentrations above the 1 ppm limit found in literatures for groundwater composition in Sellafield. Sellafield represents a unique nuclear site with a combination of nuclear power plants and fuel reprocessing plants within one site and therefore provides a good basis to compare test-stick performance against. If both extractant test-sticks can perform well in stable Sr concentrations that exceed those found in Sellafield groundwater, then there can be confidence that these test-sticks are suitable for application in most nuclear sites. The data presented here shows that as long as the stable Sr concentration in the sample (groundwater in this case) does not exceed 10 ppm for TK100 test-sticks and 200 ppm for Clevasol test-sticks then the test-sticks will operate as intended. If stable Sr concentrations should exceed these values then simple dilutions (such as 1:1 for sample:Milli-Q water, for example) can be carried out and dilution factors applied to the ^{90}Sr results obtained.

5.4.6 Chemical interferences

Investigation into chemical interferences provides information regarding ionic interferences and the impact of specific species on the performance of the test-sticks. The species selected for this investigation were Na, K, Ca and Mg – with the selection of these ions based on the proximity in chemical properties to ^{90}Sr and their plenitude in groundwater. The selected species and Sr are all members of the s-block and are either group 1 (alkali metals) or group 2 (alkaline earth metals) members and therefore possess similar chemistries. These species also form their ionic forms with ease when in solution and therefore are prevalent in groundwater systems. Combining all the above stated properties made these species ideal to evaluate the impact of interferences onto the uptake of ^{90}Sr by both TK100 and Clevasol test-sticks.

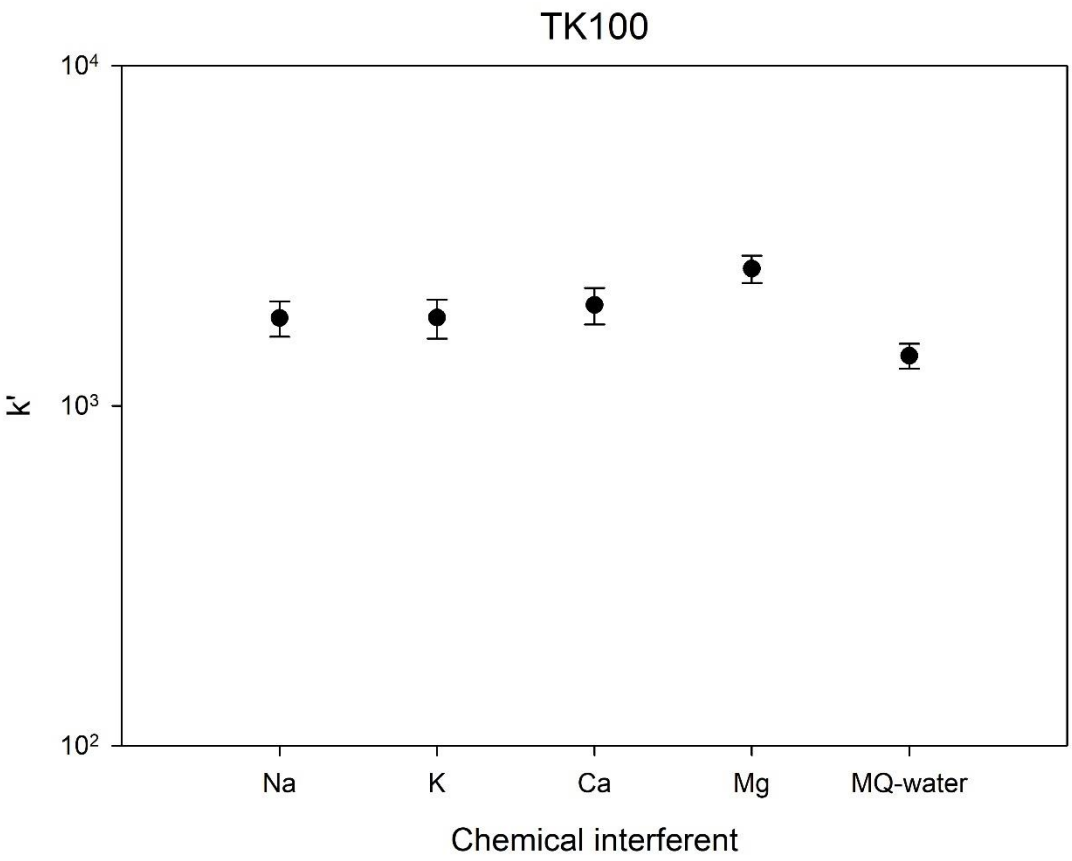

Figure 5.23: Partitioning coefficients for TK100 test-sticks with different ionic interferences present. Spiked activity of ^{90}Sr was ~10.1 Bq. Concentration of species were approximately: 94 ppm Na, 11 ppm K, 250 ppm Ca and 50 ppm Mg in Milli-Q water corresponding to NNL literature Sellafield groundwater composition. Error bars represent uncertainty calculated from counting statistics.

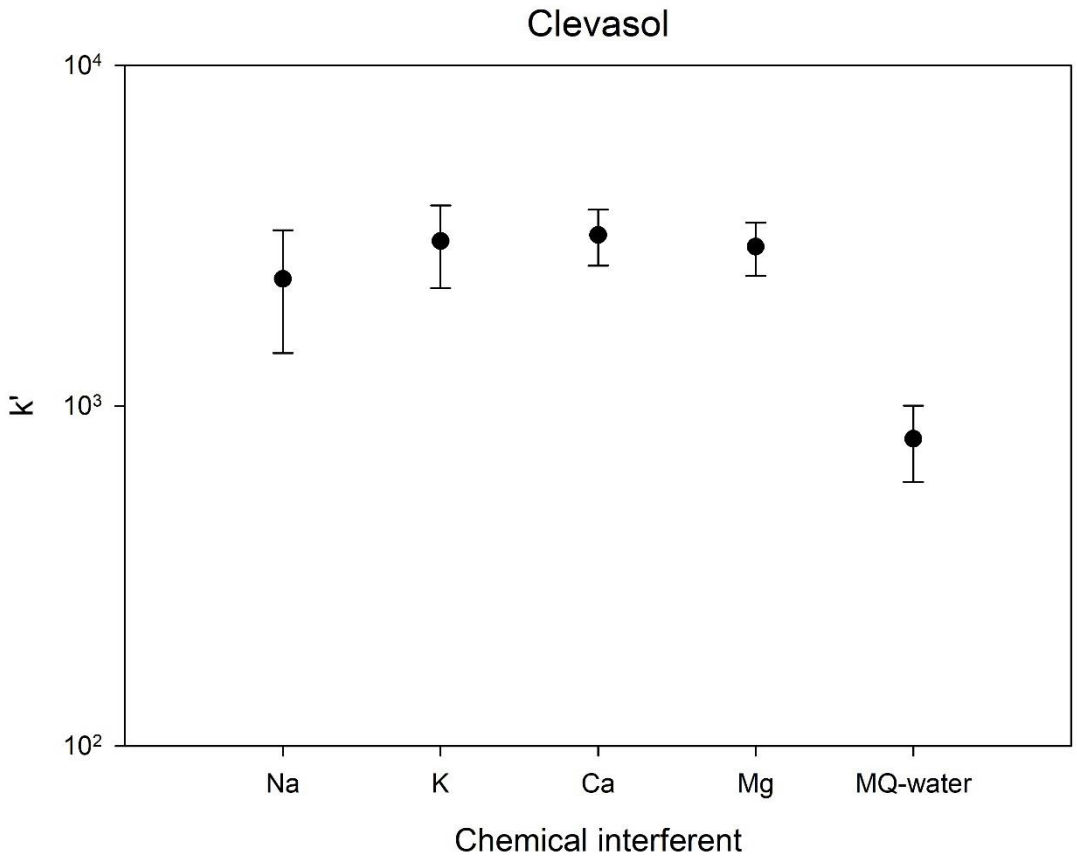

Figure 5.24: Partitioning coefficients for Clevasol test-sticks with different ionic interferences present. Spiked activity of ^{90}Sr was ~10.1 Bq. Concentration of species were approximately: 94 ppm Na, 11 ppm K, 250 ppm Ca and 50 ppm Mg in Milli-Q water corresponding to NNL literature Sellafield groundwater composition. Error bars represent uncertainty calculated from counting statistics.

Partition coefficients, k', values for TK100 test-sticks revealed minimal differences between the ionic species. Results went as far as to show Milli-Q water with the lowest obtained k' value of 1402 whilst Na, K, Ca and Mg had k' values of >1800 suggesting these species to exhibit minimal effect on test-stick uptake efficiency. This is especially surprising considering TK100 operates via size exclusion with focus on Sr uptake and a few other species with similar ionic radii such as Pb. However, literatures also showed that these measured ionic interferences should not greatly affect TK100 uptake for ^{90}Sr. Surman *et al.* discovered similar TK100 uptake efficiency for Sr to that shown here and demonstrates that utilising TK100 in a test-stick 2D geometry uptake mechanism does not impact its performance with respect to the presence of groundwater interferences. The observed k' for milli-Q water was the lowest even when compared to other ionic interferences and reasons as to why this is may be related to some conditioning effect on the extractant resin however this requires further work to determine the reasons for this behaviour. Nonetheless, these results show that TK100 test-sticks should be theoretically capable of sampling groundwater samples without the presence of Na, K, Ca or Mg species impacting the performance of the TK100 test-sticks. This

also means that TK100 is a suitable candidate for test-stick technology for groundwater sampling of ^{90}Sr [31,43,44].

Strontium partitioning for Clevasol test-sticks also showed similar findings to those of the TK100 test-sticks however, Clevasol test-sticks showed a larger difference in k' values obtained between the chemical interferences and Milli-Q water. The higher capacity of Clevasol (243 mg g^{-1} for ^{90}Sr) compared to TK100 (8 mg g^{-1}) may explain why k' values are higher between the chemical interferences and Milli-Q water. Again, the observed low k' value of milli-Q water compared to the ionic interferences suggests some conditioning effect with regards to the extractant resin and therefore requires further investigating to determine why this is observed. Clevasol test-sticks also obtained observably larger variance in measured partition coefficients, which show a larger degree of uncertainty in measured k' values. Similar k' values for all four ionic species may seem surprising when considering Clevasol is a cationic exchange extractant however the larger extractant capacity of Clevasol for ^{90}Sr (243.0 mg g^{-1}) may be able to explain why partition coefficients are similar for all four ionic species. The large capacity of Clevasol allows competition between ions at this concentration (from the NNL literature groundwater composition for Sellafield) to be minimised and uptake of ^{90}Sr to still be achieved with k' value exceeding 10^3 for all four ionic interferences. Despite both extractants exhibiting different uptake mechanism approaches (size exclusion versus ionic exchange), Clevasol's large uptake capacity may allow Clevasol to be established as a relevant candidate for ^{90}Sr test-sticks [46,47].

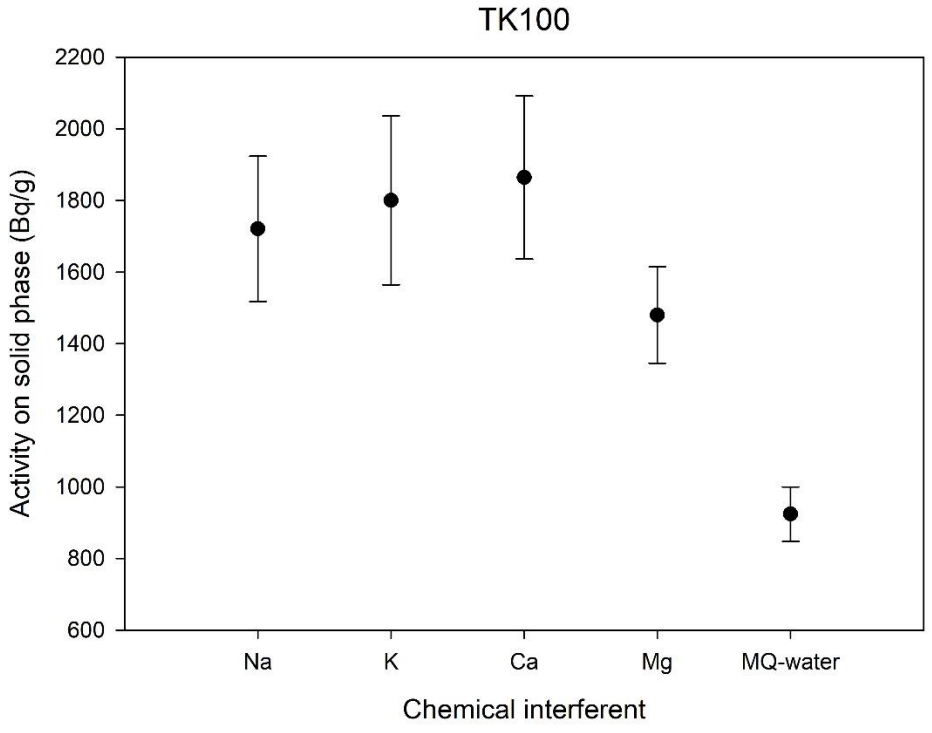

Figure 5.25: Measured activity of ^{90}Sr on TK100 test-sticks with different ionic interferences present. Spiked activity of ^{90}Sr was ~10.1 Bq. Concentration of species were approximately: 94

ppm Na, 11 ppm K, 250 ppm Ca and 50 ppm Mg in Milli-Q water corresponding to NNL literature Sellafield groundwater composition. Error bars represent uncertainty calculated from counting statistics.

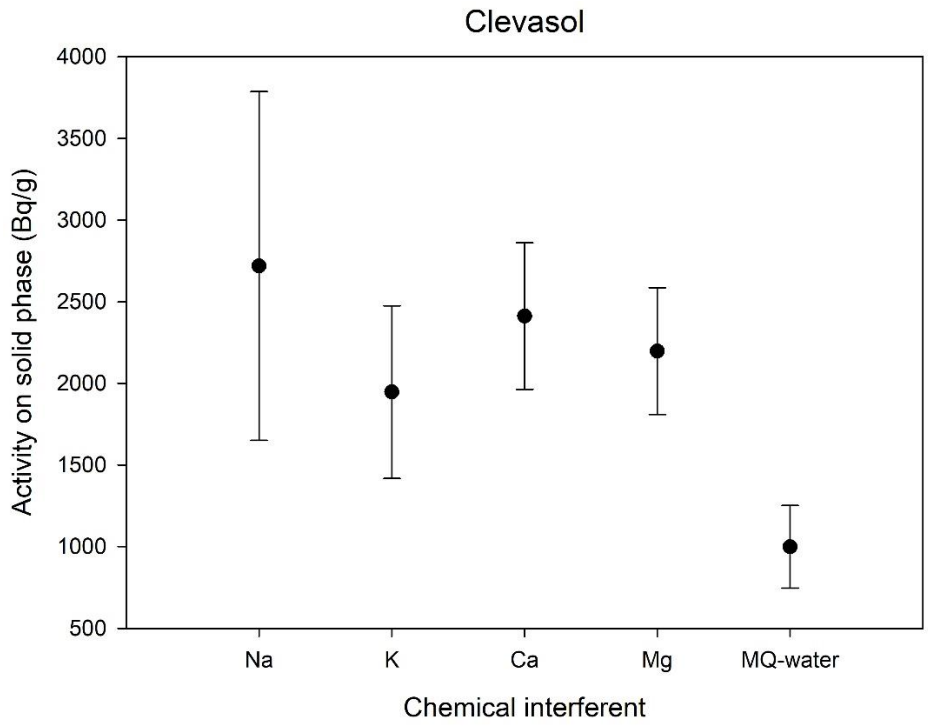

Figure 5.26: Measured activity of ^{90}Sr on Clevasol test-sticks with different ionic interferences present. Spiked activity of ^{90}Sr was ~10.1 Bq. Concentration of species were approximately: 94 ppm Na, 11 ppm K, 250 ppm Ca and 50 ppm Mg in Milli-Q water corresponding to NNL literature Sellafield groundwater composition. Error bars represent uncertainty calculated from counting statistics.

Measured activity of ^{90}Sr in TK100 test-sticks show that ^{90}Sr uptake was similar across Na, K and Ca with decreasing ^{90}Sr uptake for Mg followed by Milli-Q water. The surprising factor in these results is that Ca exhibited higher activity uptake compared to the rest of the chemical interferences and Milli-Q water. The chemical similarity between Ca and Sr seems to have not greatly affected the uptake efficiency of the TK100 test-sticks. These findings correlate well with literatures and gives confidence that the results obtained here are accurate and the TK100 extractant bound onto the test-stick is operating as hoped. Magnesium seems to show some decrease in ^{90}Sr uptake but still showed higher ^{90}Sr loadings than those for Milli-Q water. Clevasol test-sticks exhibited higher ^{90}Sr uptake activities across Na, K, Ca and Mg however, uptake activities for Milli-Q water (998 Bq g^{-1}) were similar to those obtained for TK100 test-sticks (923 Bq g^{-1}). Clevasol test-sticks did demonstrate greater result variance although this could be justified by the physical chemistry of Clevasol where the rough particle topography and lack of controlled particle sizes means that active site availability can vary greatly between particles. This is reflected in the results obtained here and

agrees well with most of the results presented in this chapter where Clevasol uptake, especially ^{90}Sr loadings, can vary greatly. Despite this, Clevasol's large uptake capacity means that Clevasol can potentially overcome this particle-to-particle variance and still operate as a suitable extractant candidate for ^{90}Sr test-sticks. Improvement in Clevasol extractant manufacture which could introduce smoother particle topography and controlled particle sizes could minimise uptake performance variance. Overall, investigation into chemical interferences demonstrated that Na, K, Ca and Mg interferences had little to no impact on both extractant's test-stick performance and therefore increases both extractant's viability to be incorporated into ^{90}Sr test-sticks for field deployment.

5.4.7 Limit of detection and count times

This chapter has discussed optimising the contact time of the test-sticks to improve the performance of test-stick performance, for both TK100 and Clevasol test-sticks. Test-stick contact time accounts for the 'separation' aspect of the test-sticks, whilst count time contributes to the 'measurement' aspect of the test-stick procedure. Lowering these count times would further improve the turnaround of results for test-stick technology. Therefore, carrying out calculations into the limit of detection (LOD) of different count times on test-stick performance would allow for test-stick procedure to speed up and comply even further with the goals set out by the NDA – provide initial characterisation in-*situ* with results obtained within 24 hours. LOD calculations can be carried out using the following Currie equation:

$$L_D = 2.71 + 4.65\sqrt{\mu_B}$$

Where L_D is the limit of detection and μ_B is the limiting (or true) mean of the instrument background. Combining this equation with the proportionality equation described earlier in this chapter, a theoretical LOD can be calculated for different count times. Limits of detection were calculated for the liquid scintillation counters used in this study (which are predominantly laboratory based instruments where background CPM = ~7) as well as theoretically for other liquid scintillation counters (LSC) which are more readily deployable in the field but where background is higher (background CPM = ~30). These tabletop LSC instruments represent what could be utilised in nuclear sites and therefore calculating count times to achieve appreciable LODs for these instruments would be beneficial. Figure 5.27 shows the calculated LODs for both the instruments used in this project (PerkinElmer 1220 Ultra Low-Level Liquid Scintillation Spectrometer) and potential instruments used in nuclear sites (such as the BetaScout tabletop LSC). LODs were calculated for Clevasol in this example and used a proportional constant, b_t, value of 0.825 (see Table 1).

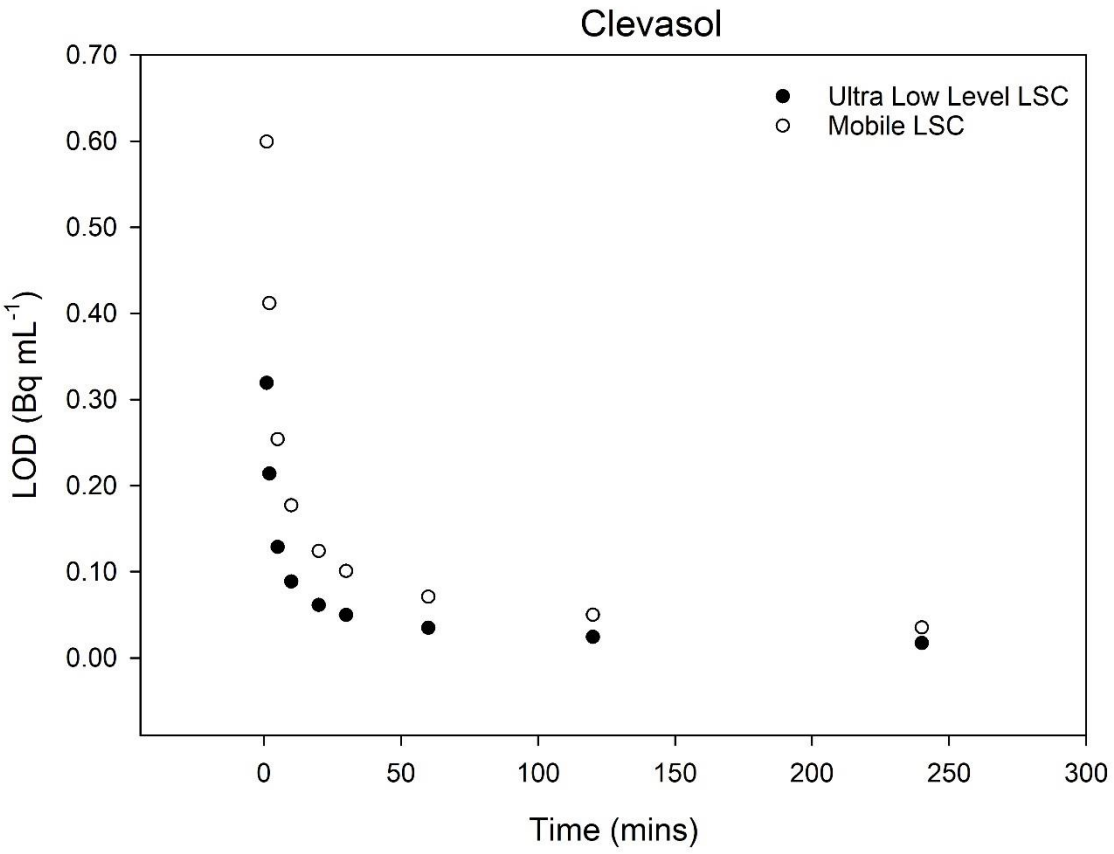

Figure 5.27: Calculated LODs for Clevasol in an unstirred system for both ultra-low level and mobile LSC instruments.

The data shown in graph 27 demonstrates that ultra low level LSC analysis of test-sticks can obtain LODs of 0.1 Bq mL^{-1} within 10 minutes. More mobile LSC instruments, depending on background CPM, can obtain the same LOD within 60 minutes. An LOD of 0.1 Bq mL^{-1} was selected as it provides sensitivity to ^{90}Sr activity ten times above that of the World Health Organisation (WHO) drinking water limit of 0.01 Bq g^{-1} ^{90}Sr. This WHO guideline limit is only used as a guide, especially when discussing groundwater samples, as this 0.01 Bq g^{-1} threshold is for drinking water limits and therefore more lenient thresholds are applied to ^{90}Sr in nuclear sites. An LOD of 0.1 Bq mL^{-1} is representative for possible applications of test-sticks in leachate of solid samples – for example leaching 1g of solid sample in 10 mL of water will be comparable to the EPR2016 guideline limit of 1 Bq g^{-1} for ^{90}Sr in solids.

Calculation of LODs using this method can provide important information regarding how long count times must be to achieve the desired sensitivity of the technique. Depending on advancements in mobile LSC instruments, this count time (of 60 minutes) can theoretically decrease, further improving test-stick technology turnaround in results for site operators.

A further example was produced for TK100, utilising a b_t constant of 1.709 and applying the same method as done above for Clevasol.

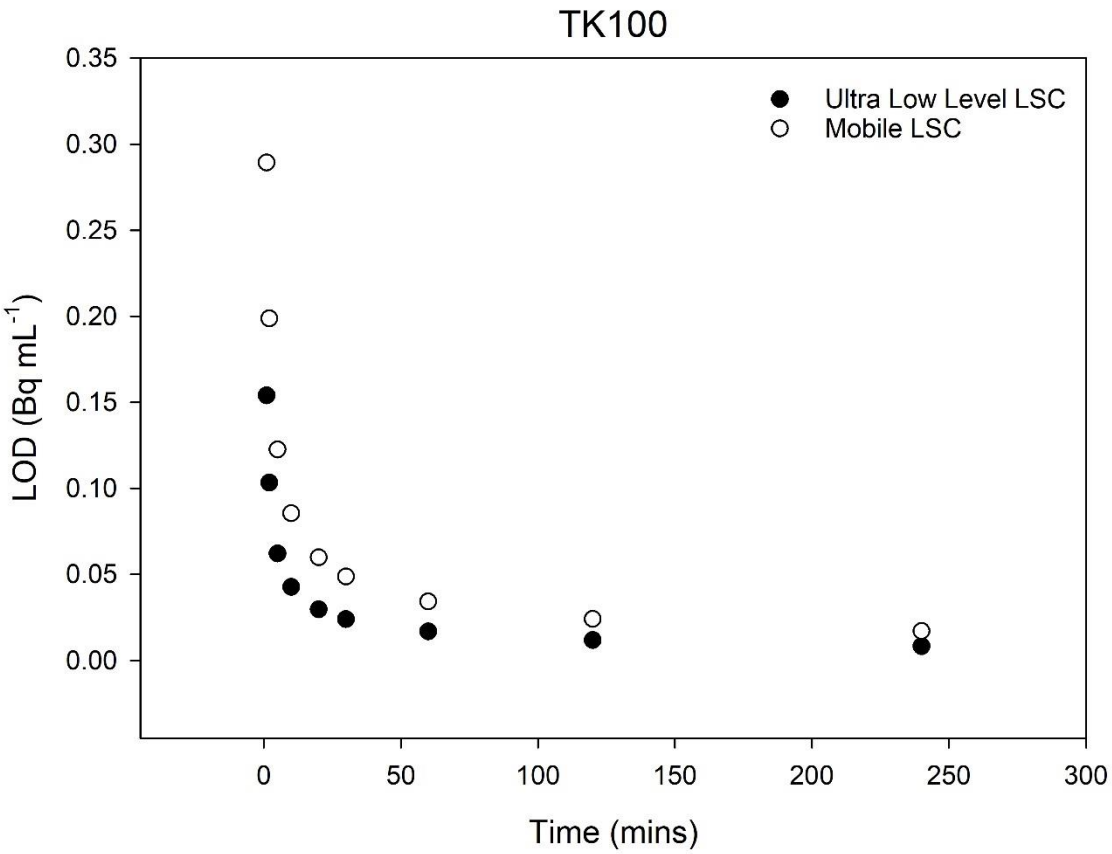

Figure 5.28: Calculated LODs for TK100 in a stirred system for both ultra-low level and mobile LSC instruments.

The calculated LOD values for TK100 showed ultra low level LSC instrument reaching the desired LOD of 0.1 Bq mL^{-1} within 5 minutes whilst mobile LSC reached this LOD in 10 minutes. These results indicate that increasing the b_t value can potentially decrease the count times required to achieve the desired LOD. This should be a further important consideration for future test-stick developments where optimisations in test-stick performance yielding in an increase in the b_t value may allow for even lower count times to be obtained. These lower count times could then reflect in even quicker turnaround time for test-stick results for site operators and other clients.

5.5 Conclusion

A set of operational conditions have been investigated in this chapter, including uptake kinetics, test-stick response, variable volume, loading capacity and the role of chemical interferences. These operational conditions were evaluated for two extractant test-sticks – TK100 and Clevasol. These extractants provided contrasting uptake mechanisms; size exclusion for TK100 and ionic exchange for Clevasol. Uptake kinetics showed that 40-minute sampling times could be used instead of 60-

minutes and similar performance would be obtained. Both test-sticks demonstrated uptake efficiencies stabilising between 40 to 60 minute sampling times suggesting that ^{90}Sr diffusion through the solid phase became the limiting step. It is believed that as contact time increases ^{90}Sr uptake also increases until remaining active sites require ^{90}Sr to diffuse further into the solid phase to reach them. These results then suggest that extending contact times further than 40-minutes is unlikely to yield grater uptake efficiencies unless test-sticks remain in solution for 24 hours or long. However, recent NDA reports have highlighted the goal of carrying out majority of initial characterisation on-site and within 24 hours. Therefore 40-minute sampling times are a good compromise between obtaining the fastest sampling times for test-stick technology whilst maximising uptake efficiency of ^{90}Sr. This applies to both extractant test-sticks.

Test-stick response experiments demonstrated the potential uptake of ^{90}Y on TK100 test-sticks. However, a possible solution was also suggested to circumvent ^{90}Y uptake which involved simply washing the test-sticks after sampling with concentrated HNO_3, instead of Milli-Q water. Regardless, both extractant test-sticks responded to ^{90}Sr activities of 0.5 Bq g^{-1} and above, which correlates well with the EPR2016 threshold limit of 1.0 Bq g^{-1} for ^{90}Sr for solid wastes. Although this guideline limit is for solid wastes, it can be used as a strong guideline for test-sticks and other rapid screening techniques to aim for. Diffusion control experiments showed that ^{90}Y was prevalent in unstirred TK100 test-sticks however, when agitation was introduced to the system ^{90}Y uptake was considerably lower than ^{90}Sr. Agitation generally improved ^{90}Sr uptake on TK100 and even Clevasol test-sticks however for the latter the improvement was negligible. Clevasol test-sticks were found to perform similarly in both unstirred and stirred systems. This presents Clevasol as a viable technique for screening of radiostrontium in large bodies of water such as old fuel ponds as well as for environmental monitoring. These applications present situations where in-*situ* sampling is preferred and agitation of the sample may be difficult to carry out. Evaluation of both extractant test-sticks in both test-stick response and diffusion control studies demonstrated the test-sticks displaying proportional uptake of ^{90}Sr. This proportional uptake mechanism forms the fundamental basis of test-stick technology and therefore observing this process in action in these experiments shows that proportional mechanism is readily established. This proportional mechanism is further strengthened when introducing agitation to the test-stick sampling system, especially for TK100 test-sticks. Variable volume studies suggested that greater uptake efficiency of ^{90}Sr was obtained at slightly lower sampling volumes of 3.0 mL, for both extractant test-sticks. However, further reducing the sample volume to 1.0 mL showed a large decrease in uptake efficiency suggesting insufficient contact of the sample with the solid phase, even with agitation of the system. Strontium loading capacity for both extractants was above the stable Sr concentrations that were found in Sellafield groundwater. This suggests that both extractant test-sticks can operate optimally under

these conditions and stable Sr loading capacity are only a concern at concentrations above 10 ppm (for TK100 test-sticks) and 200 ppm (for Clevasol test-sticks). Finally, chemical interferences experiments showed that Na, K, Ca and Mg at concentrations similar to Sellafield groundwater levels had little to no impact in both extractant test-sticks' performance.

Clevasol performance was found to contain large statistical variance calculated from mass loading experiments and counting statistics. It is believed that refinement of Clevasol manufacture that would introduce smoother particle topography and controlled particle sizes would minimise these large statistical variances. TK100 performed similarly to literatures, especially to work carried out by Surman *et al.*, which indicates test-stick technology's capability to utilise extractants without impacting greatly the performance of the extractant(s).

Chapter 6 Assessment of fundamental properties underpinning test-stick response and predicting test-stick performance under different conditions

6.1 Abstract

The performance of the test-sticks under different conditions was simulated using a LabVIEW based numerical modelling tool. Simulations were based on TK100 test-sticks using data acquired experimentally in previous works (see section 5.4.1.). TK100 was selected due to being capable of extracting ^{90}Sr in neutral pH conditions as well as being a well-known and commonly used extractant resin for ^{90}Sr separation. The numerical model looked to apply $k_{forward}$ and $k_{backward}$ constants that were determined experimentally and investigate the effect of different input variables such as sample exposure time and volume of sample. This study also focused on testing the extent of diffusion control in the performance of the test-sticks and demonstrated the time required for non-agitated samples to equilibrate. Work carried out in this chapter also looked to supplement prior work in this project and offer a theoretical explanation for some of the experimental observations in regards to uptake mechanisms. This includes the physical factors that have been observed to play the most influential role in the test-sticks' performance such as test-stick manufacture including solid phase mass loadings on the test-sticks. The numerical model looks to provide further insight into the performance of the TK100 test-stick under conditions that would otherwise be difficult to replicate in the lab and consequently provide useful information for future test-stick methodologies to incorporate.

6.2 Introduction

The large-scale nuclear decommissioning project currently being undertaken by the Nuclear Decommissioning Authority (NDA) has initiated a large drive for the development of rapid characterisation techniques. The predicted costs of the nuclear decommissioning project already exceed £100 billion pounds and are growing, along with the projected timescale for decommissioning to complete already exceeding 100 years. As the nuclear decommissioning project continues and new problems are discovered, such as characterising the Winfrith sea discharge pipeline, this projected timescale and cost will only increase further. The development of

rapid screening techniques that are easily deployed in the field and provide results within 24 hours are the current goals set out by the NDA in their 2021 baseline document. Test-stick technology looks to provide a viable candidate for rapidly screening major contaminants whilst meeting the goals set out by the NDA. These goals include a readily deployable technique with result turnaround within 24 hours. These goals look to streamline on-site characterisation and by extension the waste sentencing process. Streamlining the characterisation process would help to alleviate the pressure on off-site radiochemical labs where only samples that are found to contain radionuclides at levels near or above legislative thresholds are sent for complex analysis. This would remove occurrences where samples would be sent for off-site analysis that could take between 20 to 30 days and find that samples are not active and/or require no specialist radiochemical disposal.

The target radionuclides for these rapid screening techniques are difficult-to-measure (DTM) radionuclides as they remain difficult to measure on-site. Pure beta-emitters such as ^{90}Sr are difficult to detect on-site due to beta particle absorption by surrounding matrix which means that radiochemical separation is often a requirement to overcome this issue. Radiochemical separation is currently often carried out using chromatographic extractants with one of the most well-known extractants being crown ether size exclusion extractants. These extractants normally use the crown ether ring as the basis for the sorption of the radionuclide where the diameter of this ring will determine the selectivity of the extractant. TK100 is an industrial extractant specialised in Sr uptake that utilises a combination of a crown ether (4,4'(5')-di-t-butylcyclohexano-18-crown-6) and an organic cationic exchange resin (HDEHP - di(2-ethyl-hexyl)phosphoric acid). The HDEHP organic cationic exchanger transfers the Sr from the aqueous phase to the organic phase where the crown ether then extracts the Sr from the organic phase and situates within the crown ether ring. The role of HDEHP is to facilitate the uptake of Sr by carrying this out at more neutral pH conditions. This removes the need to add a concentrated acid for successful Sr uptake to occur as was the case with Sr-resin, the predecessor to TK100. The capability of TK100 to be applied directly into more neutral conditions without requiring the addition of concentrated acid made this extractant ideal for test-stick technology. This essentially introduces two rate steps with regards to the rate of Sr uptake by TK100, which affects both the capacity (8 mg g^{-1}) and kinetics (equilibrium reached within 30 mins) of this extractant compared to its predecessor – Sr-resin (27 mg g^{-1} and 3 mins, respectively). Extensive experiments, presented in chapters 4 and 5, have demonstrated the performance of TK100 test-sticks (as well as Clevasol test-sticks) with respect to the operational conditions of test-stick deployment as well as providing information regarding the sensitivity and precision of this technique. Experimental work has even extended as far as identifying the limits of test-stick technology (such as ^{90}Y uptake) and providing potential solutions to these limitations (agitation of the test-sticks and incorporating concentrated HNO_3 washes of the test-sticks post sampling).

However, the development of a numerical model that could both accurately simulate the performance of test-sticks as well as predict the performance of the test-sticks would be hugely advantageous. This numerical model could provide information regarding the limits of test-stick technology in scenarios that would otherwise be difficult to replicate in the lab.

This study looks to demonstrate a numerical model adapted from work on chromatographic separations and applied to test-stick technology. The input parameters required for the numerical model to operate will be extracted from a kinetic experiment that has been carried out, with a greater number of contact time samples. The numerical model will then look to simulate these kinetic experiments to demonstrate the model is working as required. Simulations regarding the performance of TK100 test-sticks with variable solid phase masses and sample volumes will be investigated. Finally, simulations of TK100 test-sticks with different solid phase:sample volume ratios will be carried out, including across different stable Sr concentrations. This work will provide information regarding how well the numerical model works and what this model predicts regarding test-stick performance based on experimental data. If successful, this numerical model could form the basis of a software capable of predicting and evaluating different extractant test-sticks' performance and therefore expedite test-stick development for different DTM radionuclides.

6.3 Methodology

6.3.1 Test-stick manufacture

Test-sticks were manufactured using cut out 4x1 cm^2 inert support with application of spray adhesive and TK100 extractant coating at the edge of the inert support in a 1x1 cm^2 area. The test-sticks were allowed to stand inside an airtight darkened container for approximately 24 to 48 hours. This was to allow the adhesive to set and bind the extractant onto the test-stick and form the solid phase. The airtight container minimised any contamination to the extractant by air or sunlight. The waiting period also allowed the adhesive to set completely and reduce any chance of the solid phase breaking down during sampling. The full test-stick manufacture procedure is described in section 3.3.2.

6.3.2 Experimental procedure

Batch uptake experiments were carried out with and without agitation and under a range of stable Sr concentrations. Once sampling had been complete, the test-sticks were removed from the sample, washed with Milli-Q water and cut into a 22 mL scintillation vial. Gold star scintillation cocktail was added (between 19 and 20 mL – dependent on whether it was a 1mL aliquot of the

aqueous phase or the test-stick solid phase) and the sample was counted for 60 minutes. The full experimental procedure is described in section 3.3.1.

6.3.3 Numerical modelling

LabVIEW 2015 was used to carry out the numerical simulations using ODE (ordinary differential equations) solver VI which solved simultaneous equations that calculated the sorption and desorption of the species, in this case ^{90}Sr. The following parameters were used:

Table 6.1: Tabulated input parameters used for test-stick simulations obtained from experimental kinetic studies. Further information regarding the variables below and what they mean please refer to Burrell thesis [56,62].

Name of input parameter	Equation notation	Description of input parameter
Forward reaction	$k_{forward}/\vec{k}$	Rate constant that dictates the 'forward' reaction – sorption of species onto the extractant
Reverse reaction	$k_{backward}/\overleftarrow{k}$	Rate constant that dictates the 'backward' reaction – desorption of species from the extractant
External reaction	$K_{external}/k_{ext}$	Rate constant that dictates the rate of transfer of the species from the bulk phase to the surface layer
Volume ratio	$\left(\frac{V_s}{V_{aq}}\right)$	Ratio of sample volume and extractive resin (test-stick) mass, in this case volume is equal to mass as the density is assumed to be 1.
Conc lumped	$[s]$	Concentration of species on extractive resin test-stick at t
Initial conc lumped	$[s]_o$	Concentration of species on extractant test-stick at t = 0

Maximum conc lumped	$[s]_E$	Maximum concentration of the species on the extractive resin test-stick, calculated from the manufacturer's (TrisKem International) product sheet [44]
Conc liq	$[aq]$	Concentration of species in aqueous phase at t
Initial conc liq	$[aq]_0$	Concentration of species in aqueous phase at t = 0
Conc surface	$[aq]_{surface}$	Concentration of species in surface layer of aqueous phase at t = 0
Conc bulk	$[aq]_{bulk}$	Concentration of the bulk system (for unstirred systems only) at t = 0
Lumped fraction	V_s	Ratio mass of solid phase
Liquid fraction	V_{aq}	Ratio mass of aqueous phase
Surface fraction	$V_{aq,(surface)}$	Ratio mass of aqueous phase in the surface layer (for unstirred systems only)
Bulk fraction	$V_{aq,(bulk)}$	Ratio mass of entire aqueous system (for unstirred systems only)

The following simultaneous equations were calculated via ODE solver VI:

$$\frac{d[s]}{dt} = \vec{k}[aq] - \overleftarrow{k}[s]$$

$$\frac{d[aq]}{dt} = \left(\overleftarrow{k}[s] - \vec{k}[aq]\right) \times \left(\frac{V_s}{V_{aq}}\right)$$

For simulations of unstirred systems, a slightly modified equation to the one above was used:

$$\frac{d[aq]_{surface}}{dt} = k_{ext}[aq]_{bulk} - k_{ext}[aq]_{surface} + \left[\left(\overleftarrow{k}[s] - \overleftarrow{k}[aq]_{surface}\right) \times \left(\frac{V_s}{V_{aq,(surface)}}\right)\right]$$

$$\frac{d[aq]_{bulk}}{dt} = \left(k_{ext}[aq]_{surface} - k_{ext}[aq]_{bulk}\right) \times \left(\frac{V_{aq,(surface)}}{V_{aq,(bulk)}}\right)$$

A further modification to the equation above is presented which was used to calculate the performance of the test-stick under different aqueous concentrations whilst still modifying the mass ratios of the solid and aqueous phases.

$$\frac{d[s]_{Sr}}{dt} = \vec{k}_{Sr}[aq]_{Sr}([s]_E - [s]_{Sr}) - \overleftarrow{k}_{Sr}[s]_{Sr}$$

$$\frac{d[aq]_{Sr}}{dt} = \left[\overleftarrow{k}_{Sr}[s]_{Sr} - \vec{k}_{Sr}[aq]_{Sr}([s]_E - [s]_{Sr})\right] \times \left(\frac{V_s}{V_{aq}}\right)$$

For further details regarding the numerical modelling simulation procedure, please refer to section 3.6.

6.3.4 Data analysis

Data acquisition from LSC instrumentation was carried out with WinQ software which provided the CPM (counts per minute) of the samples as well as the count times and dates. This data was then extracted and input into an Excel spreadsheet which calculated the activity of ^{90}Sr in samples whilst taking into account ingrowth of ^{90}Y and counting efficiencies for both ^{90}Y and ^{90}Sr. Counting efficiencies were obtained from QC (quality control) data and determined to be 95% for both radionuclides. Ingrowth data was determined from recorded separation times and count times obtained from the registry file produced by WinQ after sample counting had concluded.

Data outputted from the simulations were provided in CSV files and analysed using Excel. SigmaPlot was used for all graphical plots.

6.4 Results and discussion

6.4.1 Experimental uptake kinetics

6.4.1.1 Kinetics study utilising agitation

Application of numerical simulations to test-stick technology performance first requires an experimental data set to extract the required mathematical parameters for the numerical simulations to run as accurately as possible. These extracted parameters include the $k_{forward}$ and $k_{backward}$ as well as the mass ratio and liquid fraction values. The balance between sorption and

desorption of the species of interest onto the extractant and the rate at which this takes place are dictated by the $k_{forward}$ and $k_{backward}$ values. Mass ratio is a calculated mass-based ratio between the extractant (lumped fraction) and the aqueous sample (liquid fraction). The following uptake kinetics experiment was built on the previous kinetic studies (see section 4.3.3) by adding further contact times including at longer time intervals. This was done to provide more data points to improve the accuracy of the numerical model. This includes earlier initial time intervals starting at 1, 2, 5, 10, 15, 20, 30, 40, 50 and 60 minutes with longer time interval samples at 1440 (1 day) and 4320 minutes (3 day). This was to determine both the kinetic uptake and the 'steady-state' part of the kinetic profile where kinetic uptake performance begins to slow down and stabilise. Partition coefficients were calculated using the following equation:

$$k' = \left(\frac{A_s \cdot M_{aq}}{A_{aq} \cdot M_s}\right)$$

Where, A_s is the activity of the species on the solid phase (test-stick) in Bq, A_{aq} is the activity of the species on the aqueous phase in Bq, M_{aq} is the mass of the aqueous phase in g, M_s is the mass of the solid phase in g and k' is the partition coefficient. The k' constant describes the partitioning of the analyte, in this case ^{90}Sr, between the solid and aqueous phases.

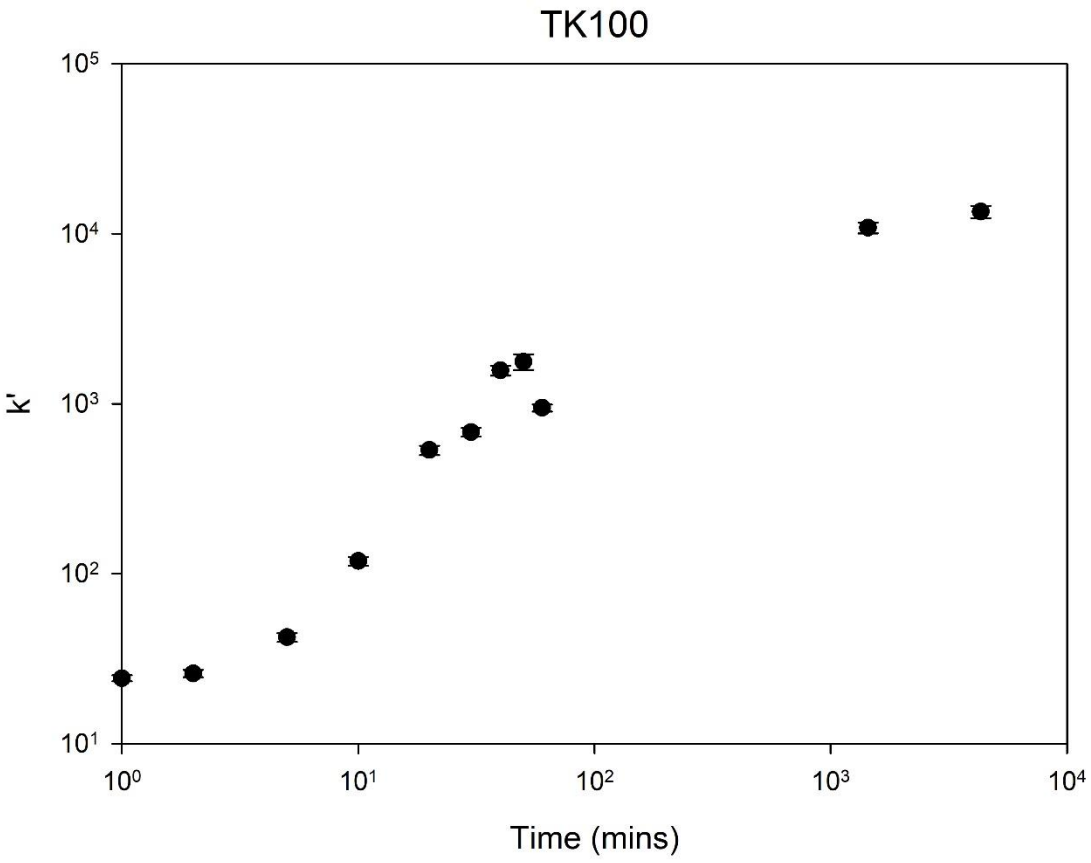

Figure 6.1: Partition coefficients obtained for stirred TK100 test-sticks ^{90}Sr uptake kinetics from 1 min to 4320 mins. Error bars represent uncertainty calculated from counting statistics.

If error bars are not visible then smaller than the data point. Activity of ^{90}Sr spike = ~11.0 Bq

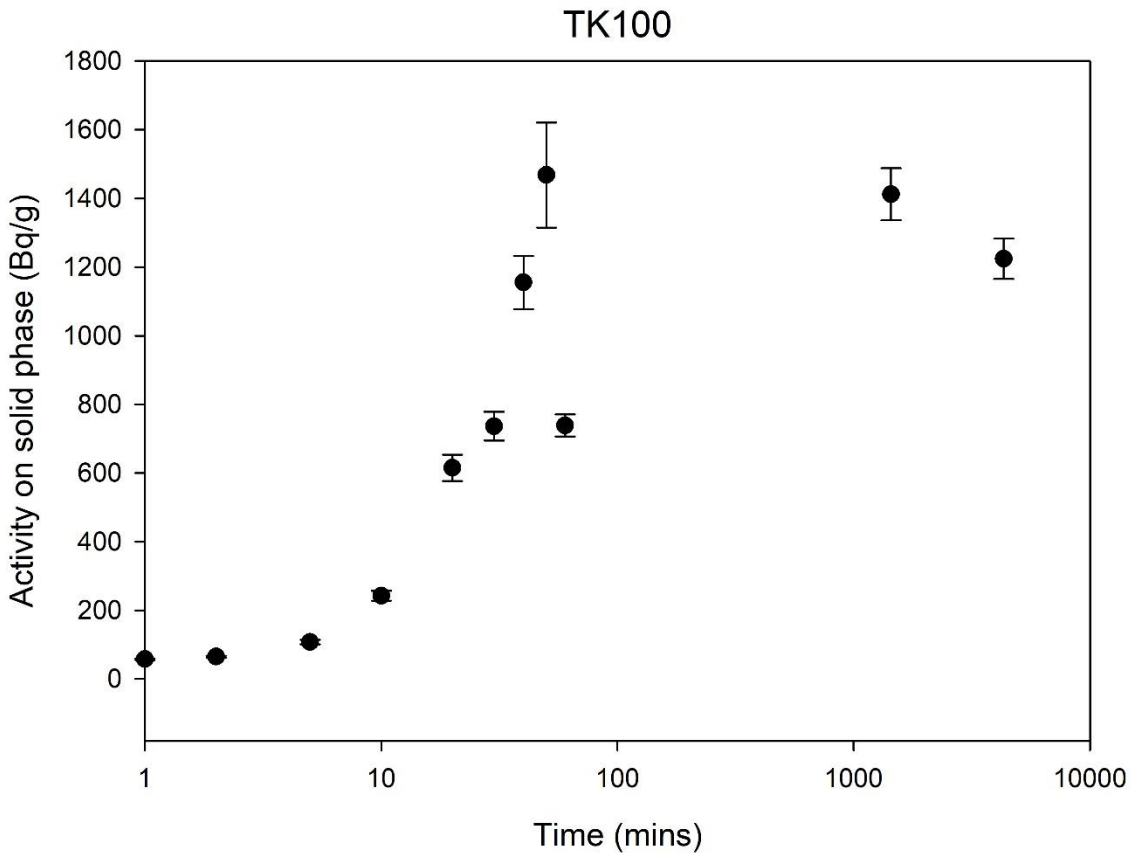

Figure 6.2: Measured activity of ^{90}Sr loaded on stirred TK100 test-sticks from 1 min to 4320 mins. Error bars represent uncertainty calculated from counting statistics. If error bars are not visible then smaller than the data point. Activity of ^{90}Sr spike = ~11.0 Bq

Kinetic data shows distribution coefficient values slowly increasing from 1 to 4 minutes (k' = 25-42) before increasing substantially up to the 40- to 50-minute mark with k' values of 1572 to 1768. Long contact times showed effective distribution coefficients to fluctuate between 10839 (24 hours) and 13497 (72 hours). A clearer trend reflected in a smoother kinetic profile within the first 60 minutes in this kinetic study compared to previous kinetic experiments is thought to be due to a combination of factors including improved manufacturing of the TK100 test-sticks over time and more controlled agitation of the test-sticks using automated sample rollers. Measured activity of ^{90}Sr on TK100 test-sticks showed ^{90}Sr activities to fluctuate between 1155 and 1576 Bq g^{-1} ^{90}Sr from 40 minutes to 4320 minutes (72 hours) further confirming that optimal ^{90}Sr uptake by TK100 test-sticks is reached within 40 minutes.

These results serve to better reflect the realistic performance of the TK100 test-sticks as this kinetics study incorporates several factors that have been recommended throughout this project including controlling agitation of the test-sticks to maximise test-sticks performance and test-stick

manufacture (although there is substantial opportunity for future work in this area as highlighted in chapter 4 and discussed briefly in the next chapter). As a result of the factors stated above (including the increased contact times and improvement in test-stick performance due to improved test-stick agitation) this kinetic study was used to generate the required mathematical parameters for input into all subsequent numerical simulations described in this chapter.

6.4.1.2 Kinetics study without agitation

Kinetic analysis of TK100 test-sticks in an unstirred system over a wide range of contact times (from 1 min to 4320 mins – 72 hours) was carried out to demonstrate the capabilities of the numerical model and highlight further the impact of agitation on the system. This experiment served to extend the application of numerical modelling to simulate test-stick performance under conditions that would otherwise be extremely difficult to replicate in the lab. Experimental conditions were kept the same as the previous experiment however agitation of the test-sticks during sampling was not carried out. Test-stick sampling was carried out at 1, 2, 5, 10, 15, 20, 30, 40, 50, 60, 1440 and 4320 mins.

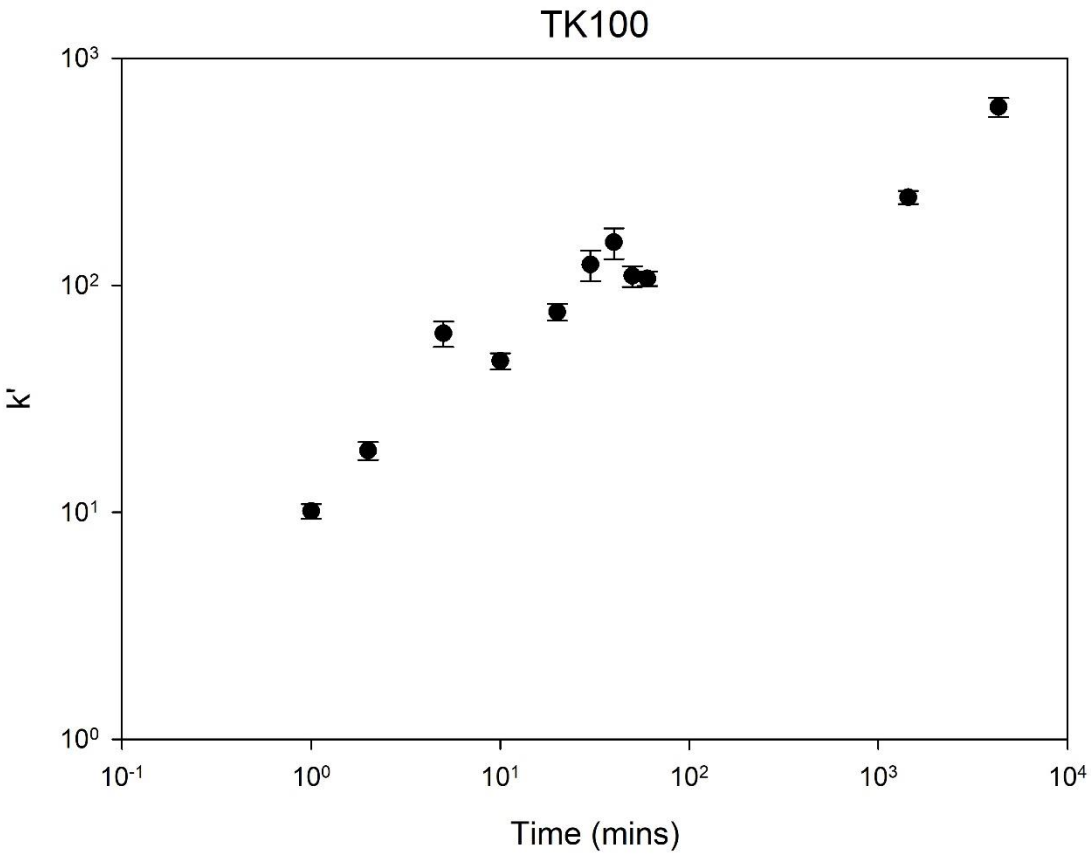

Figure 6.3: Partition coefficient obtained for unstirred TK100 test-sticks ^{90}Sr uptake kinetics from 1 min to 4320 mins. Error bars represent uncertainty calculated from counting statistics. If error bars are not visible then smaller than the data point. Activity of ^{90}Sr spike = ~11.0 Bq

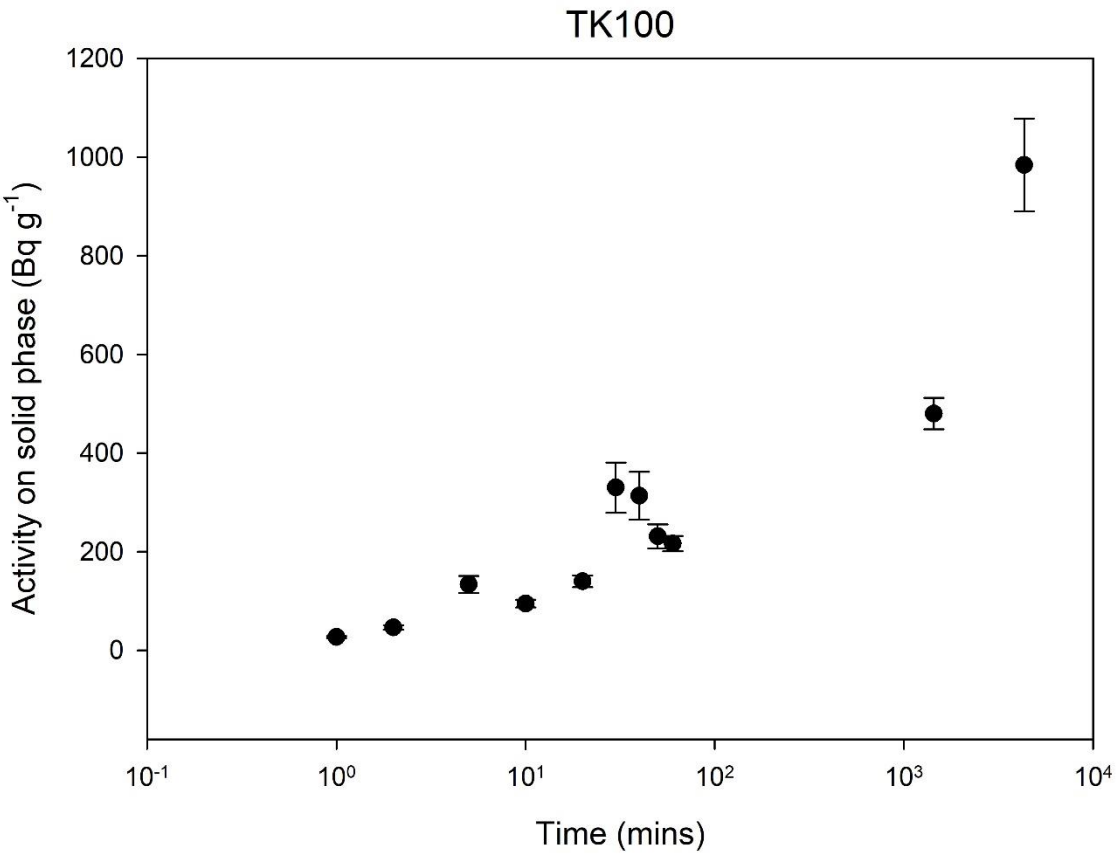

Figure 6.4: Measured activity of ^{90}Sr loaded on unstirred TK100 test-sticks from 1 min to 4320 mins. Error bars represent uncertainty calculated from counting statistics. If error bars are not visible then smaller than the data point. Activity of ^{90}Sr spike = ~11.0 Bq

An important initial observation made is the almost linear relationship of the kinetic samples' effective distribution coefficients over time. Unlike the stirred system, the unstirred test-sticks seem to continue increasing in k' values but are substantially lower than stirred test-sticks (at 72 hours, $k'_{stirred}$ = 13497, $k'_{unstirred}$ = 611) even after 72 hours. The linear trend observed for unstirred TK100 test-stick kinetics suggests that even after 72 hours kinetic equilibrium has still not been established. The reasons as to why kinetic equilibrium has not been established may be down to stagnation of ^{90}Sr uptake from poor mass transfer and chemical diffusion of ^{90}Sr through the TK100 beads meaning ^{90}Sr uptake slows down considerably. Furthermore, the TK100 beads are bound onto the solid phase of the active site where SEM analysis in previous works (see section 4.4.1.) showed 'layering' occurring which would further slow down chemical diffusion of ^{90}Sr through the solid phase. It is believed that agitation of the TK100 test-sticks increases mass transfer rate including chemical diffusion of the ^{90}Sr species into solid phase and improve ^{90}Sr sorption. Measured activity loadings of ^{90}Sr on the TK100 test-sticks show similar findings to that of the distribution coefficients where a linear relationship is present for ^{90}Sr loadings on the TK100 test-sticks over

time. Unlike the stirred system, unstirred test-sticks show no plateau in ^{90}Sr loadings on the test-sticks and therefore reinforces the idea that the unstirred TK100 test-sticks have not reached kinetic equilibrium yet. Therefore, it would be interesting to use the numeric model to investigate the theoretical time taken for total kinetic equilibrium to be established by TK100 test-sticks in an unstirred system.

6.4.2 Simulated uptake kinetics

6.4.2.1 Simulated uptake kinetics utilising agitation

Initial numerical modelling work looked to utilise the kinetic data shown above to extract the required parameters to carry out the desired simulations. These parameters would allow the numerical model to accurately reflect the test-stick performance and ergo better predict the performance of the TK100 test-sticks in different simulated conditions. The following input parameters were used for the stirred kinetic simulations:

Table 6.2: Tabulated input parameters used to run stirred TK100 test-stick simulations obtained from experimental kinetic studies. Further information regarding the variables below and what they mean please refer to table 1 and Burrell thesis [63].

$k_{forward}/\vec{k}$	2.191 x10^{-1}
$k_{backward}/\overleftarrow{k}$	2.085 x10^{-5}
$\left(\frac{V_s}{V_{aq}}\right)$	9.98 x10^{-1}
$[s]$	0
$[aq]$	2.7

All input parameters used in the simulations for each experiment will be shown in a table for the reader's reference.

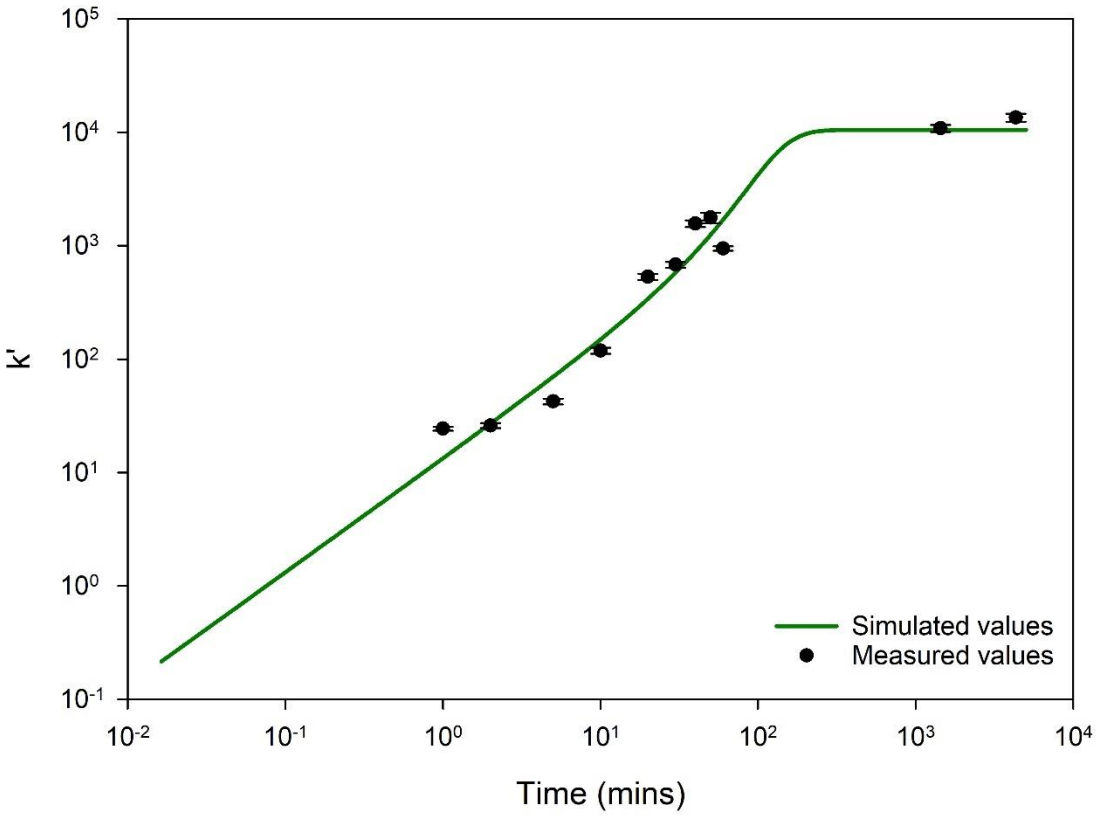

Figure 6.5: Distribution coefficients for simulation versus experimentally measured values for stirred TK100 test-sticks.

The numerical model was optimised to try and match the experimental data as closely as possible. The numerical model was able to simulate, upon adjusting variables including the $k_{forward}$ and $k_{backward}$ values, TK100 test-stick performance in a stirred system closely to that of the experimental work. Different $k_{forward}$ and $k_{backward}$ values were calculated and attempted in simulations until a best fit was achieved. This included using $k_{forward}$ and $k_{backward}$ values directly from test-stick stirred data set, $k_{backward}$ value calculated from averaged k_d values at equilibrium and $k_{forward}$ value calculated from combined stirred and unstirred datasets. The simulation which was found to best fit the experimental kinetic data (and shown in Figure 6.5) was using a $k_{forward}$ value calculated from combined stirred and unstirred datasets averaged. The $k_{backward}$ value was calculated from averaged k_d values at equilibrium (24 to 72 hours) from the stirred test-stick kinetic dataset as well as bulk-phase batch uptake data – this included both stirred and unstirred. Bulk-phase data was obtained to provide further equilibrium data points to improve the numerical model and increase simulation accuracy. Bulk-phase data is shown in the appendix for reference. This simulation was selected from observation as it was found to closely follow experimentally measured values from the kinetic study carried out in section 6.4.1.1. These input parameters were applied moving forward to different conditions to predict test-stick performance.

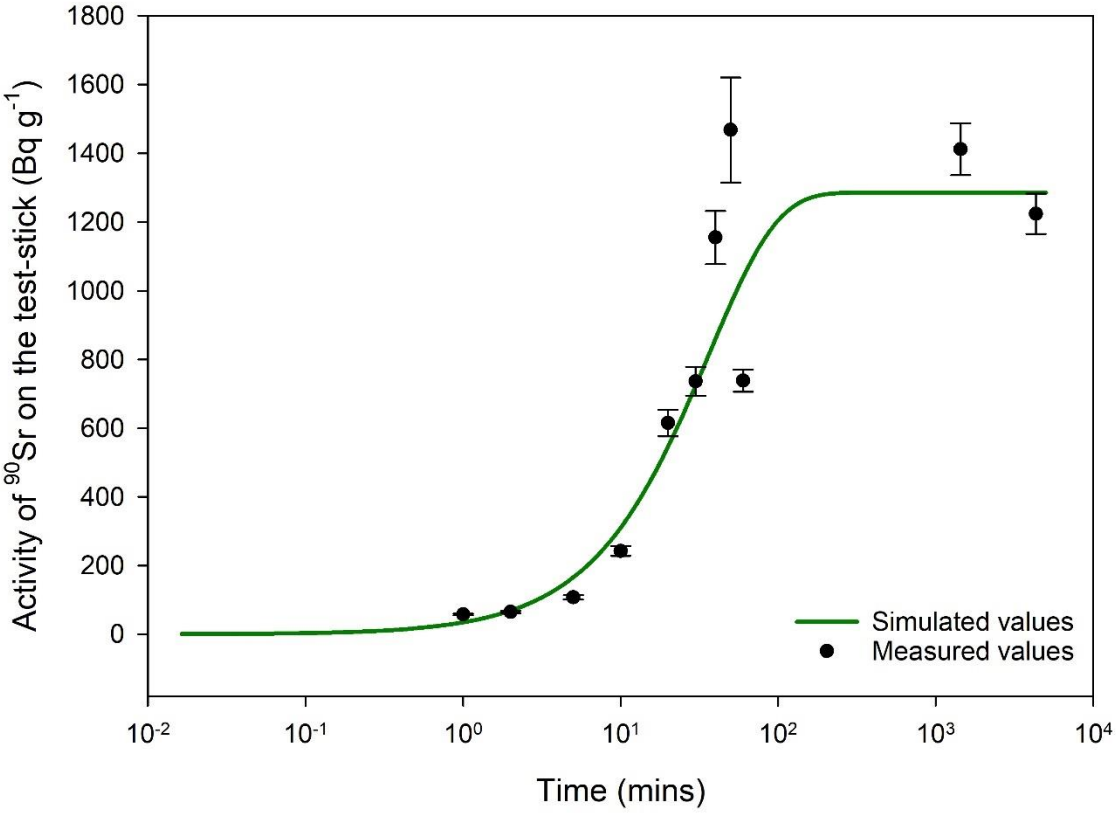

Figure 6.6: Simulated activities for ^{90}Sr loadings on stirred TK100 test-sticks versus experimentally measured.

The same simulation that produced the partition coefficient graph shown in Figure 6.5 was also utilised to obtain data regarding activity loadings of ^{90}Sr onto the TK100 test-stick over time (Figure 6.6). Here, the simulation was also found to closely follow experimental values and provided good agreement between the simulation and the measured values. The simulation described a sharp increase in activity loadings of ^{90}Sr onto the test-stick approximately after 10 minutes before beginning to reach steady-state at approximately 40-50 minutes which correlates well with experimental findings (Figure 6.2). This is further emphasised at 60-minute sampling time, where an error in sampling time of ± 5 minutes amounts to 3% change in ^{90}Sr loadings on the test-stick. An important factor demonstrated here is the numerical model's ability to accurately describe test-stick performance even between calculated partition coefficient values and activity loadings of ^{90}Sr onto the test-stick. Despite experimental data showing distribution coefficients to increase over a time span of ~24 hours before beginning to stabilise, as replicated by the simulation (Figure 6.5), activity loadings of ^{90}Sr onto the test-stick plateaued after approximately 40 minutes, which the simulation has also been able to replicate. These findings strongly suggest that the numerical model has been able to accurately predict TK100 test-stick performance over time, which hopefully allows the model to now apply this simulation to modified conditions to investigate TK100 test-stick performance. Furthermore, these findings also demonstrate the potential of this numerical model

to simulate kinetic data for different extractants. Initial work carried out by Burrell on extractants such as zirconium phosphate, UTEVA and anionic exchange resin were all applied onto either batch-uptake experiments or columns whilst work here extends this further and applies this to a 2-D surface – the solid phase of the test-stick.

6.4.2.2 Simulated uptake kinetics without agitation

Kinetic studies on TK100 test-sticks in an unstirred system presents the need for extra input variables to account for the lack of agitation to the system. Despite experimental data from the previous chapters and this chapter showing that agitation improves ^{90}Sr uptake and ergo the proportionality of ^{90}Sr uptake over an activity range, investigation into an unstirred system helps to provide information regarding the extent of the impact of agitation onto test-stick kinetics. Additionally, simulating these conditions where no agitation is present helps to understand the length of time taken for kinetic equilibrium to be established and compare against a stirred system. This numerical model can then be used to simulate any further conditions in the future for systems where agitation may not be present such as environmental conditions (sampling radioactive spills and leakages in-*situ*, for example).

Table 6.3: Tabulated parameters used to run unstirred TK100 test-stick simulations obtained from experimental kinetic studies. 'Mass ratio' has been replaced with 'lumped fraction', 'surface fraction' and 'bulk fraction'. '$k_{(external)}$' mass rate constant has also been introduced. For definition of the variables please refer to section 6.3.3. Further information regarding the variables below and what they mean please refer to Burrell thesis [63].

$k_{forward}/\vec{k}$	2.191 x10^{-1}
$k_{backward}/\overleftarrow{k}$	2.085 x10^{-5}
V_s	1.0 x10^{-3}
$V_{aq,(surface)}$	1.0 x10^{-1}
$V_{aq,(bulk)}$	8.9 x10^{-1}
$[s]$	0
$[aq]_{surface}$	2.7
$[aq]_{bulk}$	2.7

Lumped fraction was calculated from the average mass of test-stick extractant loadings for TK100 test-sticks and set to 0.001, whilst surface and bulk fractions as well as the $k_{(external)}$ were fitted via trial and error.

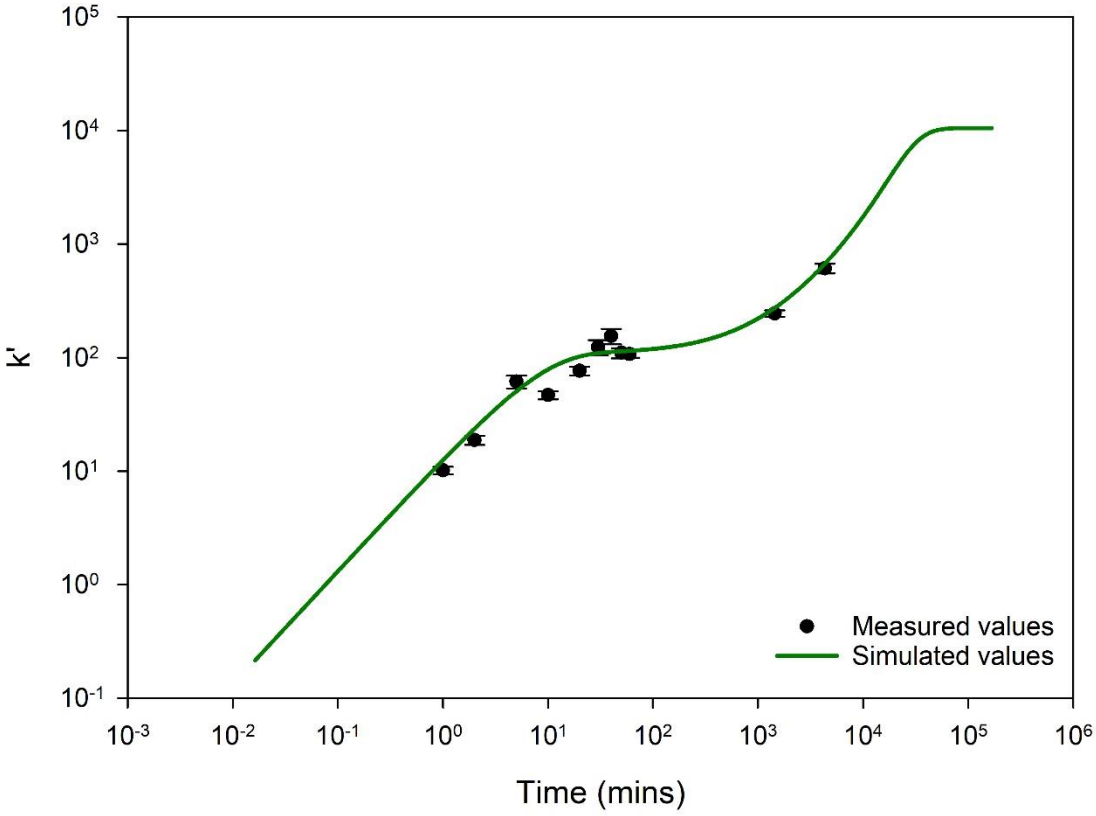

Figure 6.7: Partitioning coefficient for simulation versus experimentally measured values for unstirred TK100 test-sticks.

Trial and error fits of bulk and surface fractions dictating the relationship of masses between the three phases (bulk, surface and lumped), as well as the $k_{(external)}$ allowed for a good fit of the simulation versus the experimental values. The simulation matched the experimental values and continued to rise even past the experimental contact times of over 72 hours. The simulation was left to run and eventually found that 99% of the final kinetic partition coefficient value was reached after approximately 44 to 45 days, 95% at 33 to 35 days and 90% at ~29 days, which is in stark contrast to the 24 hours found for the stirred system. It is believed that initial rate of uptake increases similar to the stirred system, however, the rate of uptake for the unstirred system seems to slow down greatly as mass transfer begins to dominate until the kinetic equilibrium is eventually reached. It is important to note, however, that this predicted time taken for kinetic equilibrium to be established is dependent on other factors including mass of extractant loadings on test-stick (lumped fraction) and distribution of bound extractant onto the active site (whether TK100 particles are bound spatially efficient throughout the active site). This simulation is also based on a trial-and-

error fit of bulk and surface fractions as well as the $k_{external}$ value. Despite this, these findings reveal to an extreme degree the fundamental role of agitation on test-stick performance.

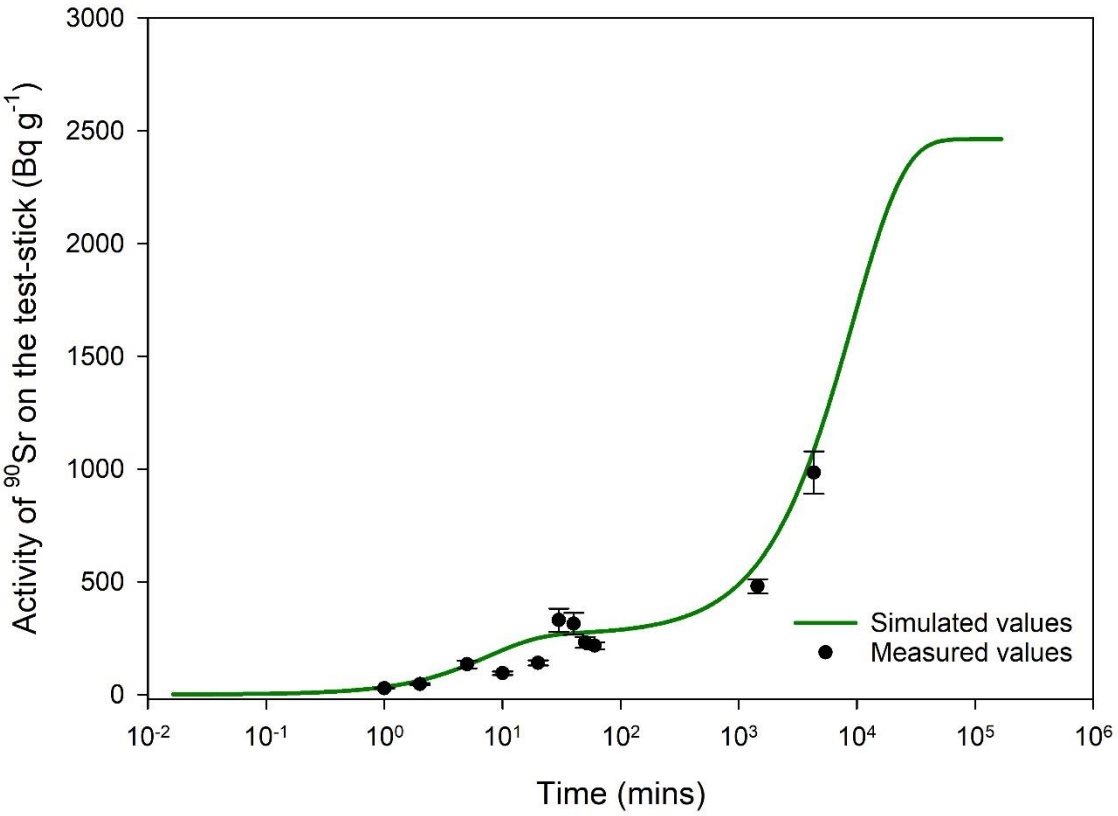

Figure 6.8: Simulated activities for ^{90}Sr loadings on unstirred TK100 test-sticks versus experimentally measured.

Numerical modelling also showed similar results for loadings of ^{90}Sr onto TK100 test-sticks where ^{90}Sr loadings increased exponentially even after 10^4 mins (>3 days). Again, it is important to note the effect of factors such as extractant loadings on the test-sticks and test-stick manufacture on the simulations shown here. However, these factors should not detract from the evidence shown here regarding the impact of agitation onto test-stick performance. This especially includes the importance of the incorporation of agitation to test-stick methodology in all works relating to test-sticks and eventual field deployment.

6.4.3 Simulated effect of variable extractant mass

An interesting and important application of this numerical model would be to simulate the performance of the TK100 test-sticks across variable extractant masses. This simulation would provide insight into how extractant loading may, or may not, impact test-stick performance and to what extent this factor may impact test-stick performance. These simulations would also give information regarding what the ideal target extractant loadings on the test-stick may be. This would

provide more information regarding the effect of variable extractant loadings onto the test-stick instead of investigating the extractant loadings of the current test-stick manufacture technique, as done in previous chapters (see section 4.3.1.). The current test-stick manufacturing technique has also been shown to contain an observable degree of human error (RSD = 25% for mass loading experiments and 16% for combined gravimetric data for TK100 test-sticks) and providing a target extractant mass loading for future developments in test-stick manufacture would be beneficial.

Table 6.4: Tabulated input parameters used to run variable mass loaded TK100 test-stick simulations.

$k_{forward}/\vec{k}$	2.191 x10^{-1}
$k_{backward}/\overleftarrow{k}$	2.085 x10^{-5}
$\left(\frac{V_s}{V_{aq}}\right)$	9.97 x10^{-1} – 9.99 x10^{-1}
$[s]$	0
$[aq]$	2.7

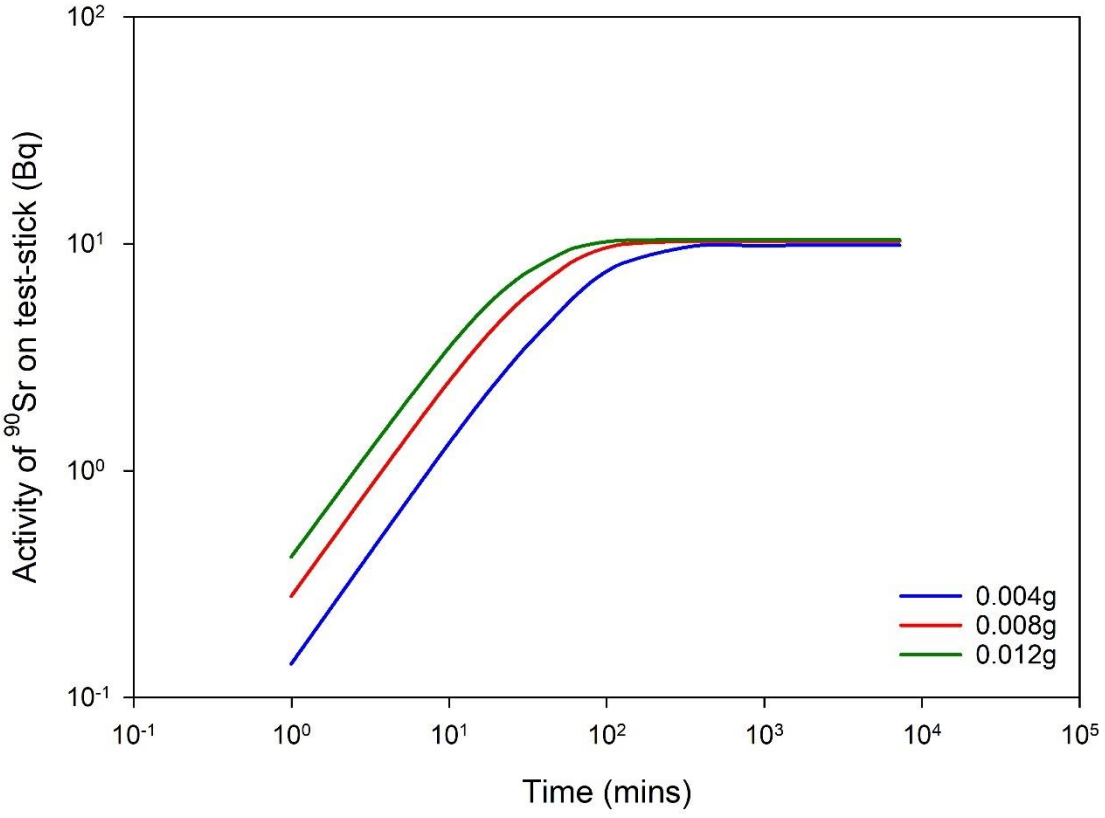

Figure 6.9: Simulated kinetic performance of different masses of TK100 loadings on stirred test-sticks in 4 mL volumes. Specifically simulating the activity of ^{90}Sr uptake onto the test-stick over time.

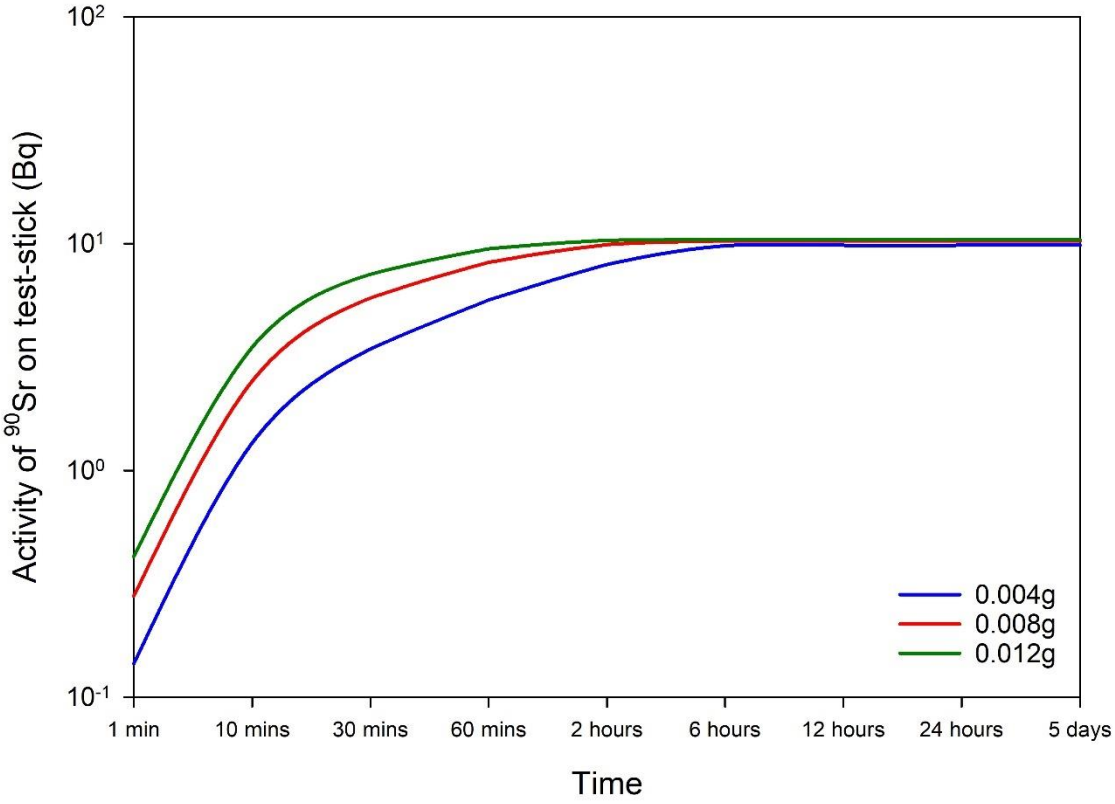

Figure 6.10: Simulated kinetic performance of different masses of TK100 loadings on stirred test-sticks, specifically simulating the activity of ^{90}Sr uptake onto the test-stick over time. Data here is shown over more concise time intervals to provide a more approachable presentation of the simulation results.

This data provides useful insight into the point at which full kinetic equilibrium is reached and fills in the gap in kinetic data points left by experimental kinetic studies where no samples for time intervals between 60 minutes and 1440 mins (24 hours) were present. It was found that at higher solid-phase masses (0.008g and 0.012g) saw test-stick performance to be similar from 30 mins onwards suggesting a mass loading window for TK100 test-sticks where kinetic performance at >30 mins onwards were found to be similar. This data corresponds extremely well to findings in the previous chapters (section 5.4.1.) where kinetic uptake for stirred test-sticks were found to plateau at approximately 40 minutes onwards. Solid phase mass effect seems to be greater at lower time intervals where higher solid phase masses were found to have higher ^{90}Sr uptake than lower extractant mass loadings – possibly demonstrating that higher loadings mean faster initial kinetics due to greater number of active sites and therefore a faster flux during initial sampling. However, these time intervals are not of interest to TK100 test-sticks as optimal sampling time for 'rapid' ^{90}Sr uptake was found to be between 40 to 60 minutes. Simulations also showed that if operators were able to allow sampling to occur up to 6 hours prior to measurement then extractant mass loadings

on TK100 test-sticks would have minimal effect on ^{90}Sr uptake. This essentially offers site operators and other potential test-stick clients a choice between carrying out sampling with optimal extractive resin loading test-sticks at shorter time intervals of 40 to 60 mins or allowing more flexible sampling times without requiring specific extractant mass loaded test-sticks (and potentially cheaper test-sticks) for in-*situ* characterisation.

6.4.4 Simulated effect of variable sample volume

A further important application of this numerical model is to not only simulate the performance of the TK100 test-stick with variable extractant mass loadings but also variable sample volumes. This investigation is especially interesting as it could dictate the extent of test-stick application from on-site sampling in nuclear decommissioning sites to more environmental samples or nuclear forensic applications such as radioactive spills. Simulating the performance of TK100 test-stick technology in variable sample volume may also serve to simulate the maximum operable sample volume for test-stick technology and therefore specify or suggest sample volume limits for test-stick technology.

Table 6.5: Tabulated input parameters used to run simulations for stirred TK100 test-sticks in variable sample volumes.

$k_{forward}/\vec{k}$	2.191 x10^{-1}
$k_{backward}/\overleftarrow{k}$	2.085 x10^{-5}
$\left(\frac{V_s}{V_{aq}}\right)$	9.9999 x10^{-1} – 9.99 x10^{-1}
$[s]$	0
$[aq]$	2.7

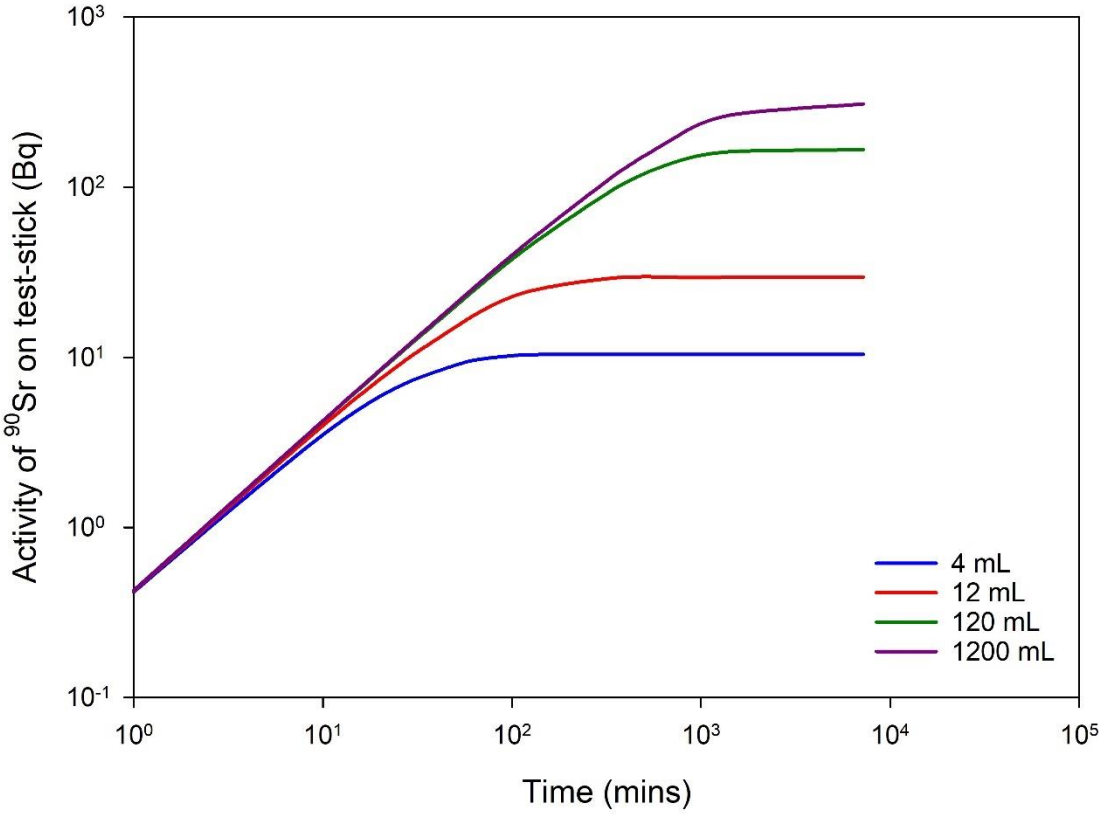

Figure 6.11: Simulated kinetic performance of stirred TK100 test-sticks in different sample volumes with constant 0.012g extractive resin mass loadings. Specifically simulating the activity of ^{90}Sr uptake onto the test-stick over time.

Simulations found text-sticks to exhibit ^{90}Sr loadings that varied considerably more than those on variable solid phase masses. Sampling in the first 10 minutes showed similar ^{90}Sr uptake performance by the test-sticks before sample volumes began to impact test-stick performance. Test-stick performance began to deviate between the different sample volumes at >20 mins and increasing sample volume begins to observably impact test-stick performance. This may be due to greater availability of free ^{90}Sr in solution at higher sample volumes compared to smaller sample volumes where limited availability of free ^{90}Sr means ^{90}Sr uptake reaches equilibrium quicker. It must be noted that these simulations were carried out over a large volume range (from 4 mL to 1.2L) and are not comparable to variable volume data shown in section 5.4.4. – as variable sample volumes investigated in this work were 1.0, 1.5, 2.0, 3.0 and 4.0 mL. Compared to this work, however, higher activity of ^{90}Sr loaded on the test-stick was simulated for 4 mL sample volumes (9.5 Bq) compared to experimental work carried out in section 5.3.3. (6.6 Bq). This disparity may be explained by test-stick simulations demonstrating optimal uptake performance of TK100 test-sticks as well as using 0.012g extractive resin mass loadings whilst experimental work is highly influenced by test-stick manufacture. This includes how well TK100 particles are mounted to the test-stick

(poor mounting may lead to TK100 particles becoming unbound during sampling, especially via agitation) and how consistent TK100 particles are distributed across the active site. These factors all contribute to the weighing uncertainties across each test-sticks' performance and highlights further the need to develop test-stick manufacture to minimise these issues (refer to chapter 4).

Despite the variance in ^{90}Sr uptake by the test-sticks across the different sample volumes, TK100 test-sticks demonstrated appreciable (>10^1 Bq) ^{90}Sr uptake and have demonstrated the potential for test-stick application in large sample volumes. However, for large sample volumes (such as from 120 to 1200 mL) it must be noted that significant deviation in ^{90}Sr loadings on the test-stick occurs at >100 mins. Therefore, if 60-minute sampling times are carried out then the same ^{90}Sr loadings are observed on the test-sticks regardless of sample volume. Interestingly, the maximum activity of ^{90}Sr loaded on the TK100 test-sticks were shown to increase with increasing sample volume reflecting the potential to increase sample volume in order to improve test-stick performance. However, it must be noted that stable Sr concentration in solution along with the test-stick capacity play an important role here and must be considered. Limit of detection may also be impacted as increasing the sample volume may mean the test-stick may be less capable of distinguishing small differences in ^{90}Sr activity from sample-to-sample. Although this may not be necessary as the test-sticks have been shown to perform well in 4 mL sample volumes, this demonstrates further potential for test-stick application as test-stick performance in terms of ^{90}Sr loadings is retained even in higher sample volumes. It must be noted, however, that this simulation assumes agitation to the system and does not account for the presence of ionic interferences including high concentrations of stable Sr. This is discussed further in the next section. Work on simulating the potential effect of ionic interferences on test-stick performance over time would be a feasible route for future work. Nonetheless, the work shown here demonstrates the potential of simulating test-stick data for different applications and conditions that would be otherwise difficult to simulate in a laboratory environment. Furthermore, these simulations also provide a measure of test-stick performance potential under different conditions – such as in large sample volumes in this case.

6.4.5 Simulated effects of further physical parameters

An important factor mentioned in the previous section was the significance of considering the role of stable Sr in solution on test-stick performance and accounting for this. This work would extend the work carried out in section 5.4.5. and simulate the performance of the TK100 test-sticks over a wider range of stable Sr concentrations and compare against a reference concentration from literature. Insight into the performance of the TK100 test-sticks under a wide range of stable Sr concentrations would confirm the suitability, or not, of TK100 test-sticks for field deployment. Furthermore, this work could also evaluate how much stable Sr concentration the test-sticks can

withstand before uptake performance starts to decrease. The maximum concentration of analyte on the test-stick ($[s]_E$) – capacity – was added to account for saturation of the extractive resin in the simulations. The value for $[s]_E$ was 0.09 mol L^{-1}, calculated from the stated capacity of TK100 (8 mg g^{-1}).

Table 6.6: Tabulated input parameters used to run simulations for TK100 test-sticks in variable initial Sr concentrations and mass ratio.

$k_{forward}/\vec{k}$	2.191 x10^{-1}
$k_{backward}/\overleftarrow{k}$	2.085 x10^{-5}
$\left(\frac{V_s}{V_{aq}}\right)$	9.83 x10^{-1} – 9.99 x10^{-1}
$[s]$	0.0
$[s]_E$	0.09
$[aq]$	1 x10^{-8} – 1 x10^{-2}

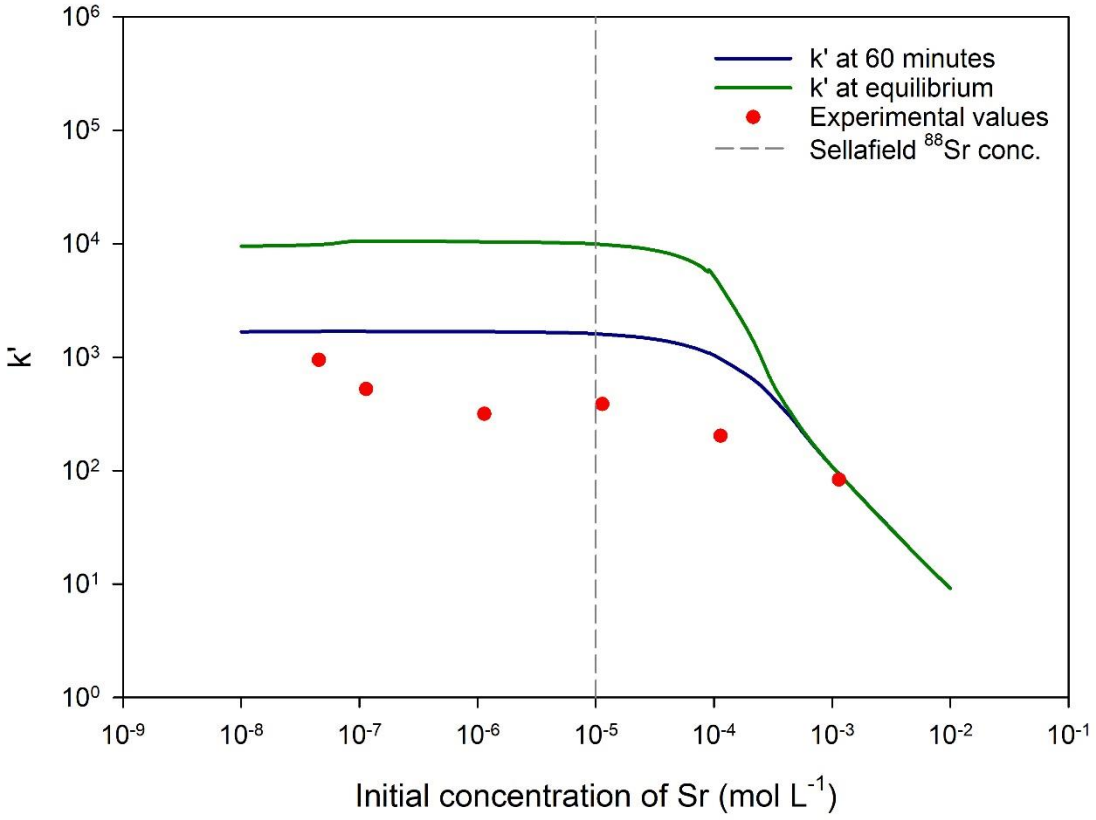

Figure 6.12: Calculated partition coefficients for TK100 test-sticks with variable initial Sr concentrations via the stirred model. This plot includes experimental values as well as the Sr concentration found in Sellafield groundwater from previous studies (grey dashed line) [64].

The first simulation involved monitoring the performance of the test-stick over different initial concentrations of Sr and obtaining the test-stick performance (in the form of k') at different times – 60 minutes and equilibrium (where the model stops). The simulations showed an expected deviation between k' values at 60 minutes and k' values at equilibrium for the variable initial Sr concentrations. The k' values were found to remain constant, for both 60 minutes and equilibrium, up to 10^{-4} mol L^{-1} of Sr where k' values began to drop steadily as the initial Sr concentration increases above the literature value. The literature value used here is the NNL report value for borehole work in Sellafield and therefore is a helpful guide for evaluating simulated test-stick performance against a real-world reference value. The simulation showed that test-stick performance remained constant even at the Sellafield concentration showing no decrease in test-stick performance and therefore demonstrates the viability of test-stick application in screening for ^{90}Sr in Sellafield groundwater. Simulation k' values are higher than those for the experimental values and this could be due to the simulation model only accounting for the performance of the extractant in a 2-D format whilst experimental values are subject to test-stick manufacture issues. These issues include

inconsistent spatial distribution of mounted extractant particles and extractant particle packing. Poor binding between the extractant particle(s) and the inert support due to unoptimised adhesive for binding small mass particles onto surfaces. Developments in adhesive and other test-stick manufacture techniques such as 3-D printing and electroplating would be beneficial to minimise result variance as well as allow test-sticks to replicate results similar to these simulations.

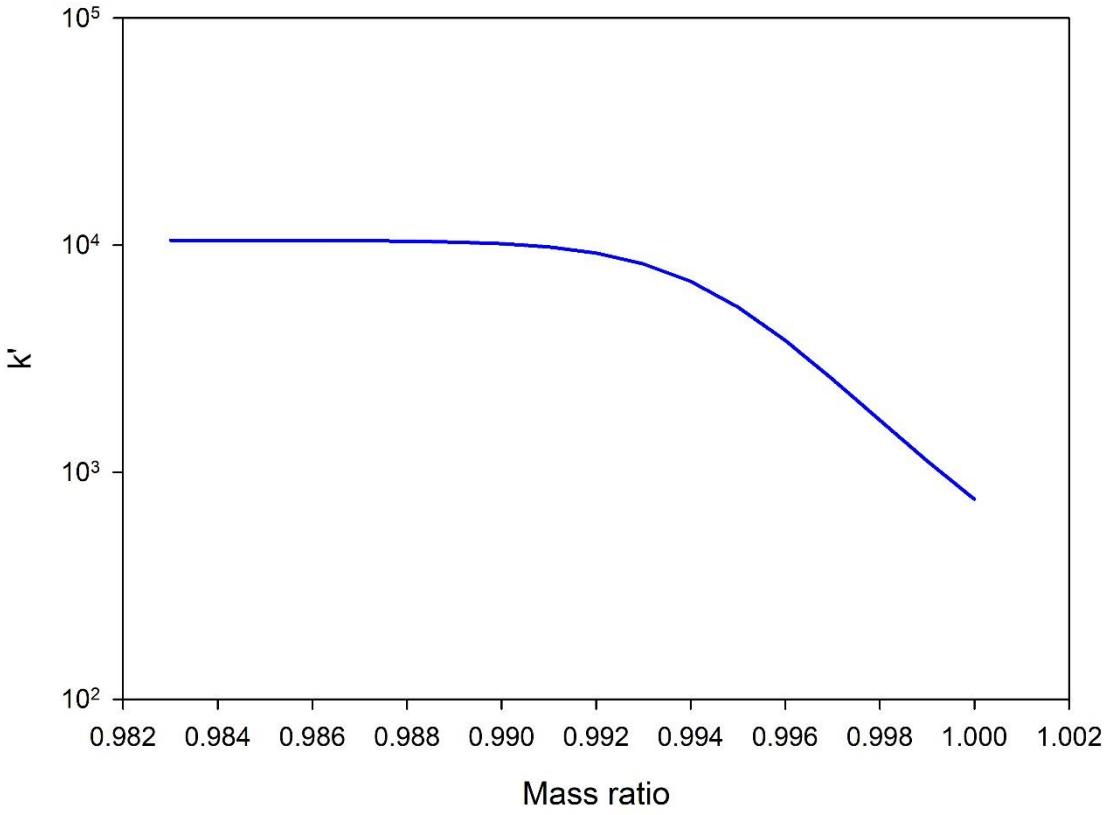

Figure 6.13: Calculated partition coefficient for variable mass ratio for TK100 test-sticks via the stirred model. Partition coefficients were obtained for 60-minute sampling times.

The next set of simulations demonstrated the performance of the test-sticks across different mass ratio values. Mass ratio is the ratio between the aqueous phase (sample) and the solid phase (test-stick extractive resin) and therefore in the case of test-sticks a mass ratio value of 0.999 equates to a value of 0.004g for the solid phase in a 4 mL total (solid phase plus aqueous sample) volume; i.e. test-stick extractant mass loading of 4 mg. This simulation work therefore indicates at which sample volume:extractant mass loading ratio test-stick performance begins to observably decrease. The numeric model revealed this to be approximately >0.992 which equates to a mass of 48 mg of extractant in 4 mL of sample volume. This shows that if test-stick solid phase masses are lower than 48 mg for sampling in a 4 mL sample then equilibrium cannot be established within 60 minutes. However, it is important to note that test-stick kinetic data (see section 6.4.1. and 6.4.2.) has shown that TK100 test-sticks can obtain a 'steady-state' system between 40 to 60 minutes where uptake

performance is appreciable. This means that despite equilibrium establishing after 60 minutes for solid phase masses <48 mg, test-sticks can still be deployed for sub-one-hour sampling times to meet the requirements of rapid screening techniques. This information can also act as a guideline for test-stick design in which test-sticks can be manufactured with the required extractant mass loadings to screen the desired sample volume. This includes bodies of water, acid work-up of decommissioning samples and acid leachate of contaminated soil samples, for example.

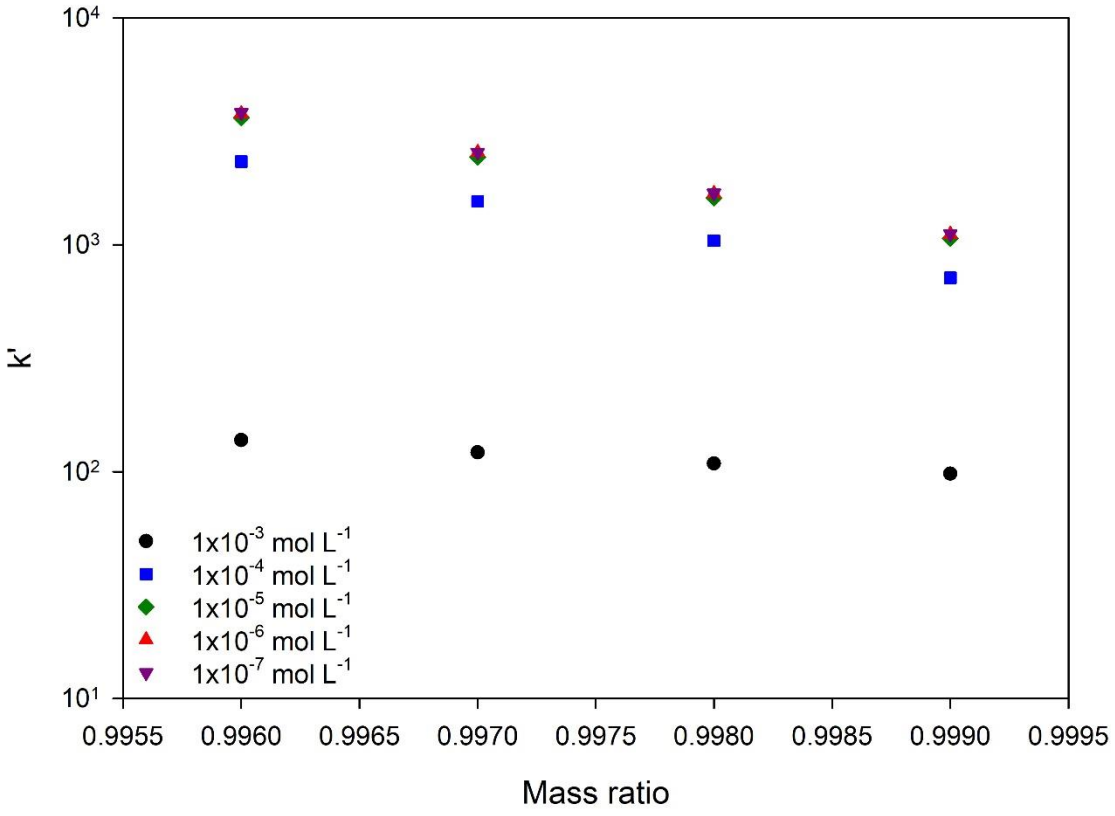

Figure 6.14: Calculated partition coefficients via the stirred model for a range of initial Sr concentrations over variable mass ratios. Partition coefficients were obtained for 60-minute sampling times.

The final set of numerical model simulations looked to demonstrate the performance of the TK100 test-stick with variable mass ratios under different initial Sr concentrations. Simulations were ran for 60 minutes to reflect current test-stick sampling methodology. This work looked to build on the previous works including variable mass ratio and variable initial Sr concentrations. The results demonstrated that at low Sr concentrations (between $1x10^{-5}$ and $1x10^{-7}$ mol L^{-1}) there was no discernible difference in test-stick performance across different mass ratio values. However, at $1x10^{-4}$ mol L^{-1} a small decrease in test-stick performance versus the lower stable Sr concentrations was observed through the mass ratios tested. Furthermore, an even larger decrease in test-stick performance was observed for $1x10^{-3}$ mol L^{-1}. The results suggest that mass ratios have less impact

on test-stick performance at Sr concentrations lower than 10^{-3} mol L^{-1} (parts per thousand – ppt). This can be useful for future test-stick design where if known concentrations of Sr in groundwater, for example, exceed ppt levels then extractant mass loadings on the test-sticks play a minimal role in test-stick performance due to stable Sr quickly occupying active sites and the test-stick reaching equilibrium within 60 minutes. These findings allow for future test-stick design to account for the effect of stable Sr concentration on test-stick performance and design TK100 test-stick with the required solid phase mass (>48 mg for a 4 mL sample) to overcome this. Furthermore, this work provides a numerical model capable of predicting test-stick performance for other extractants whilst accounting for the impact of possible interferences such as the stable isotope of the radionuclide in question on test-stick performance.

6.5 Conclusion

This chapter has presented the application of a numerical model to simulate test-stick performance of TK100 test-sticks. Experimental work on the kinetics performance of TK100 test-sticks in both stirred and unstirred systems provided the necessary data to extract the input parameters for the numerical model. This data included $k_{forward}$, $k_{backward}$ and mass ratio $\left(\frac{V_S}{V_{aq}}\right)$ data which then allowed subsequent simulations to be carried out. Bulk-phase batch-uptake data (see appendix) was also acquired to provide further data for the model to improve the accuracy of these simulations. Kinetic experiments along with simulations demonstrated further the impact of agitation on test-stick performance. Stirred test-stick systems were found to establish a steady-state system within 40 to 60 minutes and equilibrium in approximately 24 hours. Steady-state in this case describes the process where ^{90}Sr uptake slows down as active sites become occupied and ^{90}Sr uptake is controlled by mass transfer and chemical diffusion through the TK100 beads to reach remaining available active sites. Unstirred test-stick were predicted to reach equilibrium in approximately >30 days. The impact of variable extractant mass loadings on the test-stick solid phase was monitored and found to affect test-stick performance if sampling was carried out at <6 hours. At lower sampling times mass loadings on the test-sticks influenced test-stick performance. This essentially offers site operators and other potential test-stick clients the choice between controlling extractant loadings on the test-sticks (via improvements in test-stick manufacture) allowing for test-stick sampling times of 40 to 60 minutes or allowing more flexible test-stick extractant mass loadings but carry out >6 hours test-stick sampling times. This offers potential flexibility to test-sticks where test-sticks can be manufactured to meet the needs of the client whether they require cheap test-sticks for <24-hour sampling or require more rapid sampling times and therefore more controlled extractant loadings on the test-sticks. Simulations also predicted the performance of test-sticks across variable sample volumes, from the standard 4 mL to 1.2 L. These simulations showed that increasing the

sample volume could potentially increase test-stick performance as more available ^{90}Sr was present and therefore the test-sticks did not reach 'steady-state' as quickly as in smaller volumes, such as 4 mL. However, the simulation does not take into account the capacity of the extractant (8 mg g^{-1} Sr) as well as the concentration of stable Sr in solution and therefore future work can be carried out to obtain this information. Finally, simulations were carried out to determine the performance of the test-sticks across different concentrations of stable Sr. This work was also replicated to monitor the performance of the test-sticks in these different stable Sr concentrations with varying mass ratios of extractant loadings on test-sticks versus sample volume. Simulations showed the test-sticks to perform well in terms of k' values at concentrations of stable Sr higher than those reported for Sellafield groundwater ($\sim$1 x10^{-5}). This suggests that test-sticks could perform optimally in groundwater samples without Sr loading capacity of the test-sticks being reached. Simulations also suggested that test-sticks could potentially reach equilibrium in 60 minutes if extractant loadings on the test-sticks were 48 mg or higher for sampling in 4 mL samples. However, work on test-stick uptake kinetics has shown the existence of a 'steady-state' at 40 to 60 minutes for stirred test-sticks where test-stick uptake performance is appreciable, compared to test-stick performance at equilibrium (see section 6.4.1.). The simulations still further highlighted the need to optimise test-stick manufacture as controlling the solid phase mass loadings observably improves the kinetic performance of the test-sticks. Finally, the simulations found that at stable Sr concentrations exceeding 1 x10^{-3} the mass ratio of the test-sticks played almost no role in the performance of the test-sticks. Therefore, at higher concentrations of stable Sr, as long as there is no risk of saturating the test-sticks, test-stick performance is independent of extractant loading masses on the test-sticks. It must be noted that this data is influenced by saturation capacity of the specific extractant test-stick and therefore this is likely to change for different extractants, especially those with higher loading capacities such as Clevasol (243 mg g^{-1} ^{90}Sr). Overall, this work provided insight into the performance of the test-sticks over conditions which would be otherwise difficult to replicate in the lab and provide a guideline for future test-stick developments.

Chapter 7 Overall conclusion and future work

7.1 Overall conclusion

This thesis has developed and characterised test-stick technology for the rapid screening of ^{90}Sr in groundwater samples. This work has considered the impact of the test-stick manufacturing process (chapter 4) and deployment protocols (chapter 5) on test-stick performance and how these findings can be used to optimise test-stick performance in the future. A switch in approaches to test-stick technology using numerical modelling to simulate test-stick performance in conditions that would otherwise be difficult to replicate in the lab (chapter 6) was also utilised to discover further optimisations to the technique.

The manufacturing process and the key properties associated with the manufacture of the test-sticks were examined. SEM imaging provided information regarding the distribution of the extractive resin particles across the test-stick active site. These images showed an extent of 'layering' occurring on the surface of both extractive resin test-sticks. This observation was expected to impact test-stick performance and reproducibility of both extractive resin test-sticks showed this with 32% and 26% variance between test-sticks for TK100 and Clevasol, respectively. However, extractive resin mass loadings for both TK100 (25%) and Clevasol (30%) test-sticks showed similar statistical certainty to reproducibility data indicating variance in particle packing playing a role in test-stick performance reproducibility. Despite the contrasting uptake mechanisms and chemistry between both extractive resin test-sticks both exhibited similar reproducibility and mass loadings on the test-sticks. Surface area and particle size effect were found to impact TK100 test-stick performance with larger surface area and smaller particle sizes enabling the TK100 test-stick to perform better.

Test-stick deployment protocols involved evaluating the performance of both TK100 and Clevasol test-sticks under a series of conditions. Kinetic studies showed both TK100 and Clevasol test-sticks reaching a 'steady-state' system between 40 to 60 minutes indicating the potential of test-stick sampling times being reduced in future test-stick procedures. Test-stick response studies demonstrated Clevasol test-sticks to exhibit proportional uptake across a wide range of ^{90}Sr activities whilst diffusion control studies showed TK100 test-sticks required agitation to improve ^{90}Sr uptake and minimise ^{90}Y uptake. Clevasol test-sticks did not require agitation to exhibit proportional uptake of ^{90}Sr. Variable volume was shown to have minimal impact on TK100 test-stick performance above that observed in reproducibility experiments (32%) whilst Clevasol showed increasing performance with increasing sample volumes up to 4 mL. Strontium loading capacities

revealed TK100 test-sticks to approach loading capacity at 100 ppm stable Sr whilst Clevasol test-sticks could perform at higher Sr concentrations up to 1000 ppm without reaching loading capacity. Chemical interferences were investigated individually on the performance of both extractive resin test-sticks. The chemical interferences (Na, K, Ca and Mg) were shown to have minimal impact on both TK100 and Clevasol test-sticks' performance. Calculation of count times using a proportionality constant, b_t, and the Currie limit-of-detection equation calculated count times of 10 minutes for ultra low level LSC and estimated 60 minutes for more readily deployable LSC instruments. These findings demonstrated the potential of test-stick technology to fulfil the objectives set out by the NDA – carrying out 70% of initial characterisation in-*situ* with turnaround in results within 24 hours. An overall summary of test-stick optimisations for both TK100 and Clevasol, where relevant, is shown in the table below:

Table 7.1: Comparison of original conditions versus optimised conditions established from experiments carried out in this project. Note: ULLLSC = ultra low level LSC, TTLSC = tabletop LSC.

Parameters	TK100		Clevasol	
	Original	Optimised	Original	Optimised
Surface area	1 cm^2	1 cm^2	1 cm^1	
Particle size	100-150 µm	50-100 µm	-	-
Sampling time	60 minutes	40 minutes	60 minutes	40 minutes
Diffusion control	-	Yes	-	Yes
Sample volume	4 mL	4 mL	4 mL	4 mL
Count time	60 minutes	10 mins (ULL LSC) 60 mins (TTLSC)	60 minutes	10 mins (ULL LSC) 60 mins (TTLSC)

Numerical modelling provided insight into the performance of the TK100 test-sticks in conditions which were unrealistic to replicate in the lab. Test-stick performance over time using different extractive resin loadings provided further insight into the impact of these loadings onto test-stick performance. The numerical model showed that the site operators and other relevant clients could essentially have a choice between two options. The first would be controlling extractive resin loadings and therefore carrying out sampling within 40 to 60 minutes. The second would be to allow more flexible extractive resin mass loadings whilst only needing to increase sampling times to 6 hours. The latter option could also potentially make test-sticks even cheaper to suit the needs of potentially more clients whilst operating with results turnaround within 24 hours. Application of

the test-stick in a wider range of sample volumes using this numerical model showed that a wide range (from 4 mL to 1.2L) of sample volumes could be screened in 60 minutes whilst demonstrating almost identical ^{90}Sr loadings on the test-sticks. Performance of the test-stick over a range of stable Sr concentrations were also simulated and compared against Sr concentration in Sellafield groundwater, showing the test-sticks to operate well at higher concentrations of stable Sr than those recorded in Sellafield groundwater.

7.2 Future work

A reoccurring theme of future work throughout this thesis was the call for optimising the test-stick manufacture process. Optimisation of the test-stick manufacture process would bring improvements in test-stick performance including test-stick reproducibility which was shown to compare well with extractive resin mass loadings on the test-sticks, for both TK100 and Clevasol. The current method is a simplistic method where application of the spray adhesive and extractive resin mounting is done by the operator. A test-stick manufacturing process which could guarantee tightly packed monolayer extractive resin active sites would help to reduce the variance observed in some of the data, especially for ^{90}Sr loadings on the test-sticks. These variances in ^{90}Sr loadings were observed for both extractive resin test-sticks but especially Clevasol test-sticks. This observation was explained in SEM imaging where Clevasol particles were shown to be inconsistent in particle sizes (200 ± 100 μm) compared to TK100 (100-150 μm, for most TK100 test-sticks). Furthermore, these SEM images showed Clevasol particles to have a rough exterior with no degree of homogeneity, compared to TK100 particles which were shown to be smooth bead-like particles. Future work could include sourcing Clevasol or any other future extractive resins with improved manufacturing where homogenous surface topography and more constrained particle sizes are obtained. This would also make it easier for future test-stick manufacturing methods to tightly pack the particle into a monolayer extractive resin surface on the test-sticks. Future work could include adapting the ^{90}Sr test-stick presented here to other DTM radionuclides such as ^{99}Tc and build a catalogue of different radionuclide test-sticks for rapid screening the DTM radionuclide of choice (Table 1). This test-stick catalogue would then facilitate the development of multi-extractant test-sticks where a test-stick could be manufactured with multiple extractive resins to screen for a number of radionuclides. Once sampling was complete, MES test-sticks would be analysed via solid plate scintillators which would provide spatial resolution of the test-sticks including information regarding radionuclide uptake on each of the different active sites.

Table 7.2: Example of other potential DTM radionuclides which test-sticks could be developed for as well as extractive resins to manufacture said test-sticks with.

Radionuclide	Extractive resin
^{99}Tc	TEVA[65], **TK-TcScint**[66]
^{59}Fe	Actinide resin[67], TRU resin[68]

Further works, highlighted in **bold** in table 1, are combining extractive resins with scintillators to expedite the process even further. This would potentially remove the need to add scintillator cocktails or use scintillation plates and therefore only a photomultiplier (PM) tube system would be needed. This would streamline test-stick technology even further and require minimal equipment to carry out rapid in-*situ* characterisation. Streamlining of the characterisation process with targeted result turnaround time within 24 hours would bring savings in costs and time to the current nuclear decommissioning project – and test-stick technology presents itself as a viable candidate to support this objective.

Appendix A Supplementary information for Chapter 5

Derivation for the simultaneous equations, to solve for the activity of both ^{90}Sr and ^{90}Y, are shown below:

$$c_1 = k_1 A_{Sr-90} + k_2 A_{Y-90}$$

$$c_2 = k_3 A_{Sr-90} + k_4 A_{Y-90}$$

Rearranging to give A_Y,

$$c_2 - k_3 A_{Sr-90} = k_4 A_{Y-90}$$

$$A_{Y-90} = \frac{c_2}{k_4} - \frac{k_3}{k_4} A_{Sr-90}$$

Substituting into equation for c_1,

$$c_1 = k_1 A_{Sr-90} + k_2 A_{Y-90}$$

$$c_1 = k_1 A_{Sr-90} + k_2 \left(\frac{c_2}{k_4} - \frac{k_3}{k_4} A_{Sr-90}\right)$$

$$c_1 = k_1 A_{Sr-90} + \frac{c_2 k_2}{k_4} - \frac{k_2 k_3}{k_4} A_{Sr-90}$$

Grouping terms for $A_{Sr\text{-}90}$,

$$c_1 = \left(k_1 - \frac{k_2 k_3}{k_4}\right) A_{Sr-90} + \frac{c_2 k_2}{k_4}$$

$$c_1 - \frac{c_2 k_2}{k_4} = \left(k_1 - \frac{k_2 k_3}{k_4}\right)$$

$$\frac{\left(c_1 - \frac{c_2 k_2}{k_4}\right)}{\left(k_1 - \frac{k_2 k_3}{k_4}\right)} = A_{Sr-90}$$

Solving for ^{90}Y,

$$c_1 = k_1 A_{Sr-90} + k_2 A_{Y-90}$$

$$c_1 - k_1 A_{Sr-90} = k_2 A_{Y-90}$$

$$A_{Y-90} = \frac{c_1 - k_1 A_{Sr-90}}{k_2}$$

Appendix B Supplementary information for Chapter 6

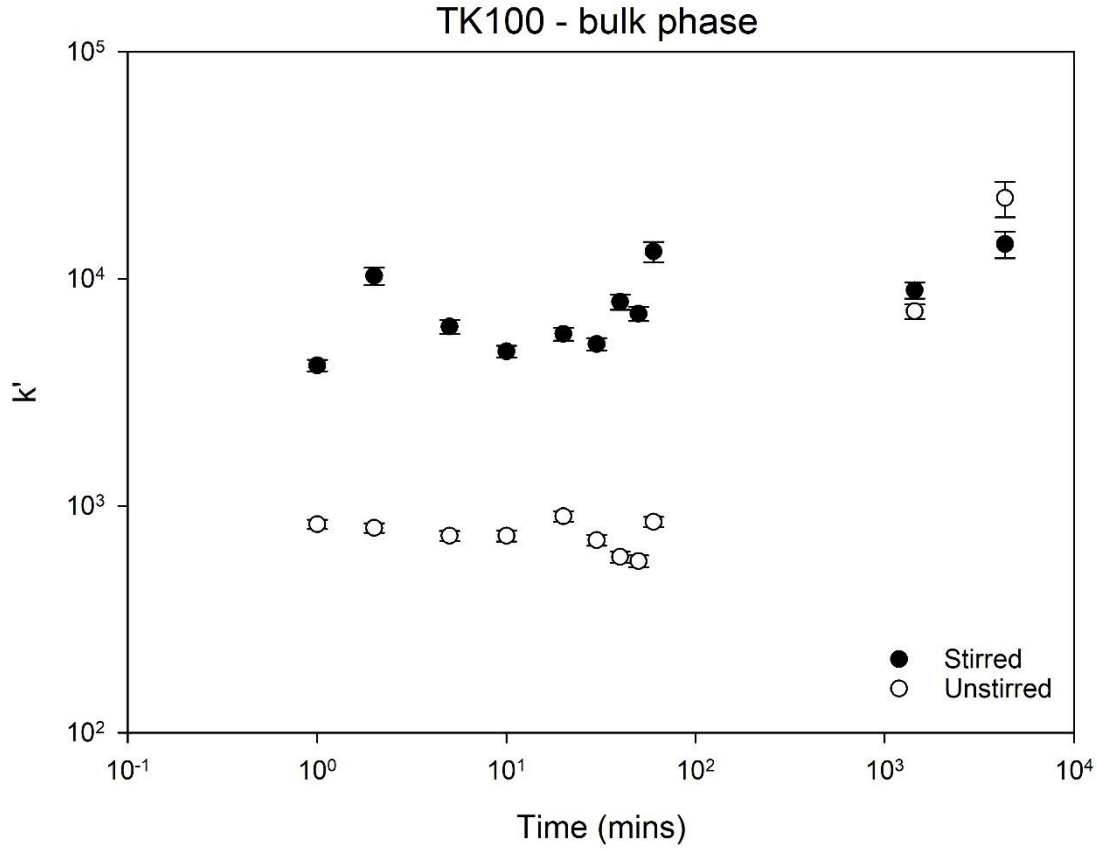

Figure 7.1: Partition coefficients of bulk-phase TK100 extractive resin between 1 min and 72 hours.

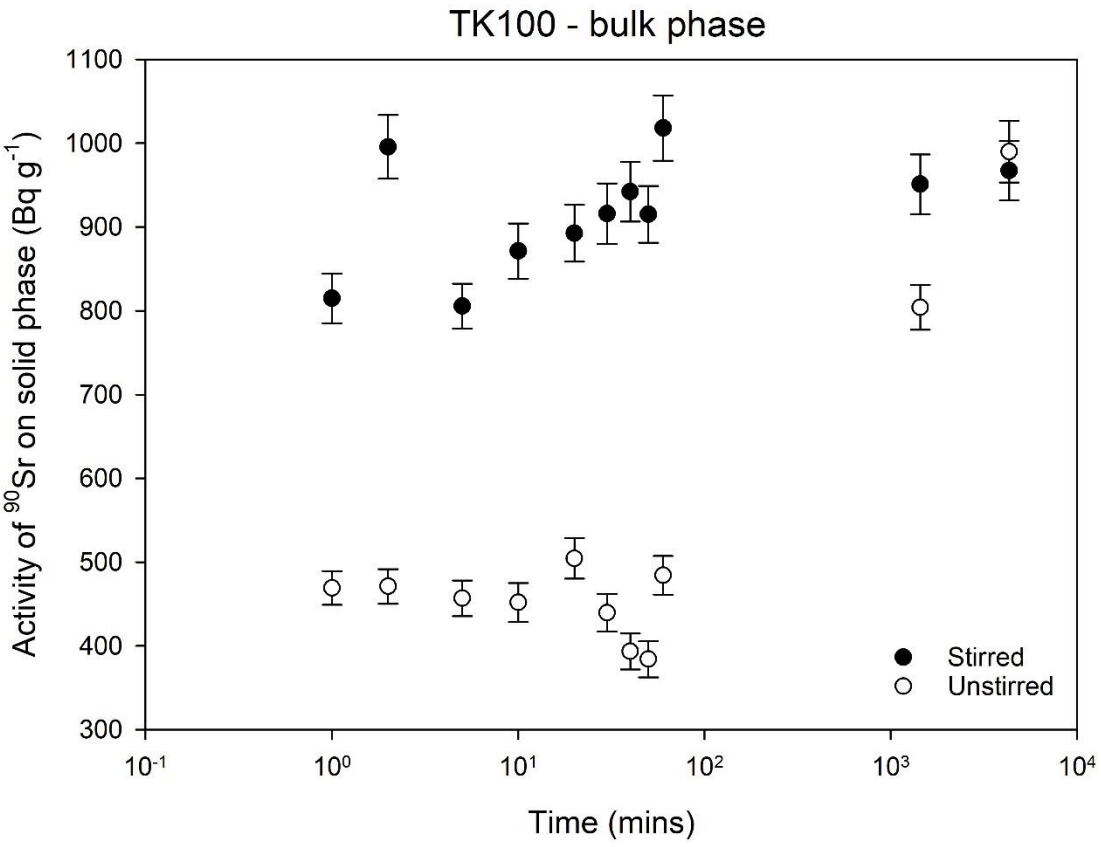

Figure 7.2: Measured ^{90}Sr loadings on bulk-phase TK100 extractive resin between 1 min and 72 hours.

List of References

1. Arnold L. A Letter from Oxford: The History of Nuclear History in Britain. *Minerva*. 2000;38(2):201-219. doi:10.1023/A:1026553128414

2. Atomic Energy Act of 1946 US. United States. Published 1946. Accessed August 2, 2021. https://web.archive.org/web/20170903230822/https://www.osti.gov/atomicenergyact.pdf

3. Atomic Energy Act 1946. United Kingdom. Published 1946. Accessed August 2, 2021. https://www.legislation.gov.uk/ukpga/Geo6/9-10/80/data.pdf

4. Atomic Energy Authority Act 1954. United Kingdom. Published 1954. Accessed August 2, 2021. http://www.legislation.gov.uk/ukpga/Eliz2/2-3/32

5. Elliott D. *Nuclear Power Past, Present and Future*. IOP Publishing; 2017. doi:10.1088/978-1-6817-4505-3

6. House of Commons Trade and Industry Committee. *The Nuclear Decommissioning Authority Pre–Legislative Scrutiny of the Draft Nuclear Sites and Radioactive Substances Bill*.; 2003. https://publications.parliament.uk/pa/cm200203/cmselect/cmtrdind/968/968.pdf

7. Nuclear Decommissioning Authority. *Nuclear Decommissioning Authority Business Plan 2018 to 2021*.; 2018. Accessed October 30, 2018. https://assets.publishing.service.gov.uk/government/uploads/system/uploads/attachment_data/file/695245/NDA_Business_Plan_2018_to_2021.pdf

8. Authority ND. The NDA Operating Model Guidance on the Roles of the Site Licence Company and the Parent Body Organisations Doc No NSG 31 The NDA Operating Model Guidance on the Roles of the Site Licence Company and the Parent Body Organisations Doc No NSG 31. Published online 2013:1-16.

9. Nuclear Decommissioning Authority. *Strategy Effective from April 2016*.; 2016. Accessed June 14, 2018. https://assets.publishing.service.gov.uk/government/uploads/system/uploads/attachment_data/file/512836/Nuclear_Decommissioning_Authority_Strategy_effective_from_April_2016.pdf

10. Nuclear Decommissioning Authority. *Strategy Effective from March 2021*.; 2021.

11. Elísio S, Joyce MJ, Graham J, Greenhalgh B. An advanced blind-tube monitoring instrument

to improve the characterization of subsurface radioactive plumes. *EPJ Web Conf*. 2021;253:08005. doi:10.1051/epjconf/202125308005

12. How do we manage radioactive waste? | UK Radioactive Waste Inventory (UKRWI). Accessed October 12, 2021. https://ukinventory.nda.gov.uk/about-radioactive-waste/how-do-we-manage-radioactive-waste/

13. International Atomic Energy Agency. *Strategy and Methodology for Radioactive Waste Characterization*.; 2007.

14. Nuclear Decommissioning Authority. NDA Technical Baseline Executive Summary NDA Technical Baseline. 2016;(1):48-58. Accessed January 10, 2018. https://www.gov.uk/government/uploads/system/uploads/attachment_data/file/573486/NDA-Technical-Baseline-October2016_Issue1.pdf

15. EPR. The Environmental Permitting (England and Wales) Regulations. SI 2016/1154. 2016;(1154).

16. Emptage M, Loudon D, Mcleod R, Milburn H, Row N. Characterisation : Challenges and Opportunities – A UK Perspective. *PREDEC Int Symp Prep Decommissioning*. Published online 2016:1-10.

17. IAEA. Determination and Use of Scaling Factors for Waste Characterization in Nuclear Power Plants. Published online 2009:124. http://www-pub.iaea.org/books/iaeabooks/7985/Determination-and-Use-of-Scaling-Factors-for-Waste-Characterization-in-Nuclear-Power-Plants

18. Furukawa M, Takagi Y. 90Sr Analysis Using Inductively Coupled Plasma Mass Spectrometry with Split-Flow Injection and Online Solid-Phase Extraction for Multiple Concentration and Separation Steps. In: *Agricultural Implications of the Fukushima Nuclear Accident (III): After 7 Years*. ; 2019:235-248. doi:10.1007/978-981-13-3218-0

19. Croudace IW, Warwick PE, Reading DG, Russell BC. Recent contributions to the rapid screening of radionuclides in emergency responses and nuclear forensics. *TrAC - Trends Anal Chem*. 2016;85:120-129. doi:10.1016/j.trac.2016.05.007

20. Bliznyuk VN, Seliman AF, Ishchenko AA, Derevyanko NA, Devol TA. New Efficient Organic Scintillators Derived from Pyrazoline. *ACS Appl Mater Interfaces*. 2016;8(20):12843-12851. doi:10.1021/acsami.6b02719

21. Sun Y, Yang S, Chen Y, Ding C, Cheng W, Wang X. Adsorption and Desorption of U(VI) on

Functionalized Graphene Oxides: A Combined Experimental and Theoretical Study. *Environ Sci Technol*. 2015;49:4255-4262. doi:10.1021/es505590j

22. Russell B, García-Miranda M, Ivanov P. Development of an optimised method for analysis of 90 Sr in decommissioning wastes by triple quadrupole inductively coupled plasma mass spectrometry. *Appl Radiat Isot*. 2017;126:35-39. doi:10.1016/j.apradiso.2017.01.025

23. Buchtela K. Radiochemical Methods - Gamma-Ray Spectrometry. In: Worsfold P, Townshend A, Poole C, eds. *Encyclopedia of Analytical Science: Second Edition*. Second. Elsevier Inc.; 2005:72-79. doi:10.1016/B0-12-369397-7/00525-2

24. Buchtela K. Gas Ionization Detectors. In: L'Annunziata MF, ed. *Handbook of Radioactivity Analysis*. Elsevier Inc.; 2004:123-178. doi:10.1016/B978-012436603-9/50007-7

25. L'annunziata MF. Solid Scintillation Analysis. In: *Handbook of Radioactivity Analysis*. Academic Press; 2003:1021-1115.

26. Dyer A. *An Introduction to Liquid Scintillation Counting*. First. Heyden; 1974.

27. Keith-Roach M, Achterberg EP. Radiochemical Methods - Uranium. *Encycl Anal Sci Second Ed*. Published online January 1, 2004:44-49. doi:10.1016/B0-12-369397-7/00521-5

28. Willard HH, Goodspeed EW. Separation of Strontium, Barium, and Lead from Calcium and Other Metals. *Ind Eng Chem Anal Ed*. 1936;8(6):414-418. Accessed May 8, 2019. https://pubs.acs.org/sharingguidelines

29. Otto JB, Blank WK, Dahl DA. A nitrate precipitation technique for preparing strontium for isotopic analysis. *Chem Geol (Isotope Geosci Sect*. 1988;72:173-179. Accessed May 8, 2019. https://pdf.sciencedirectassets.com/273274/1-s2.0-S0168962200X00425/1-s2.0-0168962288900656/main.pdf?x-amz-security-token=AgoJb3JpZ2luX2VjEEsaCXVzLWVhc3QtMSJIMEYCIQCfwGgEeVBgBD0GlnKSpXdMyR0LN01aJOuYXi4FPhdWTQIhAIOWRYiORTvWV76KTEyCMCUhwTZnO4OPrGz1B497FW84K

30. Horwitz E, Dietz ML, Fisher DE. Separation and Preconcentration of Strontium from Biological, Environmental, and Nuclear Waste Samples by Extraction Chromatography Using a Crown Ether. *Anal Chem*. 1991;63(5):522-525. doi:10.1021/ac00005a027

31. Horwitz E, Chiarizia R, Dietz ML. A novel strontium selective extraction chromatographic resin. *Solvent Extr Ion Exch*. 1992;10(2):313-336. doi:10.1080/07366299208918107

32. Egorov OB, O'Hara MJ, Grate JW. Equilibration-based preconcentrating minicolumn sensors

for trace level monitoring of radionuclides and metal ions in water without consumable reagents. *Anal Chem*. 2006;78(15):5480-5490. doi:10.1021/ac060355m

33. O'Hara MJ, Burge SR, Grate JW. Automated Radioanalytical System for the Determination of 90 Sr in Environmental Water Samples by 90 Y Cherenkov Radiation Counting. *Anal Chem*. 2009;81(3):1228-1237. doi:10.1021/ac8021407

34. Uesugi M, Watanabe R, Sakai H, Yokoyama A. Rapid method for determination of 90Sr in seawater by liquid scintillation counting with an extractive scintillator. *Talanta*. 2018;178:339-347. doi:10.1016/j.talanta.2017.09.041

35. Tayeb M, Dai X, Sdraulig S. Rapid and simultaneous determination of Strontium-89 and Strontium-90 in seawater. *J Environ Radioact*. 2016;153:214-221. doi:10.1016/j.jenvrad.2016.01.003

36. Amano H, Sakamoto H, Shiga N, Suzuki K. Method for rapid screening analysis of Sr-90 in edible plant samples collected near Fukushima, Japan. *Appl Radiat Isot*. 2016;112:131-135. doi:10.1016/j.apradiso.2016.03.026

37. Vos Van Avezathe A, Brandhoff PN, Van Bourgondien MJ, Krijger GC. Rapid screening methods for beta-emitters in food samples. *J Environ Radioact*. 2015;141:130-137. doi:10.1016/j.jenvrad.2014.12.010

38. LabLogic Systems, Southern Scientific. *WILMA: On-Line Water Radioactivity Monitor*.; 2016. Accessed June 26, 2019. www.southernscientific.co.uk

39. Carconi P, De Felice P, Fazio A, et al. Characterization and calibration of a novel detection system for real time monitoring of radioactive contamination in water processed at water treatment facilities. *Appl Radiat Isot*. 2017;126:138-145. doi:10.1016/j.apradiso.2017.01.023

40. Warwick PE, Croudace IW. Rapid on-site radionuclide screening of aqueous waste streams using dip-stick technologies and liquid scintillation counting. *J Radioanal Nucl Chem*. Published online 2017. doi:10.1007/s10967-017-5413-9

41. TrisKem International. *Sr-Resin Product Sheet*. Vol 0.; 2016.

42. Kabai E, Hornung L, Savkin BT, Poppitz-Spuhler A, Hiersche L. Fast method and ultra fast screening for determination of 90 Sr in milk and dairy products. *Sci Total Environ*. 2011;410-411:235-240. doi:10.1016/j.scitotenv.2011.09.052

43. Surman JJ, Pates JM, Zhang H, Happel S. Development and characterisation of a new Sr selective resin for the rapid determination of 90 Sr in environmental water samples. *Talanta*. 2014;129:623-628. doi:10.1016/j.talanta.2014.06.041

44. TrisKem International. *TK100 / TK101 Product Sheet*. Vol 0.; 2014.

45. Mohamud H, van Es EM, Sainsbury T, et al. Progress towards the development of a rapid analytical approach for separation of226Ra using dibenzo-18-crown-6 ether functionalised silica (SiO2) disks. *Radiat Phys Chem*. 2017;140(February):57-60. doi:10.1016/j.radphyschem.2017.02.020

46. LemerPax. *CLEVASOL; A Novel Cation Exchange Resin for Isotope Capture*.; 2019.

47. Türler A, Yakushev A. BOPOR Patent. Published online 2010:1-16. https://register.dpma.de/DPMAregister/pat/register?AKZ=1020080646822

48. Singer DM, Johnson SB, Catalano JG, Farges F ßois, Brown GE. Sequestration of Sr(II) by calcium oxalate—A batch uptake study and EXAFS analysis of model compounds and reaction products. *Geochim Cosmochim Acta*. 2008;72:5055-5069. doi:10.1016/j.gca.2008.07.020

49. Froidevaux P, Pittet PA, Bühlmann D, Bochud F, Straub M. Ion-imprinted resin for use in an automated solid phase extraction system for determining 90 Sr in environmental and human samples. *J Radioanal Nucl Chem*. 2021;330:797-804. doi:10.1007/s10967-021-07974-8

50. Novoselov KS, Geim AK, Morozov S V, et al. Electric Field Effect in Atomically Thin Carbon Films. *Science (80-)*. 2000;306(5696):666-669. doi:10.1126/science.1102896

51. Mohamud H, Ivanov P, Russell BC, Regan PH, Ward NI. Selective sorption of uranium from aqueous solution by graphene oxide-modified materials. *J Radioanal Nucl Chem*. Published online 2017. doi:10.1007/s10967-018-5741-4

52. Bubeníková M, Ecorchard P, Szatmáry L, Mrózek O, Salačová P, Tolasz J. Sorption of Sr(II) onto nanocomposites of graphene oxide-polymeric matrix. *J Radioanal Nucl Chem*. 2018;315:263-272. doi:10.1007/s10967-017-5688-x

53. Hummers WS, Offeman RE. Preparation of Graphitic Oxide. *Trans Amer Electrochem Soc*. 1958;80(6):1339-1339. doi:10.1021/ja01539a017

54. Paek SH, Lee SH, Cho JH, Kim YS. Development of rapid one-step immunochromatographic assay. *Methods*. 2000;22(1):53-60. doi:10.1006/meth.2000.1036

55. Horwitz E, Dietz ML, Chiarizia R, Diamond H, Maxwell SL, Nelson MR. Separation and preconcentration of actinides by extraction chromatography using a supported liquid anion exchanger: application to the characterization of high-level nuclear waste solutions. *Anal Chim Acta*. 1995;310:63-78. Accessed June 20, 2018. https://ac.els-cdn.com/000326709500144O/1-s2.0-000326709500144O-main.pdf?_tid=e1437049-8b6a-4381-8a34-d965c33b23a2&acdnat=1529507138_6d72112ab3dc8fa678328205a7670ba6

56. Burrell FM. *Development of Numerical Simulation Methods to Support Emerging Rapid and Automated Radioanalytical Techniques*. University of Southampton; 2017.

57. Burrell FM, Warwick PE, Croudace IW, Walters WS. Development of a numerical simulation method for modelling column breakthrough from extraction chromatography resins. *Analyst*. 2021;146:4049. doi:10.1039/d0an02251a

58. Nuclear Decommissioning Authority. *NDA Research and Development 2016*.; 2016.

59. Chandler SD. *Radioactive Waste Control and Controversy : The History of Radioactive Waste Regulation in the UK*. Gordon and Breach Science Publishers; 1997. Accessed January 10, 2018. https://books.google.co.uk/books?id=nuE_MTfLODsC&pg=PA66&dq=sellafield+history&hl=en&sa=X&ved=0ahUKEwj5toeT3s3YAhUaOsAKHURGAa4Q6AEIMzAC#v=onepage&q=sellafield history&f=false

60. IAEA. *Organization and Management for Decommissioning of Large Nuclear Facilities, STI/PUB/399*.; 2000.

61. Bond A, Palerm J, Haigh P. Public participation in EIA of nuclear power plant decommissioning projects: a case study analysis. *Environ Impact Assess Rev*. 2004;24:617-641. doi:10.1016/j.eiar.2004.02.002

62. Burrell FM, Warwick PE, Croudace IW, Walters WS. Development of a numerical simulation method for modelling column breakthrough from extraction chromatography resins. *Analyst*. 2021;146(12):4049-4065. doi:10.1039/d0an02251a

63. Burrell FM. *Development of Numerical Simulation Methods to Support Emerging Rapid and Automated Radioanalytical Techniques*. 2017.

64. James Graham. *MSSS GEMS Phase 2: Characterisation of Soils and Strontium Sorption Batch Testing*.; 2015.

65. TrisKem International. *TEVA Product Sheet*. Vol 33.; 2015.

66. TrisKem International. *PRODUCT SHEET TK-TcScint Packing Order N°. Form Particle Size Conditions of Utilization*.; 2021. Accessed March 30, 2022. https://www.triskem-international.com/scripts/files/6167ea10645210.08957338/PS_TK-TcScint-Resin_EN_210902.pdf

67. PRODUCT SHEET Actinide Resin TM (AC Resin). Accessed March 30, 2022. www.triskem-international.com

68. TrisKem International. *TRU Resin Product Sheet*.; 2015. Accessed June 27, 2018. http://www.triskem-international.com/scripts/files/5b0bc8e8d03117.86838612/TRU RESIN-EN.pdf